Synthesis of acene based organic gelators. Examination of the spectroscopical, photochemical and rheological properties

Vom Fachbereich für Chemie und Pharmazie

der Technischen Universität Carolo-Wilhelmina

zu Braunschweig

zur Erlangung des Grades eines

Doktors der Naturwissenschaften

(Dr. rer. nat.)

genehmigte

D i s s e r t a t i o n

von Jens Reichwagen

aus Hamburg

1. Referent: Professor Dr. H. Hopf

2. Referentin: Professor Dr. M. Mazik

eingereicht am: 03.02.2005

mündliche Prüfung (Disputation) am: 18.04.2005

Vorveröffentlichungen der Dissertation

Teilergebnisse aus dieser Arbeit wurden mit Genehmigung der Gemeinsamen Naturwissenschaftlichen Fakultät, vertreten durch den Betreuer der Arbeit, in folgenden Beiträgen vorab veröffentlicht:

Publikationen

Jens Reichwagen, Henning Hopf, André Del Guerzo, Jean-Pierre Desvergne, and Henri Bouas-Laurent: Photodimers of a Soluble Tetracene Derivative. Excimer Fluorescence from the Head-to-Head Isomer, *Org.Lett.*, **2004**, *6, 12*, 1899-1902.

André Del Guerzo, Colette Belin, Henri Bouas-Laurent, Jean-Pierre Desvergne, Jens Reichwagen, Henning Hopf: Photochromism ans Self-Assembly of Soluble Tetracenes, *Mol. Cryst. Liq. Cryst.*, in press.

Jens Reichwagen, Henning Hopf, André Del Guerzo, Colette Belin, Henri Bouas-Laurent, Jean-Pierre Desvergne: Synthesis of 2,3-substituted tetracenes and evaluation of their self-assembling properties in organic solvents, *Org. Lett.*, **2005**, *7, 6*, 971-974.

Tagungsbeiträge

Reichwagen, J., Hopf H., Desvergne J.-P., Bouas-Laurent H.: Synthese und Eigenschaften organischer Gelbildner; 2,3 Didecyloxytetracen (DDOA) (Poster) 13. Vortragstagung der LIEBIG-Vereinigung für Organische Chemie der Gesellschaft Deutscher Chemiker (ORCHEM 2002), Bad Nauheim (2002).

Reichwagen, J., Hopf, H., Del Guerzo, A. Desvergne, J.-P., Bouas-Laurent, H.: Alkoxiacene: Spektroskopie, Gel-Bildung und Photochemie einer variablen Substanzklasse (Poster) Jahrestagung der GDCh 2003, München (2003).

André Del Guerzo, Jens Reichwagen, Henning Hopf, Colette Belin, Henri Bouas-Laurent, Jean-Pierre Desvergne: Self-Assembled Fibers with Tunable Optical Properties: Organogels of Anthracene and Tetracene Derivatives (Poster), HRSMC & EPA Summer School "New Perspectives in Photochemistry" Egmond aan Zee (2003).

André Del Guerzo, Colette Belin, Henri Bouas-Laurent, Jean-Pierre Desvergne, Jens Reichwagen, Henning Hopf: Self-Assembling and Photochemical Properties of soluble Tetracenes, XXth IUPAC Symposium on Photochemistry, Granada (2004).

Del Guerzo, A., Belin, C., Bouas-Laurent, H., Desvergne, J.-P., Reichwagen, J., Hopf, H.: Photochromism and Selfassembling of Soluble Tetracene Derivatives (Poster), ISOP'04, Arcachon (2004)

Die vorliegende Arbeit wurde in der Zeit von Oktober 2001 bis November 2004 am Institut für Organische Chemie der Technischen Universität Braunschweig unter der Leitung von Prof. Dr. H. Hopf angefertigt.

This study could not have been carried out and completed without the help of numerous persons.

I would like to express my sincere gratitude to Prof. Dr. Henning Hopf for the possibility to perform this study, for his encouragement, advice and his interest.

Further, I am very grateful to Prof. Dr. Monika Mazik for agreeing to be the co-referee of my thesis.

For the opportunity to study and do research at the Université Bordeaux in 2002 and 2003, I would like to thank Prof. Dr. Henri Bouas-Laurent and Prof. Dr. Jean-Pierre Desvergne.

I am very grateful to Ms. Petra Holba-Schulz for the measurement of high resolution and 2D NMR spectra; Ms. Karin Kadhim for measuring UV and IR spectra; Dr. Ulrich Papke and Ms. Doris Döring for the measurement of high and low resolution mass spectra.

For the measurement of AFM and fluorescence spectra, as well as valuable discussions about photophysical techniques, I am thankful to Mme. Colette Belin and Dr. André Del Guerzo.

I would like to express further my sincere gratitude to Dr. Kerstin Ibrom for many valuable discussions about my work in general and about NMR spectroscopy.

For financial support of this study, I would like to thank the "Fonds der Chemischen Industrie".

Last, but nor least, I thank all my colleagues for the incountable valuable discussions, the support and the enjoyable working atmosphere I experienced throughout these years.

Table of contents

1 Introduction

Low molecular mass gelators (LMMOGs) have in recent years been the target of growing scientific interest. Even though they played a minor role in the organic literature during the 1970s, new developments and new structures of LMMOGs have been reported over the past 20 years. The focus on this class of gel forming substances has two reasons. For the organic chemist LMMOGs play an important role (in comparison to polymeric gelators, systematization *vide infra*) because they can be examined by structure effect relationships and are subject of rational synthetic approaches.

The second reason is the widespread use of gels in industrial applications, pharmaceutical applications and "everyday life".

This range of applications can be explained by the great diversity of structures that are displayed on the microscopic and mesoscopic scale. Gels often show thermoreversibility, exhibit a great chemical sensitivity and, as will be shown later in this work, a large diversity of nanostructures.

A short summary of applications for gels may illustrate the importance of gel-like materials.[1a] Reverse micellar systems (microemulsions) involving gels are used in biocatalysis, biomembrane mimetics, extraction processes and the preparation of microparticles. In waste disposal, gels are frequently involved in the recovery of spilled crude oil or the disposal of used cooking oil. The application of organogels in drug delivery can be illustrated by the example of active enzymes and bacteria entrapped in apolar gels of gelatin. Many aqueous gels or complex mixtures of surface-active components in water and oil are utilized for ointments or macromolecular separations, protein crystallizations, etc. One final example is the use of gels containing ester groups for the gelification of electrolyte solutions for lithium battery applications.

Like with many new gelators, the first discovery that simple acene structures can form gels in low concentrations with organic solvents, was made accidentally.

In 1991 Bouas-Laurent et al. discovered the gel forming abilities of 2,3-didecyloxy-anthracene (**1**) (2,3-DDOA) in the course of photochemical investigations on substituted anthracenes.[2] Similarly substituted naphthalenes or benzenes do not form gels under similar conditions. Angular substitution (like in the case of dialkoxy-phenanthrenes) does not lead to gel forming substances, too.[2]

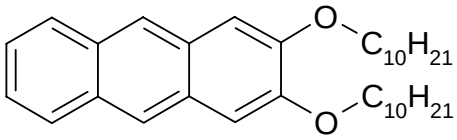

1

This led to one of the primary question of this work. Would 2,3-dialkoxy-tetracenes **2**, until now not described in the literature, exhibit gel forming properties or is gel formation a unique property of substituted anthracenes?

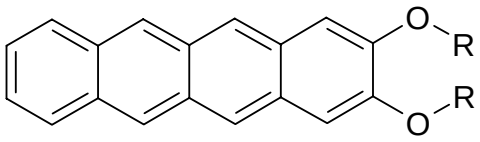

2 R = C_nH_{2n+1}

On the other hand it was surprising to note that 2,3-didecyloxy-anthracene (**1**) does not form photodimers upon irradiation.[3] Surprising, because anthracene itself[4] and most of the known alkoxy substituted anthracenes are known to undergo [4+4] photocycloadditions.[3 ,4]

Like anthracene and its derivatives, tetracene is known to undergo photodimerization,[5, 6, 7] but no examples of the photochemistry of substituted tetracenes are known so far.

Those two properties, gel forming ability and lack of photodimerization, of 2,3-DDOA (**1**), led to the primary goal of this work: synthesis of 2,3-dialkoxy substituted tetracenes and, if possible, even longer acenes, analysis of the gel forming properties and photochemical properties of those new substances. Last, but not least, comparison of those properties to the photochemistry and photophysics of other substituted tetracenes.

2 Polyacenes as low molecular mass gelators

2.1 Introduction

It is hard to give a universal definition of a gel. To give some information on how to classify acene (anthracene, tetracene, pentacene and others) based gelators, different definitions and characteristics of gelators, as given in the recent literature, will be considered.

Bungenberg de Jong[8] defines a gel as a "system of solid character, in which the colloidal particles somehow constitute a coherent structure,…". Another definition, more suited to classify existing systems, is provided by P. H. Hermans[8] who is giving three propositions to define a gel. "(a) They are coherent colloid systems of at least two components; (b) they exhibit mechanical properties characteristic of a solid; (c) both the dispersed component and the dispersion medium extend themselves continuously throughout the whole system."

The drawback with this definition, as with many others, is that a broad variety of "gel-like systems" occurring in every day life fail to fulfill the definition. It is thus easier, to accept the limits and to present a structural classification of gels. This is done by P. J. Flory,[9] by ordering but not defining the described gels. He classifies gels on the basis of structural criteria into four types:[9]

A) Well ordered lamellar structures, including gel mesophases.

B) Covalent polymeric networks; completely disordered.

C) Polymer networks formed through physical aggregation; predominantly disordered, but with regions of local order.

D) Particulate, disordered structures.

The first type (A) of gels is represented by soap gels, phospholipids and clays. Examples for the second type (B) are vulcanized rubbers, structures of elastin and polyfunctional condensation polymers. The third class (C) is represented by systems like *i*-carrageen or alginate gels. Flocculent precipitates like V_2O_5 gels or aggregated proteins form the fourth class of gels (D).

Especially gelators of the third type have caused increasing interest in recent years. The main distinction from the other classes of gelators is that mainly molecules of finite size are giving order and solid like behavior to large amounts of an appropriate solvent. The gels formed are

often thermoreversible and in many cases only small amounts of the gelator (typically < 2 wt%)[1a] are needed to form the viscoelastic liquidlike or solidlike material.

To show the structural versatility of organic gelators, some examples are described in the next chapter.

2.2 Classes of organogelators

Terech and Weiss, who have reviewed the field of organic gelators extensively[1a] describe eight major classes of organic gelators and their applications.

2.2.1 Fatty acid derivatives

Substituted fatty acids and their monovalent metal salts, like 12-hydroxy-octadecanoic acid (**3**) have long been used to harden organic liquids, e.g. in the lubrication industry.[1b]

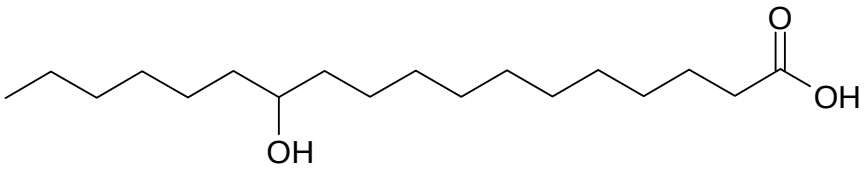

3

The range of organic liquids which can be gelified by this family of molecules extends from alkanes, CCl_4, and aromatic solvents to more polar solvents, like nitrobenzene. As this type of gelator contains an asymmetric carbon center, their aggregates can be chiral. The preferential reflection of circularly polarized light by the gels of **3** indicate that the fibers are twisted in a way that is related to their molecular chirality. It has to be pointed out that the enantiomorphic relationship do not fully explain the gel forming ability in organic liquids as racemic (*d,l*)-**3** produces organogels consisting of fibers interconnected by platelike contact zones.

Next to monovalent salts of fatty acids, divalent or trivalent metal soaps have been used in lubricating applications. Examples are C_{16}DP-Al **4** or **5**.[1c] The degree of non saturation and the length of the lipophilic part of the gelator, the nature of the metal ion and the type of solvent influence the solubility of the metal ion soap and hence its gel forming abilities.

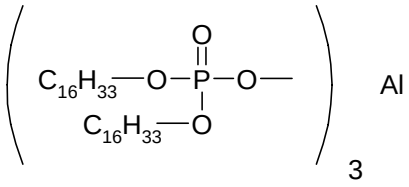

4

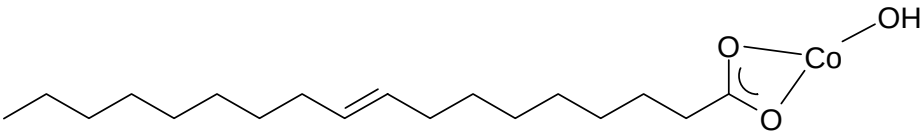

5

It is interesting to note that aggregates of the aluminum salt of dihexadecyl-phosphate (C_{16}DP-Al) are formed even at concentrations of 0.01 wt%, far below the critical gelator concentration, while at higher concentration fibrous aggregates of gels in hydrocarbons have been observed by single electron microscopy (SEM).

2.2.2 Steroid derivatives

The range of steroid derivatives that show gel forming abilities is quite broad. One rather simple structure is dihydrolanosterol (DHL) (**6**), which forms gels at 1-10 wt% with different oils (mineral, synthetic, animal or silicone).

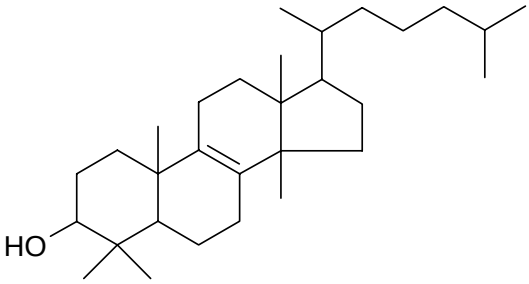

6 (DHL)

Other steroid derivatives, like deoxycholic, cholic, apocholic, and lithocholic acid and their salts thicken aqueous salt solutions. Some relationships between the structure of a molecule and the gel formation are provided by the fact that remarkably stable gels of hydrocarbon liquids can be obtained if the steroid has a hydroxyl group at C_3 and an amine functionality at the 17a-aza position, like in STNH **7**.[1d]

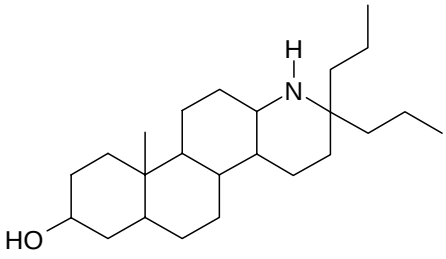

7 (STNH)

Other facts which determine the gel forming abilities of steroids are the position of unsaturated functionalities. Two allyl groups at C_{17} inhibit gelation, but a double bond at $C_{5,6}$ does not.

The steroid gel structures could be derived by small angle neutron scattering (SANS). These data show that the aggregates are very long, rigid fibers, possibly symmetrical double helices with a diameter of 99 Å. The structure contains further "contact points" that are formed by specific overlap through fusion or coiling of two or more individual fibers over distances much longer than their diameters. As for other gels, the TEM measurements of STNH indicate that fiber interactions are (pseudo) crystalline zones in a heterogeneous network, with a solidlike behavior.

2.2.3 Anthryl derivatives

Bouas-Laurent, Desvergne et al. discovered in 1991 that even a very simple molecule like 2,3-DDOA (2,3-didecyloxy-anthracene) (**1**) is able to gel various alkanes, alcohols, aliphatic amines and nitriles.[2] Oxidation of the condensed ring system to the related quinone **8** keeps the gelling ability, but the lower homologue 2,3-dialkoxy-naphthalene shows no gel forming ability.

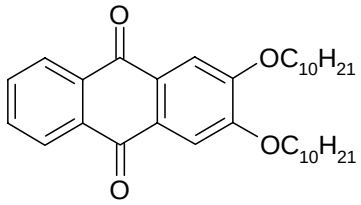

8

The solution to gel phase transition of 2,3-DDOA (**1**) varies over a wide temperature range, depending on the solvent and the gelator concentration. In comparison to other gelators, the 2,3-DDOA (**1**) gels show a magnitude of elasticity, which suggests that the interaction zones are permanent crystalline microdomains at a given temperature.

2.2.4 Gelators containing steroidal and condensed aromatic rings

A combination of the gelators described in Chapter 2.1.2 and 2.1.3 can be seen in the class of gelators containing steroidal and condensed aromatic rings. In contrast to STNH, the gelation ability of which relies upon the presence of a hydroxyl group at C_3, this class of molecules are functionalized at C_3 and cannot be H-bond donors. This type of gelators (ALS) consist of an aromatic group (A) connected to a steroidal moiety (S) via a linking group (L). This versatility makes the analysis of gel interactions easier, as any of the three building units can be changed and some of the molecular attributes, like luminescence or chirality can be used to investigate changes in the path from isotropic phase to the gel phase.

Two main subgroups have been described by Weiss and Terech, the first being anthryl and anthraquinone bearing steroid-based gelators. Cholesteryl-4-(2-anthryloxy)butanoate (CAB) (**9**) and cholesteryl-anthraquinone-2-carboxylate (CAQ) (**10**) are examples of these ALS gelators[1e].

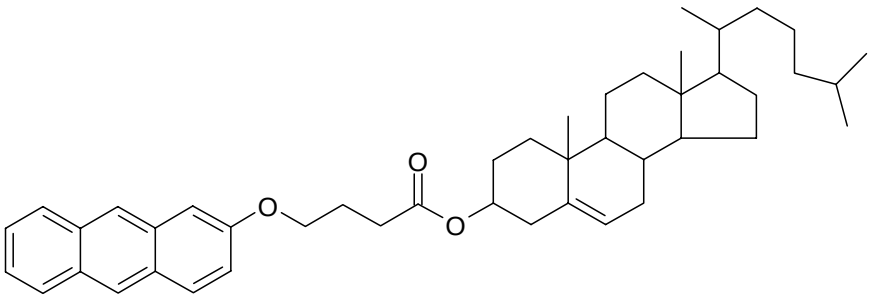

9 (CAB)

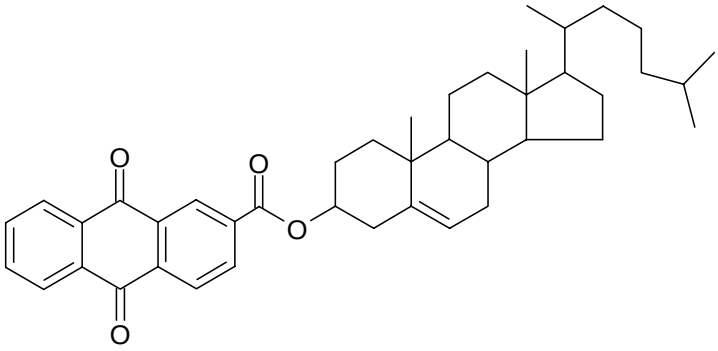

10 (CAQ)

CAB forms gels with a wide variety of solvents like hydrocarbons, alcohols, aldehydes esters, and amines, many of which are luminescent. When the correlation of the gel forming abilities with the three structural components is examined, it is noticed that neither a 1-pyrenyl analogue of CAB (containing four nonlinearly fused rings in the A position) nor a 2-naphthyl analogue of CAQ (containing only two fused rings) are capable of forming gels with any of a variety of liquids. A remarkable fact is the induction of thixotropy that can be accomplished by addition of a small amount of the non gelling CMAQ **11** to normal samples of CAQ **10** and 1-octanol.

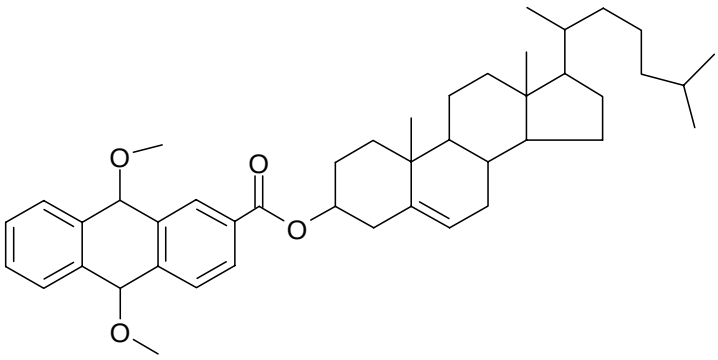

11

One major difference between ALS-type gelators and gelators of the 2,3-DDOA-type is the swelling of the strands of steroid based organogelators.[10] The steroid unit allows inclusion of solvent molecules, when they are of the right molecular shape and electronic compatibility with the lipophilic external shell of the ALS. In contrast, gelators without the steroidal moiety (like 2,3-DDOA (**1**)) form gels with dry crystalline nodes, which gives rise to almost superimposable diffraction patterns of the solid substance and the gel phases.

The second subgroup of the gelators containing steroidal and aromatic rings are azobenzene steroid based gelators. They exhibit a highly polar azobenzene group linked to C_3 of a steroidal moiety. One sample of this type of gelator is substance **12** which gels, depending on the phenyl-ether (OMe to $OC_{10}H_{21}$), solvents like *n*-alkanes, cyclohexane, ethers, esters, alcohols and polar aprotic solvents like acetone or DMF.[1f]

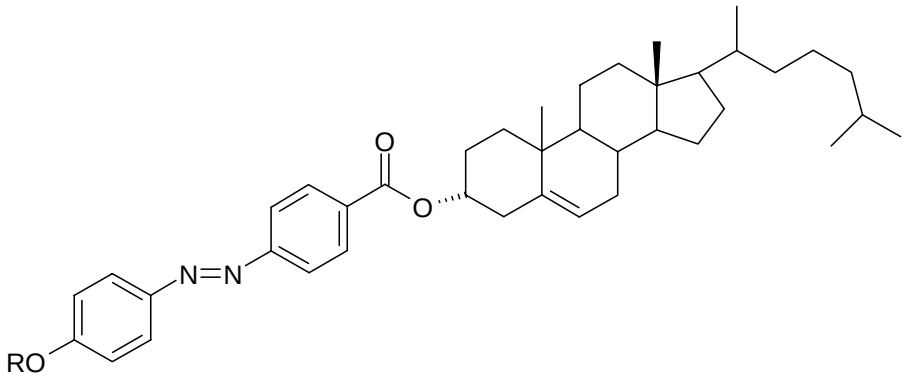

12

Like with other steroid based gelators (with substitution on C_3) the α- and β-anomers preferentially gel apolar and polar liquids, respectively. It could be witnessed by the greater efficiency of gelators with an odd number of C-atoms on a substituent attached to the azobenzene moiety that there is a delicate lipophobic/lipophilic structural balance governing gel formation in this type of gelator.

2.2.5 Amino acid type organogelators

This type of gelator has a very divers appearance. One example is the urea derivative 2-octyldodecyl-4-[[(1-naphthylamino)carbonyl]amino]benzoate (**13**) which forms lyotropic gels at 4 wt%.[1g] Another example is an amide, *N*,*N'*,*N''*-tristearyltrimesamide (TSTA) (**14**) which forms gels with a variety of polar liquids, including 1,2-dichloroethane, nitrobenzene, DMSO and others. Other members are amino acid derived, like *N*-benzyloxy-carbonyl-*L*-alanine-4-hexadecanoyl-2-nitrophenyl-ester (**15**) which forms gels with methanol and cyclohexane through networks of intermolecular hydrogen bonds between the N-H and the C=O parts of the urethane group.

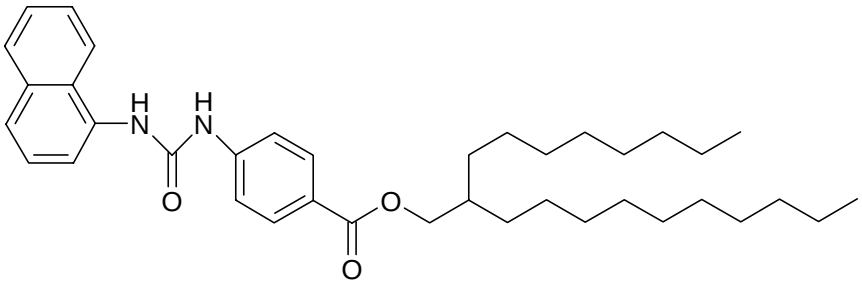

13

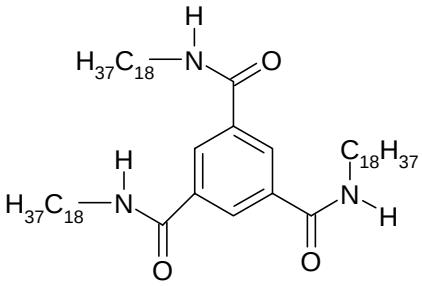

14 (TSTA)

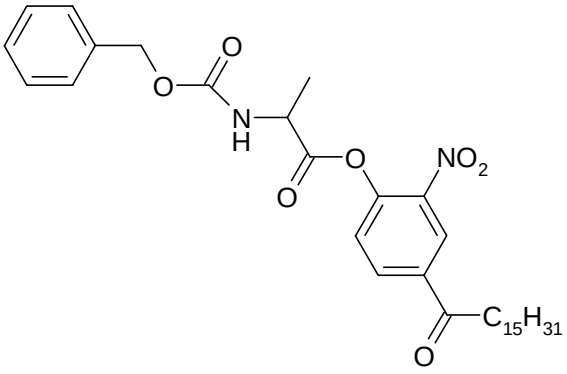

15

A wide variety of organic liquids can be thickened by oligomers of some amino acid derivatives like **16** (R = $CH_2CH_2CO_2Me$, n = 4.2, m = 12) or even cyclic structures like the cyclo-dipeptide **17** (R^1 = $CH(CH_3)_2$ and R^2 = $(CH_2)_2CO_2(CH_2)_2CHMe(CH_2)_3CHMe_2$).

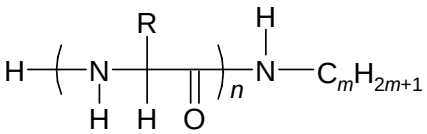

16

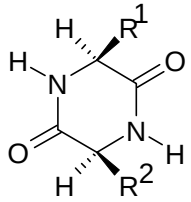

17

Even some structurally simple tertiary amines and related tertiary and quaternary ammonium halide salts form viscoelastic, thermally reversible gels with organic liquids ranging from DMF to dodecane. Like with other gelators, the mode of gelation involves a network of interconnected strands.

2.2.6 Organometallic compounds

Next to metal salts of fatty acids (see Chapter 2.1.1) different organometallic compounds form gels with organic solvents. One example is the mononuclear copper β-diketonate **18** whose disc-like molecules are shaped favorably to stack and form rodlike aggregates.[1h]

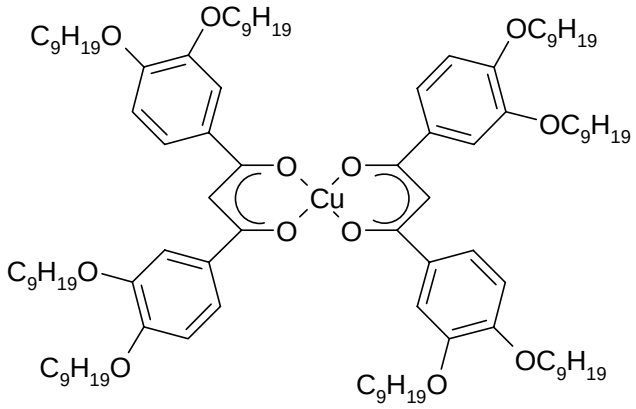

18

In this case, like with other gelators, the similarity to the field of liquid crystals can be seen. Derivative **18** forms both, a neat thermotropic discotic mesophase and an organo-gel with ca. 99% of cyclohexane. Next to the mononuclear copper compounds, various binuclear copper tetracarboxylates and even binuclear rhodium carboxylates have been investigated. At concentrations below 1 wt% they form gel-like materials with hydrocarbons.

Another type of organometallic gelator exhibits not a transition metal oxygen bond but a transition metal nitrogen system. The zinc *meso*-tetrakis(*p*-carboxy-phenyl)porphyrin (**19**) forms gels, like the copper compounds, with hydrocarbons and has been investigated by Marchon and coworkers.[1i]

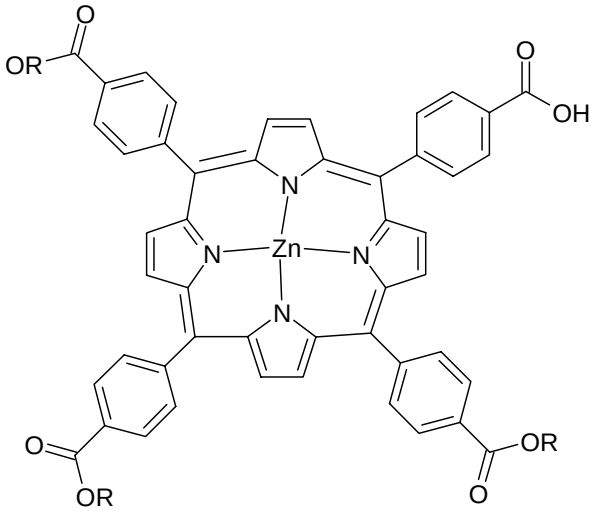

19

2.2.7 Miscellaneous types of gelators

This group of LMMOGs is characterized by two properties. First it is subdivided in a quite large number of structurally different subgroups. Secondly some of the members, while still not polymers, show large oligomeric structures with molecular weights up to 2300 mass units.

The first subunit are macrocyclic gelators like calix[*n*]arenes (*n* = 4-8), substituted with long alkanoyl chains. As one example a calix[8]arene bearing dodecanoyl chains is given.

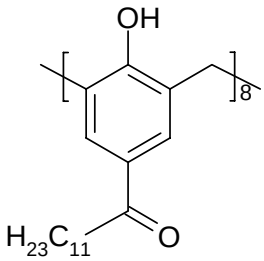

20

20 forms gels with liquids like alkanes, carbondisulfide, toluene and selected alcohols. It is worth noting that related open structures with two or one phenolic ring are only weak gelators or even non gelators. This indicates that a minimum number of intermolecular interaction sites per gelator molecule is needed.

The second subgroup is based on sorbitol and other polyol derivatives. Examples are 1,3:2,4-di-*O*-benzylidene-D-sorbitol as a chiral polyalcohol, forming gels with a variety of solvents like hexadecane, ethanol or dimethyl-phthalate. Interestingly, the racemic sorbitol derivative does not form gels.

Another sugar based gelator is cellobiose-octa(decanoate) **21**, another example of a structure at the border between liquid crystalline and gel forming behavior (depending upon the concentration and temperature in hexadecane).[1j]

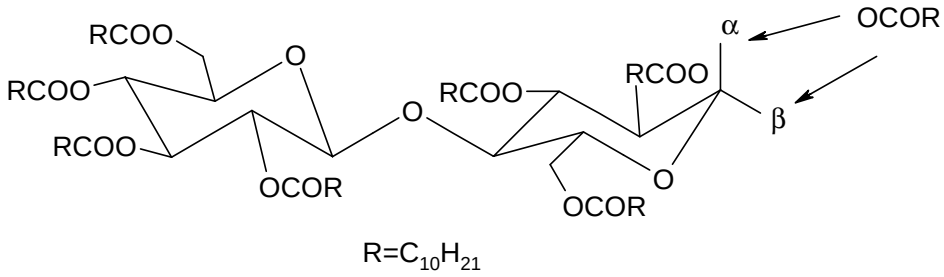

21

A structurally rather simple gelator for *n*-alkanes are partially fluorinated *n*-alkanes (F_nH_m). They form birefringent gels when $n = 12$ and $8 < m < 20$. With this gelator, in contrast to many other alkane gelling substances, cyclic alkanes (like cyclohexane) are not gelled.

Another interesting molecule in this group, being a LMMOG with a rather high molecular mass, is β-cyclodextrin (β-CD), which is a cyclic heptamer of α-1,4-linked glucosidic units. β-CD forms gels with pyridine (when both, gelator and solvent are rigorously dried) or with toluene and chloroform (in the presence of small amounts of water), showing the strong dependency of gel formation from the measurement conditions.

The last gelator in this chapter is again of rather simple structure. Sodium bis(2-ethylhexyl)-phosphate **(22)** forms large reverse micelles in *n*-heptane, found to consist of semiflexible rods when grown in the absence of water.

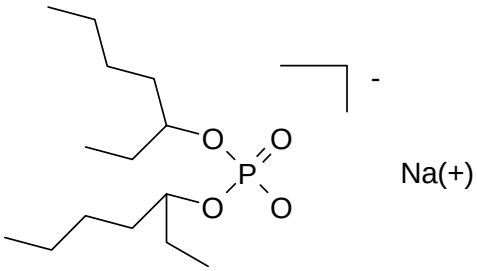

22

2.2.8 Two component systems

This last chapter in the summary of LMMOGs is dedicated to systems, the gelling ability of which is due to the mixture of different compounds. The single components do not or only poorly gel organic liquids. One example is the mixture of aminopyrimidine **23** and dialkylbarbituric acid **24**.[1k]

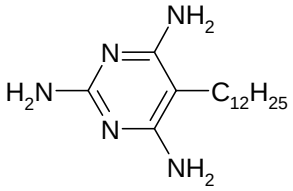

23

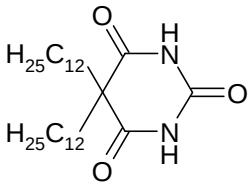

24

Stable organogels of **23**/**24** mixtures (1:1 molar ratio) are formed in cyclohexane in concentrations as low as 1.1 wt%. The strands which form the gel are built by N-H/C=O intermolecular hydrogen bonds. Another interesting mixture which forms gels in toluene has been found in the course of the asymmetric hydrocyanation of 3-phenoxy-benzaldehyde. The gelation proceeds due to complexation between the two optically active ingredients, **25** and **26**.

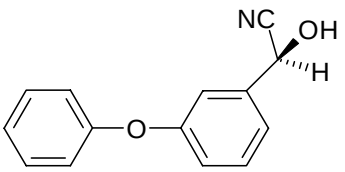

25

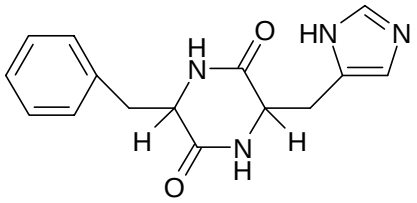

26

Besides these distinct mixtures, where sometimes the ratio of the two components can be varied only in small steps, two component gelators are known, where one compound can form gels in the presence of a broader variety of "co-gelators". One example is the mixture of sodium-bis(2-ethylhexyl)-sulfosuccinate (**27**) with a variety of phenols. These mixtures form gels with nonpolar liquids in concentrations below 0.5 wt%.

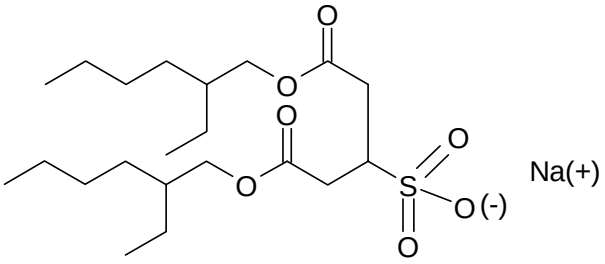

27

This summary of some of the gelators known today shows two interesting points. On the one hand there is a broad variety of systems that form gels under various conditions. On the other, it is still challenging to synthesize specific gelators. Many systems are simply encountered by luck and than further investigated. This is one of the reasons, why the systematic investigation of acene gelators, as presented in this study, is of interest. The discovery of the gel forming abilities of 2,3-DDOA (**1**) gives rise to the hope that a full class of LMMOGs has been discovered, with **1** only being the first member.

2.3 Synthesis of gel forming tetracenes

2.3.1 Synthetic strategies

Three general approaches will be discussed here to find synthetic routes leading to 2,3-dialkoxy-tetracenes **2**.

First of all it is useful to look at the known synthesis of 2,3-DDOA (**1**) and to attempt an enlargement of the ring-system along similar lines (strategy A).

The second approach is directed at an iterative construction of tetracene systems. This starts with smaller ring systems (benzenes or naphthalenes) enlarging them in a sequence of repetitive reactions. Here it is important to keep the desired 2,3-disubstitution pattern in mind (strategy B).

Last, but not least, tetracene systems can be build up by connection of one and two ring systems, where the connecting reaction gives the fourth ring. Like in the iterative approach, the substitution pattern is to be kept in mind (strategy C).

These three approaches will be discussed in the following chapters.

2.3.1.1 Strategy A

Different strategies were used to synthesize 2,3-DDOA[11] and they seem to be a valid first key step to build a 2,3-dialkoxy-tetracene **2** system as well. Bouas-Laurent et al. used two strategies, using 2,3-dialkoxy-9,10-anthraquinone (**8**) as a key intermediate. Both strategies rely retrosynthetically on three steps as indicated in Scheme 1. The functionalization of the anthracene core is leading to a 9,10-anthraquinone **8**. Functional group interconversion transforms the alkoxy-phenyl-ether to the corresponding phenol **28**. The last retrosynthetical step is the formation of the 9,10-anthraquinone core, the main difference between the two strategies presented by Bouas-Laurent et al.[11]

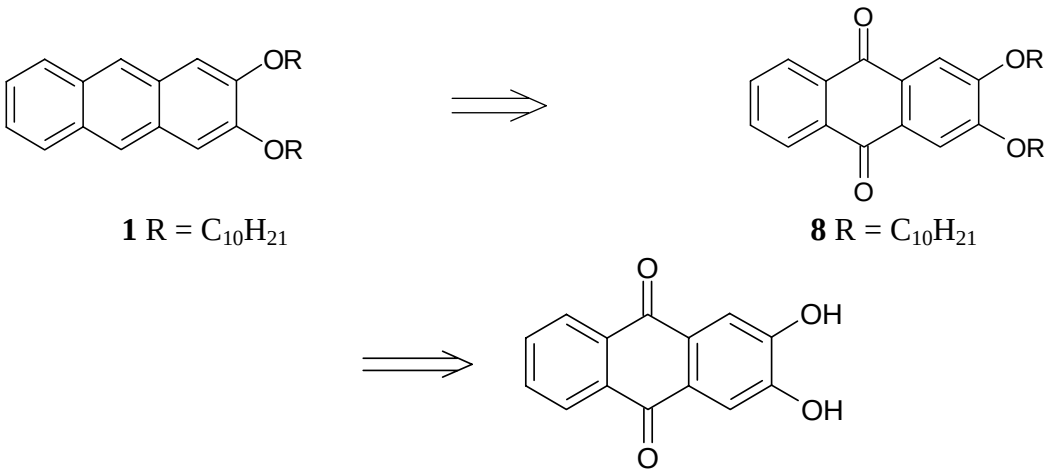

1 R = $C_{10}H_{21}$ **8** R = $C_{10}H_{21}$

28

Scheme 1 Retrosynthesis of 2,3-DDOA (1)

Synthetically, using a Friedel-Crafts acylation, 1,2-dihydroxy-benzene (**29**) is first coupled with phthalic anhydride (**30**) to intermediate **31**, which is subsequently cyclized to the target system **28**.

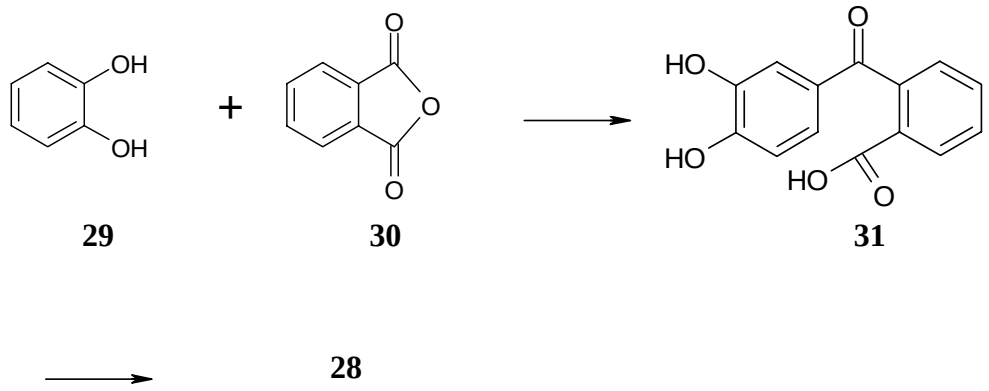

29 **30** **31**

28

Scheme 2 Synthesis of 2,3-dihydroxy-anthra-9,10-quinone (28)

The resulting intermediate (**28**) is then alkylated and reduced to yield 2,3-DDOA (**1**).

Different problems prohibit the use of this "Friedel-Crafts approach" to synthesize analogous tetracenes. To synthesize the desired tetracene core, either 2,3-dihydroxynaphthalene (**32**) or naphthalene-2,3-dicarboxylic-acid-anhydride (**34**) have to be used to arrive at the bishydroxy-tetracene-quinones **33** or **35** (see Scheme 3).

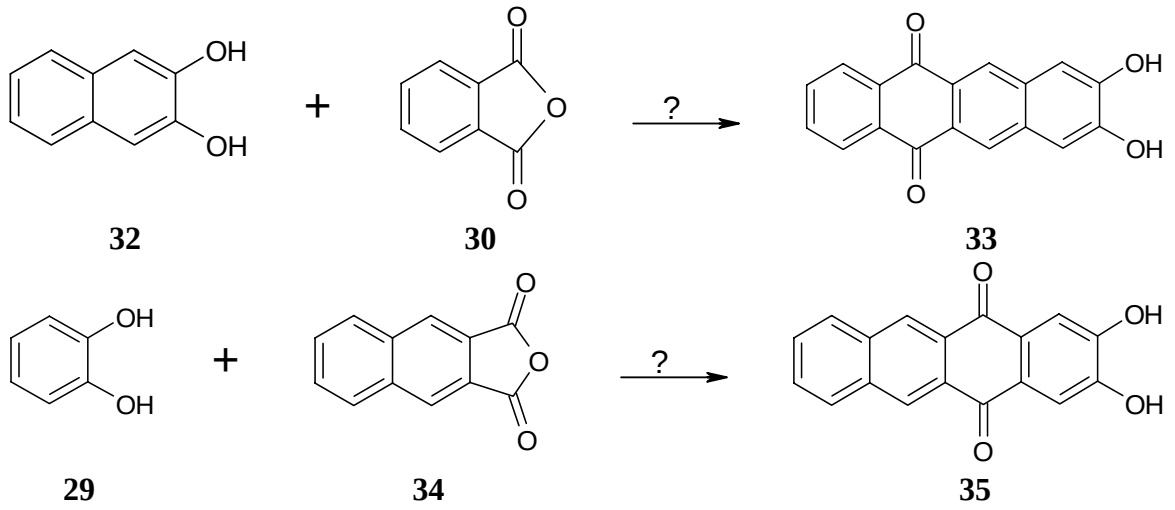

Scheme 3 Synthesis of possible dihydroxy-tetracene-quinones by Friedel-Craft reactions

It is likely to assume that bisphenol **32** is acylated in *o*-position relative to the activating hydroxy functions. On the other hand, intermediate **34** is not commercially available and has to be synthesized from naphthalene-2,3-dicarboxylic-acid.

The second approach described by Bouas-Laurent et al., uses the Diels-Alder addition of 2,3-dimethoxy-butadiene (**37**) to 1,4-naphthoquinone (**36**). The Diels-Alder-adduct is directly oxidized to form 2,3-dimethoxy-9,10-anthraquinone (**38**).

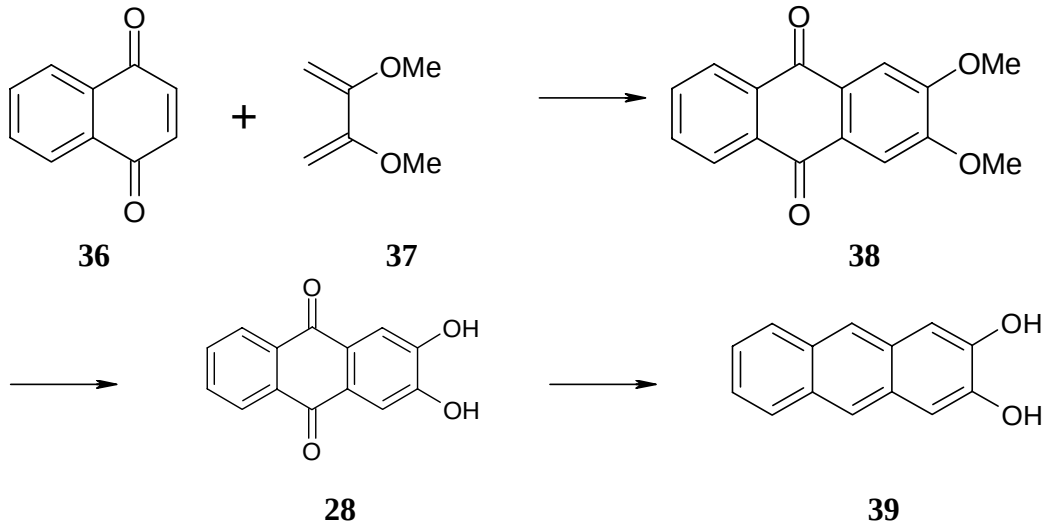

36 **37** **38** **28** **39**

Scheme 4 **Synthesis of 2,3-dihydroxy-anthracene (39) as precursor of 2,3-DDOA (1)**

Intermediate **38** is further demethylated, the resulting bisphenol **28** is reduced and the dihydroxyanthracene **39** is alkylated to yield 2,3-DDOA (**1**).

Principally, this approach could be used to build up tetracene systems, if small modifications are introduced. Instead of naphthalene-1,4-quinone (**36**), the higher homologue anthracene-1,4-quinone (**40**) must be used. Even though it is not commercially available, it can be obtained from commercially available chinizarin (1,4-dihydroxy-anthra-9,10-quinone) in 98% yield by reduction with $NaBH_4$.[12]

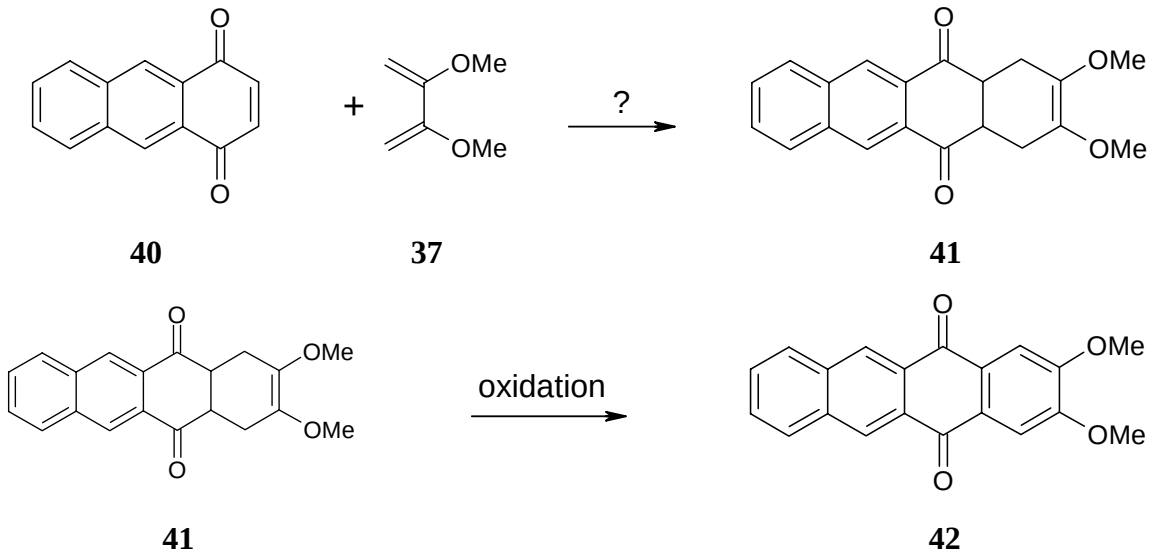

40 **37** **41** **41** **42**

Scheme 5 **Possible synthesis of 42 by Diels-Alder reaction**

Only the poor yield of the Diels-Alder reaction between the smaller naphthoquinone **36** and diene **37** (61% dropping to 19% with larger amounts of reagent)[11] made it a good idea to look for different alternatives first.

2.3.1.2 Strategy B

Two different strategies to build up tetracenes by an iterative approach have been reported. Only those strategies which include the 2,3-disubstitution pattern seem worth to be investigated further, as it appears unlikely that this substitution pattern can be incorporated after the synthesis of the tetracene core e. g. by bromination or other classical aromatic substitution routes.

Bowles and coworker [13] have described the synthesis of 2,3-disubstituted naphthalenes and anthracenes via desilylative halogenation, cycloaromatisation and alkynylation of precursors such as **43**.

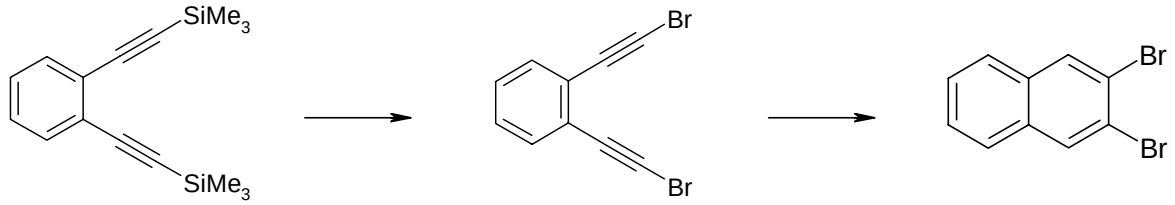

43 **44** **45**

Scheme 6 Synthesis of 2,3-disubstituted acenes by iterative reactions

This reaction sequence can be used to prepare 2,3-dibromo-naphthalene (**45**) in moderate yields. Extension to the corresponding 2,3-dibromo-anthracene is possible, too. A further extension of the ring system is prohibited by the poor solubility of the product of the desilylative halogenation of bis(trimethylsilylethynyl)-anthracene. The reaction leads to an inseparable mixture of products.[13]

A further approach is based on the synthesis of tetracene-2,3-dicarboxaldehyde (**48**), presented by Mallouli et al.[14] The basic idea consists in the condensation of phthalic dialdehyde (**46**) with 2,5-dimethoxy-tetrahydrofuran (**47**), leading to extended aromatic *o*-dialdehydes.

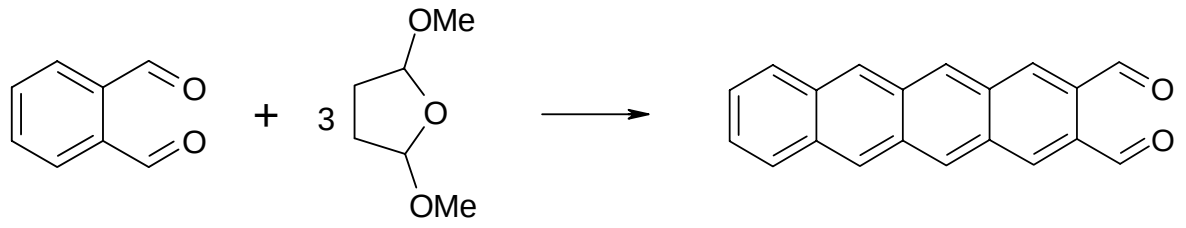

46 **47** **48**

Scheme 7 Synthesis of tetracene-2,3-dicarboxaldehyde (48) by condensation

Major drawbacks of this approach are the poor yields concerning the tetracene dialdehyde **48** (17% published[14]) and the high probability of severe separation problems. It is likely to assume that a mixture of all possible homologous *o*-dialdehydes from phthalic-dialdehyde to tetracene-dialdehyde will be present.

Other problems could appear in further transformations, since the activation of the *o*-dialdehyde prohibits the direct transformation of the dialdehyde to a diformiate by Baeyer-Villiger oxidation, for example.[15] Further functional group interconversion would at least include transformation of the aldehyde to a methyl ketone by a Grignard or methyl lithium reagent, oxidation and than Baeyer-Villiger oxidation to the acetate.

The general drawbacks of the presented iterative tetracene synthesis led to the planning of consecutive synthetic approaches.

2.3.1.3 Strategy C

Numerous reactions to build up six membered rings and even aromatic rings are known. The best known are Diels-Alder additions, aldol condensations, and especially the Robinson annulation.

When an approach is considered that involves the construction of one ring in the course of the synthetic protocol, two plus one aromatic ring have to be present in the starting materials already.

One route, involving tetracene-quinones as key intermediates has been examined in the course of my diploma thesis. It is briefly summarized here.[16]

Following the above mentioned 2+1+1 ring approach, it is possible to use a double aldol condensation between a hydroquinone and a dialdehyde. This synthesis, published by Lepage et al.[17] has been used to synthesize several differently substituted anthraquinones. One possibility leads to 2,3-naphthalene-dialdehyde (**52**) and 1,4-dihydroxy-2,3-dimethoxybenzene (**53**), as presented in the following scheme.

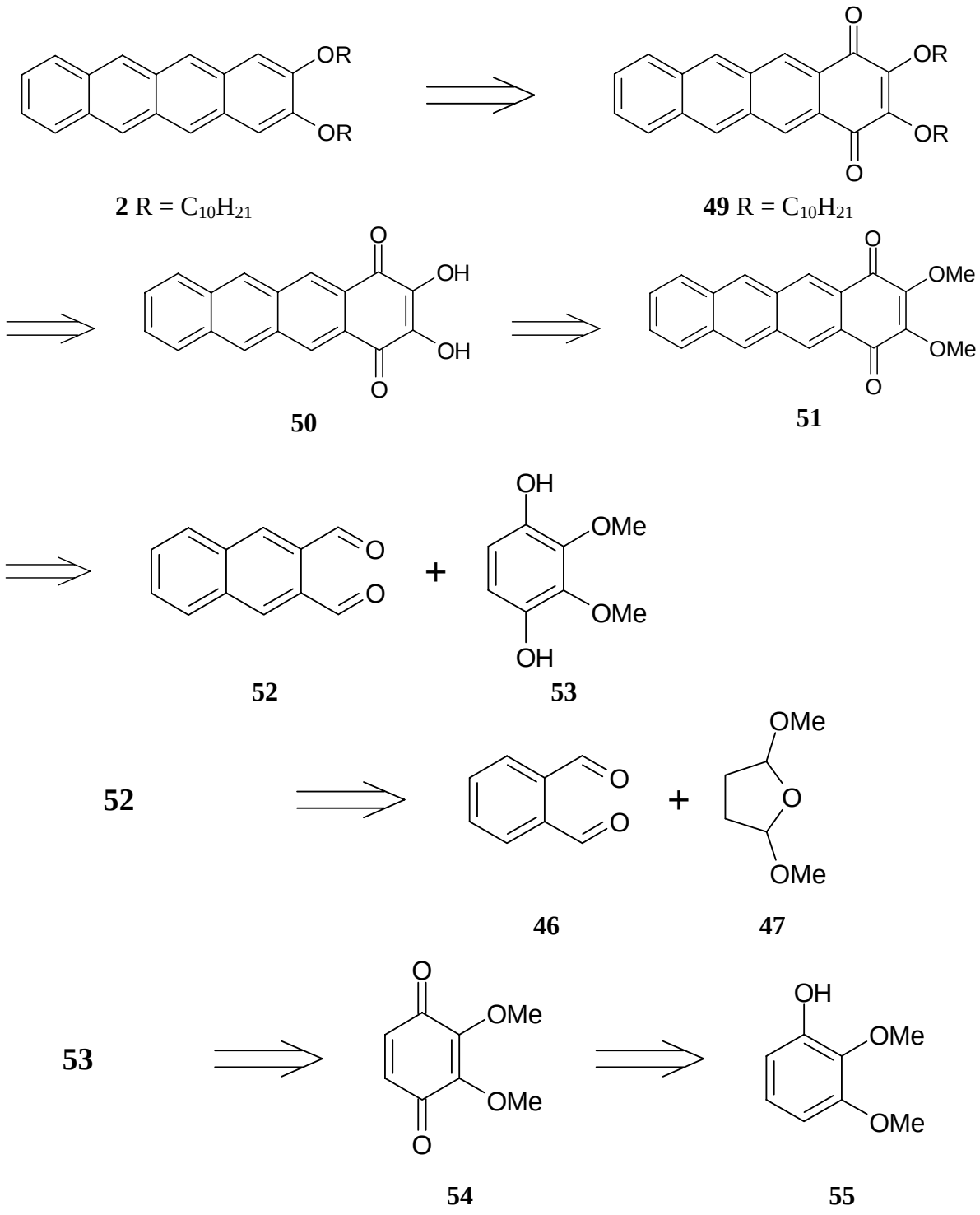

Scheme 8 **Retrosynthesis of 2,3-dialkoxy-tetracenes 2, aldol condensation pathway I**

The first step of the retrosynthesis comprises the functionalization of the tetracene core, leading to a substituted tetracene-1,4-quinone **49**. This intermediate can be further simplified by cleavage of the alkoxy-ethers, leading to the corresponding phenol **50**. The next two steps involve the retrosynthetical protection of the phenol and the cleavage of the tetracene-1,4-quinone, leading to the two main fragments, dialdehyde **52** and the substituted hydroquinone **53**.

Although it is possible to follow this pathway up to the 2,3-dialkoxy-tetracene-1,4-quinone **49** (yield 2% over 6 steps), the reduction of the quinone to the corresponding hydrocarbon failed, possibly due to the activation of the quinone system by the directly connected alkoxy functions.[16]

This set back led to the idea of investigating the "inverted approach", using phthalic-dialdehyde **46** and 1,4-dihydroxy-6,7-dimethoxy-naphthalene (**57**) as reactants for the aldol condensation.

2.4 Retrosynthesis of 2,3-dialkoxy-tetracenes (2) via aldol condensation, second approach

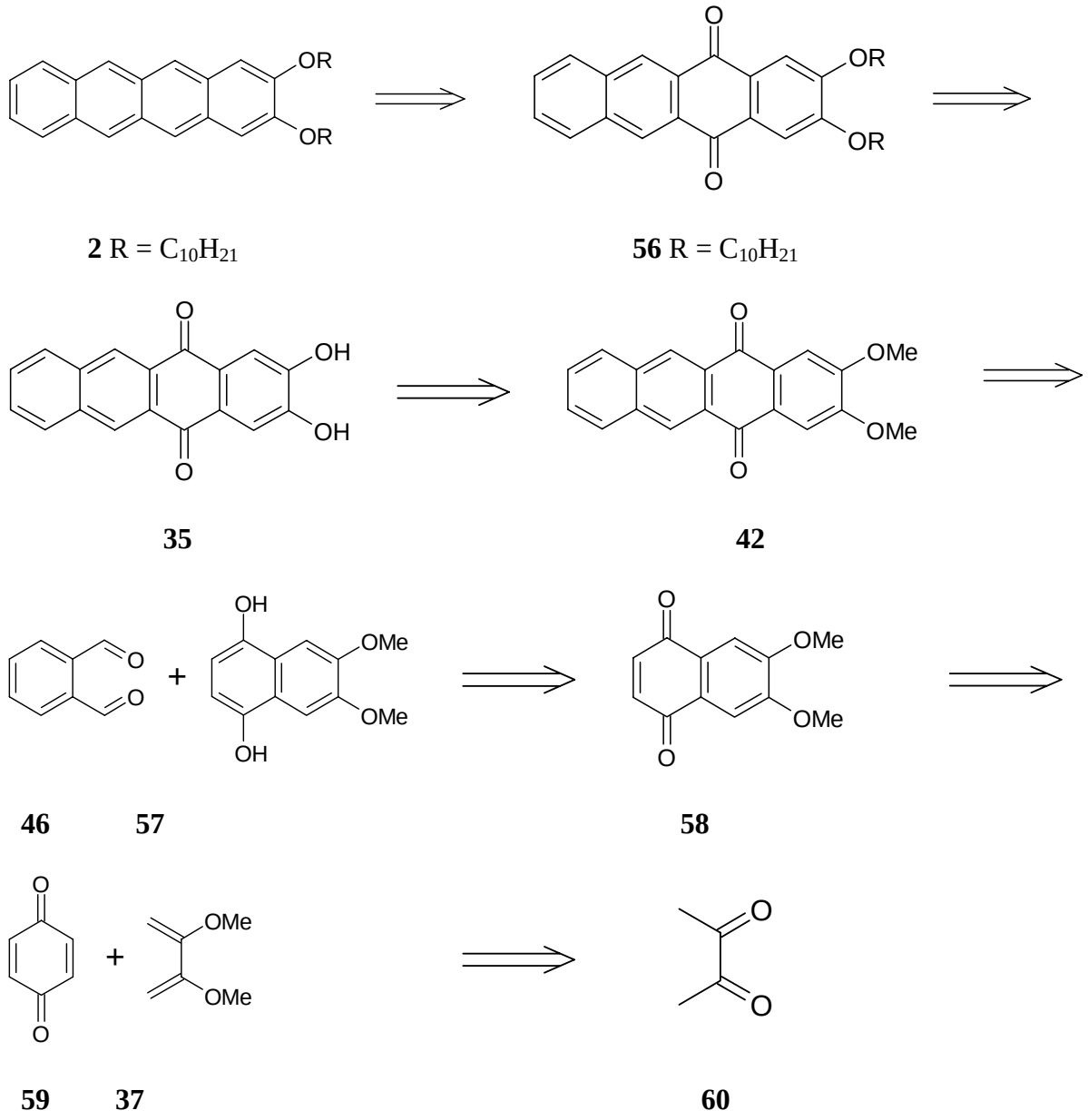

Scheme 9 **Retrosynthesis of 2,3-dialkoxy-tetracenes (2), aldol condensation pathway II**

The first step of the retrosynthesis is again the functionalization of the tetracene core, leading to the dialkoxy-tetracene-quinone **61**. Subsequently, the alkoxy chains are retrosynthetically converted to phenol-functions and those are protected as methoxy ethers.

The key step is the retrosynthesis of the tetracene ring system, now leading to a benzene fragment and a naphthalene fragment. Phthalic-dialdehyde (**46**) is commercially available. The naphthalene fragment, 1,4-dihydroxy-6,7-dimethoxy-naphthalene (**57**) is not, it is not even known in the literature. It can be derived from 6,7-dimethoxy-naphthoquinone (**58**), which can be transformed back to benzoquinone (**59**) and 2,3-dimethoxy-buta-1,3-diene (**37**), a commercially available and easy to synthesize compound. Following these ideas, the synthesis of differently substituted 2,3-dialkoxytetracenes (**2**) was possible and will be presented in detail in the following chapter.

2.5 Synthesis of 2,3-dialkoxy-tetracenes (2)

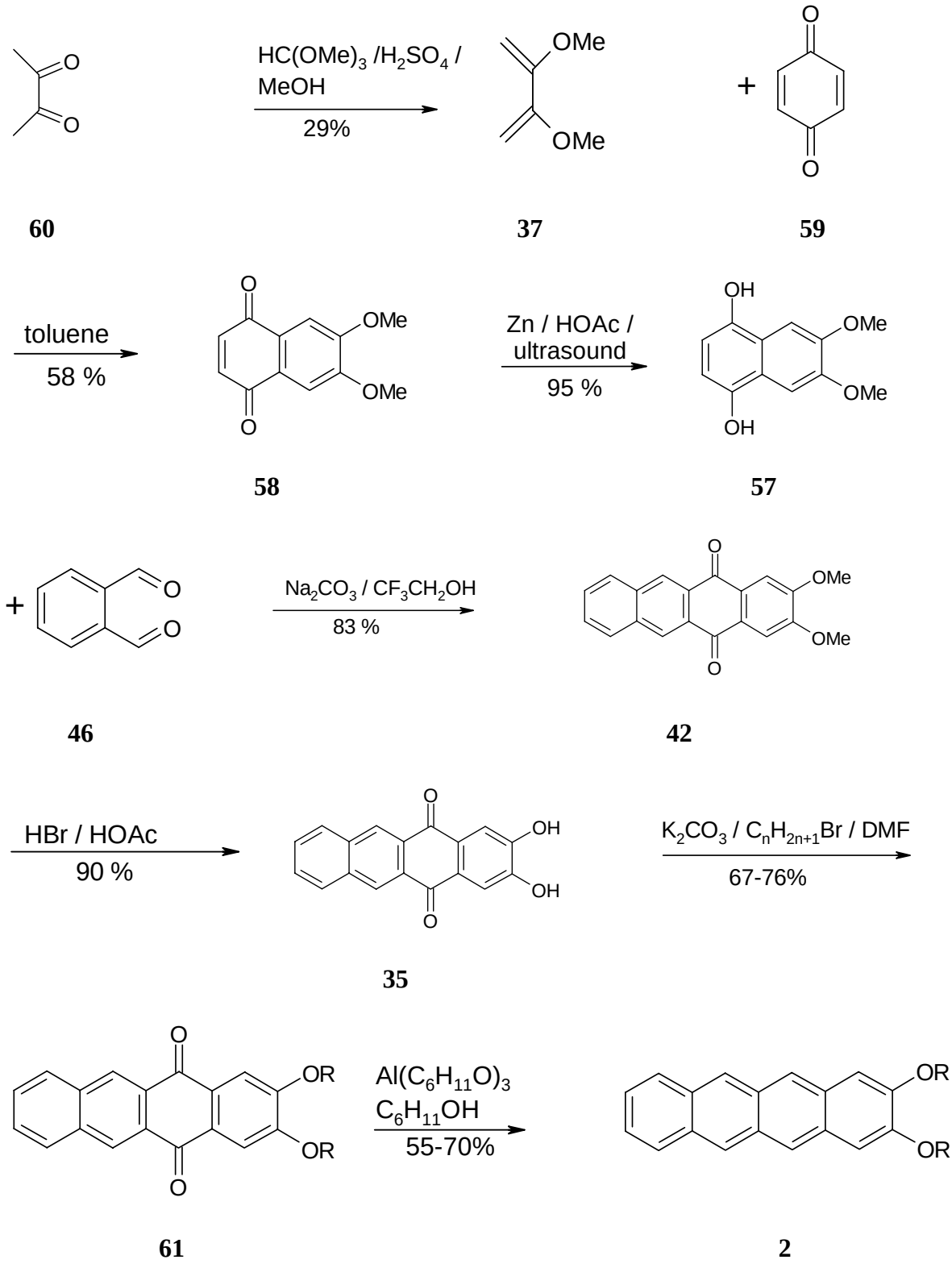

Scheme 10 **Synthesis of 2,3-dialkoxy-tetracenes (2) by aldol condensation**

2.5.1 Explanation of the individual synthetic steps

The different steps of the above shown synthesis will be presented in the order in which they were carried out. The spectroscopic data, especially of substances not described in the chemical literature, will be discussed.

2.5.1.1 2,3-Dimethoxy-buta-1,3-diene (37)

Even though 2,3-dimethoxy-1,3-butadiene (**37**) is a commercially available substance, it is easy to synthesize following the method described by Bouas-Laurent et al.[11] The only drawback is the problem of slow polymerization of the diene **37** during purification by distillation. Therefore a 90% purity (determined by gas chromatography) was considered to be acceptable and the compound was stored under an atmosphere of N_2 and at low temperatures prior to use (see Chapter 7.3.1.1).

2.5.1.2 6,7-Dimethoxy-1,4-naphthoquinone (58).

The synthesis of 6,7-dimethoxy-1,4-naphthoquinone (**58**) has first been published by Adams et al.[18] in 1941: 6,7-dimethoxy-naphthalene-1-ol was oxidized with $K_2Cr_2O_7$. One more recent synthetic approach is the TEMPO oxidation of 1,2-diethynyl-4,5-dimethoxybenzene, published by Grissom et al. in 1995.[19] In the course of this study, the Diels-Alder addition of 2,3-dimethoxy-buta-1,3-diene (**37**) to benzoquinone (**59**), published in 1996 by Zhang, Fox and Hadfield,[20] was chosen. Two problems, though, have to be faced. First of all, the dienophile is symmetrical, offering the possibility of double addition, which would lead to an anthraquinone system. Secondly, the primary adduct **62** would have to be oxidized to yield **58**.

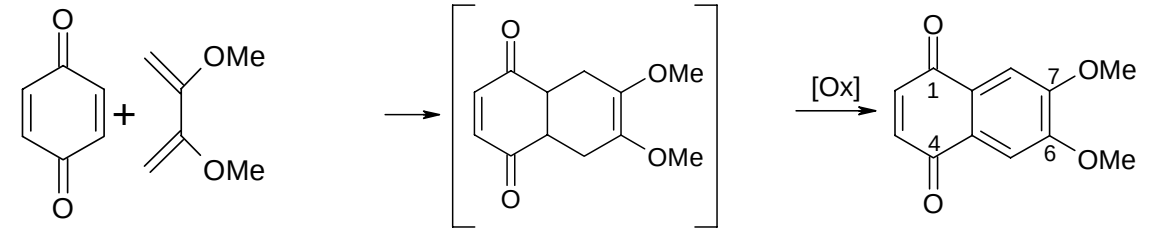

59 **37** **62** **58**

Scheme 11 **Diels Alder addition/oxidation to 6,7-dimethoxy-1,4-naphthoquinone (58)**

Both problems can be solved by using a threefold excess of **59**. This leads to the formation of the mono adduct and oxidation of the intermediate **62** to the desired product *in situ*. With this excess of benzoquinone, the yield of the reaction improves in comparison to the procedure given in the literature (33% [20]) to 58% (see Chapter 7.3.1.2).

In contrast to the given procedure, the addition was carried out in toluene and for the work-up recrystallization, rather than column chromatography, was used.

The structure of **58** was determined using HMBC and HSQC experiments, leading to the following correlation:

Entry	δ (H)	multiplicity	correlation
a	7.49	s	8/5-H
b	6.88	s	3/2-H
c	4.03	s	10/9-H

Table 1 **^{1}H NMR correlation of 58**

Entry	δ (C)	multiplicity	correlation	HSQC	HMBC
A	184.5	s	C-4/1	-	a,b
B	153.5	s	C-7/6	-	a,c
C	138.3	d	C-3/2	b	-
D	126.7	s	C-8a/4a	-	a
E	107.8	d	C-8/5	a	-
F	56.5	q	C-10/9	c	-

Table 2 **^{13}C NMR correlation of 58**

The structural assignment is further supported by the 70 eV mass spectrum, showing [M^+] at *m/z* = 218 and characteristic fragments at *m/z* = 203 and 188, deriving from a loss of one and two CH_3 fragments. The UV/Vis absorption spectrum is dominated by strong maxima at 208 and 268 nm, while the color of **58** is derived from two unstructured absorption maxima at 352 and 410 nm. The characteristic IR absorptions for the quinone system are 1655 (C=O) and 1584 (C=C), as well as 1254 cm^{-1} (aromatic ether).

2.5.1.3 Reduction of 6,7-dimethoxy-1,4-naphthoquinone (58)

As 1,4-dihydroxy-6,7-dimethoxy-naphthalene (**57**) has, until now, not been described in the literature, procedures for the reduction of other known naphthoquinones had to be used as guidelines. Classical conditions to reduce quinones to the corresponding hydroquinones have been known for a long time. Plimpton used tin and hydrochloric acid as early as 1880 to perform this reaction.[21] Other commonly used systems are hydrogen with Pd on charcoal (Laatsch et al.[22]) or sodium azide with hydrochloric acid (Papageorgiou et al.[23]). When the original work of Adams et al. is considered[18] 6,7-dimethoxy-naphtho-1,4-quinone (**58**) was in fact reduced, using Zn dust in acetic anhydride with acetic acid and sodium acetate. This procedure led to the formation of 1,4-diacetoxy-6,7-dimethoxy-naphthalene, an acylated form of the desired hydroquinone.

In the course of this work, the reduction of the naphthoquinone **58** to the corresponding hydroquinone was carried out, using Zn in acetic acid (without acetic anhydride) as reductant and ultrasound conditions to shorten reaction times. This procedure is adapted from the reduction of the unsubstituted 1,4-naphthoquinone (**36**) (see Chapter 7.3.4.1) published by Marchand et al. in 1991.[24]

The given procedure was chosen for the short reaction times and excellent yields that were reported (< 5 min and 100% for naphthoquinone (**36**)).[24]

While the reaction is generally fast (around 1.5 h, depending on the reaction scale) special care has to be taken during work-up to prevent reoxidation (see Chapter 7.3.1.3). Furthermore, it is worth to note that the reaction times differ largely with the quality of the Zn surface. The activation of the metal, using diluted hydrochloric acid and afterwards methanol and ether to dry the activated metal has advantages. For general synthetic procedures it is sufficient to remove the solvent after the completion of the reaction (detected by TLC) and use the crude product directly in the aldol condensation without further purification.

The structure of the product was assigned by comparison of the ^{1}H- and the ^{13}C NMR data with the one taken for the unsubstituted 1,4-dihydroxy-naphthalene (**95**) (see Chapter 7.3.4.1). This indirect approach had to be taken due to the reoxidation of **57** that complicates the measurement of multidimensional NMR spectra.

Further proof of the assigned structure derives from the 70 eV mass spectrum, showing [M^+] at *m/z* = 220 as well as from the IR spectrum, lacking the characteristic intense quinone-bands at 1655 (C=O) and 1584 cm^{-1} (C=C).

2.5.1.4 Condensation of 1,4-dihydroxy-6,7-dimethoxy-naphthalene (57) with phthalic dialdehyde (46).

The key step of the synthesis of 2,3-dialkoxy-tetracenes (**2**) is the aldol condensation of hydroquinone **57** with phthalic-dialdehyde **46** under basic conditions in trifluorethanol. Reactions of this type have been published by Serpaud and Lepage in 1977. They synthesized differently substituted polycyclic quinones and heterocyclic quinones.[17] The facile synthesis of tetracene-5,12-quinone (**94**) (see Chapter 7.3.4.2), used later in this work to synthesize 5,12-DDOT (**85**), has already been described. More recently, Martín et al. used the same approach to prepare *N*,*N*'-dicyanoquinonediimine for studies on electrically conducting charge transfer complexes.[25]

The reaction proceeds smoothly by refluxing the two starting compounds in the presence of sodium carbonate (see Chapter 7.3.1.4). The low solubility of the product drives the reaction and makes work-up easier. After the end of the reaction the mixture can be diluted with water to dissolve the sodium carbonate. The reaction leads to the key intermediate 2,3-dimethoxy-tetracene-5,12-quinone (**42**) in 83% yield.

The mechanism of the reaction can be assumed as follows: the hydroquinone **57** is deprotonated to the hydroquinonate **63**. This intermediate, from its carbanion resonance structure, attacks one of the aldehyde functions of **46** as a nucleophile. The resulting alcoholate is protonated to form the aldol adduct. This intermediate is not stable under the reaction conditions but eliminates directly (no intermediate can be detected by TLC monitoring of the reaction) to the aromatic quinone. Repetition of this sequence leads to the 2,3-dimethoxy-tetracene-5,12-quinone (**42**).

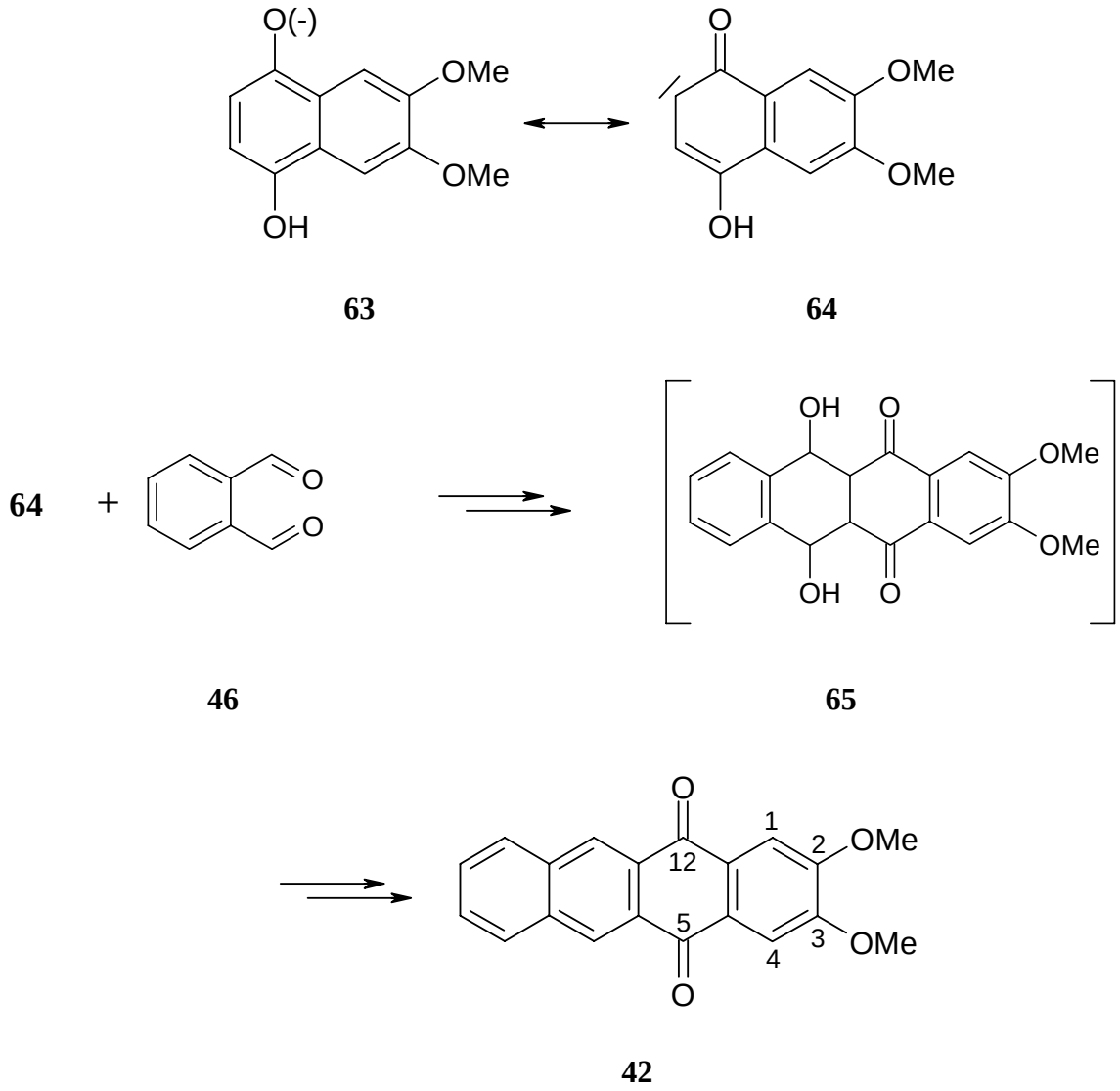

Scheme 12 **Aldol-condensation of 46 to 57 leading to 2,3-dimethoxy-tetracene-5,12-quinone (42)**

The structure of the tetracenequinone **42** was determined mainly by one- and two dimensional NMR spectra. The coupling constants of the signals 10/7-H and 9/8-H were calculated iteratively, the relative error of the calculation (R-factor) equals 0.46%. HSQC and HMBC experiments then provided the correlations shown in Table 3 and Table 4. As **42** is the parent system of all 2,3-dialkoxy-tetracene-5,12-quinones further synthesized in the course of this investigation, the ^{1}H and the ^{13}C NMR spectra are reproduced for a better understanding (see Figure 1 and Figure 2)

Entry	δ (H)	multiplicity	coupling (J or N [Hz])	correlation
a	8.78	s		11/6-H
b	8.08	m_c (AA'XX')	$^3J_{AX/A'X'}$ = 8.3 Hz $^4J_{AX'/A'X}$ = 1.2 Hz $^5J_{AA'}$ = 0.7 Hz $^3J_{XX'}$ = 6.9 Hz	10/7-H
c	7.77	s		4/1-H
d	7.68	m_c (AA'XX')	$^3J_{XA/X'A'}$ = 8.3 Hz $^4J_{X'A/XA'}$ = 1.2 Hz $^5J_{AA'}$ = 0.7 Hz $^3J_{XX'}$ = 6.9 Hz	9/8-H
e	4.08	s		14/13-H

Table 3 **^{1}H NMR correlation of 42**

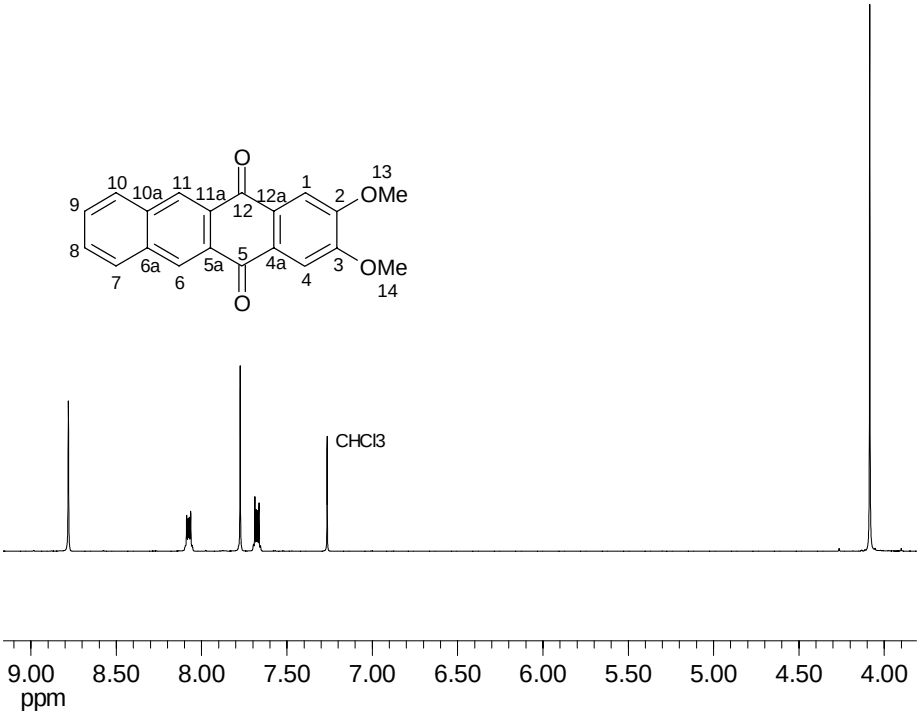

Figure 1 **^{1}H NMR spectrum of 42**

Entry	δ (C)	multiplicity	correlation	HSQC	HMBC
A	182.2	s	C-12/5	-	a,c
B	153.9	s	C-3/2	-	c,e
C	135.0	s	C-10a/6a	-	a,b,d
D	130.1	d	C-10/7	b	d
E	129.9	s	C-11a/5a	-	a
F	129.5	s	C-12a/4a	-	f
G	129.3	d	C-9/8	a	b
H	129.2	d	C-11/6	d	b
I	108.5	d	C-4/1	c	-
J	56.6	q	C-14/13	e	-

Table 4 **^{13}C NMR correlation of 42**

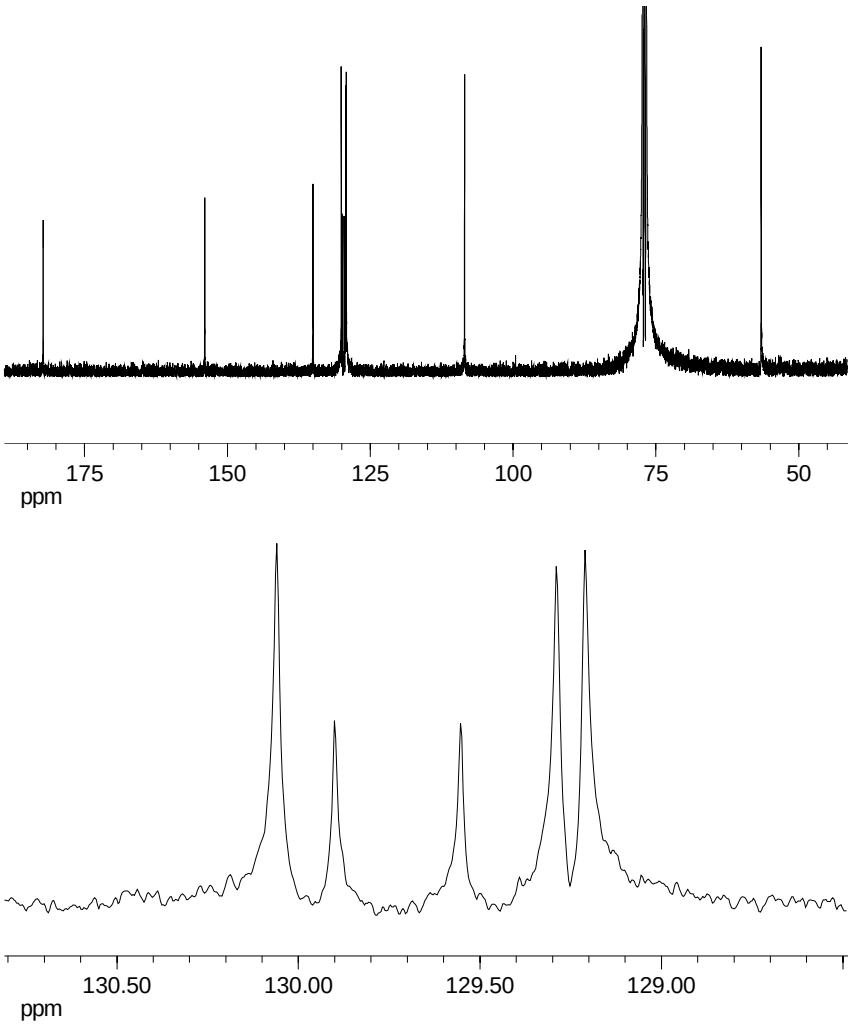

Figure 2 **^{13}C NMR spectrum of 42**

The ^{1}H NMR spectrum exhibits, next to the OCH_3-groups with δ = 4.08 ppm, two singlets (δ = 8.78 and 7.77) for the 11/6 and 4/1-H adjacent to the quinone system. 10/7 and 9/8-H are represented by a characteristic AA'XX' system with $\delta_{(center)}$ = 8.08 and 7.68 ppm. The lower field signal corresponds to the 10/7-H. This can be explained by the stronger deshielding of those protons which are near to the second ring of the naphthalene subsystem. Similar spectroscopic features can be found in all of the tetracenequinones, pentacene quinones and as well in the tetracenes and pentacenes (*vide infra*).

The ^{13}C NMR spectrum shows characteristic low-field signals for the quinone C=O (182.2 ppm) and the C(aryl)-OR (153.9 ppm). The lowest field quaternary carbon is C-6a/10a junction of the naphthalene subsystem, belonging to two aromatic rings. The signals D to H show only little difference in chemical shifts but are still resolved well enough to be assigned.

The structural assignment is further supported by the 70 eV mass spectrum (*m/z* = 318 for [M^+], loss of one CH_3-fragment leading to *m/z* = 303, loss of CO from that fragment leading to *m/z* = 275).

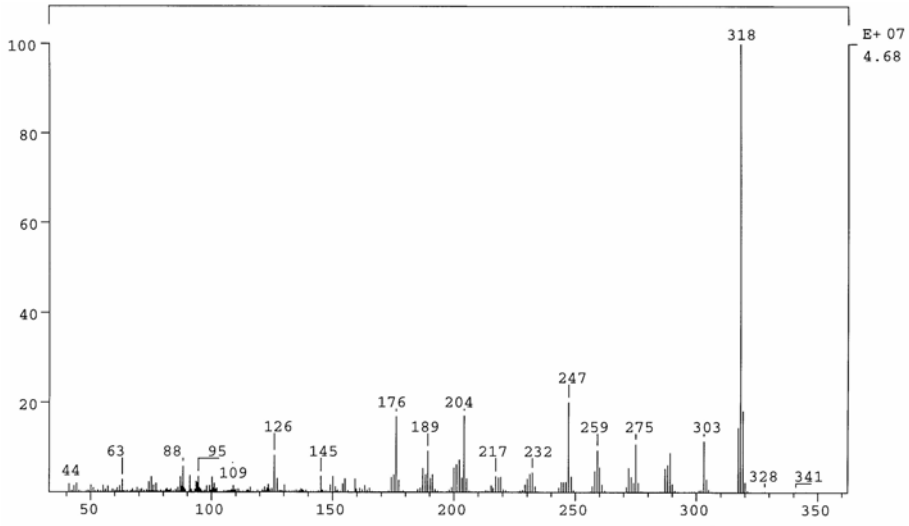

Figure 3 70 eV mass spectrum of 42

Characteristic IR absorptions originate from the quinone system, with 1666 (C=O) and 1579 (C=C), as well as 1252 cm^{-1} (aromatic ether). The UV spectrum shows intense absorptions in the far (204 and 236 nm) as well as in the near (298 nm) UV. The intense yellow orange color of **42** is caused by a broad absorption band at 386 nm.

2.5.1.5 Demethylation of 2,3-dimethoxy-tetracene-5,12-quinone (42).

The cleavage of aromatic methoxy ethers is a widely used synthetic step. Today the most commonly used reactant is BBr_3 in different solvents (DCM or hexane),[26] a mixture commercially available. Even though it is possible to demethylate 2,3-dimethoxy-tetracene-5,12-quinone (**42**) in this fashion, the reaction proceeds very slowly and leads to a mixture of unreacted starting material, the singly demethylated compound and only 10% of the desired product (after direct alkylation of the mixture, see Chapter 7.3.1.5.c). Other reported procedures rely on metal halides like NaI/SiI_4[27] or Lewis acids like AlI_3.[28]

Still, the classical procedure, using strong Broenstedt acids, is widely used. The procedure is only limited by the stability of the starting material and product under the harsh conditions (acidity and temperature). Reagents employed are reaching from HI (with various coreactants like acetic acid anhydride)[29] to mixtures of aqueous HBr with glacial acetic acid.[30] The demethylation is generally a S_N type reaction, where the strong acid activates the ether oxygen by protonation, and the acid anion attacks as the nucleophile at the methyl group. Another classical method is the use of the "protected" acid HCl as pyridine hydrochloride.[31] This offers the advantage of high reaction temperatures (the melting point of pyridine hydrochloride is around 150 °C) and the absence of free acid in a still strongly nucleophilic system.

In the course of this study three techniques of demethylation have been examined:

1) Demethylation by BBr_3

In the course of this study, the procedure failed, possibly due to the low solubility of the 2,3-dimethoxy-tetracene-5,12-quinone (**42**) even in DCM.

Even after several days of stirring a suspension of 2,3-dimethoxytetracene-5,12-quinone (**42**) in DCM with a solution of BBr_3 in DCM, only a minor part of the starting material was demethylated, as could be determined after alkylation (see Chapter 7.3.1.5.c).

2) Demethylation by HBr/HOAc

Due to the high reaction temperatures (48% HBr refluxing at 128 °C) and the simple reaction conditions (the starting material is suspended in HBr-solution and refluxed for several days), this procedure is well suited for reactions on a large scale (see Chapter 7.3.1.5.a).

The major drawback of this procedure is its two phase nature. It is nearly impossible to obtain fully deprotected 2,3-dihydroxy-tetracene-5,12-quinone (**35**). As the reaction mixture is only soluble in polar aprotic solvents like DMF or DMSO, a separation on this stage of the reaction path is not advisable. Separation and purification is accomplished on the stage of the 2,3-dialkoxy-tetracene-5,12-quinones (**61**) after alkylation of the crude mixture.

3) Demethylation by pyridine•HCl

The reaction of aromatic methyl ethers with pyridine•HCl (see Chapter 7.3.1.5.b) proceeds in principle by the same pathway as the demethylation using strong acids. Advantageous is the shorter reaction time (3 h with pyridine•HCl versus 48 h with HBr•HOAc). Disadvantageous is the availability of the pyridinium salt. It has either to be prepared under rigorously dried conditions or purchased and stored under Ar, as the salt is highly hygroscopic. The reaction proceeds smoothly under inert conditions leading to the demethylated product **35**. Again traces of the singly demethylated compound can be found due to the reaction in two phases (the starting material is not fully soluble in the molten mixture).

Thus both procedures, using HBr•HOAc or pyridine•HCl can be used in parallel with similar results.

The structure of 2,3-dihydroxy-tetracene-5,12-quinone (**35**) was determined, using one- and two dimensional NMR spectroscopy. The solvent chosen for the NMR spectra was DMSO-d_6, since **35** is only poorly soluble in $CDCl_3$.

Entry	δ (H)	multiplicity	coupling (*J* or *N* [Hz])	correlation
a	10.68	s (broad)		OH
b	8.68	s		11/6-H
c	8.21	m_c (AA'XX')	*N* = 9.4 Hz	10/7-H
d	7.73	m_c (AA'XX')	*N* = 9.5 Hz	9/8-H
e	7.57	s		4/1-H

Table 5 **^{1}H NMR correlation of 35**

N represents the sum of the coupling constants from the most low-field to the most high-field shifted signal of the AA'XX' or the AA'XX' signal.

Entry	δ (C)	multiplicity	correlation	HSQC	HMBC
A	183.3	s	C-12/5	-	b,e
B	151.8	s	C-3/2	-	e
C	134.4	s	C-10a/6a	-	b,c,d
D	130.0	d	C-10/7	c	b,d
E	129.8	s	C-11a/5a	-	b
F	129.4	d	C-9/8	d	c
G	128.4	d	C-11/6	b	c
H	128.0	s	C-12a/4a	-	e
I	113.1	d	C-4/1	e	-

Table 6 **^{13}C NMR correlation of 35**

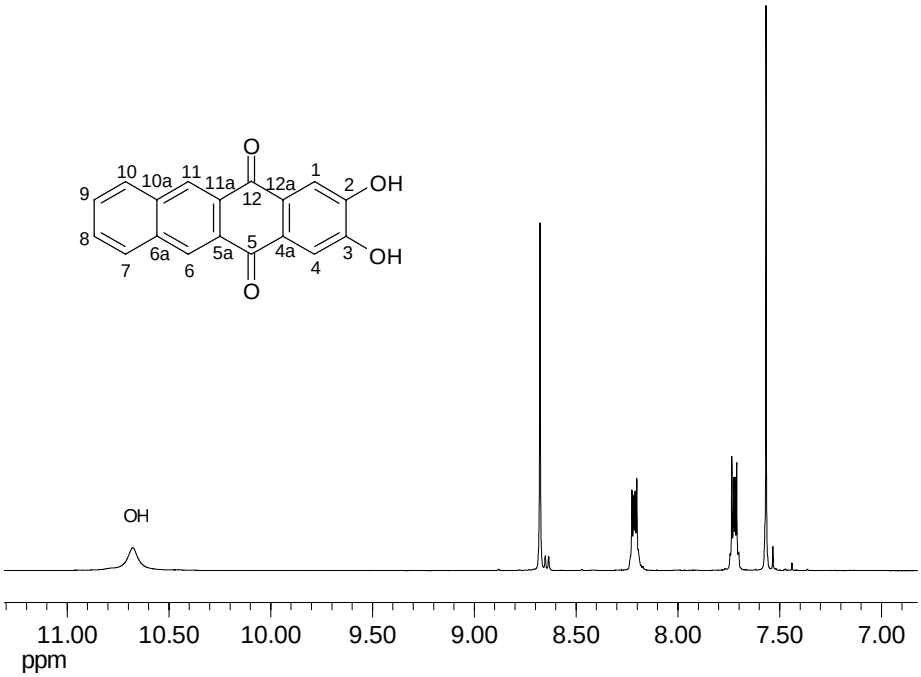

Figure 4 **^{1}H NMR spectrum of 35**

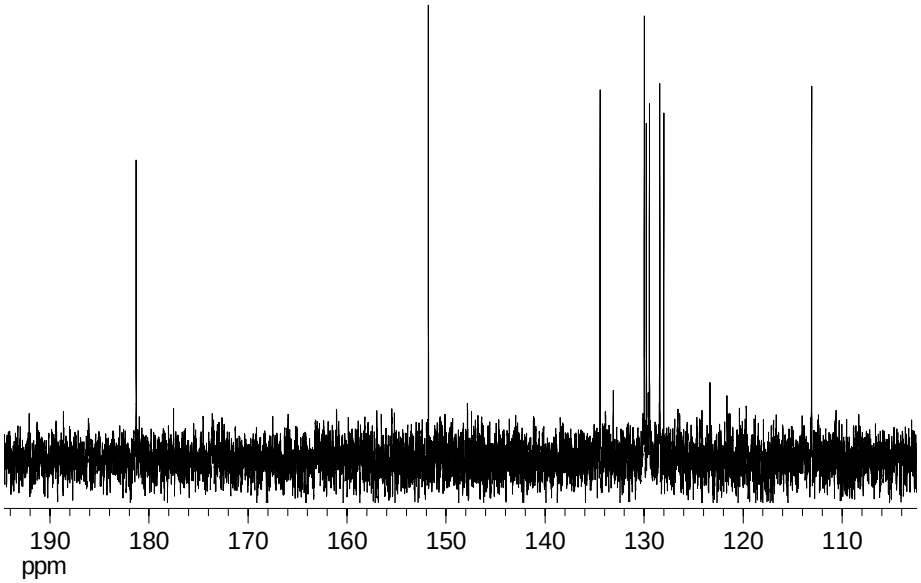

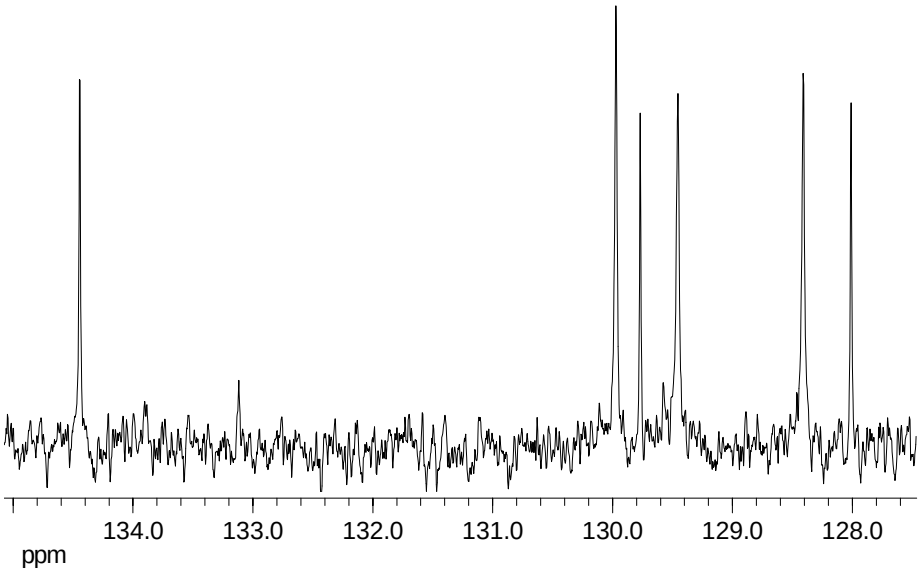

Figure 5 **^{13}C NMR spectrum of 35 (with magnification of C-10a/6a, 10/7, 11a/5a, 9/8, 11/6 and C-12a/4a)**

When the NMR-spectra of **35** are compared to those of **42** (precursor) or the alkylated products (see Chapter 2.5.1.6), characteristic differences are observed. It is interesting to note that the order of the signals for C-12a/4a, C-9/8 and C-11/6 changes from F,G,H in the methoxy quinone **42** and the alkoxy quinones **106** to **108** to H,F,G. Similarly, in the ^{1}H NMR spectrum of **35**, 4/1-H and 9/8-H change the order of appearance relatively to the alkylated species.

Further evidence of the assigned structure is provided by the 70 eV mass spectrum, showing [M^{+}] at *m/z* = 290 and characteristic fragments at *m/z* = 262 and 234 resulting from the loss of one and two CO fragments. The signal at *m/z* = 304 can be assigned to traces of the partially demethylated side product that can not be separated from the main product at this stage of the synthesis.

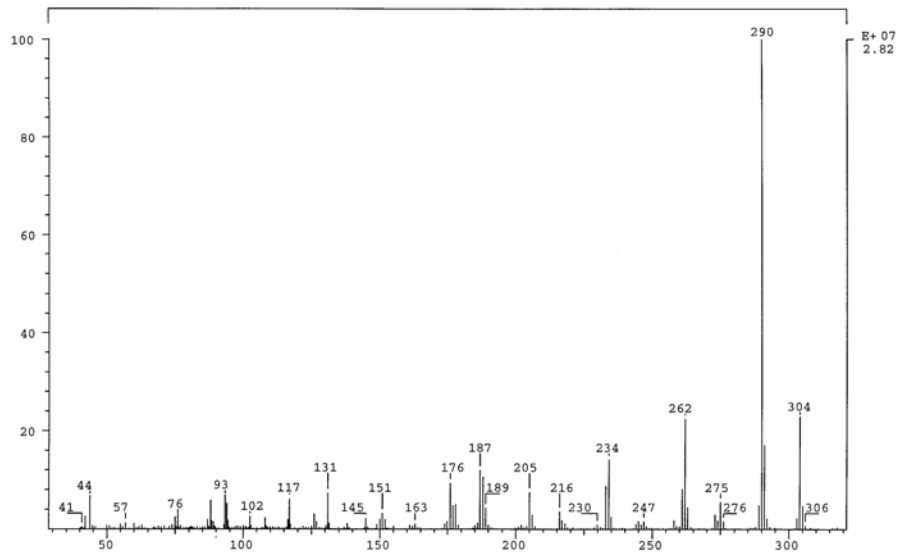

Figure 6 70 eV mass spectrum of 35

The IR data are in good agreement with the proposed structure, showing the quinone C=O/ C=C system at 1670 and 1575 cm^{-1}, while the aromatic methoxy ether absorption at 1252 cm^{-1} is missing. A strong band at 3270 cm^{-1} can be assigned to the OH-absorption of the phenol. The UV/Vis absorption spectrum shows the same strong UV absorption at 298 nm as the starting material, while the change in color (from yellow-orange to green) can be explained by the bathochromic shift of the visible absorption to 536 nm.

2.5.1.6 Alkylation of 2,3-dihydroxy-tetracene-5,12-quinone (35)

After the deprotection of **42**, the reaction path is followed by alkylation of the free phenolic OH functions.

Like the cleavage of methyl-phenyl ethers, this is a widely used synthetic step. The reaction is a variation of the classical Williamson ether synthesis,[32] known since the late 19th century. Since phenols are relatively acidic, a weak base, often K_2CO_3, suffices to deprotonate them. From the variety of possible solvents (acetone, THF or DMF) only DMF is used, due to the poor solubility of the 2,3-dihydroxy-tetracene-5,12-quinone (**35**). The alkylation is carried out with four different *n*-alkyl-bromides (*n*-butyl-bromide, *n*-hexyl-bromide, *n*-decyl-bromide and *n*-hexadecyl-bromide). The yields are generally good (67% for C_4H_9Br to 71% for $C_{16}H_{33}Br$, see Chapter 7.3.1.6 to 7.3.1.9).

As the demethylation is often not carried out with full conversion of the starting material, it is possible to separate unreacted 2,3-dimethoxy-tetracene-5,12-quinone (**42**) and partially demethylated/realkylated side product from the desired 2,3-dialkoxy-tetracene-5,12-quinones **61** by column chromatography on silica using DCM/pentane as a mobile phase.

As usual the structures of the four alkoxy-tetracene-quinones were assigned by ^{1}H- and ^{13}C NMR spectroscopy, the spectroscopic data of the 2,3-dihexyloxy-tetracene-5,12-quinone **107** is presented as an example.

Entry	δ (H)	multiplicity	coupling (*J* or *N* [Hz])	correlation
a	8.77	s		11/6-H
b	8.07	m_c (AA'XX')	*N* = 9.5 Hz	10/7-H
c	7.74	s		4/1-H
d	7.66	m_c (AA'XX')	*N* = 9.5 Hz	9/8-H
e	4,21	t	^{3}J = 6.7 Hz	19/13-H
f	1.94-1.87	m		chain
g	1.59-1.49	m		chain
h	1.43-1.32	m		chain
i	0.94-0.91	m		24/18-H

Table 7 **^{1}H NMR correlation of 107**

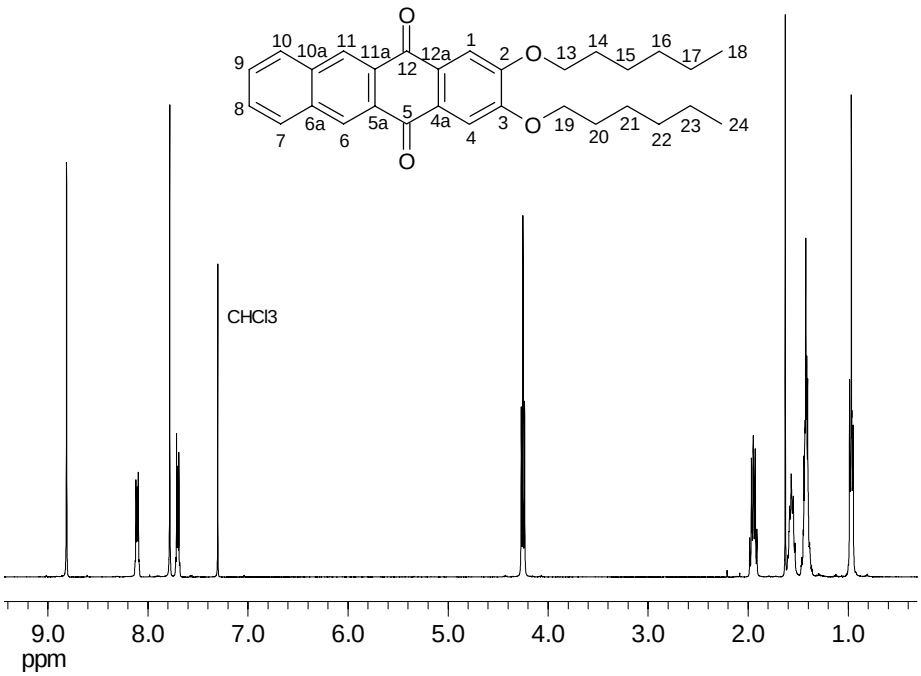

Figure 7 **^{1}H NMR spectrum of 107**

As the ^{13}C NMR signals D,E and F,G,H are very close ($\Delta\delta$=0.036 ppm and 0.051/ 0.094 ppm), HSQC and HMBC spectra were recorded for the quinone **107** and **108**, both leading to the same result. Especially the ^{13}C NMR signals D and E were assigned by comparison of the DEPT spectra. The alkoxy quinones **106** and **56** were assigned by comparison with those results and no deliberate HSQC and HMBC spectra were measured.

Entry	δ (C)	multiplicity	correlation	HSQC	HMBC
A	182.4	s	C-12/5	-	a,c
B	153.9	s	C-3/2	-	c,e
C	135.0	s	C-10a/6a	-	a,b,d
D	130.04	s	C-11a/5a	-	a
E	130.02	d	C-10/7	b	a,d
F	129.22	s	C-12a/4a	-	c
G	129.17	d	C-9/8	d	b
H	129.1	d	C-11/6	a	b
I	109.4	d	C-4/1	c	-
J	69.4	t	C-19/13	e	f
K-N	31.5-22.6	t	chain	-	-
O	14.0	q	C-24/18	i	h

Table 8 **^{13}C NMR correlation of 107**

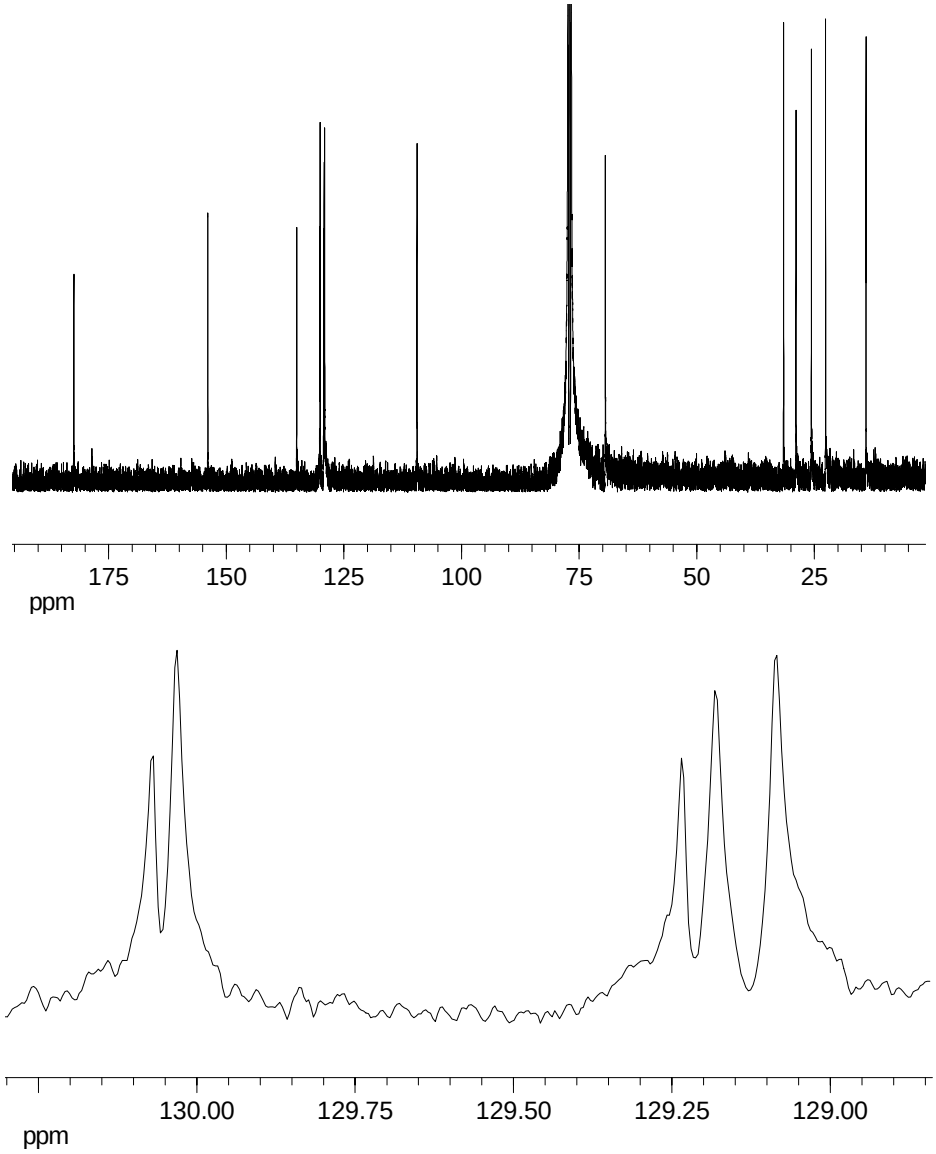

Figure 8 **^{13}C NMR spectrum of 107 with amplification of C-11a/5a, 10/7, 12a/4a, 9/8 and C-11/6**

70 eV mass spectroscopy gives the answer regarding the degree of alkylation. NMR-spectroscopy does not offer results of the same quality, as ^{13}C NMR signals tend to show equal chemical shifts in the case of **56** and **108** and the calculation of the chain length, using the ^{1}H NMR integrals becomes less reliable with the number of H-atoms.

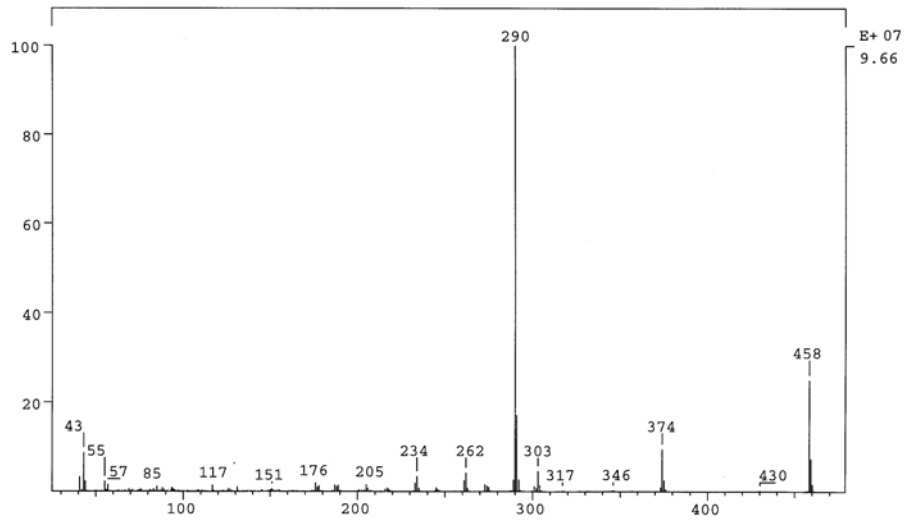

Figure 9 **70 eV mass spectrum of 107**

The fragmentation of all the 2,3-dialkoxy-tetracene-5,12-quinones (**42**, see Chapter 7.3.1.4, as well as **106**, **107**, **56** and **108**, see Chapters 7.3.1.6-7.3.1.9) is very similar. The most intensive signals are the [M^+] (*m/z* = 318, 402, 458, 570 and 738) and the fragments resulting from the cleavage one and two C_nH_{2n} chains (*m/z* = 303, 346, 374, 430, 514 and 289, 290). When the UV spectra of the different alkoxy tetracene-quinones are compared, only small differences can be observed.

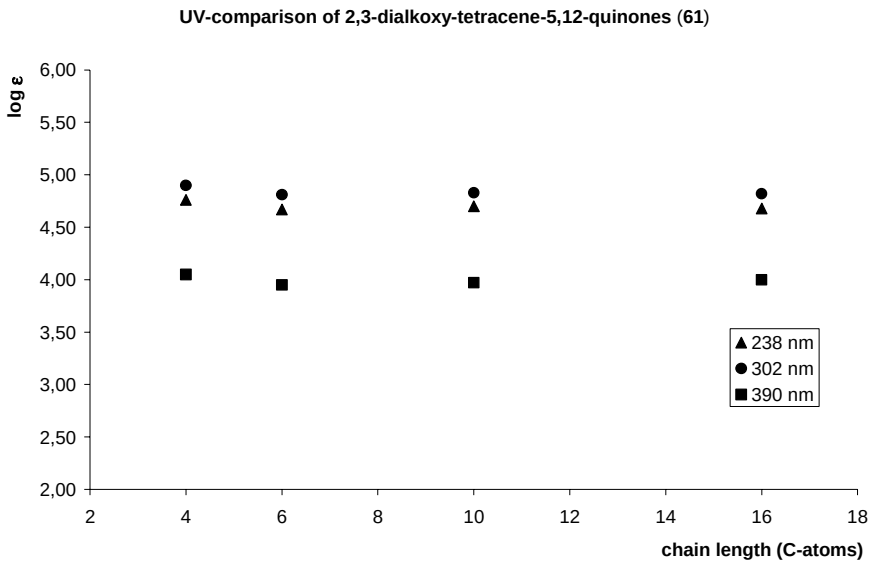

Figure 10 **Comparison of the UV-data of 2,3-dialkoxy tetracene-5,12-quinones (61)**

The spectra show three main absorptions, the most intense at 238 nm, while the yellow color of the tetracene-quinones can be explained by the broad unstructured absorption at 390 nm.

The IR spectra of the different 2,3-dialkoxy-tetracene-5,12-quinones **61** are also quite similar to each other, only the intensity of CH_2-vibrations between 2949 and 2847 cm^{-1} is increasing with chain length, as expected.

2.5.1.7 Reduction of 2,3-dialkoxy-tetracene-5,12-quinones (61)

The last step of the described sequence is the reduction of the 2,3-dialkoxy-tetracene-5,12-quinones (**61**) to the corresponding 2,3-dialkoxy-tetracenes (**2**).

The reduction of different 9,10-anthraquinones to the corresponding anthracenes has long been known. A commonly used system is Zn dust in concentrated ammonia solution. This reaction has already been published in 1905 by Lagodzinski.[33] The same procedure is still used, especially with Zn that has been activated by $CuSO_4$ (Diederich et al.)[34] Only the extremely poor solubility of the tetracene quinones, and even more of the pentacene quinones (see Chapter 2.8.1.2) prevented the application of this easy to carry out and cheap reduction procedure.

Modern reduction reagents like $NaBH_4$[35] react under milder reaction conditions and provide better yields but are generally carried out in solvents like 2-propanol or THF. Both solvents do not solubilize the 2,3-dialkoxy-tetracene-5,12-quinones **61**, offering only a remote chance of reaction in contrast to the reduction of 2,3-didecyloxy-9,10-anthraquinone (**8**) that can be reduced by $NaBH_4$ in 2-propanol.[11]

These problems kept in mind, a variation of the Meerwein-Ponndorf-Verley (MPV) reduction was used.[36] The classical Meerwein-Ponndorf-Verley reduction was published in 1925 and 1926[37, 38]. It has nowadays generally been replaced by hydride reduction ($NaBH_4$, $LiAlH_4$) when the conversion of carbonyl functions into alcohols is considered. Still a valuable tool of modern chemistry is the variation of the MPV reduction using cyclohexyl alumina alkoxide ($Al(OC_6H_{11})_3$) in cyclohexanol for the reduction of quinones to the corresponding aromatic hydrocarbons under mild conditions. The only limit of this reaction is the relatively high temperature applied preventing the use of the MPV process for temperature sensitive compounds. Current examples of the application are the reduction of anthraquinones to anthracenes, published in 1994 by Müllen et al.,[39] or the reduction of tetrachloropentacenequinone to tetrachloropentacene, presented in 2003 by Wudl et al.[40]

The reaction proceeds via a six-membered transition state **68** between the alumina alkoxides and the ketone (or quinone) to be reduced. After the cleavage of this intermediate, the alcohol forming the alkoxide is obtained as the ketone, while the original carbonyl-function is reduced. The driving force of the classical MPV reduction is the removal of the resulting acetone (from *iso*-propanol) by distillation, pushing the equilibrium towards the product.

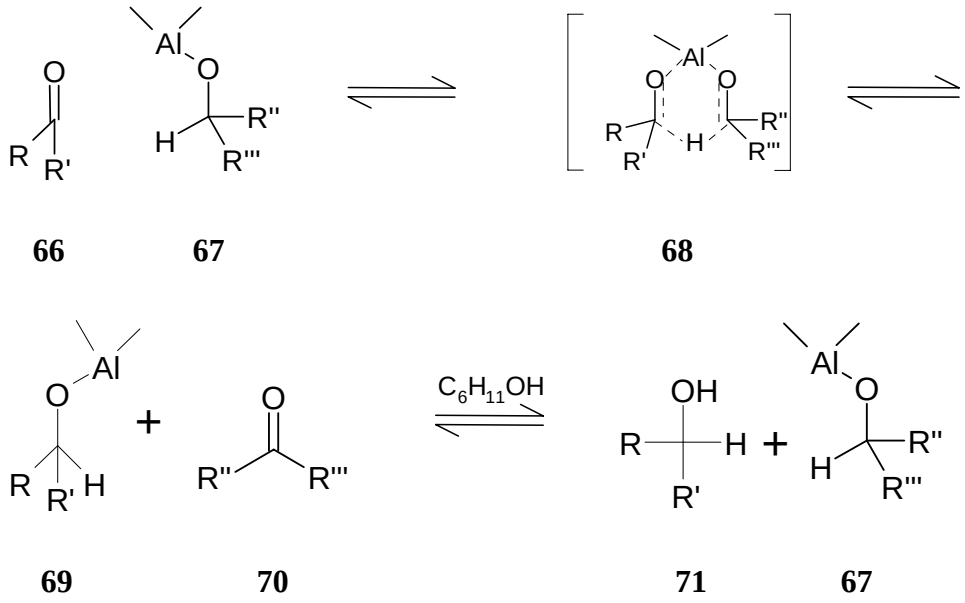

66 **67** **68**

69 **70** **71** **67**

Scheme 13 **Mechanism of the Meerwein-Ponndorf-Verley (MPV) reduction**

In the modern version of the MPV reduction, using the alkoxide of cyclohexanol instead of $Al(O^iPr)_3$, the driving force is different.

The high boiling point of the cyclohexanol (162 °C) leads to the *in situ* elimination of water of the intermediate **71**, a hydroquinone in the case of the quinone reduction. Hence, the aromatic hydrocarbon is obtained directly and the aromatization is the driving force of the reduction.

A specific advantage of the MPV reduction in the present study is the suppression of gel formation that begins with the 2,3-dialkoxy-tetracene-quinones if they are substituted with long chains.

The reaction conditions have to be slightly adopted to the different chain-length of the 2,3-dialkoxy-tetracene-5,12-quinones **61**. As the degradation of the tetracene starts to become more pronounced with the higher solubility of the C-16 tetracenes, careful TLC monitoring is necessary to prevent on the one hand a drop in reaction yield, on the other the presence of unreacted quinone that is not easy to separate from the desired product.

The 2,3-dialkoxy-tetracenes **2** can be further purified by recrystallization from ethyl acetate under addition of methanol to prevent the formation of gels, as those gels include large amounts of solvent and impurities.

The NMR spectra of the 2,3-dialkoxy-tetracenes **2** were assigned, using the HSQC and HMBC data of the 2,3-dibutoxy-tetracene (**109**). The correct order of the C-atoms in the chain can not be assigned, since usually the HMBC experiment shows coupling via 2 or 3 bonds. The coupling constants for the AA'XX'-spin system were, again, calculated by iterative methods, using the WinDAISY software. The relative error of the calculation (R-factor) equals 0.75%. Unlike in the case of the tetracene-quinones, the $\Delta\delta$ values of the aromatic ^{13}C-signals are large enough (more than 1.0 ppm) to assign the other alkoxy tetracenes by comparison, using only one alkoxy tetracene, **109**, as reference. This substance was chosen, because of the acceptable solubility and the lack of gel-formation even in a saturated solution.

Entry	δ (H)	multiplicity	coupling (J or N [Hz])	correlation
a	8.52	s		11/6-H
b	8.37	s		12/5-H
c	7.95	m_c (AA'XX')	$^3J_{AX/A'X'}$ = 8.7 Hz $^4J_{AX'/A'X}$ = 1.2 Hz $^5J_{AA'}$ = 0.9 Hz $^3J_{XX'}$ = 6.5 Hz	10/7-H
d	7.35	m_c (AA'XX')	$^3J_{XA/X'A'}$ = 8.7 Hz $^4J_{X'A/XA'}$ = 1.2 Hz $^5J_{AA'}$ = 0.9 Hz $^3J_{XX'}$ = 6.5 Hz	9/8-H
e	7.13	s		4/1-H
f	4.16	t	^3J = 6.6 Hz	17/13-H
g	1.96-1.89	m		chain
h	1.63-1.54	m		chain
i	1.01	t	^3J = 7.4 Hz	20/16-H

Table 9 **^{1}H NMR correlation of 109**

Entry	δ (C)	multiplicity	correlation	HSQC	HMBC
A	150.3	s	C-3/2	-	e,f
B	131.0	s	C-10a/6a	-	a,c
C	129.7	s	C-11a/5a	-	a,b
D	129.1	s	C-12a/4a	-	b,e
E	128.2	d	C-10/7	c	a
F	125.4	d	C-11/6	a	b
G	124.6	d	C-9/8	d	c
H	123.3	d	C-12/5	b	a,e
I	105.3	d	C-4/1	e	b
J	68.5	t	C-17/13	f	g,h
K	31.1	t	chain	g	f,h,i
L	19.4	t	chain	h	f,g,i
M	13.9	q	C-20/16	i	g,h

Table 10 **^{13}C NMR correlation of 109**

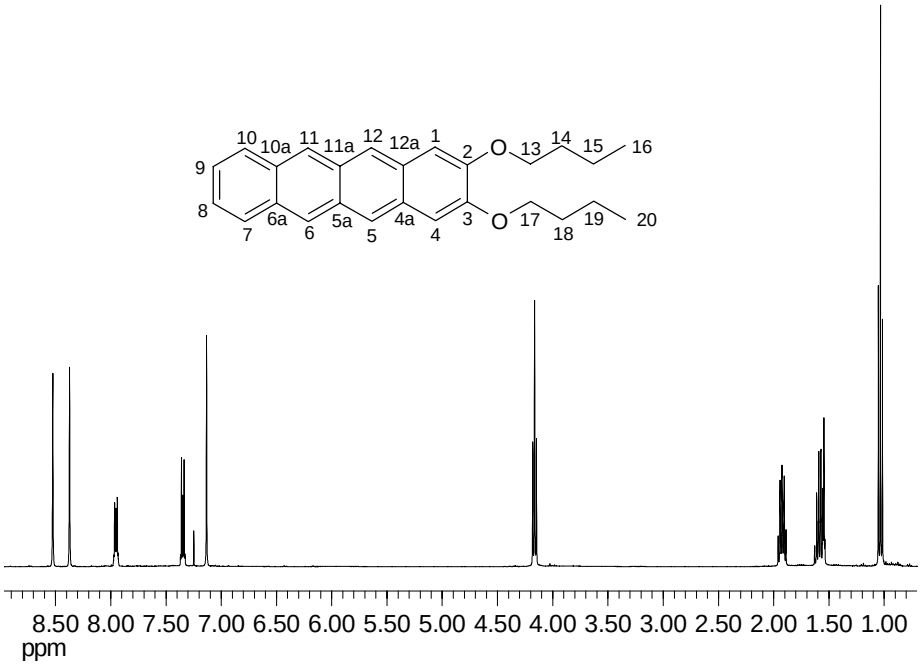

Figure 11 **^{1}H NMR spectrum of 109**

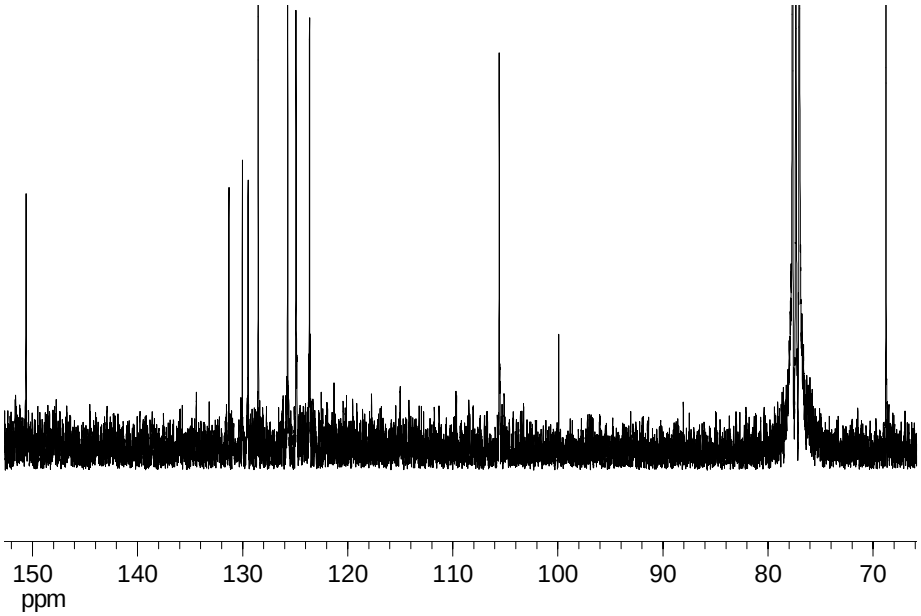

Figure 12 **^{13}C NMR spectrum of 109 (aromatic part including C-17/13)**

Further evidence of the structures derives from the 70 eV mass spectrum. The differently substituted tetracenes all show a very similar fragmentation. It is explained for the case of the 2,3-dibutoxy-tetracene (**109**).

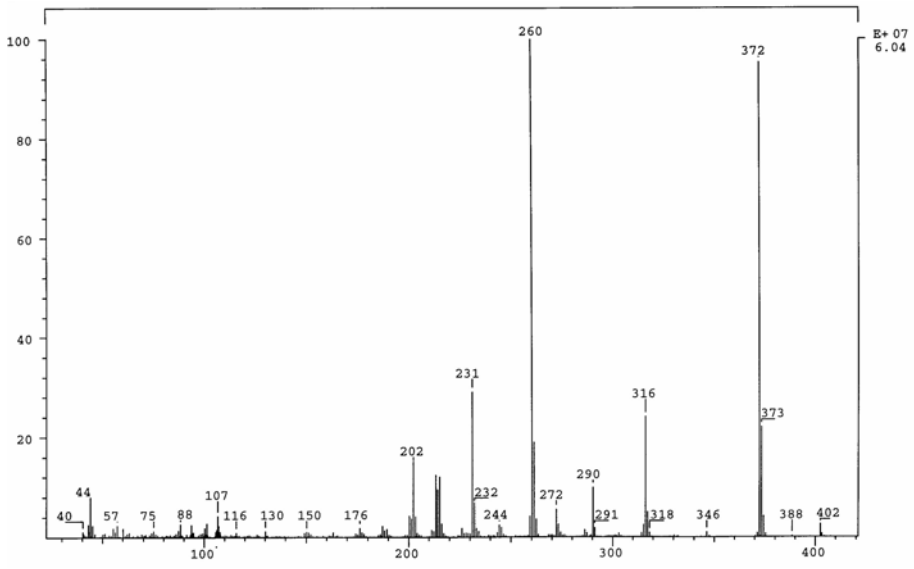

Figure 13 **70 eV mass spectrum of 109**

The two most intense signals derive from [M^+] at *m/z* = 372 and a fragment with *m/z* = 260 which can be explained by the loss of two C_4H_8 groups. This last fragment is characteristic, as it can be observed in all the mass spectra of 2,3-dialkoxy substituted tetracenes (see Chapter 7.3.1.11-7.3.1.14).

Like in the case of the 2,3-dialkoxy-tetracene-quinones **61** (see Chapter 2.5.1.6), the UV-spectra of the differently substituted 2,3-dialkoxy-tetracenes **2** are very similar. This is shown in the Figure 14 and explainable by the similarity of the chromophore.

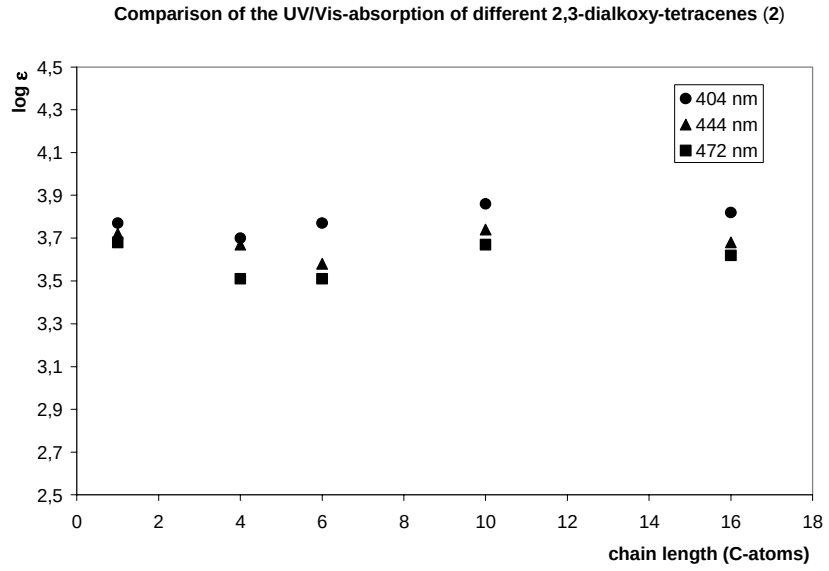

Figure 14 UV/Vis comparison of differently substituted 2,3-dialkoxy-tetracenes 2

The IR-spectra of the different tetracenes are also again similar, with only the CH_2-vibrational bands in the area of 2900 cm^{-1} increasing in intensity with the chain length.

2.5.2 Variations of the synthesis

To have a more versatile approach to substituted tetracenes (especially when reducible groups are considered), it was tried to deprotect and alkylate the tetracene core at the end of the synthesis, rather than reducing the tetracene-quinones in the last step.

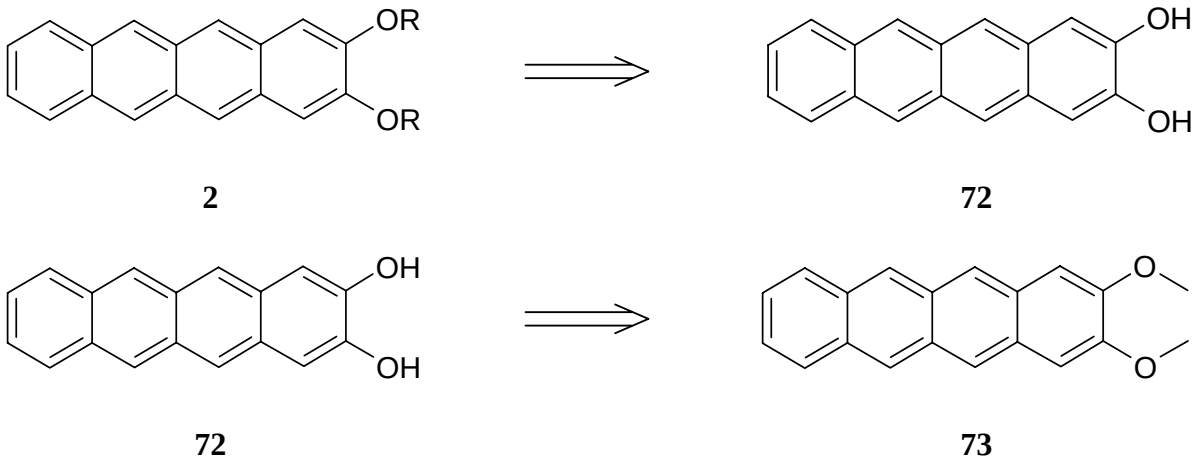

Scheme 14 Retrosynthesis of 2 via 2,3-dihydroxy-tetracene (72)

As reported in the overview of LMMOGs (see above), many structures of acene gelators are known, not containing simple alkoxy chains. To adopt the synthesis presented here, substituents should be attached as late as possible in the synthesis. This prevents incompatibilities of the substituents with the reduction procedure of the tetracene-quinone core and shortens the preparative effort when a large number of differently substituted tetracenes has to be synthesized.

A possible intermediate would be 2,3-dihydroxy-tetracene (**72**), substituted in the following synthesis. Hence the possibility to demethylate 2,3-dimethoxy-tetracene (**73**) was examined.

Of the three demethylation reactions used throughout the course of this work, only the demethylation with BBr_3 and the demethylation with pyridine/HCl were examined, as the reaction with HBr under atmospheric conditions seemed inappropriate, due to the instability of tetracenes towards oxygen.

Generally, the reaction mixture of the demethylation was not examined directly by NMR spectroscopy but alkylated using $C_6H_{13}Br$ or $C_{10}H_{21}Br$ under standard conditions (see Chapter 7.3.1.14.1). The resulting mixture was separated by column chromatography and the degree of demethylation was determined based on this result.

Even by variation of the reaction conditions (solvent, temperature and inert atmosphere), the yield of the desired 2,3-dialkoxy-tetracene **2** could not be improved beyond 16% (see Chapter 7.3.1.14.1) by using BBr_3, even if Nuckolls et al. used the approach to demethylate 2,3-dimethoxy-tetracene (**73**) with BBr_3 in investigations of semiconductor effects of 2,3-dihydroxy-tetracene (**72**) on aluminum oxide surfaces.[41] When pyridine•HCl was used at different temperatures, either no reaction took place or the starting material was destroyed (see Chapter 7.3.1.14.2).

Until now, no competitive strategy to the alkylation of 2,3-dihydroxy-tetracene-quinone (**35**) and reduction of the yielding 2,3-dialkoxy-tetracene-quinones **61** could be found. Still, by demethylation of 2,3-dimethoxy-tetracene (**73**), 2,3-dihydroxy-tetracene (**2**) could be synthesized even if it has not been isolated in substance as published by Nuckolls et al.[41]

2.6 Synthesis of gel forming pentacenes

2.6.1 Introduction

Since 2,3-DDOA **1** is not unique as a gel-forming acene (see Chapter 3) but only the lowest homologue of a class of gel-forming substances, it is of principal interest to see, how far the acene system can be extended, while gel formation is still possible. So the attempt to prepare gel forming pentacenes is a logical step.

But there are further reasons to enlarge the synthetic principle presented in the previous chapter.

During the last few years, pentacene has attracted much interest as component in organic thin film transistors (OTFTs).[42, 43] The main problem is the poor solubility that only allows for vacuum deposition of the acene. Two concepts are used to circumvent this drawback. First the thermoreversible Diels-Alder addition/ reversion proposed by Dehaen et al. or Afzali et al.[42, 43] The second approach lies in the use of substituted pentacenes as presented by Anthony et al. or Suzuki et al.[44, 45] to change solubility and electronic properties of the pentacenes.

This dual interest, possible formation of gel forming pentacenes and improvement of the solubility for the possible application in OTFTs, led to the extension of the already successful synthesis of 2,3-alkoxy-tetracenes **2** to the corresponding pentacenes **74**.

2.7 Retrosynthesis of 2,3-dialkoxypentacenes (**74**)

When 2,3-dialkoxy-pentacenes **74** are retrosynthetically examined like the corresponding 2,3-dialkoxy-tetracenes **2** (see Chapter 2.4), the best cleavage is the one leading to two naphthalene subunits. A further advantage is the application of known starting materials, such as naphthalene-2,3-dialdehyde (**52**) and hydroquinone **57**, rather than finding a synthetic path towards a corresponding 1,4-dihydroxy-anthracene.

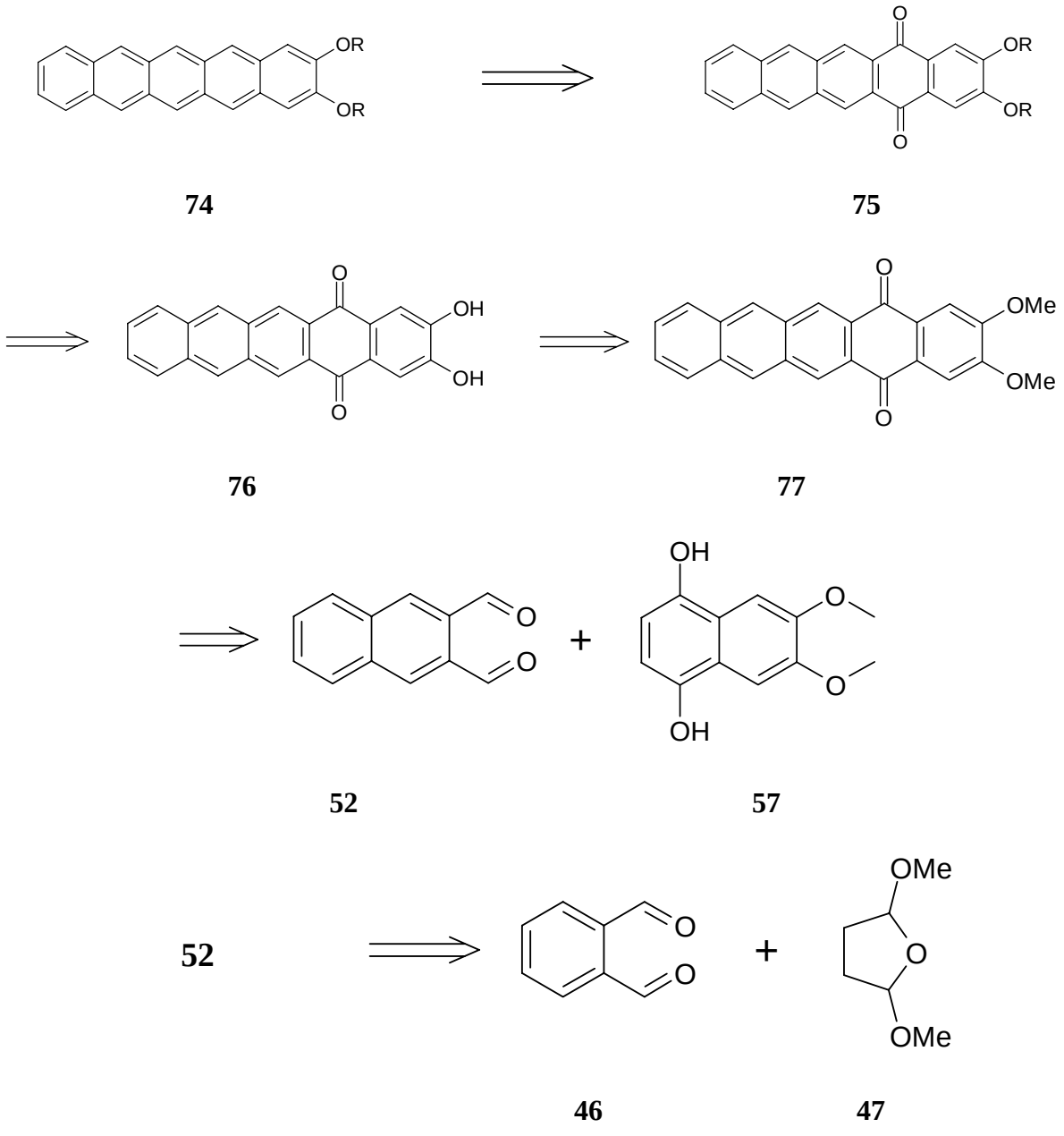

Scheme 15 **Retrosynthesis of 2,3-dialkoxy-pentacenes** (**74**)

Following Scheme 15 the retrosynthetic examination of **74** leads by oxidation of the pentacene core to the corresponding pentacene-5,14-quinone **75**. Cleavage of the alkoxy-phenyl ether and protection of the resulting phenol **76** leads to 2,3-dimethoxy-pentacene-5,14-quinone (**77**). This intermediate can be analyzed back to two naphthalene subunits, the dialdehyde **52** and the *p*-dihydroxy-naphthalene **57**. The former can be further traced back to the lower homologue **46**, the retrosynthesis of the latter is explained in Scheme 9.

2.8 Synthesis of 2,3-dialkoxy-pentacenes (**74**)

Some difficulties noted during the synthesis of 2,3-dialkoxy-tetracenes **2** can be expected to be comparable in the case of the pentacenes series. These are:

Poor solubility of the 2,3-dimethoxy-pentacene-5,14-quinone (**77**), leading to slow demethylation.

Even poorer solubility of the 2,3-dihydroxy-pentacene-5,14-quinone (**76**), leading to a slow alkylation and severe problems in purifying **76**.

High sensitivity of the pentacenes towards oxygen combined with low solubility hampering purification and limiting gel formation to compounds with at least C_{10} chains (see Chapter 3.1). The solution to these problems is presented in the following chapters.

2.8.1 Explanation of the individual synthetic steps

The synthesis of 2,3-dialkoxy-pentacenes **74** follows the synthesis of the 2,3-dialkoxy-tetracenes **2**, with only two major differences. First, the dialdehyde to be condensed with 1,4-dihydroxy-6,7-dimethoxy-naphthalene (**57**) is the higher homologue of **46**, naphthalene-2,3-dialdehyde (**52**). The second difference can be found in the poor solubility of all 2,3-dialkoxy-pentacene-5,14-quinones **75** and the corresponding 2,3-dialkoxy-pentacenes **74**, which complicates the work. The reduction of the 2,3-dialkoxy-pentacene-5,14-quinones **75** to the 2,3-dialkoxy-pentacenes **74** was thus carried out under argon to prevent oxidation of the substrate.

2.8.1.1 Synthesis of naphthalene-2,3-dialdehyde (**52**)

The synthesis of **52** has first been published by Cook et al. in 1949.[46] The given procedure though (oxidation of anthracene with OsO_4 followed by cleavage with periodic acid) is not suitable to produce larger amounts of the substance due to the complicated procedure and the high price of OsO_4.

An improvement can be found in the synthesis by Weygand et al.[47] published in 1950. This reaction sequence is building on naphthalene-2,3-dicarboxylic acid. It is first reduced to the diol and subsequently partially oxidized. Unfortunately, this synthesis can only be carried out in small amounts since the oxidant is SeO_2.[47]

Another synthesis, using functional group interconversion of a substituted naphthalene, has been published by Ried et al. in 1956.[48] 2,3-Dimethyl-naphthalene is brominated in two steps to provide 2,3-bis-dibromomethyl-naphthalene. This intermediate is hydrolyzed by aqueous potassium oxalate which gives the desired dialdehyde **52** in an overall yield of 34%. It is a serious drawback though that 2,3-dimethyl-naphthalene is not anymore available commercially as a side product of tar production as described by Ried.[48]

This makes it necessary to look for synthetic approaches in which the naphthalene nucleus is build up from cheap and available precursors.

Two strategies to synthesize naphthalene-2,3-dicarboxaldehyde (**52**) from benzenic subunits are described in the literature. Givens et al. have published a synthesis in 1986,[49] using α,α,α´,α´-tetrabromo-*o*-xylene. This precursor is converted with NaI to the dibromo-*o*-quinomethide which is trapped in a Diels-Alder addition with maleic acid anhydride. Work-up leads to the 2,3-naphtalene-dicaboxylic acid, which is, similar to the approach published by Weygand, reduced to the diol and then oxidized to the dialdehyde. The overall yield of this sequence is 32%.

The second approach, published by Mallouli and Lepage,[14] exploits the condensation of 1,4-dioxobutane, *in situ* prepared from 2,5-dimethoxy-tetrahydrofuran (**47**), to *o*-phthalic dialdehyde (**46**), catalyzed by piperidine and carried out in a mixture of glacial acetic acid and water. One advantage is the relatively good solubility of the starting material and the naphthalene-2,3-dicarboxaldehyde (**52**). This allows purification (separation of traces of anthracene-2,3-dicarboxaldehyde) by recrystallization or by sublimation, as the melting points of the two major aldehydes differ by 80 °C. Even if this synthesis gives the desired dialdehyde only in a poor yield (19%), the short and easy to perform transformation makes it more suitable than the longer route described by Givens.

The structure assignment of the product was carried out by HMBC and HSQC experiments. as summarized in Table 11 and Table 12.

Entry	δ (H)	multiplicity	coupling (*J* or *N* [Hz])	correlation
a	10.64	s		9/10-H
b	8.45	s		4/1-H
c	8.06	m_c (AA'XX')	*N* = 9.4 Hz	8/5-H
d	7.75	m_c (AA'XX')	*N* = 9.5 Hz	7/6-H

Table 11 **^{1}H NMR correlation of 52**

Entry	δ (C)	multiplicity	correlation	HSQC	HMBC
A	192.2	s	C-10/9	a	b
B	134.46	d/ s	C-4/1 or C-8a/4a	b	a,b,c,d
C	134.45	d/ s	C-4/1 or C-8a/4a	b	a,d,c,d
D	132.8	s	C-3/2	-	a,b
E	130.0	d	C-7/6	d	c
F	129.6	d	C-8/5	c	b,d

Table 12 **^{13}C NMR correlation of 52**

Especially the aldehyde proton singlet at δ = 10.64 and the two aromatic signals deriving from an AA'XX'-spin system ($\delta_{centrum}$ = 8.06 und δ = 7.75), attributed to 6/7-H and 8/9-H are characteristic. The low resolution mass spectrum shows signals with *m/z* = 184 [M^+] and *m/z* = 155. This latter peak results from a loss of one aldehyde function (CHO, *m/z* = 29). The UV spectrum displays λ_{max} = 258 nm and the absorption with the longest wavelength at λ = 360 nm consistent with the light yellow color of the product. The IR spectrum is dominated by a strong band at 1683 cm^{-1}, corresponding to the carbonyl function.

2.8.1.2 Synthesis of 2,3-dimethoxy-5,14-pentacene-quinone (77)

Like in the case of 2,3-dialkoxy-tetracene-5,12-quinones **61**, the main reaction is an aldol condensation between naphthalene-2,3-dialdehyde (**52**) and a hydroquinone (1,4-dihydroxy-6,7-dimethoxy-naphthalene (**57**)) (see chapter 2.5.1.4). With 89% the yield of the reaction is slightly better than the yield of the condensation described above, possibly due to the very low solubility of the pentacene-quinone product. Structural assignment is provided by NMR-data as well as 70 eV EI mass spectrometry. The NMR spectroscopy is hampered by the poor solubility in $CDCl_3$. Hence only a ^{1}H NMR spectrum could be obtained and the signals were assigned by comparison with the better soluble 2,3-didecyloxy-pentacene-5,14-quinone (**112**).

This leads to the following assignment:

Entry	δ (H)	multiplicity	coupling (*J* or *N* [Hz])	correlation
a	9.00	s		13/6-H
b	8.67	s		12/7-H
c	8.07	m_c (AA'XX')	*N* = 9.7 Hz	11/8-H
d	7.81	s		4/1-H
e	7.59	m_c (AA'XX')	*N* = 9.7 Hz	10/9-H
f	4.10	s		16/15-H

Table 13 **^{1}H NMR data of 77**

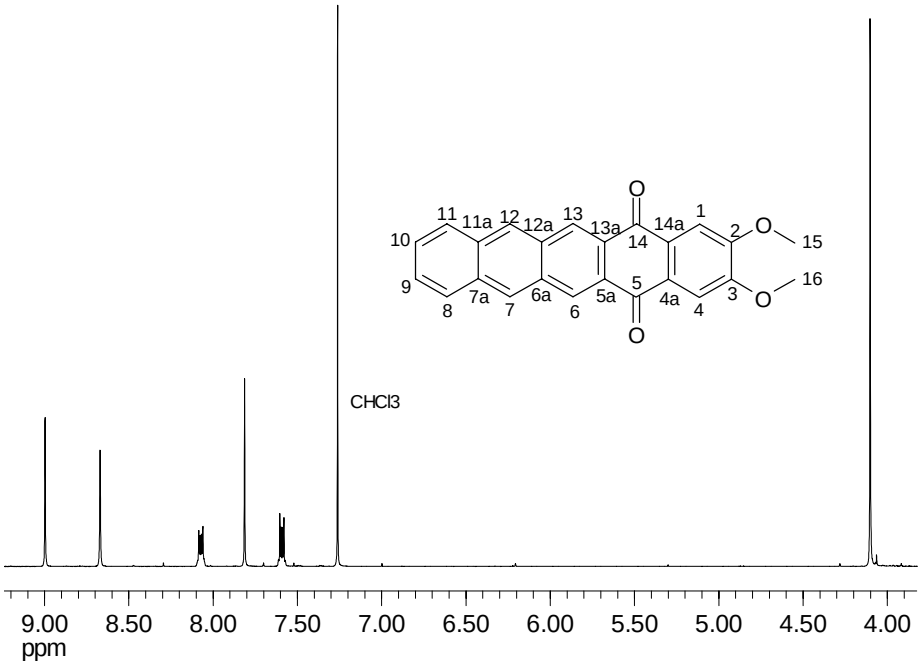

Figure 15 **^{1}H NMR spectrum of 77**

Comparison of the spectra of the two 2,3-dialkoxy-pentacene quinones **75** was possible, as it could be proven that the relative order of the ^{13}C and ^{1}H signals did not change with the degree of alkylation (only the hydroxy quinone being an exception, see Chapter 2.5.1.5) in the tetracene-quinone series. The same insensitivity of the quinone core towards the alkyl chain can thus be assumed. It was, indeed, shown to be the case for 2,3-didecyloxy-pentacene-5,14-quinone (**112**) and 2,3-dihexadecyloxy-pentacene-5,14-quinone (**113**) (see Chapters 7.3.3.4 and 7.3.3.5).

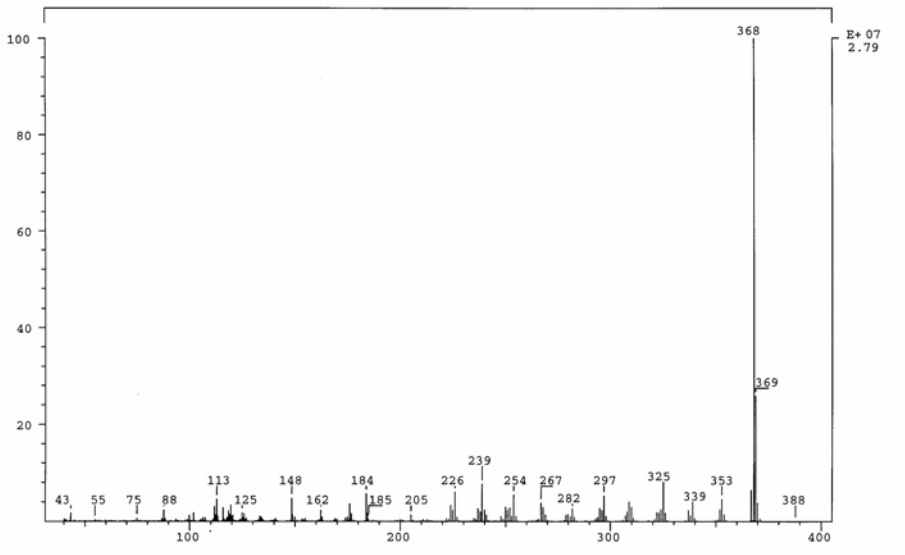

Figure 16 **70 eV mass spectrum of 77**

The 70 eV mass spectrometry displayed [M^+] at *m/z* = 368 and a very atypical fragmentation with fragments of nearly equal intensity at *m/z* = 353 (loss of CH_3), 339 (loss of CH_3+CH_2), 325 (further loss of CH_2), 309 (loss of O). IR spectroscopy shows characteristic absorptions for the quinone system (1664 (C=O) and 1582 cm^{-1} (C=C)) as well as the aryl-O-CH_3 vibration at 1208 cm^{-1}. The UV-spectrum is characterized by three important absorptions, at 262, 340 and, corresponding to the color, at 456 nm.

2.8.1.3 Demethylation of 2,3-dimethoxy-pentacene-5,14-quinone (77)

As far as solubility and reactivity of 2,3-dimethoxy-pentacene-5,14-quinone (**77**) are concerned, the compound resembles 2,3-dimethoxy-tetracene-5,12-quinone (**42**). Thus only demethylation using HBr/HOAc and pyridine•HCl were applied.

Because of its low solubility, 2,3-dimethoxy-pentacene-5,14-quinone (**77**) has to be refluxed for several days in HBr/HOAc to yield the 2,3-dihydroxy-pentacene-5,14-quinone (**76**). The intermediate **76** was not characterized but directly alkylated and separated from unreacted **77** and only partially demethylated **77** at the stage of the alkoxy-pentacene-quinones (see Chapter 2.8.1.4).

2.8.1.4 Alkylation of 2,3-dihydroxy-pentacene-5,14-quinone (76)

The crude mixture resulting from demethylation of **76** was generally alkylated without further purification, which is prevented by the poor solubility of 2,3-dihydroxy-pentacene-5,14-quinone (**76**) and 2,3-dimethoxy-pentacene-5,14-quinone (**77**). Compared to the well established reaction of 2,3-dihydroxy-tetracene-5,12-quinone (**35**), the alkylation has to be carried out with longer reaction times. This is necessary to compensate for the low concentration of the hydroxyquinone **76** present in the reaction mixture. On the other hand the application of bromides as long as C_{22} is hampered by their low solubility in DMF, leading to a decrease in reaction efficiency. This prevented the synthesis of 2,3-dialkoxy-pentacene-5,14-quinones **75** substituted with chains longer than C_{16}, decomposition of the starting material occurring after prolonged reflux. Since the minimum chain length for gelification of the tetracenes was shown to be between C_6 and C_{10} (see Chapter 3), only two derivatives of 2,3-dialkoxy-pentacene-5,14-quinones **75**, bearing C_{10} and C_{16} chains were synthesized. (see Chapter 7.3.3.4 and 7.3.3.5).

The yields of the Williamson synthesis were good (62% in the case of C_{10}, 57% in the case of C_{16}, both including demethylation) but lower than the yields obtained in the 2,3-dialkoxy-tetracene-5,12-quinone **61** series. This is possibly due to the imperfect demethylation at the earlier stage. The unreacted **77** was not recovered during column chromatography. Since only the 2,3-dihexadecyloxy-pentacene-quinone (**113**) leads to a gel forming derivative (see Chapter 3.2), only its spectral data are discussed in depth. The structure was assigned using one and two dimensional NMR spectroscopy as well as 70 eV mass spectrometry (*vide infra*).

Entry	δ (H)	multiplicity	coupling (*J* or *N* [Hz])	correlation
a	8.96	s		13/6-H
b	8.64	s		12/7-H
c	8.05	m_c (AA'XX')	*N* = 9.7 Hz	11/8-H
d	7.75	s		4/1-H
e	7.57	m_c (AA'XX')	*N* = 9.7 Hz	10/9-H
f	4.21	t	^3J = 6.6 Hz	31/15-H
g	1.95-1.88	m		32/16-H
h	1.56-1.22	m		33-45/ 17-29-H
i	0.88	t	^3J = 6.8 Hz	46/30-H

Table 14 **^{1}H NMR correlation of 113**

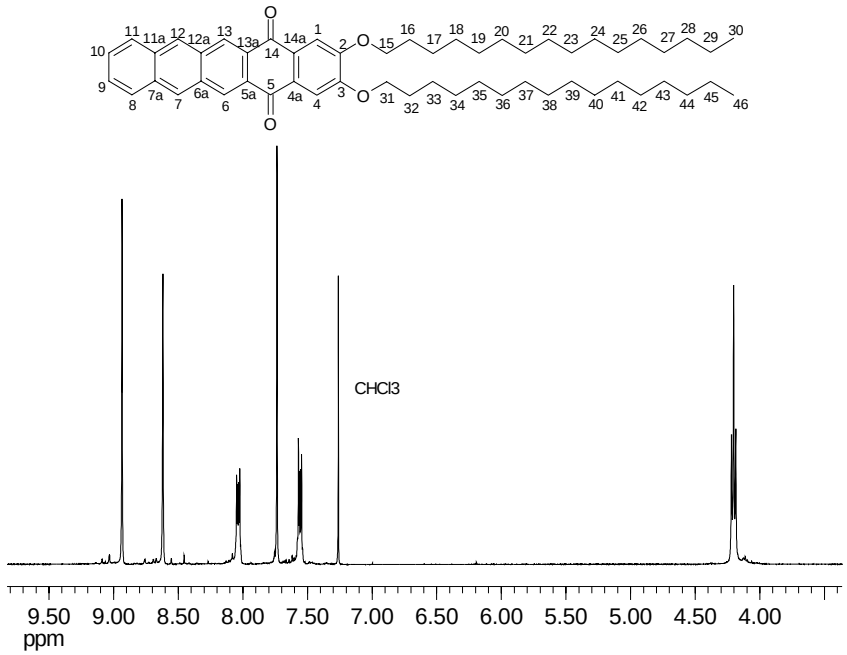

Figure 17 **^{1}H NMR spectrum of 113 (alkyl chain excluded)**

Entry	δ (C)	multiplicity	correlation	HSQC	HMBC
A	182.1	s	C-14/5	-	a,d
B	154.0	s	C-3/2	-	d,f
C	133.5	s	C-11a/7a	-	b,c,(e)
D	131.7	s	C-12a/6a	-	a,b
E	130.7	d	C-13/6	a	b
F	129.8	d	C-12/7	b	a,(c)
G	129.7	s	C-14a/4a	-	d
H	129.2	s	C-13a/5a	-	a
I	128.6	d	C-11/8	c	b,e
J	127.3	d	C-10/9	e	c
K	109.4	d	C-4/1	d	-
L	69.4	t	C-31/15	f	g
M	31.9-22.7	t	chain	-	-
N	14.1	q	C46/30	i	h

Table 15 **^{13}C NMR correlation of 113**

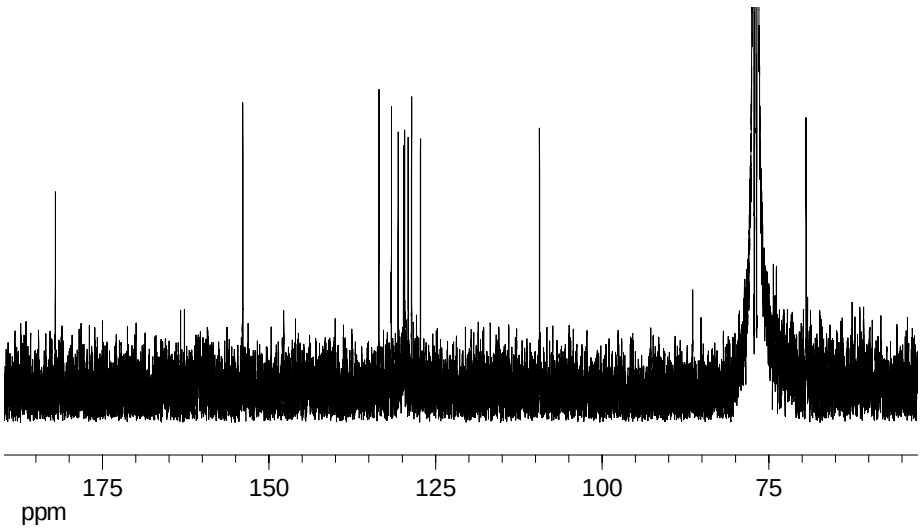

Figure 18 **^{13}C NMR spectrum of 113 (aromatic part, including C-31/15)**

When the ^{1}H NMR spectra of the 2,3-dialkoxy-tetracene-5,12-quinones **61** are compared with those of the 2,3-dialkoxy-pentacene-5,14-quinones **75**, it can be seen that the relative order of the signals is maintained. The new singlet b (12/7-H) simply inserts.

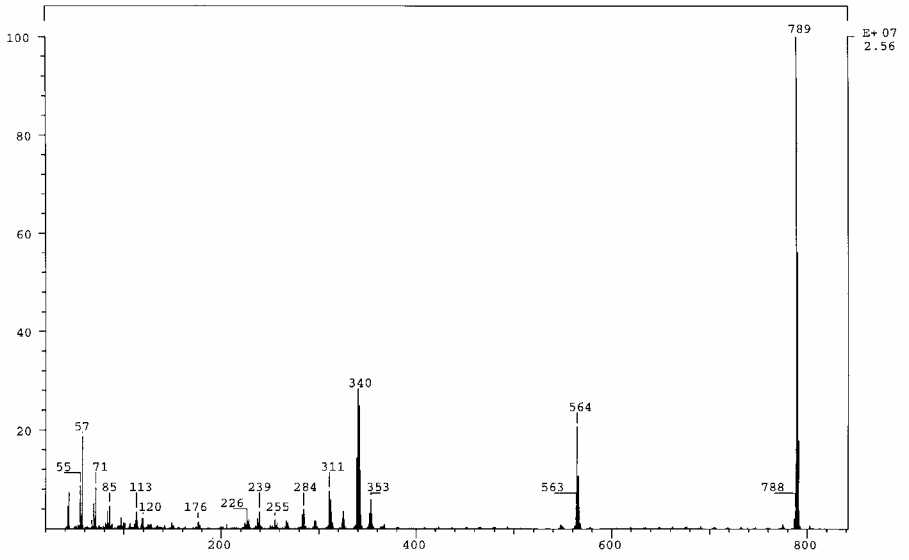

Figure 19 70 eV mass spectrum of 113

As expected the fragmentation pattern of the 2,3-dialkoxy-pentacene-5,14-quinones **75** is very similar to the one of the 2,3-dialkoxy-tetracene-5,12-quinones **61** (see Chapter 2.5.1.6). The signal of the highest intensity is $[M^+]$ (*m/z* = 789 instead of *m/z* = 788 due to the high amount of H in the sample). By the loss of one (*m/z* = 564) and two (*m/z* = 340) $C_{16}H_{32}$ chains the main fragments are created. IR- and UV/Vis- spectra again support the assigned structure (see Chapter 7.3.3.5).

2.8.1.5 Reduction of 2,3-dialkoxy-pentacene-5,14-quinones (75)

As pentacenes are even more sensible towards oxygen than tetracenes,[50] all reaction and work-up procedures have to be carried out in an atmosphere of Ar. The desired product **114** is even less soluble than the starting material. This limits structural assignment in the case of the 2,3-didecyloxy-pentacene (**114**) to solid state techniques (IR and 70 eV mass spectrometry), mainly relying on the high resolution mass spectrum (see Chapter 7.3.3.6). In the case of the 2,3-dihexadecyloxy-pentacene (**115**), the solubilizing effect of the longer alkyl chains not only leads to gel formation (see Chapter 3.3) but allows full characterization of the substance by one and two dimensional NMR spectroscopy as well as 70 eV mass spectrometry, IR spectroscopy and UV/Vis spectrometry. Still, under general measurement conditions 2,3-dialkoxy-pentacene **115** is only sparsely soluble and prone to oxidation when dissolved.

Thus the NMR spectra were measured in freeze thaw degassed 1,1,2,2-tetrachloroethane-d_2 in a sealed NMR-tube at 81 °C. Even under these conditions, traces of decomposition products can be observed in the NMR spectrum. The UV/Vis spectrum was taken equally under freeze thaw degassed conditions in 1,1,2,2-tetrachloroethane. It has to be mentioned that the UV/Vis spectrum could only be taken qualitatively due to the low solubility (see Chapter 7.3.3.7).

Entry	δ (H)	multiplicity	coupling (J or N [Hz])	correlation
a	8.83	s		13/6-H
b	8.63	s		12/7-H
c	8.40	s		14/5-H
d	7.94	m_c (AA'XX')	N = 9.8 Hz	11/8-H
e	7.33	m_c (AA'XX')	N = 9.9 Hz	10/9-H
f	7.11	s		4/1-H
g	4.18	t	^3J = 6.5 Hz	31/15-H
h	1.98-1.91	m		chain
i	1.63-1.56	m		chain
j	1.48-1.31	m		chain
k	0.92	t	^3J = 6.8 Hz	46/30-H

Table 16 **^{1}H NMR correlation of 115**

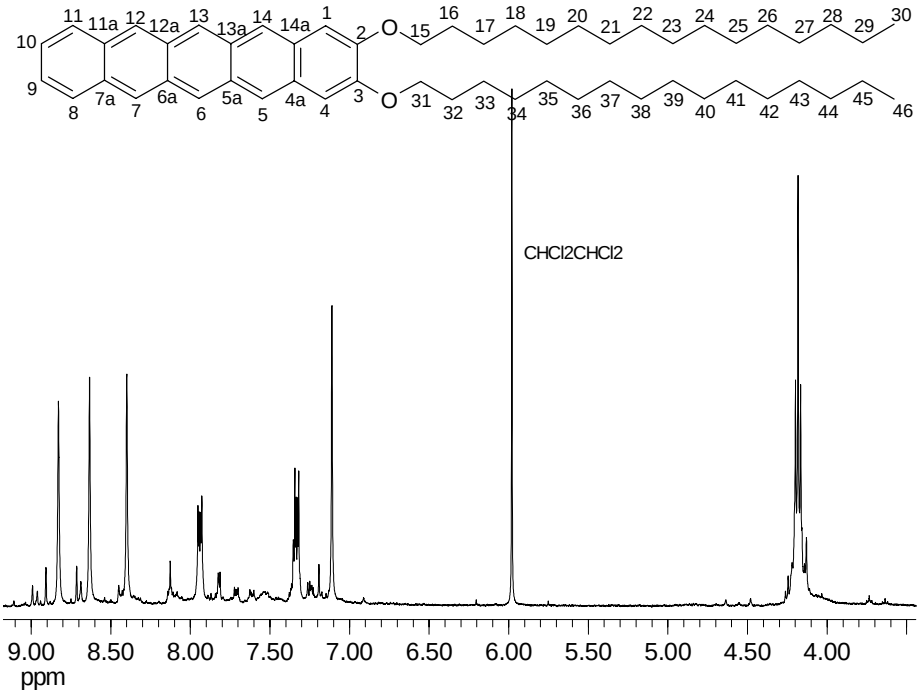

Figure 20 **^{1}H NMR spectrum of 115 (aromatic part including 31/15-H)**

Entry	δ (C)	multiplicity	correlation	HSQC	HMBC
A	150.8	s	C-3/2	-	f,g
B	131.2	s	C-11a/7a	-	b,d
C	129.7	s	C-13a/5a or C-12a/6a	-	a,b,c
D	129.5	s	C-14a/4a	-	c,f
E	128.2	d	C-11/8	d	b
F	125.9	d	C-12/7	b	a
G	125.1	d	C-13/6	a	b,c
H	124.7	d	C-10/9	e	d
I	122.9	d	C-14/5	c	a,f
J	105.8	d	C-4/1	f	c
K	68.9	t	C-31/15	chain	chain
L-S	31.7-22.4	t	chain	chain	chain
T	13.8	q	C-46/30	chain	chain

Table 17 **^{13}C NMR spectrum of 115**

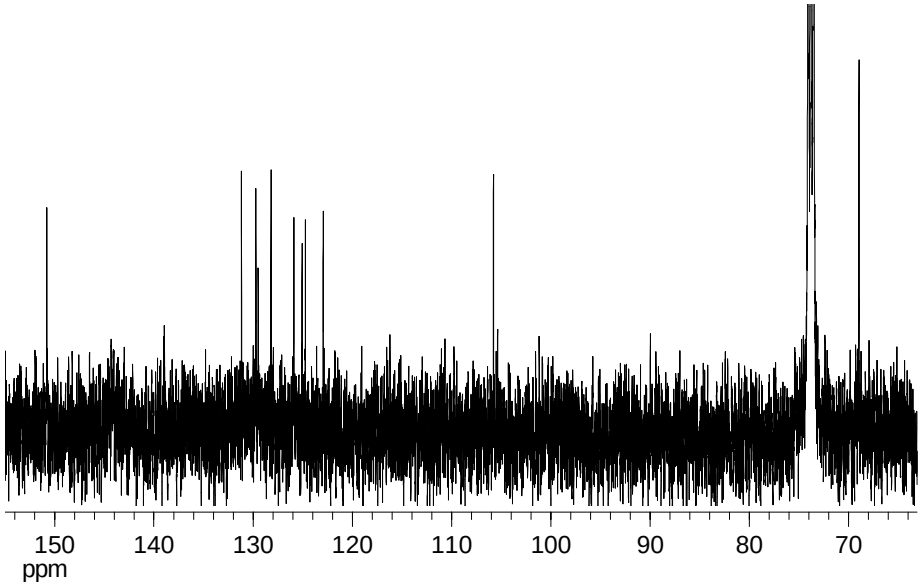

Figure 21 **^{13}C NMR spectrum of 115 (aromatic area including C-31/15)**

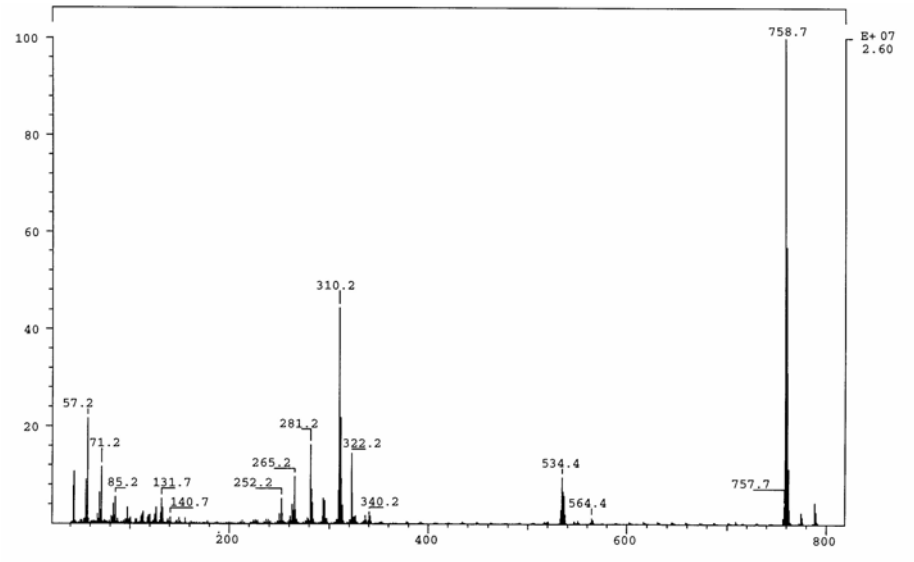

Figure 22 70 eV mass spectrum of 115

The first technique to prove the structure of the 2,3-dialkoxy-pentacenes (**114** and **115**) was 70 eV mass spectrometry. Both high- and low resolution spectra were measured, as combustion analysis did not give proper results. This can be seen in the case of the 2,3-dialkoxy-tetracenes **2** as well. It can be explained by the high carbon content of the tetracene and pentacene core as well as the fact that polycondensed aromatic substances are often found in soot, proving their resistance towards combustion.

The low resolution 70 eV mass spectrum of **115** shows three main signals. The $[M^+]$ with *m/z* = 758 is the base signal. Cleavage of one $C_{16}H_{32}$ fragment leads to the *m/z* = 534 signal, the cleavage of the second $C_{16}H_{32}$ fragment to the *m/z* = 310 signal. This fragmentation pattern is comparable to the one found in the 2,3-dialkoxy-tetracene **2** series (see Chapter 2.5.1.7).

In the case of the 2,3-didecyloxy-pentacene (**114**), only the 70 eV mass spectrum and the IR spectrum were measured, as mentioned above. Only the 2,3-dihexadecyloxy-pentacene (**115**) was (under special conditions, *vide supra*) soluble enough to form gels and to be further examined.

UV/Vis spectrometry shows electronic absorptions at 309, 321 and 348 nm as well as absorptions in the visible range at 433, 498, 536 and 580 nm, in good agreement with the dark blue to violet color of **115** in solution.

2.9 Synthesis of gel forming anthracenes

2.9.1 Introduction

If 2,3-dialkoxy-tetracenes **2** in low concentration are incorporated in gels formed by 2,3-DDOA (**1**), the question arises whether these different acene-gelators interact in the gel.

To perform initial experiments on cooperative gel formation between 2,3-DDOA (**1**) and 2,3-DDOT (**86**), 2,3-DDOA (**1**) was synthesized as described in the following chapter.

In general, the synthesis as summarized in Scheme 4 follows the known approach, published by Bouas-Laurent et al. (see Chapter 2.3.1.1).[11] Only minor adaptations to the well established procedures for the 2,3-dialkoxy-tetracene- and 2,3-dialkoxy-pentacene synthesis were introduced and will be explained in the following chapters.

2.10 Retrosynthesis

The examination of 2,3-didecyloxy-anthracene (**1**) leads to the first intermediate, 2,3-dialkoxy-anthra-9,10-quinone (**8**). Standard protective group chemistry provides the key intermediate, 2,3-dimethoxy-anthra-9,10-quinone (**38**). This can be build up mainly by two strategies, proposed by Bouas-Laurent et al.[11] (see Chapter 2.3.11).

In the present work, only the first approach was used, since the Friedel-Crafts reaction between 2,3-dihydroxy-benzene (**29**) and phthalic anhydride (**30**) has been described to include "tedious work-up" and suffers from the drastic reaction conditions.[11] A third approach, not included in the cited literature, would be the aldol condensation of 1,4-dihydroxy-2,3-dimethoxy-benzene (**53**) to phthalic dialdehyde (**46**), leading to a substituted anthracene-1,4-quinone **78**.

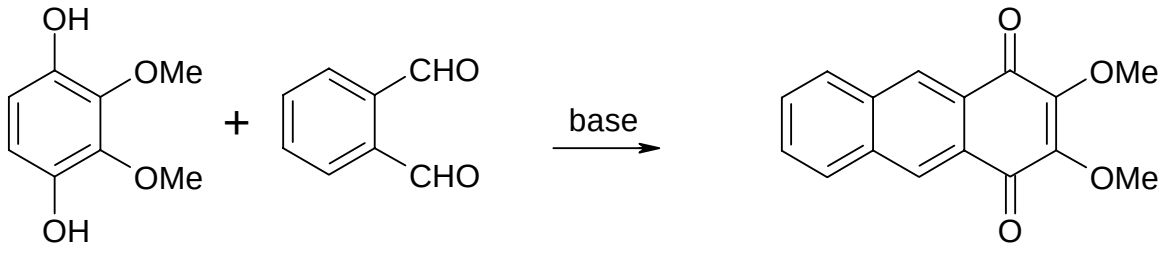

53 **46** **78**

Scheme 16 **Possible synthesis of 78 via aldol condensation**

Because of the problems mentioned in Chapter 2.3.1.3, this approach was not further pursued.

The Diels-Alder approach is well known from the synthesis of 6,7-dimethoxy-naphthalene-1,4-quinone (**58**) (see Chapter 2.5.1.2) and was thus used in this study.

2.11 Synthesis of 2,3-didecyloxy-anthracene (1)

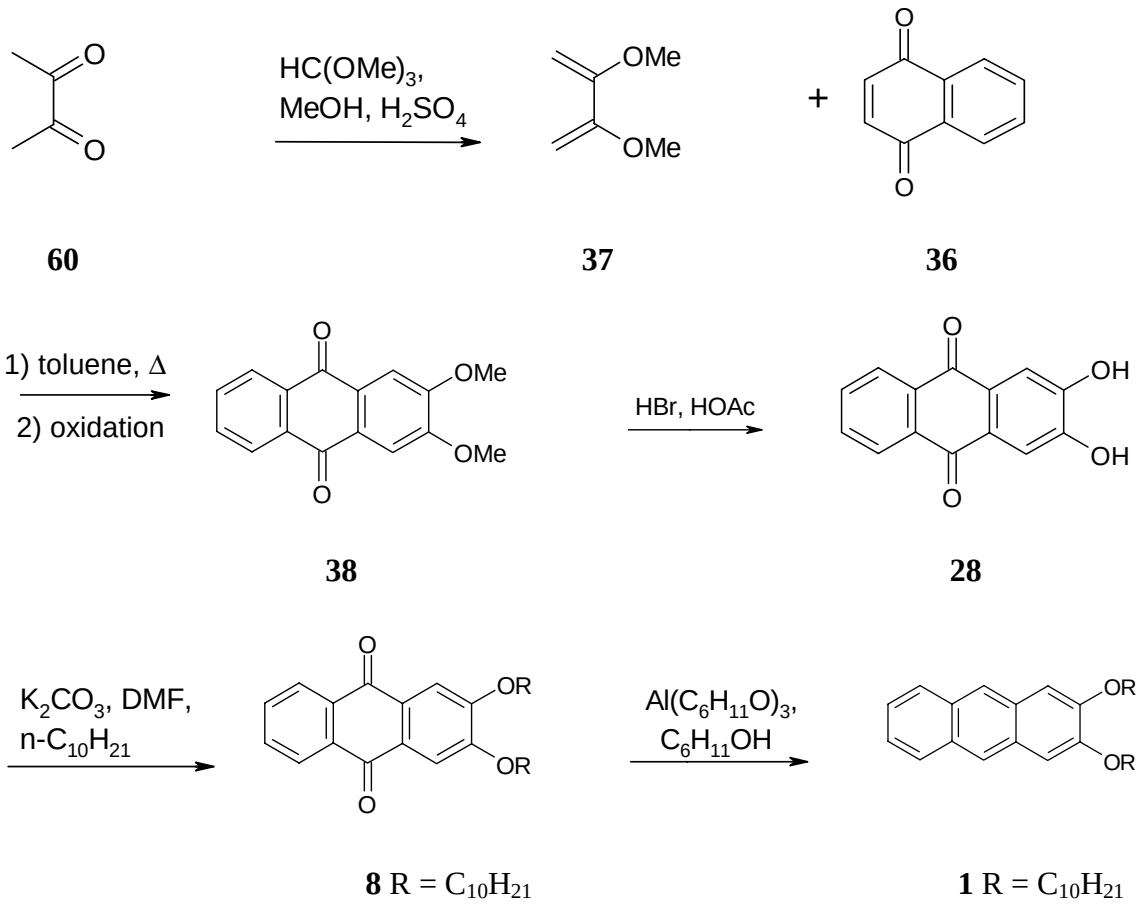

60 **37** **36** **38** **28**

8 R = $C_{10}H_{21}$ **1** R = $C_{10}H_{21}$

Scheme 17 **Synthesis of 2,3-didecyloxy-anthracene (1)**

2.11.1 Explanation of the individual synthetic steps

2.11.1.1 Synthesis of 2,3-dimethoxy-anthra-9,10-quinone (38)

As mentioned in Chapter 2.3.1.1, two ways are possible to synthesize 2,3-dimethoxy-anthra-9,10-quinone (**38**), both of which have been described by Bouas-Laurent et al. in 1997.[3] The first alternative is the Friedel-Crafts acylation, first published as the ring closure of 2-veratroyl-benzoic acid by Lagodzinski et al. in 1895.[51] The other possibility is the Diels-

Alder addition of 2,3-dimethoxy-buta-1,3-diene (**37**) to naphthalene-1,4-quinone (**36**). This synthesis was first published by Johnson et al. in 1941[52] and was used in the present investigation because of the simpler work-up.[11] When compared to the addition of **37** to benzoquinone (**59**) two major differences have to be mentioned (see Chapter 7.3.2.1). First, the addition can only take place once. Therefore the diene **37** is used in excess. On the other hand, naphthoquinone is, unlike benzoquinone, not able to oxidize the primary adduct. Hence the Diels-Alder addition is followed by an oxidation step with air in basic solution. To make work-up easier, the oxidation was carried out without the separation and purification of the primary adduct. The spectroscopic data (^{1}H NMR and ^{13}C NMR) agree well with the data provided in the literature.[11] Further proof was drawn from the 70 eV mass spectrum with [M^+] at *m/z* = 268 and characteristic fragments at *m/z* = 253 and 238, resulting from the loss of one and two CH_3-groups. The IR-spectrum exhibits characteristic bands at 1655 and 1572 cm^{-1} for the quinone system and 1224 cm^{-1} for the aromatic methoxy ether.

2.11.1.2 Demethylation of 2,3-dimethoxy-9,10-anthraquinone (38)

The higher solubility of the anthraquinone **38** in comparison to 2,3-dimethoxy-tetracene-5,12-quinone (**42)** makes it possible to use modern reagents and mild conditions (BBr_3 in DCM) as published by Bouas-Laurent et al.[11] Still, the convenient and cheap demethylation using strong acids that was used with good success in the course of this work is applicable to the lower homologue of the tetracenequinone. The reaction time is comparatively short (24 h, see Chapter 7.3.2.2) and the relatively high solubility allows good conversions.

The spectroscopic data provided in Chapter 7.3.2.2 is in good agreement with the ^{1}H NMR, ^{13}C NMR and IR data provided by Bouas-Laurent et al.[11]

2.11.1.3 Alkylation of 2,3-dihydroxy-anthracene-9,10-quinone (28)

The classical Williamson conditions, using DMF as solvent and potassium carbonate as base were used successfully as described in the literature.[11] The spectral data of the resulting 2,3-didecyloxy-anthracene-9,10-quinone (**8**) agree with the published data[11] (see Chapter 7.3.2.3).

2.11.1.4 Reduction of 2,3-didecyloxy-anthracene-9,10-quinone (8)

The procedure to reduce 2,3-didecyloxy-anthra-9,10-quinone (**8**) to the corresponding dialkoxy-anthracene **1**, published by Bouas-Laurent at al.[11] is a two step reduction using $NaBH_4$ in *iso*-propanol. The higher solubility of anthraquinones in contrast to alkoxy-tetracene-quinones **61** makes this low temperature procedure possible. Still, the gel formation of the product 2,3-DDOA (**1**), a good gelator for alcohols, causes problems. Bouas-Laurent et al. circumvented these by changing the order of reduction/substitution.[11] In this study, a different approach was chosen to prevent gel formation, the proven high temperature reduction using $Al(OC_6H_{11})$. The relatively high solubility of 2,3-DDOA (**1**) in DCM led to a different work-up, the extraction after decomposition of the alumina species in contrast to filtration and recrystallization (see Chapter 7.3.2.4).

The spectroscopic data (^1H NMR, ^{13}C NMR, IR-spectroscopy and 70 eV mass spectrum) are in good agreement with the data published by Bouas-Laurent et al.[11]

3 Examination of the gel forming abilities of 2,3-dialkoxy-acenes

The techniques to examine gel formation can be subdivided into three main groups. The first and most obvious group contains rheological tests like the "inverted tube test", following the "definition" given by Lloyd, quoted by Terech and Weiss[1a] who stated that "if it looks like "Jello", it must be a gel". The second possibility is to observe spectroscopic changes, when a solution of a possible gelator is cooled and by this transferred into the gel-state. UV/Vis- and fluorescence spectroscopy can provide these "indirect" evidences for gel formation. The last, and most interesting group of techniques contains direct structural determinations of the gel. Measurement of the microscopic structures involved can be accomplished by electron microscopy, neutron scattering or scanning probe microscopy techniques.

The use of the three types of gel determination will be presented for the acene gelators in the following chapters.

3.1 2,3-Dialkoxy-tetracenes 2

3.1.1 Inverted test tube examinations

A first test to evaluate the gel forming properties of different solvents and gelators is the “inverted tube” method. A precisely weighed sample of the finely powdered gelator is transferred into a sample tube (length 6 cm, diameter 0.7 cm). A known volume of the solvent to be tested is added. The tube is capped and the content homogenized in an ultrasound bath. The suspension is warmed until dissolution of the gelator. Upon cooling to room temperature, a solidification of the whole liquid indicates gel formation. Other possible results are the precipitation of the gelator, the lack of solubility or the gelator staying dissolved. In this last case, the sample can be cooled to -24 °C if the solvent allows such a treatment.

This test was used to gain a first impression of the gelification properties and to screen a broad variety of solvents.

The full data of the inverted tube tests is given in Appendix I A. To summarize those results, the following table is given:

solvent	c (DDOT) [mol/L]•10^{-3}	c (DHdOT) [mol/L]•10^{-3}	remarks
n-hexanol	4.9	2.4 (VS)	no stable gel with 2,3-DHdOT
n-octanol	5.0	1.0	
n-decanol	4.6	1.2	
n-hexane	10.1	1.2	
n-heptane	-	0.9	no stable gel with 2,3-DDOT
n-nonane	-	1.6	no stable gel with 2,3-DDOT
n-$C_{14}H_{30}$	-	1.4	no stable gel with 2,3-DDOT
cyclohexane	3.9	0.8	
MCH	10.0	1.0 (VS)	
$CHCl_3$	18	-	2,3-DDOT only at -24 °C
DCM	9.1	7.5	2,3-DDOT only at -24 °C
DMF	4.6	-	no stable gel with 2,3-DHdOT
acetone	-	3.5	no stable gel with 2,3-DDOT

Table 18 **Results of the inverted tube tests for 2,3-DDOT (86) and 2,3-DHdOT (111)**

Before the results of the inverted tube tests on 2,3-dialkoxy-tetracenes **2** are summarized and explained, a picture of inverted tubes containing 2,3-DDOA-, 2,3-DHdOT- and 2,3-DHdOP gels is shown to illustrate the examination technique.

Figure 23 **Picture of inverted tubes (2,3-DDOA (1)/ methanol; 2,3-DHdOT (111)/ cyclohexane; 2,3-DHdOP (115)/ 1,1,2,2-tetrachloroethane)**

The table shows that the best solvents used for the formation of gels with 2,3-dialkoxy-tetracenes **2** are apolar or fairly polar solvents like long chain alcohols or alkanes. While the alkanes form gels more easily, the alcohols have a broader boiling range, allowing more gelator to be dissolved at higher temperatures. Moreover, it can be stated that the gel forming abilities of 2,3-DHdOT (**111**) are (in terms of concentration) sometimes one order of magnitude better than the ones of 2,3-DDOT (**86**). It has to be kept in mind though that the molecular weight of the 2,3-DHdOT (**111**) is 31% higher than the one of 2,3-DDOT (**86**). This diminishes the advantage of 2,3-DHdOT (**111**), when gel forming abilities in mg/mL are considered.

Table 18 further illustrates the difficulties of this kind of test. The border between viscous solutions and gels is flexible and it depends on the geometry of the tubes, the ambient conditions and the sample. For the best results only freshly recrystallized samples should be used, as oxidation of the sample can influence the result.

3.1.1.1 Influence of the chain length of different 2,3-dialkoxy-tetracenes 2 on gel formation

To gain an impression on the influence of the chain length upon the gel formation properties of 2,3-dialkoxy-tetracenes **2**, inverted tube experiments were carried out for five different 2,3-dialkoxy-tetracenes **2** in cyclohexane and hexanol. The results are summarized in the following tables, the abbreviations used are as follows: P = precipitation upon cooling, IS = sample is insoluble at boiling temperature, VS = viscous solution, S = gelator stays dissolved without increase of the viscosity, G = gel formation.

Cyclohexane

sample	β [g/L]	c [mol/L]	result	β [g/L]	c [mol/L]	result
2,3-DMOT	1.99	$6.90 \bullet 10^{-3}$	IS	1.00	$3.47 \bullet 10^{-3}$	P
2,3-DBOT	2.03	$5.45 \bullet 10^{-3}$	P	0.96	$2.58 \bullet 10^{-3}$	P
2,3-DHOT	2.00	$4.67 \bullet 10^{-3}$	VS	1.00	$2.33 \bullet 10^{-3}$	S
2,3-DDOT	2.05	$3.79 \bullet 10^{-3}$	G	1.02	$1.89 \bullet 10^{-3}$	VS
2,3-DHdOT	1.97	$2.77 \bullet 10^{-3}$	G	1.00	$1.41 \bullet 10^{-3}$	VS

Table 19 **Influence of the chain length of 2,3-dialkoxy-tetracenes 2 on gel formation (solvent: cyclohexane)**

Table 19 shows that in cyclohexane (generally the best solvent for gel formation of 2,3-dialkoxy-tetracenes **2**) the minimum chain length is around C_6 with a critical concentration of 2 g/L (in the case of 2,3-DHOT (**110**) $5 \bullet 10^{-3}$ mol/L).

Hexanol

sample	β [g/L]	c [mol/L]	result	β [g/L]	c [mol/L]	result
2,3-DMOT	1.96	$6.78 \bullet 10^{-3}$	P	0.98	$3.39 \bullet 10^{-3}$	L
2,3-DBOT	1.95	$5.23 \bullet 10^{-3}$	P	1.01	$2.70 \bullet 10^{-3}$	P
2,3-DHOT	2.01	$4.69 \bullet 10^{-3}$	VS	1.00	$2.33 \bullet 10^{-3}$	L
2,3-DDOT	2.01	$3.72 \bullet 10^{-3}$	G	0.99	$1.82 \bullet 10^{-3}$	VS
2,3-DHdOT	1.96	$2.77 \bullet 10^{-3}$	G	0.97	$1.36 \bullet 10^{-3}$	G

Table 20 **Influence of the chain length of 2,3-dialkoxy-tetracenes 2 on gel formation (solvent: hexanol)**

In hexanol the critical chain length again is C_6 (at 2 g/L, for 2,3-DHOT (**110**) $5 \bullet 10^{-3}$ mol/L) also, proving that the choice of the solvent, when gel formation is possible, is only of secondary importance.

This result is in good agreement with the idea of "dry gels". This term explains a gel formation that unlike in the case of steroid gelators (see Chapter 2.2.2) includes no solvent molecules gelator structures.[1a] This mode of gel formation is common in the case of 2,3-DDOA (**1**), and for this reason could be expected for other acene gelators as well.

In summary the inverted tube test provides a first insight into the gel forming efficiency of the different 2,3-dialkoxy-tetracenes **2**. Furthermore, it allows a broad scan of solvents. The minimum chain length for gel formation is around C_6, while the critical concentration is in the range of 1 to $10 \bullet 10^{-3}$ mol/L. On the average one molecule of gelator thus immobilizes 2000 molecules of solvent. Even though the described technique is very useful, it should be mentioned that no precise information on the structure of the gel formation or its thermodynamics can be derived.

To get these results, further measurements are necessary.

3.1.2 Spectroscopic examination of the gel formation

For a more detailed investigation of the gel structure UV/Vis spectroscopic measurements often prove to be helpful. Tetracenes are colored compounds, showing good absorption in the visible range. Furthermore, as shown by the work of Bouas-Laurent et al., 2,3-DDOA gels exhibit solid state structures, giving a distinct bathochromic shift of the UV/Vis absorption upon gel formation.[53] As the same mode of gel formation can be suspected for 2,3-dialkoxy-tetracene **2** gelators, similar changes in the UV spectrum of the gelator can be expected.

For 2,3-DDOA (**1**) in methanol, the following changes have been observed: the first absorption band (300-400 nm) possesses a well resolved fine structure with defined vibronic maxima at λ = 338, 347, 365 and 385 nm. Especially the last of those vibronic bands (probably corresponding to the 0-0 transition) shows an apparent bathochromic shift ($\Delta\nu$ = 700 cm^{-1}). Those two features point to a great loss of freedom of orientation for the molecules in the gel.[53]

The UV/Vis spectra of 2,3-DDOT (**86**) and 2,3-DHdOT (**111**) in different solvents were measured to gain a more detailed insight in the temperature/concentration dependence of the gel formation. Furthermore, to have the spectral properties of a fully immobilized gelator, the spectrum of 2,3-DHdOT (**111**) in solid KBr was determined (see Figure 24).

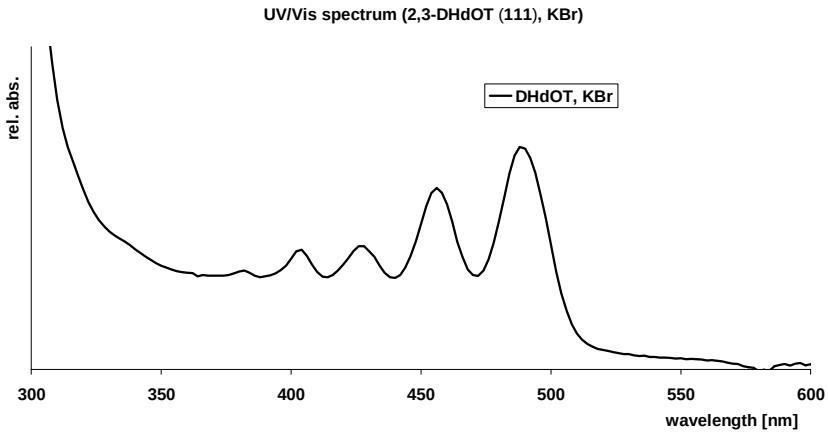

Figure 24 **UV/Vis spectrum of 111 in solid state (KBr-pellet)**

Only the bathochromic absorption (deriving from excitation to the first excited state) is shown in Figure 24. Like in the case of 2,3-DDOA (**1**), a well structured absorption is shown with λ = 382, 404, 426, 456 and 488 nm, the last absorption probably corresponding to the 0-0 transition with the highest degree of "allowedness" and by this the highest excitation.

The spectrum was taken, using 0.2 mg of 2,3-DHdOT (**111**) in a KBr pellet and measured using a pure pellet as a blind.[54]

This spectrum is compared with the spectrum of 2,3-DHdOT (**111**) in isotropic solution as well as in the gel state (see Figure 25) by taking temperature dependent UV/Vis spectra of the gelator in appropriate solvents.

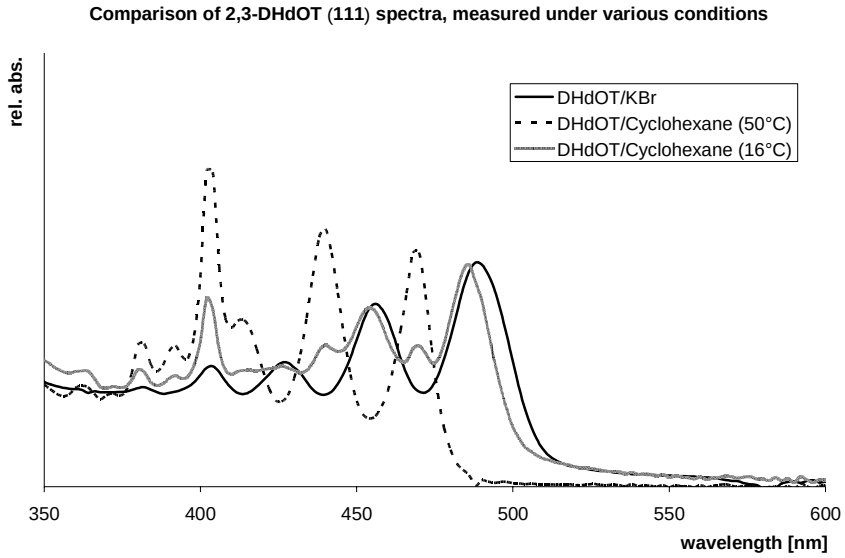

Figure 25 **Comparison of 2,3-DHdOT (111) absorption spectra, measured under various conditions**

The temperature dependent measurements were carried out with the following technique: A precisely weighed sample of the gelator was diluted with the appropriate amount of solvent to reach the desired concentration. The sample was then treated in an ultrasound bath and warmed to complete dissolution of the gelator. The solution was transferred in a 1 mm UV/Vis cuvette which was closed to prevent solvent evaporation. The UV/Vis measurements were carried out in a water heated cell holder. The temperature was measured using a Pt thermocouple, measuring the temperature in a copper spacer directly adjacent to the 1 mm cuvette. At each temperature point (see thermodynamic measurements Chapter 3.1.3), the temperature was kept for 3 min to equilibrate the sample prior to taking the corresponding UV/Vis spectrum.

Figure 25 shows the spectral changes when going from the isotropic state to the gel state. The gel spectrum resembles the one takes in solid state: the most bathochromic absorption of the isotropic solution (λ = 470 nm) is shifted to λ = 486 nm. This equals a shift of $\Delta\bar{\nu} = 701\text{cm}^{-1}$, resembling the value found for 2,3-DDOA (**1**) in methanol.[53] This is a first indication that the modes of gel formation for 2,3-DDOA (**1**) and 2,3-DHdOT (**111**) are similar.

It is a further advantage of the UV/Vis technique that, as indicated above, different temperatures can be measured for one sample. So the half melting points and the half formation points can be determined for different gelators, solvents and concentrations as presented in the following chapter.

3.1.3 Thermodynamic data of the gel formation

The thermodynamic properties of the different gelators (2,3-DDOT (**86**), 2,3-DHdOT (**111**) and mixtures of 2,3-DDOA (**1**)/2,3-DDOT (**86**) (see Chapter 3.4)) in different solvents were calculated from the temperature dependent UV/Vis spectra of the solutions at different concentrations. The full graphical data are presented in Appendix I B. In this chapter, only an illustrating example and the results will be presented.

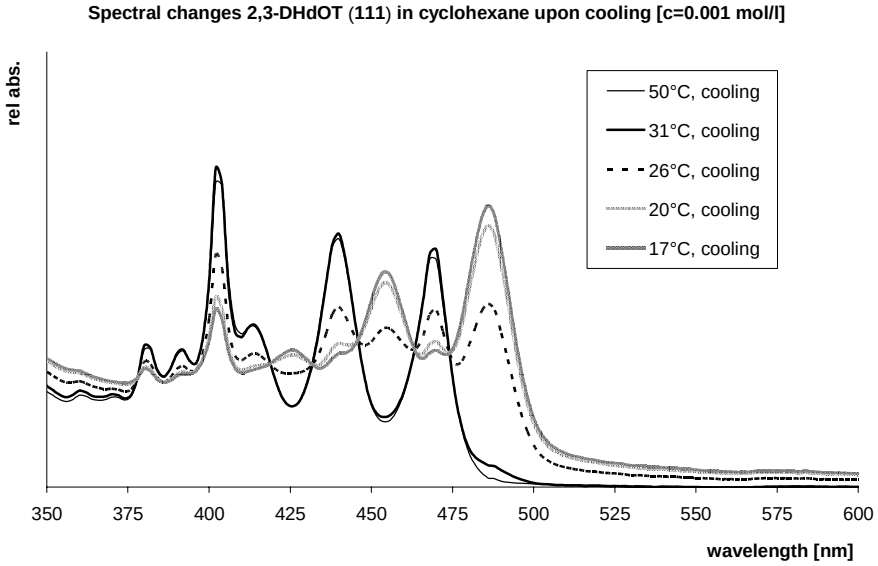

Figure 26 **Spectral changes upon cooling a sample of 2,3-DHdOT (111) in cyclohexane from 50 ° to 17 °C**

Figure 26 shows the beginning of the gel formation (evolution of the absorption at λ = 486 nm) around 31 °C upon cooling a sample of 0.718 mg/mL 2,3-DHdOT (**111**) in cyclohexane. The precise half formation point was calculated on the basis of the optical densities at λ = 486 nm as shown in Figure 27.

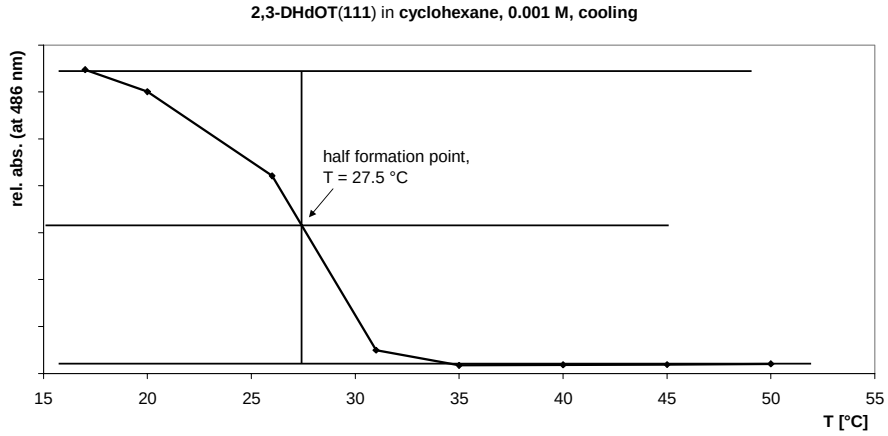

Figure 27 Graphical determination of the half formation point of the gel

Using this graphical method, it is possible to determine the half formation points (and half melting points) with an accuracy of ±2 °C, depending on the applied concentration of the gelator and the quality of the S-curve (*vide infra*).

When the same sample is reheated, the melting of the gel can be observed, leading to the half melting point at a given temperature. It should be noted that the formation of the gel at a given concentration and the melting at the same concentration does not occur at the same temperature, but with a certain hysteresis.

When the procedure described above is applied to different concentrations, a phase transition diagram can be plotted as in Figure 28, which shows the mentioned hysteresis between gel formation and the melting of a gel.

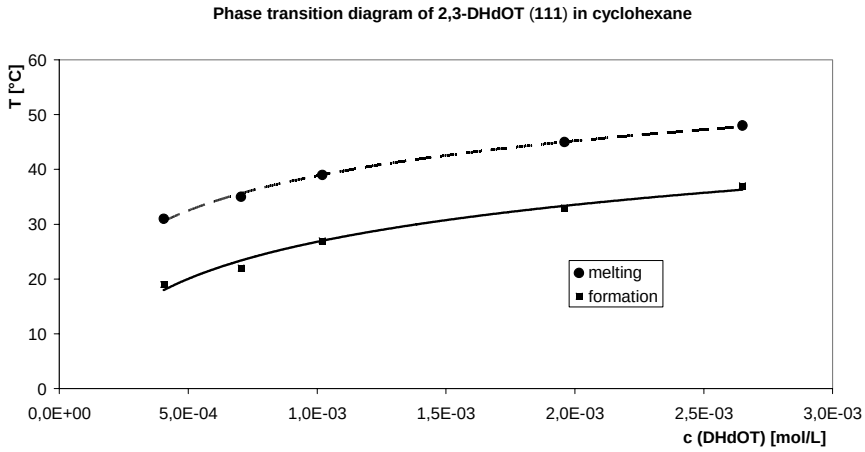

Figure 28 Phase transition diagram (2,3-DHdOT (111) in cyclohexane)

The thermodynamic parameters (ΔH, ΔS and ΔG) can be calculated from the absorption versus temperature data. The absorption at the turning-point of the diagram was transferred into the molar fraction (ϕ), using the Lambert-Beer law and evaluated using Equation 1 and Equation 2.[53]

$$\ln(\phi) = \frac{\Delta H_F}{R} \cdot \frac{1}{T_F} - \frac{\Delta S_F}{R}$$ **Equation 1**

for the formation of the gel upon cooling respectively

$$\ln(\phi) = -\frac{\Delta H_M}{R} \cdot \frac{1}{T_M} + \frac{\Delta S_M}{R}$$ **Equation 2**

for the melting of the gel upon heating

This calculation leads to the following Figure 29

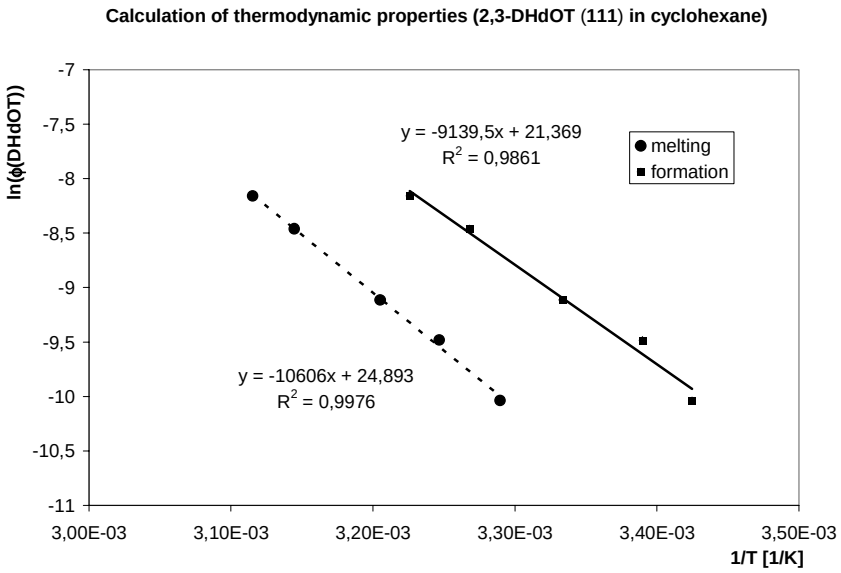

Figure 29 Calculation of the thermodynamic properties of 2,3-dialkoxy-tetracene 2 gels

The thermodynamic analysis was performed for gels composed of 2,3-DDOT (**86**) as well as 2,3-DHdOT (**111**) with cyclohexane and hexanol as solvents. This led to the following results:

substance/ solvent	formation/ melting	ΔH (kJ/ mol)	ΔS (kJ/ mol•K)	ΔG (kJ/ mol)
2,3-DDOT/ cyclohexane	formation	-78	-0,19	-21 (298 K)
	melting	123	0,32	27 (298 K)
2,3-DDOT/ hexanol	melting	73	0,15	28 (298 K)
2,3-DHdOT/ cyclohexane	formation	-76	-0,18	-23 (298 K)
	melting	88	0,21	26 (298 K)
2,3-DHdOT/ hexanol	melting	89	0,19	33 (298 K)

Table 21 Thermodynamic properties of 2,3-DDOT (86) and 2,3-DHdOT (111) (solvent: cyclohexane or hexanol)

For the measurements of the gelators in hexanol, only the melting-data are given. In this case gel formation is in competition with the precipitation of the substance. When cooling the solution slowly (to record the gel formation data), precipitation is favored, while fast cooling leads to the formation of a gel.

Table 21 shows that even though the ΔS and ΔH values differ quite strongly, the ΔG values are rather constant. This is another indication that dry gels are formed and the gel formation is, when taking place, independent of the solvent and depend only slightly on the structure of the acene gelator.

This conclusion is further supported by comparison with the thermodynamic data on the 2,3-DDOA (**1**) gelification, published by Bouas-Laurent et al.[55]

Substance/ solvent	Formation/ melting	ΔH (kJ/mol)	ΔS (kJ/mol•K)	ΔG (kJ/mol)
2,3-DDOA/ heptane	formation	-60	-0,155	-13,5 (298 K)
	melting	92	0,246	18,2
2,3-DDOA/ ethanol	melting	93	0,218	27,6

Table 22 Thermodynamic data of the 2,3-DDOA (1) gel formation

Again, the ΔG values are of the same order of magnitude as the values obtained for the tetracene derivatives (*vide supra*).

It should be mentioned that the described method of determining gel formation and gel melting is not without problems and the thermodynamic data can only be taken approximately.

The difficulties of the method are of principal and of technical nature. In principle the evolution of the UV absorption at 486 nm indicates the formation of solid state structures. This is a necessary but not a sufficient condition for a macroscopic immobilization (gel formation) of the solvent, as sometimes only thickened fluids are obtained with a given concentration of the gelator.

The technical problems, which determine the relative error of the measurements, depend on the solvent used for gel formation and on the concentration of the gelator. Especially when cyclohexane is used, the minimum concentration of the gelator can not be reduced very much, as the melting point of the solvent (6 °C) limits the degree of possible cooling. On the other hand, the spectrometer specifications generally allow only absorptions of around 2-3 until the Lambert-Beer law is not longer followed linearly. This limits the upper amount of gelator that can be applied. The other difficulty, the tendency of the gelator to precipitate in certain solvents when the solution is cooled slowly, has already been mentioned.

These restrictions should be kept in mind, when data of different thermodynamic measurements (e.g. DSC, differential scanning calorimetry, and other UV/Vis or fluorescence techniques) are compared.

Still, the measurements show a reasonable order of magnitude for the thermodynamic properties of gel formation and melting and provide another indication of the mode of gel formation of acene gelators.

3.1.4 AFM-measurements on 2,3-dialkoxy-tetracene 2 gels

3.1.4.1 General introduction to AFM measurements[56]

Atomic force microscopy is one technique from the group of scanning probe microscopy techniques. In this group of techniques, a fine probe (usually a sharp tip) is scanned across a sample surface by means of piezoelectric translators. The signal measured is recorded as a function of the lateral position. Scanning tunneling microscopy (STM) and atomic force microscopy (AFM) have gained the highest importance among the different probe techniques so far.

The AFM can further be defined as scanning force microscopy, as different forces (attractive or repulsive) are the basis of the measurement.

In the AFM, a sharp tip is mounted on a soft lever and it is scanned across the sample surface, while generally the tip is in contact with the surface. The force acting on the tip changes according to the sample topography, resulting in a varying deflection of the lever. The deflection is measured by means of laser beam deflection and detected by a double segment photodiode.

As cantilevers silicon nitride with integrated pyramidal tips (base 4µm×4µm, height 4µm) is commonly used, displaying a nominal radius of curvature of the tip apex of 20 to 50 nm. Ideally, the tip is terminated by a single atom.

Two measurement modes can be applied, the contact mode and the tapping mode (explained later). In the contact mode, the AFM tip always touches the sample surface. This leads to an interatomic repulsive force at the contact area due to penetration of the electronic shells of the tip and substrate atoms. In addition, long-range forces (Coulomb, dipole-dipole etc.), which can be attractive or repulsive, can occur but only the varying repulsive interatomic force allows high-resolution imaging of surfaces. The measurements can be operated in two different force modes, the constant force mode and the constant height mode, depending on the sample roughness and sample size. In the constant height mode, a higher scan rate can be achieved, but the danger of destruction of the tip on the surface ("tip crash") is higher.

In the tapping mode, the cantilever is vibrated above the sample surface in such a way that the tip is just slightly tapping the surface while scanning across it. In this way the force load can be reduced significantly and shear forces that could scratch off material can practically be

eliminated. In the tapping mode AFM, the surface topography is accessible by monitoring the oscillation amplitude of the cantilever, which is influenced by the damping due to tip-sample interaction.

The analytical potential of the AFM technique is based on the following possibilities:

1) On the one hand, atomic resolutions can be achieved, on the other hand imaging on areas larger than 100µm square is possible. This can be used to zoom in on details with high resolution without changing the sample.

2) AFM images contain direct depth information which is important for roughness determinations and can be displayed in topography images.

3) As no conducting surface is necessary, further sample preparation can be avoided (which could lead to artifacts introduced by the coating process).

4) In situ measurements (even under liquids and in air) and short measurement times allow direct observation of surface processes with high resolution.

All those advantages can be used to get a further insight in the structures that form the acene gels.

3.1.4.2 Sample preparation and measurements

All AFM measurements were carried out at the Laboratoire de Physico-Chimie Moléculaire, (CNRS, UMR 5803) Université Bordeaux 1, by Mme. Colette Belin.

Direct measurement of the surface of a freshly prepared gel (2,3-DHdOT (**111**) or 2,3-DDOT (**86**) in alkanes or long chain alcohols) was not possible due to shrinking of the gel after formation on a mica-surface. This shrinking leads to exclusion of solvent on the surface, thus crashing the tip of the AFM cantilever on the solvent surface in both, contact or tapping mode.

To get insight of the structures formed, measurements on xero gels were carried out. Those xero gels were produced by heating a solution of the gelator (between 0.4 and 1.0 mg per mL) in the chosen solvent until complete dissolution. This solution was applied on a freshly cleaved mica surface and the solvent was slowly allowed to evaporate while cooling to room temperature. After this procedure the samples were generally measured in the tapping mode (low or high resolution) to prevent scratching of the sample surface.

Measurements were carried out, using 2,3-DDOT (**86**) in butanol or nonane and 2,3-DHdOT (**111**) in nonane, which gave the best results. In the second case, especially when low concentrations were applied, single fibers of the gelator could be grown on the surface.

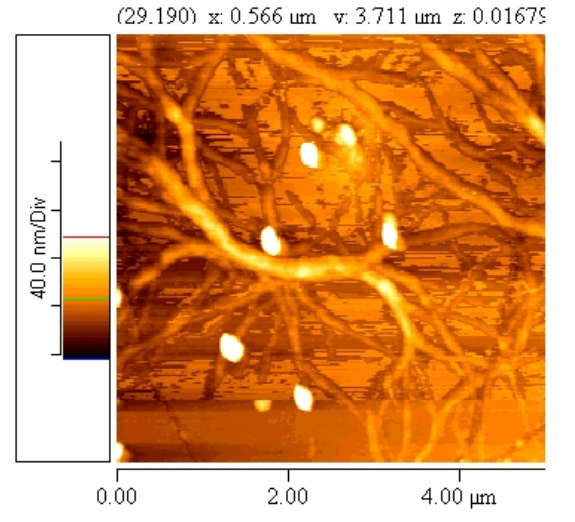

Figure 30

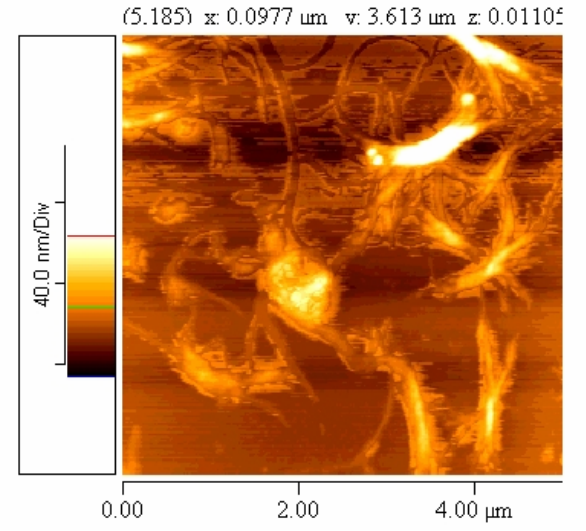

Figure 31

Figure 30 shows an AFM picture of 2,3-DDOT (**86**) in nonane (0.4 mg/ mL) in the size of 5×5 µm and a height profile of 160 nm ranging from white to black. Even though bundles of fibers can be seen, the tendency to aggregate (and by this to precipitate) is still strong. Figure 31 shows the same sample after treating the sample in a vacuum oven for some minutes at 80 °C. The structures shown before are collapsed to larger bundles.

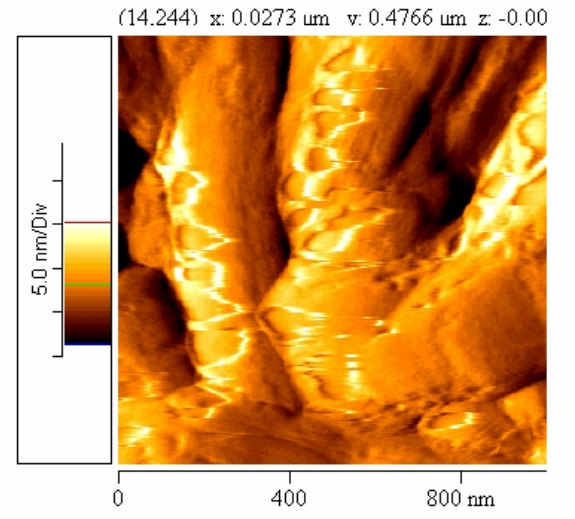

Figure 32

Figure 32 shows a sample of 2,3-DDOT (**86**) in butanol (0.5 mg/mL) in the size of 1×1 µm and a height profile of 25 nm ranging from white to black. Even though thick structures can be observed, butanol is not the solvent of choice for the investigation if the fine structures formed in the gel and probably present in gels formed at low concentrations. It was chosen because the slower evaporation should make the formation of gels (prior to evaporation of the solvent) easier.

The measurements on 2,3-DDOT (**86**) had shown the possibility of gaining further insight in the gel forming structures. To have a better estimation of the size of these structures (if possible by examination of single strands) more diluted samples of 2,3-DHdOT (**111**) in nonane were measured.

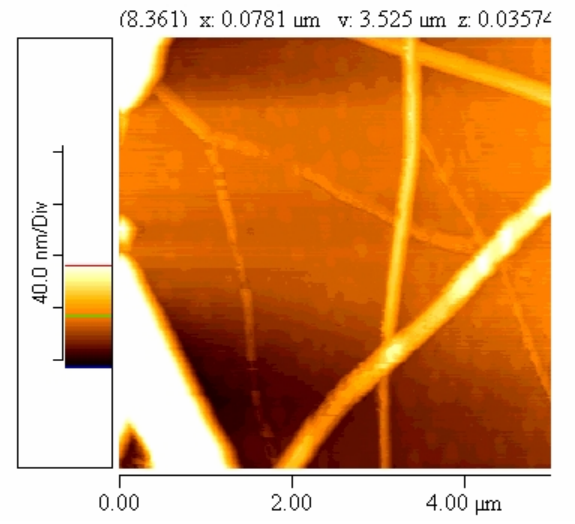

Figure 33

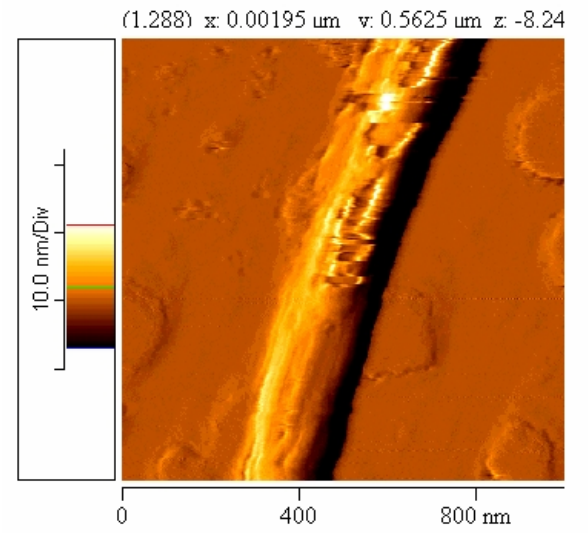

Figure 34

Figure 33 shows a sample of 2,3-DHdOT (**111**) in nonane (0.5 mg/mL) in the size of 5×5 µm and a height profile of 160 nm ranging from white to black. Next to large fiber bundles (lower left part of the picture) some small fibers and fiber ramifications can be detected. One of those small fibers was selected for further investigation in Figure 34. Here, the size of the small fibers can be estimated to be in the range of 200 nm (diameter) and several µm (length).

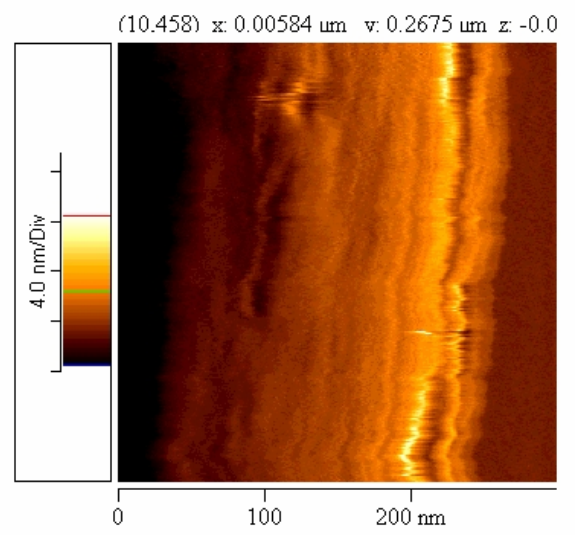

Figure 35

The single fiber shown in Figure 35 was chosen for high resolution (low voltage) measurements to see how the fiber is further structured. Figure 35 shows some finer substructure along the length axis of the fiber. The fiber exhibit a length of 100-200 nm and a width of around 20 nm. Further measurements have to be made to go to molecular levels. When the calculated data for 2,3-DHdOT (**111**) are considered (length approximately 3 nm, width approximately 0.5 nm) it can be estimated that the observed deformation corresponds to several 2,3-DHdOT (**111**) molecules.

In summary the AFM measurements on 2,3-DHdOT (**111**) and 2,3-DDOT (**86**) show that 2,3-DHdOT forms at low concentration a very distinct network of fine fibers, while 2,3-DDOT shows a stronger bundled structure. The thickness of a single fiber of 2,3-DHdOT can be as low as 200 nm in diameter.

3.2 2,3-Dialkoxy-pentacenes 74

Two major problems limit the examination of the 2,3-dialkoxy-pentacene **74** gel formation. The extremely low solubility in most solvents and the high instability of the 2,3-dialkoxy-pentacenes **74** when dissolved and exposed to oxygen.

This restricts especially quantitative measurements, as generally a minor part of the gelator decomposes upon heating, even if Ar saturated solvents are used.

3.2.1 Inverted tube tests

All solvents for inverted tube tests have to be purged with argon to prevent decomposition of the sample. Even though, a slight decomposition can not be prevented, leading to only rough values of critical concentrations in the inverted tube tests (see Appendix I A).

Gel formation was only observed in high boiling halogenated solvents like chloroform and 1,1,2,2-tetrachloroethane, the second being the best solvent for gel formation with 2,3-dialkoxy-pentacenes **74** so far. Furthermore, only 2,3-DHdOP (**115**) has shown gel forming ability, so far.

3.2.2 UV/Vis measurements

UV/Vis measurements of pentacene gels were not possible, again because of the instability of the 2,3-dihexadecyloxy-pentacene (**115**). To have at least some insight into the UV spectroscopy of the formed structures, UV spectra in solid KBr were measured for comparison with the spectrum in isotropic solution.

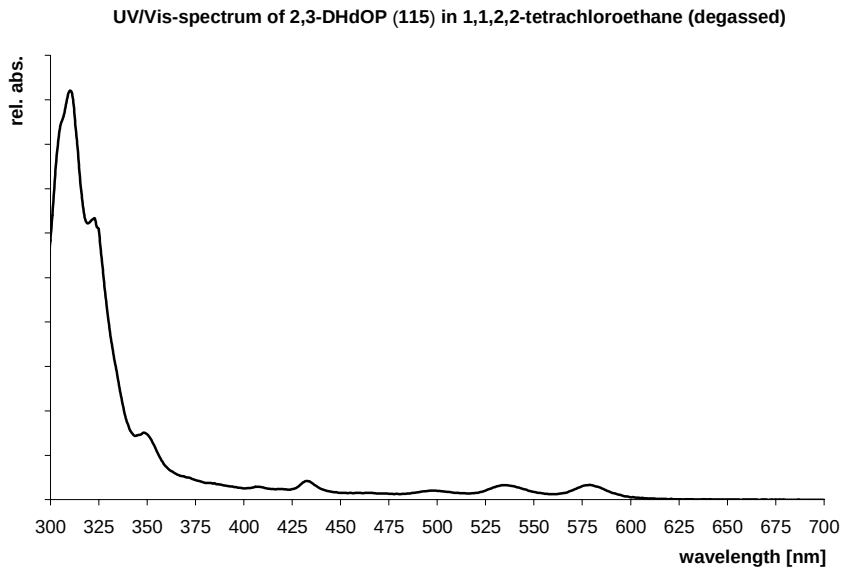

Figure 36 UV/Vis spectrum of 2,3-DHdOP (115) in 1,1,2,2-tetrachloroethane (degassed)

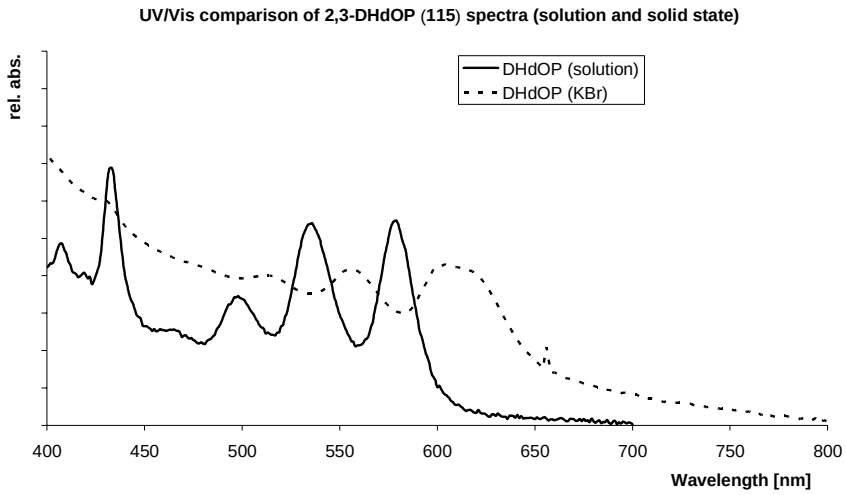

Figure 37 **UV/Vis spectrum of 2,3-DHdOP (115) in KBr compared to the spectrum in isotropic phase**

Again, like in the case of 2,3-DDOA (**1**) and 2,3-DHdOT (**111**) (*vide supra*), a bathochromic shift upon formation of solid structures can be observed. The longest wavelength absorption, probably corresponding to the 0-0 transition, is shifted from λ = 579 nm in the isotropic solution to (around) λ = 604 nm in the solid state. This is equivalent to $\Delta\bar{\nu} = 715$ cm^{-1}, roughly the value found for gel formation of the other mentioned gelators. The same mode of dry gels can be assumed, although a definitive proof still has to be found.

3.2.3 AFM-measurements

The sample preparation in the case of 2,3-DHdOP (**115**) (for the AFM measurements in chloroform), is much less facile and the results are ambiguous.

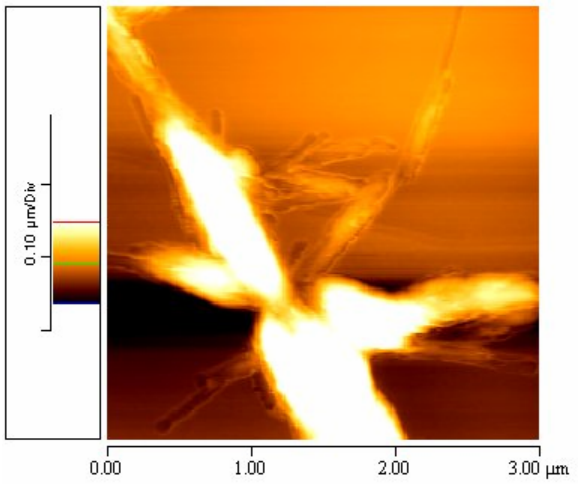

Figure 38

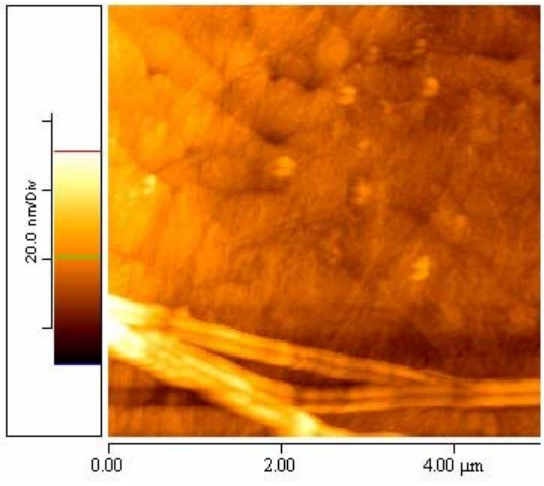

Figure 39

Figure 38 shows a sample of 2,3-DHdOP (**115**) in chloroform (size 3×3 µm) with a height profile of 200 nm ranging from white to black. Next to some crystalline fibers, a star like precipitation can be observed. In Figure 39, a different part of the same sample shows (as in the case of the 2,3-DHdOT (**111**) measurements) rodlike structures, but of much larger dimensions (diameter around 400 nm).

These AFM measurements of 2,3-DHdOP (**115**), are only of exploratory nature and further investigations (if possible under inert conditions) are clearly desirable.

3.3 Comparison of gel forming acenes (2,3-DDOA, 2,3-DDOT/ 2,3-DHdOT, 2,3-DHdOP)

In summary, gel formation of the different 2,3-dialkoxyacenes is characterized by the following features:

The mode of gel formation involves dry gels, meaning that no solvent is incorporated into the structures formed by the gelator.

The gel formation can be monitored with UV/Vis spectroscopy by a distinct bathochromic shift of the 0-0 vibrational absorption of the lower energy band. This shift is nearly independent of the gelator and represents the formation of solid state structures as examined by UV/Vis spectroscopy in KBr. With $\Delta\bar{\nu} \approx 700$ cm^{-1} the bathochromic shift is nearly independent of the aromatic core of the gelator.

From UV/Vis spectra, taken at different temperatures and concentrations, thermodynamic data of the gel formation and (to a wider extent) gel melting process could be derived.

Examination of the microscopically formed structures by AFM measurements lead to a first impression of the size of the formed structures, which is in the range of 200 nm (diameter).

One major difference of the three known classes of 2,3-dialkoxyacenes is the type of solvents, with which gels are formed (short chain alcohols for 2,3-DDOA (**1**), hydrocarbons for 2,3-DHdOT (**111**) and high boiling halogenated solvents for 2,3-DHdOP (**115**)). Another difference, even though expected, is the optimal chain length for gelification (C_{10} for anthracenes, C_{16} for tetracenes, C_{16} [and probably longer] for pentacenes).

3.4 Mixed gels between 2,3-DDOA (1) and 2,3-DDOT (86)

One advantage of the acene gelators is the fact that the spectroscopic properties as well as the gel forming properties can be varied, depending on the aromatic core.

To investigate whether the addition of small amounts of 2,3-DDOT (**86**) to a solution of 2,3-DDOA (**1**) would interact on the gel formation of the 2,3-DDOA (**1**), further UV/Vis-experiments were performed.

Critical for this experiments were the choice of the solvent and the concentration, both allowing the UV/Vis monitoring of the 2,3-DDOA (**1**) gel formation, while a small amount of 2,3-DDOT (**86**) (still visible in the UV) could be applied.

3.4.1 Spectroscopic examination of the mixed-gel-formation

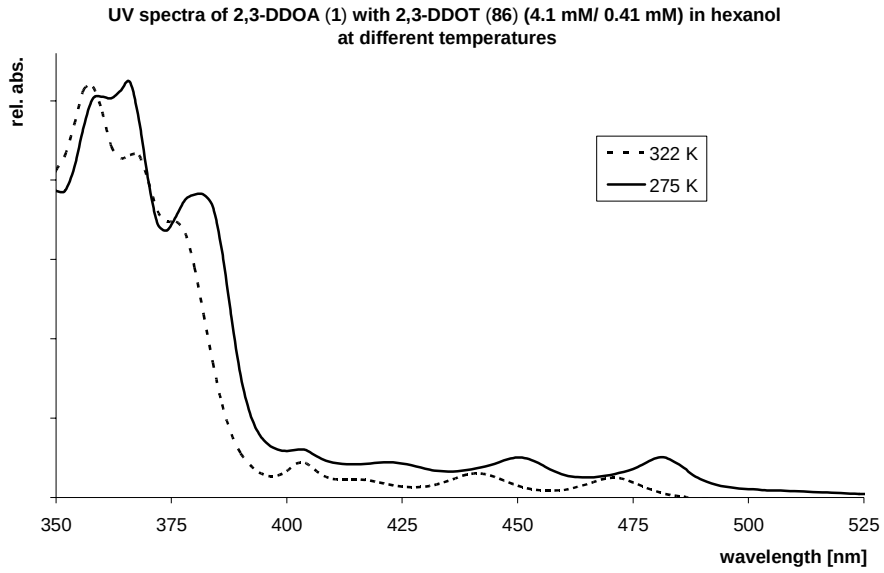

Figure 40 UV/Vis spectrum of a mixture of 2,3-DDOA (1) with 2,3-DDOT (86) (4.1 mM/ 0.41 mM) in isotropic solution and the gel state (solvent: hexanol).

Figure 40 shows the UV/Vis spectra of a solution of 2,3-DDOA (**1**) in hexanol doped with 10 mol-% of 2,3-DDOT (**86**). The solution at 322 K shows the properties of the isotropic solution for both, 2,3-DDOA (**1**) and 2,3-DDOT (**86**). When this solution is cooled to 275 K, characteristic changes of the spectral features as described in Chapter 3.1.2 are found, indicating the formation of solid structures both in the case of 2,3-DDOA (**1**) and 2,3-DDOT (**86**).

When the sample is warmed again, recording the UV/Vis spectra at several temperature points after equilibration, it can be seen that the "half-melting-points" of the anthracene- and the tetracene structures correspond (see Appendix I B). They can be found to be 305 K for 2,3-DDOA (**1**) and 307 K for 2,3-DDOT (**86**).

As DDOA is known to form gels at low concentrations and low temperatures with MCH, the experiment above was repeated with lower concentrations of 2,3-DDOA and 2,3-DDOT, again maintaining the 1:10 molar ratio. The spectra were measured in an Oxford cryostat with electrical heating. Again, a gel was formed at low temperature (220 K) which was then warmed stepwise, until the UV spectrum resembled the one of the isotropic solutions of 2,3-DDOA and 2,3-DDOT (see Figure 41 and Appendix I B for the S-curve of the melting process).

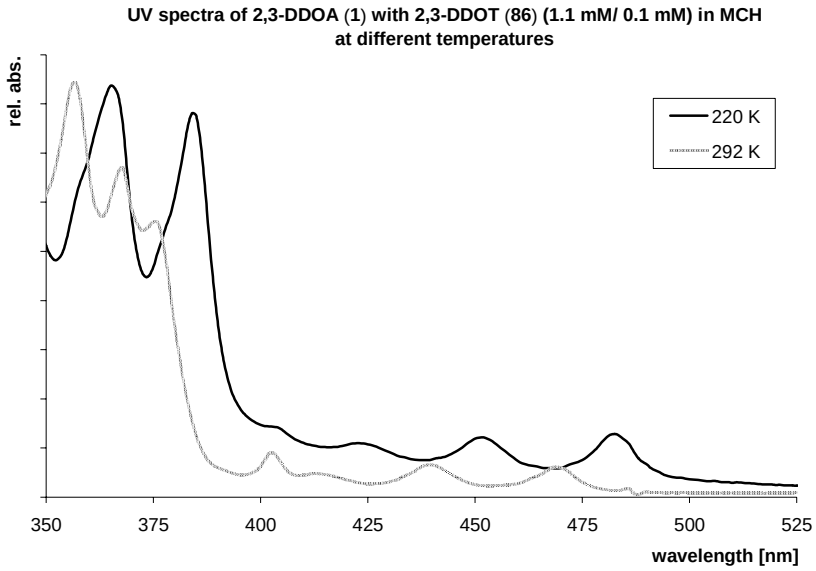

Figure 41 **UV/Vis spectrum of a mixture of 2,3-DDOA (1) with 2,3-DDOT (86) (1.1 mM/ 0.1 mM) in isotropic solution and gel state (solvent: MCH).**

Even under these conditions, the "half-melting-points" of the 2,3-DDOA and the 2,3-DDOT structures respectively, agree well (269 K for 2,3-DDOA and 272 K for 2,3-DDOT).

To conclude the preliminary measurements on cooperative behavior of 2,3-DDOA (**1**) and 2,3-DDOT (**86**), it can be stated that small amounts of 2,3-DDOT (**86**) seem to be incorporated in the 2,3-DDOA (**1**) network when a 2,3-DDOA gel is formed. Still, the field of mixed gels should be further investigated (formation of dry gels of 2,3-DDOA doped with 2,3-DDOT, fluorescence measurements on mixed structures), before the mode of interaction between different acene gelators can be determined. This will be of special interest for the

investigation of energy transfer between the different aromatic cores, one possible application of mixed gels.

4 Photochemistry

4.1 Introduction

While ca. 4000 publications on the photochemistry of anthracenes have appeared in the literature between 1967 and 1998,[4] investigations of the photochemistry of tetracenes are still rare. This is mainly due to the low solubility of tetracene and many of its derivatives. Another problem to be dealt with is the easy oxidation of tetracene compared to anthracene. Last, but not least, the number of substituted tetracenes known today is small, compared to the huge number of substituted anthracenes.

Before the photochemical behavior of substituted tetracenes will be discussed it is instructive to summarize that of the corresponding anthracenes.

Following the Woodward-Hoffmann rules for photochemical reactions,[57] two possible reactions can take place when anthracene is irradiated. The [2+2] photocycloaddition, leading to substituted cyclobutanes, is one possible mode of addition. It is often found in the case of alkene irradiation, but is not found for anthracenes. The other mode is the [4+4] photocycloaddition, leading to tricyclo[4.2.2.$2^{2,5}$]dodecanes. This is the typical reaction of anthracene and substituted anthracenes when exposed to UV light.

Another question of principle interest in the photodimerization of anthracenes concerns the regioselectivity of the photoaddition. Either the center-ring or the outer rings of the anthracene can react to form photoproducts, as illustrated by **79** and **80** (which can form in the shown *syn*-configuration or its *anti*-isomer). A third possibility would lead to a "mixed dimer", resulting from the addition between an outer and the center ring, leading to **81**, shown in Scheme 18.

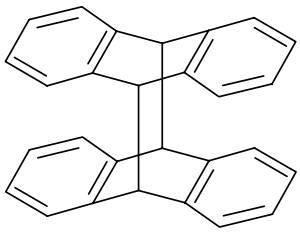

79

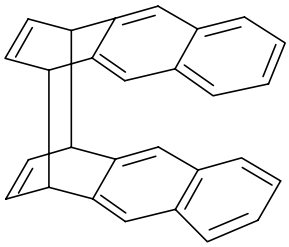

80

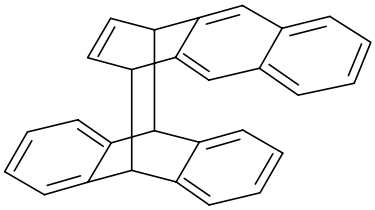

81

Scheme 18 Possible photoproducts of the [4+4] cycloaddition of anthracene

One reason, why anthracenes undergo smooth photocycloaddition, mainly involving the 9,10-positions, is the formation of four benzene subunits. From the thermodynamic point of view, the concept of Hess-Schad resonance energies can be applied, and the photoproducts can be compared with dihydroacenes.[58] This leads to the resonance energy (RE) of 0.78β units in dihydroanthracene compared to 0.66 β units in anthracene.[58] This is in good agreement to the results of anthracene photodimerization, presented in the current literature (*vide infra*).

A dimer of the third type has been described by Desvergne et al. in 1988.[59] The comprehensive examination of alkoxy substituted anthracenes (substitution in the 2,6/ 1,4/ 1,5/ 1,8/ 9,10 and 2,3-position) presented[59, 2, 3] led to the following results:

Three of the differently substituted anthracenes give classical [4+4] dimers of the type **79**. 2,6-Disubstituted alkoxy-anthracenes lead mainly to the 9,10-1',4' product and the 9,10-disubstituted as well as the 2,3-disubstituted derivatives do not give any photodimers. In the case of the 9,10-dialkoxyanthracene, this can be explained by steric hindrance at the most reactive positions.[3] With other substituents at these positions, many photodimers are known.[60, 61] Still, in the case of the 2,3-dialkoxy-anthracenes, this can not be the reason. Some work has been published, examining the photophysical and photochemical properties of 2,3-dialkoxy-anthracenes[62] and it is of some interest to see, if 2,3-disubstituted tetracenes will react similarly.

4.2 General technique

To compare the results of the different irradiations (see Chapter 7.3.5), experiments were carried out under similar conditions. The following problems had to be considered: poor solubility of some tetracenes, danger of photooxidation, possibility of thermal monomerization or monomerization when irradiated at lower wavelength.

Taking the above mentioned problems into consideration, the irradiations of the different alkoxy-tetracenes were carried out in the following fashion: Argon saturated solvent (cyclohexane) to prevent photooxidation, irradiation with a 1000 W halogen lamp through durane glass to filter out the UV part of the light, irradiation in a sealed glass vessel without cooling to solubilize the educts. Only the problem of thermal monomerization could not be eliminated. Therefore, photoproducts and product distribution are those obtained at thermal equilibrium.

4.3 Tetracene (**82**)

Before the results on the photodimerization of substituted tetracenes will be discussed, the major insights from the photochemistry of anthracenes (*vide supra*) will be applied to the photodimerization of the parent hydrocarbon **82**, the only example of a photodimerization of a tetracene up to now.

4.3.1 Possible photoproducts of tetracene (**82**)

Applying the thermodynamic principles on the photochemistry of anthracenes discussed above to tetracene (**82**), only two of six possible photoproducts appear reasonable.

In the case of tetracene/dihydrotetracene the values for the Hess-Schad resonance energies are 0.75 and 0.94 β units, making the photodimerization of tetracene and its derivatives even more favorable than the dimerization of anthracenes.

As the terminating rings are to be considered inert, the possible photodimers of tetracene (**82**) are the centro symmetric dimer (tetracene-D1) (**83**) and the plano symmetric dimer (tetracene-D2) (**84**)

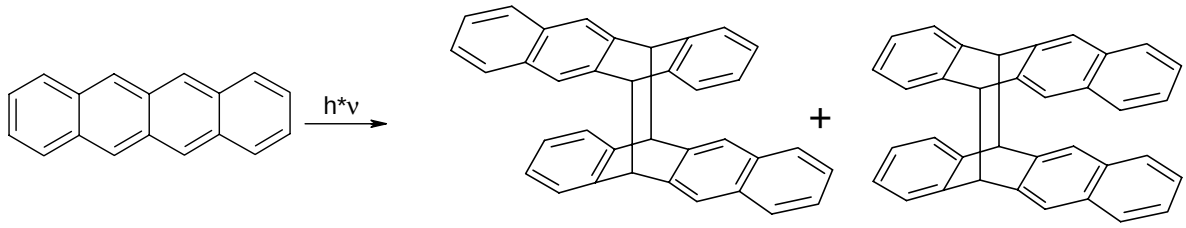

82 tetracene-D1 (**83**) tetracene-D2 (**84**)

Scheme 19 Photodimerisation of tetracene (**82**)

First, only one of these dimers has been reported[63] but Bouas-Laurent et al.[7] have shown that both dimers are formed upon irradiation of tetracene in benzene at boiling temperature, using a 500 W high pressure mercury lamp.

The loss of symmetry, when tetracene is substituted, leads to a greater variety of possible photoproducts. Of special interest in this investigation are two modes of substitution, 5,12-disubstitution, as in **85** and 2,3-disubstitution, as in **86**:

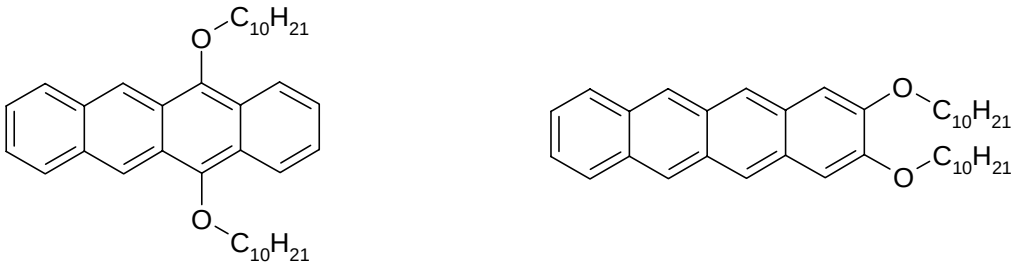

85 **86**

5,12-Dialkoxy-tetracenes can be regarded as homologues of the 9,10-disubstituted anthracenes, which show photocycloaddition depending on the size and electronic effects of the substituents (*vide supra*). On the other hand 2,3-dialkoxy-tetracenes (**2**), are the homologues of the 2,3-disubstituted anthracenes, which are not known to undergo photodimerization until now.

Of some interest are the possibilities to distinguish between the different dimers.

The tetracene dimers and the dimers of substituted tetracenes can be divided in two subgroups, the centrosymmetric dimers (head-to-tail, htt) and the planosymmetric dimers (head-to-head, hth), depending on the relative orientation of the naphthalene- and the benzene subunit.

The best way to distinguish those dimers would be X-ray analysis of single crystals. Application of this technique is problematic, when the photodimers of tetracenes are

examined. In the course of this study, it was not possible to grow single crystals of any dimers (see Chapters 4.3.2, 4.4, 4.5 and 4.6) obtained by irradiation of tetracene or substituted tetracenes.

Other possibilities consist of through space NMR measurements (ROESY) that were used effectively in the case of unsymmetrical dimers (see Chapter 4.6).

A general approach, used in this study is the evaluation of characteristic differences in the UV/Vis spectra or the ^{1}H NMR shifts as described in the individual chapters concerning the photodimerizations.

4.3.2 Irradiation of tetracene (**82**)

The irradiation of tetracene (**82**) on a preparative scale, along with the structural assignment of the two dimers formed, is presented by Lapouyade et al.[7]

It can be seen that the planosymmetric dimer **84** (discovered later) is better soluble than the centrosymmetric dimer **83**, one reason why, until now, no NMR data on **83** are available and the structural assignment was performed by IR spectroscopy and chemical means.[7]

To have access to the two dimers (as reference material to distinguish between the different products obtained by irradiation of mixed samples, see Chapter 4.6), a sample of tetracene (**82**) was irradiated and the reaction mixture separated according to the procedure published by Lapouyade et al.[7]

Only the better soluble **84** could be characterized by one- and two dimensional NMR experiments (HSQC, HMBC). To demonstrate the similarity of the two substances and gain further spectroscopic data, solid state ^{13}C NMR experiments were performed on both **83** and **84**.

Entry	δ (H)	multiplicity	coupling (*J* or *N* [Hz])	correlation
a	7.49	m_c (BB'YY')	*N* = 9.4 Hz	10/7/10´/7´-H
b	7.39	s		11/6/11´/6´-H
c	7.17	m_c (BB'YY')	*N* = 9.5 Hz	9/8/9´/8´-H
d	6.98	m_c (AA'XX')	*N* = 8.7 Hz	4/1/4´/1´-H
e	6.85	m (AA'XX')	*N* = 8.7 Hz	3/2/3´/2´-H
f	4.84	s		12/5/12´/5´-H

Table 23 **^{1}H NMR correlation of tetracene-D2 (84)**

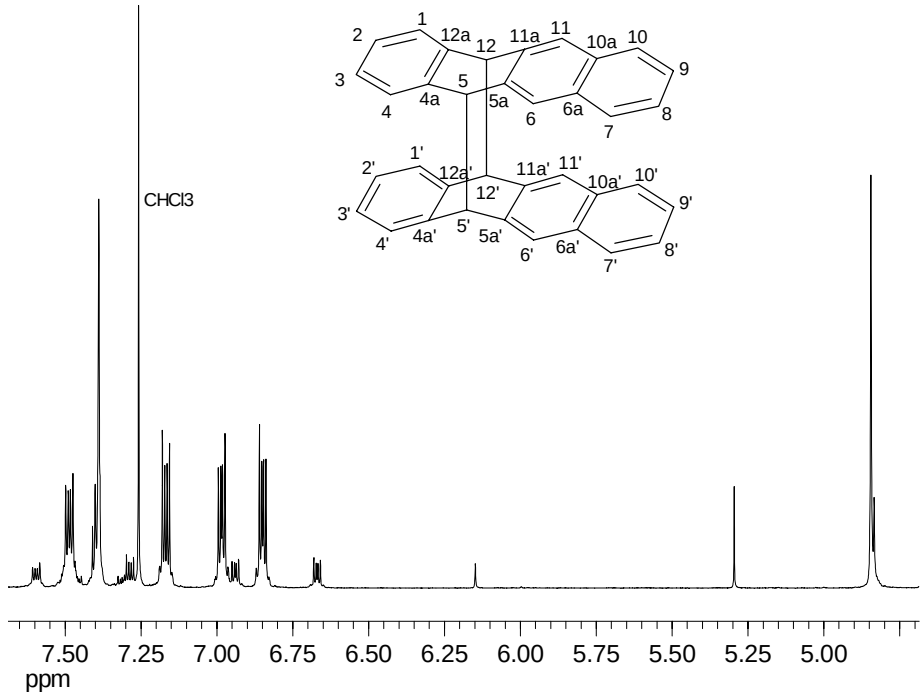

Figure 42 **^{1}H NMR spectrum of 84**

Entry	δ (C)	multiplicity	correlation	HSQC	HMBC
A	143.0	s	C-12a/4a/12a´/4a´	-	d,f
B	141.0	s	C-11a/5a/11a´/5a´	-	b,f
C	132.0	s	C-10a/6a/10a´/6a`	-	a,b,c
D	127.14	d	C-4/1/4´/1´	d	e,f
E	127,12	d	C-10/7/10´/7´	a	b,c
F	125.9	d	C-3/2/3´/2´	e	d
G	125.4	d	C-11/6/11´/6´	b	a,(c),f
H	125.0	d	C-9/8/9´/8´	c	a
I	53.8	d	C-12/5/12´/5´	f	(-)

Table 24 **^{13}C NMR correlation of tetracene-D2 (84)**

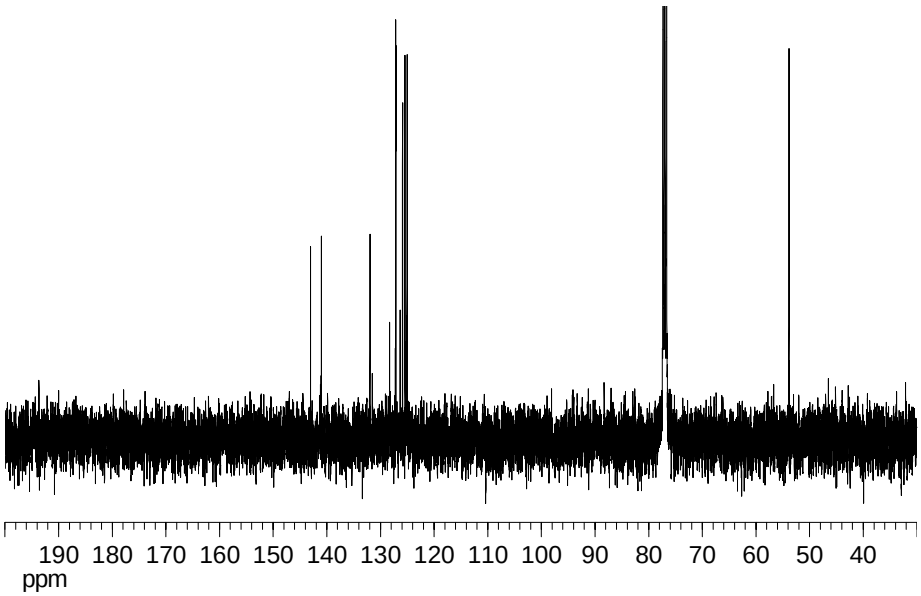

Figure 43 **^{13}C NMR spectrum of 84**

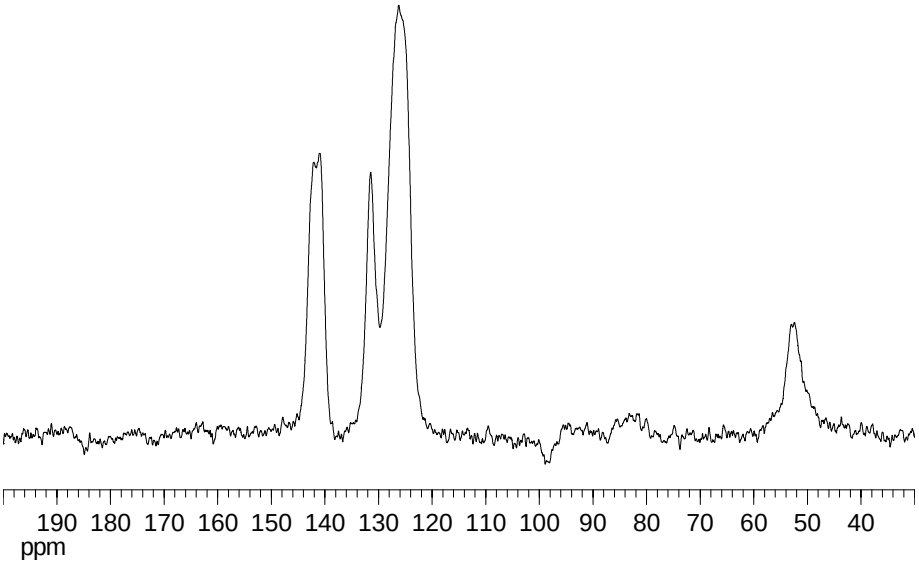

Figure 44 **^{13}C solid state NMR spectrum of 84**

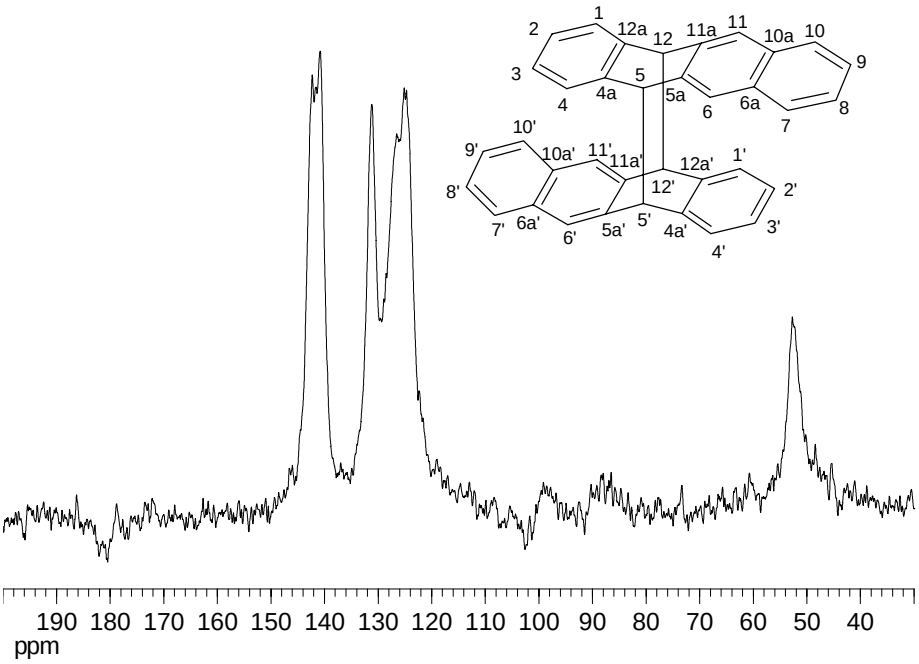

Figure 45 **^{13}C solid state NMR spectrum of 83**

When the spectra of **84** (solution and solid state) and **83** (solid state) are compared, a common main structure can be detected. C-12a/4a/12a´/4a´ and C-11a/5a/11a´/5a´ (signal A and B of the spectrum in solution) are represented in the solid state spectrum of **84** with one signal ranging from δ = 144 to 139 ppm. Signal C of the solution spectrum is represented by a slimmer solid state signal between δ = 133.6 and 129.6 ppm. Signals D-H are not further resolved in the solid state spectrum and lead to one broad signal between δ = 129.6 and 122.0 ppm. the bridgehead C-signal (C-12/5/12´/5´), at 53.8 ppm in the solution spectrum of **84** is resembled in the solid state spectrum by a signal between δ = 55.0 and 50.0 ppm.

The similarity between **84** and **83** can now be deduced from the similarity between the solid state NMR spectra of the two substances as shown in Figure 44 and Figure 45. The spectrum of **83** exhibits the same four signal groups (δ = 145-138.8, 133.8-129.4, 129.4-120 and 54.4-49.5 ppm) as the solid state spectrum of **84**.

Those data assist the data derived from IR and UV/Vis spectra reported in the literature.[7] As **83** and **84** were, until this study, the only photodimers of tetracene, the differentiation between the hth- and the htt dimer were problematic. Some evidence was taken from the difference in solubility (the planosymmetric dimer is better soluble) but the only other spectroscopic measurements performed (UV/Vis and IR spectra) did not lead to further evidence. The main distinction published was performed by chemical means (synthesis and isolation of tetrahydrotetracene-dimers and aromatization of those, comparison to the separated photodimers).[7]

As more tetracene dimers are now available, indirect evidence will be used and applied to the dimers **83** and **84** (*vide infra*).

4.4 2,3-Disubstituted tetracenes

4.4.1 Possible photoproducts

The reduced symmetry of 2,3-disubstituted tetracenes in comparison with tetracene (**82**), leads to an increase of possible photoproducts, even when only the two center rings are considered to react. Again, the products can be subdivided into two groups, head-to-head (hth, the naphthalene subunits of both decks are above each other) and head-to-tail (htt, naphthalene subunits on different sides of the junction). The possible photodimers are presented in Scheme 20. It is likely to assume that both groups of dimers are easily separable by column chromatography, because of the difference in the dipole moments. Still, it might be difficult to separate the members of each group.

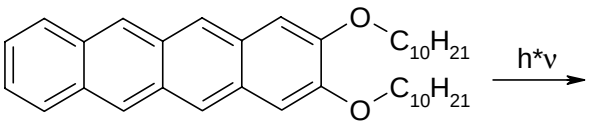

86

Head-to-head-dimers

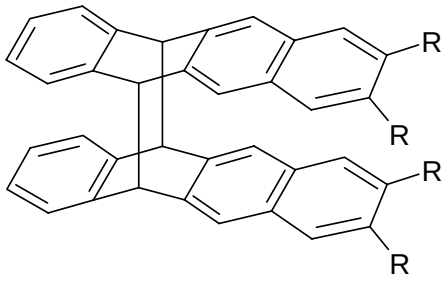

87

Head-to-tail dimers

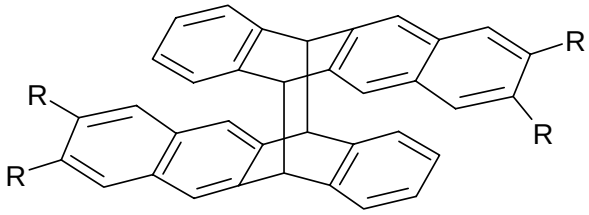

88

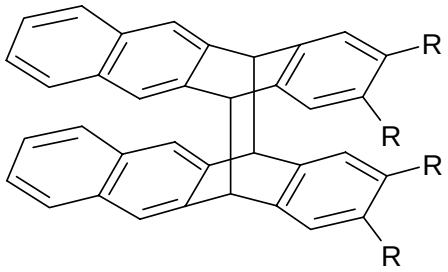

89

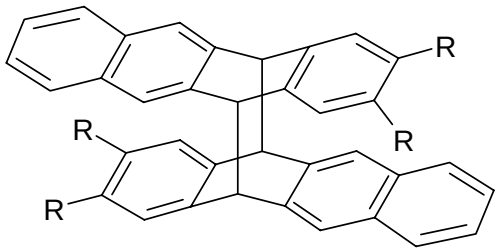

90

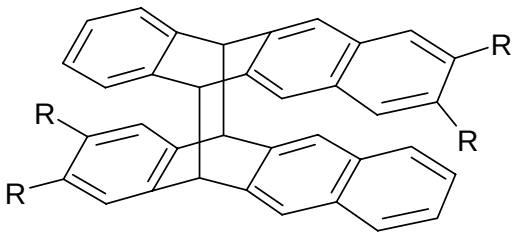

91

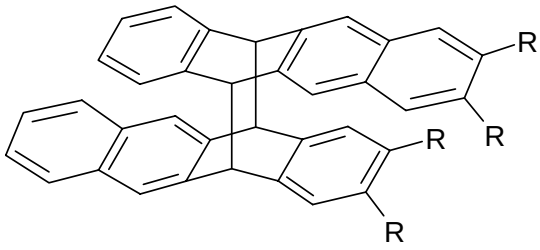

92

Scheme 20 Possible photodimers of 2,3-disubstituted tetracenes (in this study: R = $C_{10}H_{21}$)

4.4.2 Irradiation of 2,3-DDOT (**86**)

When a sample of 2,3-DDOT in cyclohexane is irradiated for 24 h, four dimers could be isolated as the major products, plus a fifth dimer, detected in trace amounts by TLC. The dimers were characterized by one and two dimensional NMR spectroscopy. The spectroscopic data of the dimers are presented below, the distinction between hth and htt dimers is presented in Chapter 4.4.2.1

2,3-DDOT-D1 (**87**)

Entry	δ (H)	multiplicity	coupling (*J* or *N* [Hz])	correlation
a	7.20	s		12/5/12'5'-H
b	6.94	m_c (AA'XX')	*N* = 8.6 Hz	10/7/10'/7'-H
c	6.81	m_c (AA'XX')	*N* = 8.7 Hz	9/8/9'/8'-H
d	6.80	s		4/1/4'/1'-H
e	4.74	s		11/6/11'/6'-H
f	3.94-3.91	m		23/13/23'/13'-H
g	1.80-1.77	m		chain
h	1.44-1.42	m		chain
i	1.31-1.26	m		chain
j	0.89-0.86	m		22/32/22'/32'-H

Table 25 **^{1}H NMR correlation of 87**

Entry	δ (C)	multiplicity	correlation	HSQC	HMBC
A	148.8	s	C-3/2/3'/2'	-	d,f
B	143.6	s	C-10a/6a/10a'/6a'	-	b,c,e
C	139.2	s	C-11a/5a/11a'/5a'	-	a,e
D	127.5	s	C-12a/4a/12a'/4a'	-	a,d,e
E	127.0	d	C-10/7/10'/7'	b	c,e
F	125.6	d	C-9/8/9'/8'	c	b
G	124.0	d	C-12/5/12'/5'	a	d,e
H	107.9	d	C-4/1/4'/1'	d	a
I	68.7	t	C-23/13/23'/13'	f	-
J	53.9	d	C-11/6/11'/6'	e	-
K-R	31.9-22.7	t	chain	-	-
S	14.1	qu	C-32/22/32'/22'	-	-

Table 26 **^{13}C NMR correlation of 87**

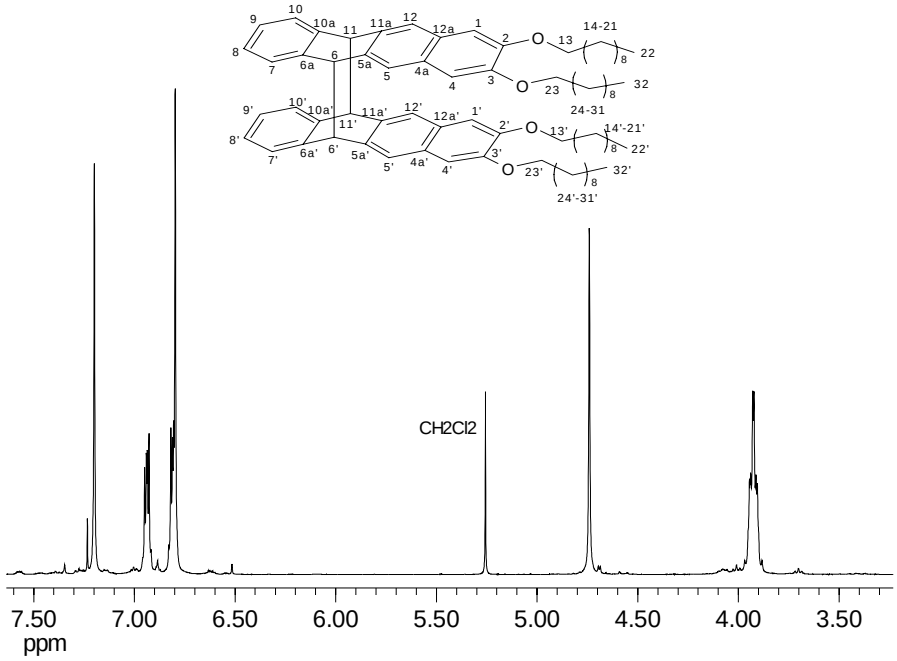

Figure 46 **^{1}H NMR spectrum of 87 (including O-CH$_2$)**

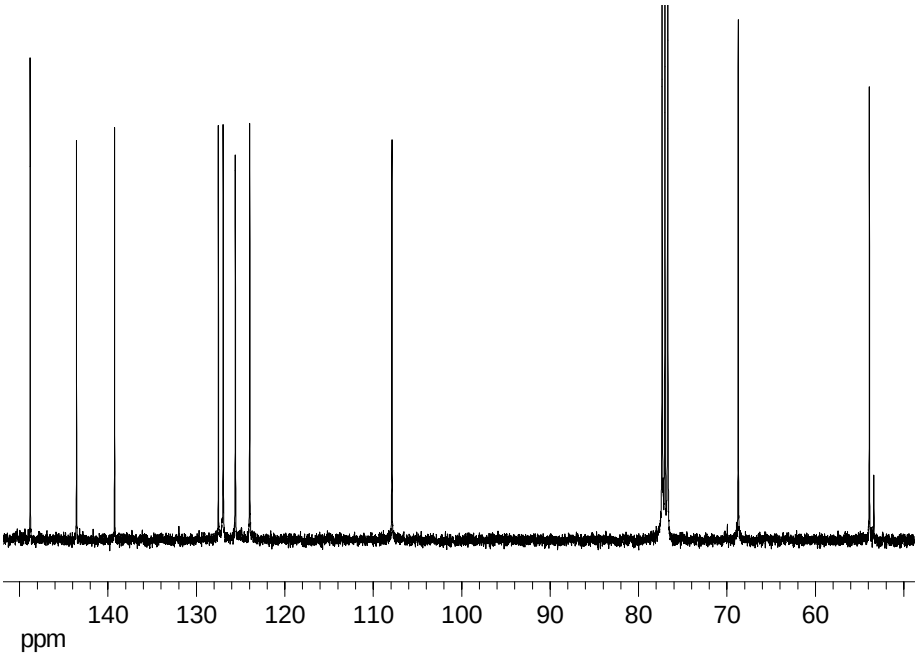

Figure 47 **^{13}C NMR spectrum of 87 (alkyl chains excluded)**

2,3-DDOT-D2 **92**

Entry	δ (H)	multiplicity	coupling (J or N [Hz])	correlation
a	7.57	m_c (AA'XX')	N = 9.4 Hz	10/7-H
b	7.35	s		11/6-H
c	7.27	m_c (AA'XX')	N = 9.4 Hz	9/8-H
d	7.20	s		12'/5'-H
e	6.89-6.87	m		4'/1'-H and 10'/7'-H
f	6.62	m_c (AA'XX')	N = 8.6 Hz	9'/8'-H
g	6.51	s		4/1-H
h	4.69	s		11'/6'-H
i	4.68	s		12/5-H
j	4.03-3.99	m		23'/13'-H
k	3.72-3.68	m		23/13-H
l	1.91-1.82	m		chain
m	1.59-1.44	m		chain
n	1.37-1.25	m		chain
o	0.90-0.86	m		32/32'/22/22'-H

Table 27 **^{1}H NMR correlation of 92**

Entry	δ (C)	multiplicity	correlation	HSQC	HMBC
A	149.0	s	C-3'/2'	-	e,j
B	146.9	s	C-3/2	-	g,k
C	143.2	s	C-10a'/6a'	-	e,f,h,i
D	141.7	s	C-11a/5a	-	b,h,i
E	139.2	s	C-11a'/5a'	-	d,h,i
F	136.1	s	C-12a/4a	-	g,h,i
G	132.0	s	C-10a/6a	-	a,b,c
H	127.7	s	C-12a'/4a'	-	d,e
I	127.10	d	C-10/7	a	b,c
J	127.05	d	C-10'/7'	e	f,h
K	125.6	d	C-9'/8'	f	e
L	124.93	d	C-9/8	c	a
M	124.88	d	C-11/6	b	a,i
N	123.9	d	C-12'/5'	d	e,h
O	115.1	d	C-4/1	g	i
P	108.0	d	C-4'/1'	e	d
Q	69.9	t	C-23/13	k	-
R	68.9	t	C-23'/13'	j	-
S	53.9	d	C-11'/6'	h	d,e,i*
T	53.5	d	C-12/5	i	b,g,h*
U-AE	31.9-22.7	t	chain	-	-
AF	14.1	qu	C-32/32'/22/22'	-	-

Table 28 **^{13}C NMR correlation of 92**

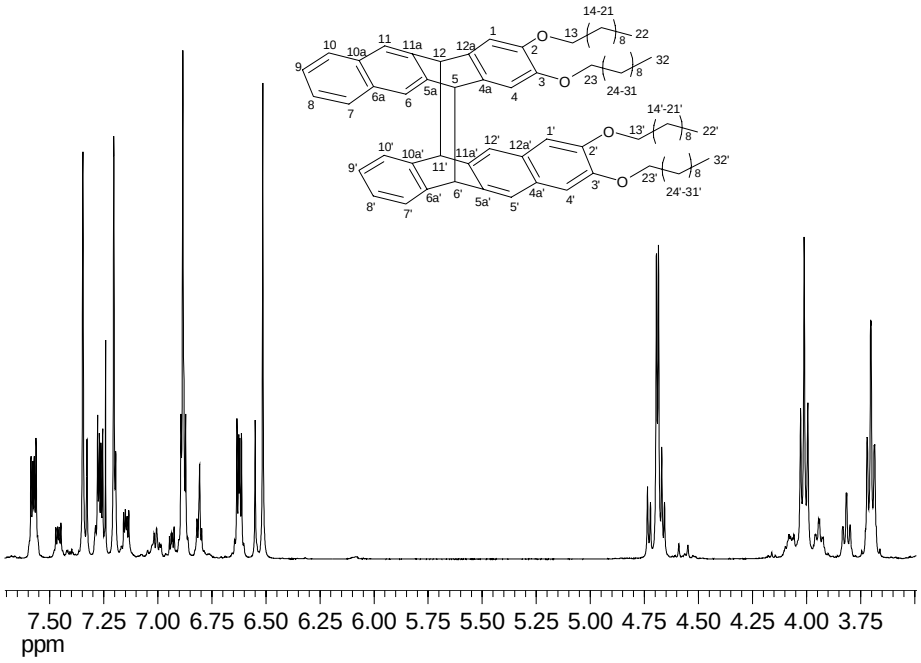

Figure 48 **^{1}H NMR spectrum of 92 (including O-CH_2)**

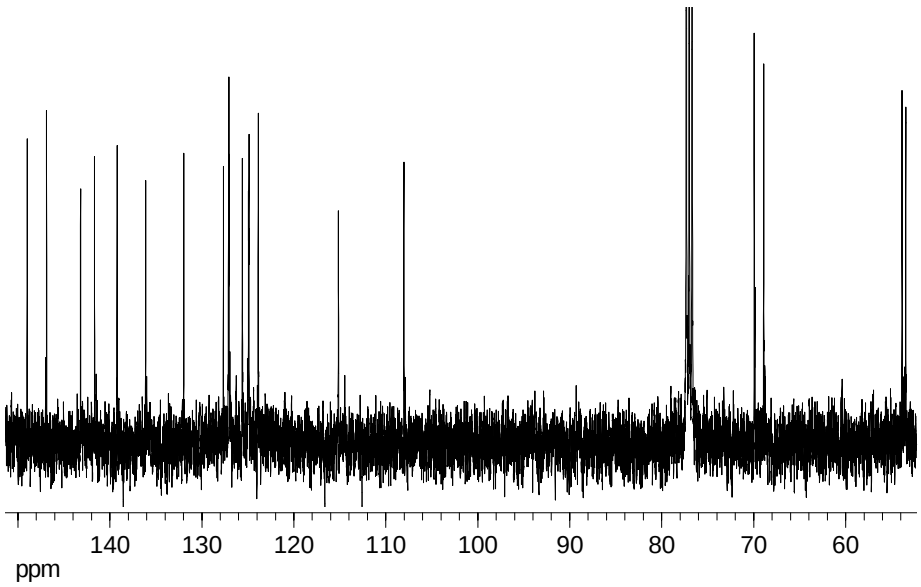

Figure 49 **^{13}C NMR spectrum of 92 (alkyl chains excluded)**

2,3-DDOT-D3 **88**

Entry	δ (H)	multiplicity	coupling (*J* or *N* [Hz])	correlation
a	7.12	s		12/5/12'/5'-H
b	6.83	m_c (AA'XX')	*N* = 8.7 Hz	10/7/10'/7'-H
c	6.81	s		4/1/4'/1'-H
d	6.59	m_c (AA'XX')	*N* = 8.7 Hz	9/8/9'/8'-H
e	4.66	s		11/6/11'/6'-H
f	3.98-3.89	m		23/13/23'/13'-H
g	1.79-1.73	m		chain
h	1.44-1.35	m		chain
i	1.30-1.20	m		chain
j	0.83-0.80	m		32/22/32'/22'-H

Table 29 **^{1}H NMR correlation of 88**

Entry	δ (C)	multiplicity	correlation	HSQC	HMBC
A	148.8	s	C-3/2/3'/2'	-	c
B	143.2	s	C-10a/6a/10a'/6a'	-	b,d,e
C	139.4	s	C-11a/5a/11a'/5a'	-	a,e
D	127.5	s	C-12a/4a/12a'/4a'	-	a,c
E	127.0	d	C-10/7/10'/7'	b	d,e
F	125.5	d	C-9/8/9'/8'	d	b
G	123.8	d	C-12/5/12'/5'	a	c,e
H	107.8	d	C-4/1/4'/1'	c	a
I	68.7	t	C-23/13/23'/13'	f	g
J	53.8	d	C-11/6/11'/6'	e	a,b,(e)
K-R	31.9-22.7	t	chain	-	-
S	14.1	qu	C-32/22/32'/22'	j	i

Table 30 **^{13}C NMR correlation of 88**

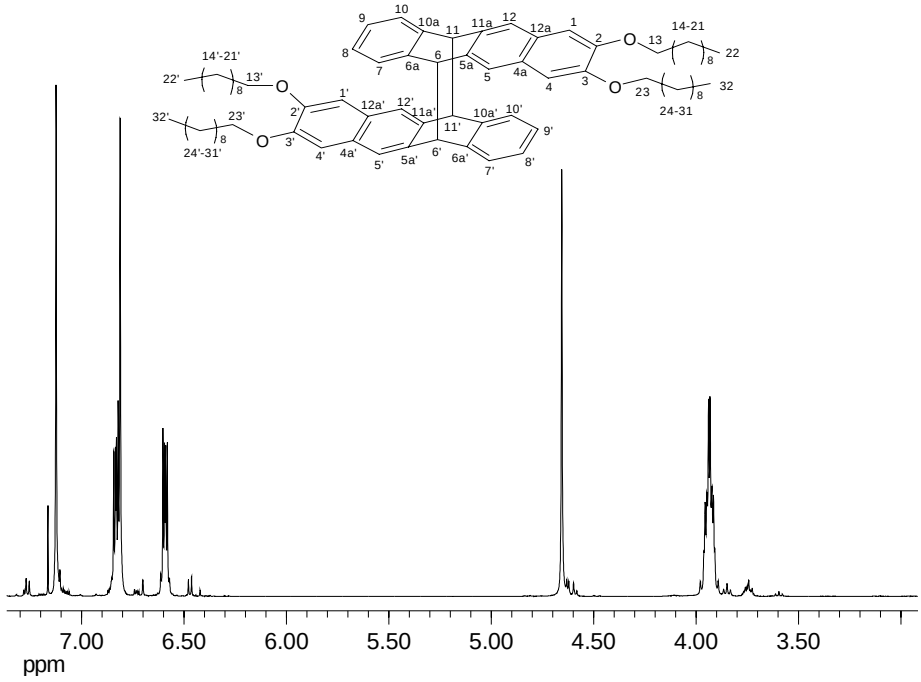

Figure 50 **^{1}H NMR spectrum of 88 (including O-CH_2)**

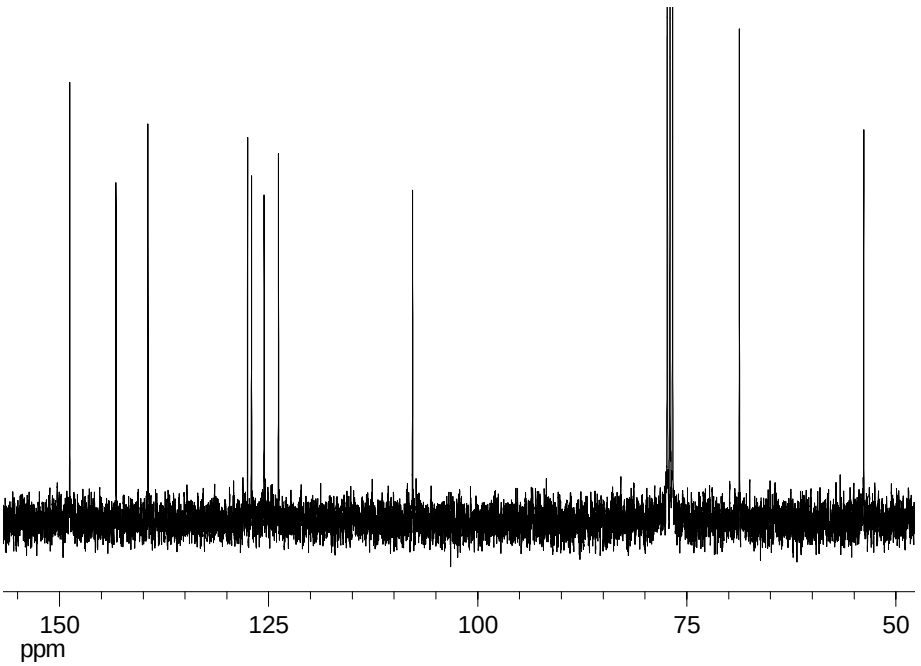

Figure 51 **^{13}C NMR spectrum of 88 (alkyl chains excluded)**

2,3-DDOT-D4 **91**

Entry	δ (H)	multiplicity	coupling (*J* or *N* [Hz])	correlation
a	7.49	m_c (AA'XX')	*N* = 9.4 Hz	10/7-H
b	7.34	s		11/6-H
c	7.18-7.16	m		9/8-H and 12'/5'-H
d	6.93	m_c (AA'XX')	*N* = 8.7 Hz	10'/7'-H
e	6.80	m_c (AA'XX')	*N* = 8.6 Hz	9'/8'-H
f	6.77	s		4'/1'-H
g	6.53	s		4/1-H
h	4.70	s		11'/6'-H
i	4.69	s		12/5-H
j	3.92	t	^3J = 6.7 Hz	23'/13'-H
k	3.84-3.78	m		23/13-H
l	1.79-1.75	m		chain
m	1.69-1.65	m		chain
n	1.42-1.25	m		chain
o	0.90-0.86	m		32/22/32'/22'-H

Table 31 **^{1}H NMR correlation of 91**

Entry	δ (C)	multiplicity	correlation	HSQC	HMBC
A	148.7	s	C-3'/2'	-	f,j
B	146.9	s	C-3/2	-	g,k
C	143.3	s	C-10a'/6a'	-	d,e,h
D	141.5	s	C-11a/5a	-	b,i
E	139.2	s	C-11a'/5a'	-	c,h
F	136.2	s	C-12a/4a	-	g,i
G	131.9	s	C-10a/6a	-	a,b,c
H	127.5	s	C-12a'4a'	-	c,f
I	127.1	d	C-10/7	a	b,c
J	126.9	d	C-10'/7'	d	e,h
K	125.7	d	C-9'/8'	e	d
L	125.0	d	C-11/6	b	a,i
M	124.9	d	C-9/8	c	a
N	124.0	d	C-12'/5'	c	f,h
O	114.9	d	C-4/1	g	i
P	107.8	d	C-4'/1'	f	c
Q	69.9	t	C-23/13	k	-
R	68.7	t	C-23'/13'	j	-
S	53.9	d	C-11'/6'	h	c,d,i*
T	53.5	d	C-12/5	i	b,g,h*
U-AG	31.9-22.7	t	chain	-	-
AH	14.1	qu	C-32/22/32'/22'	-	-

Table 32 **^{13}C NMR correlation of 91**

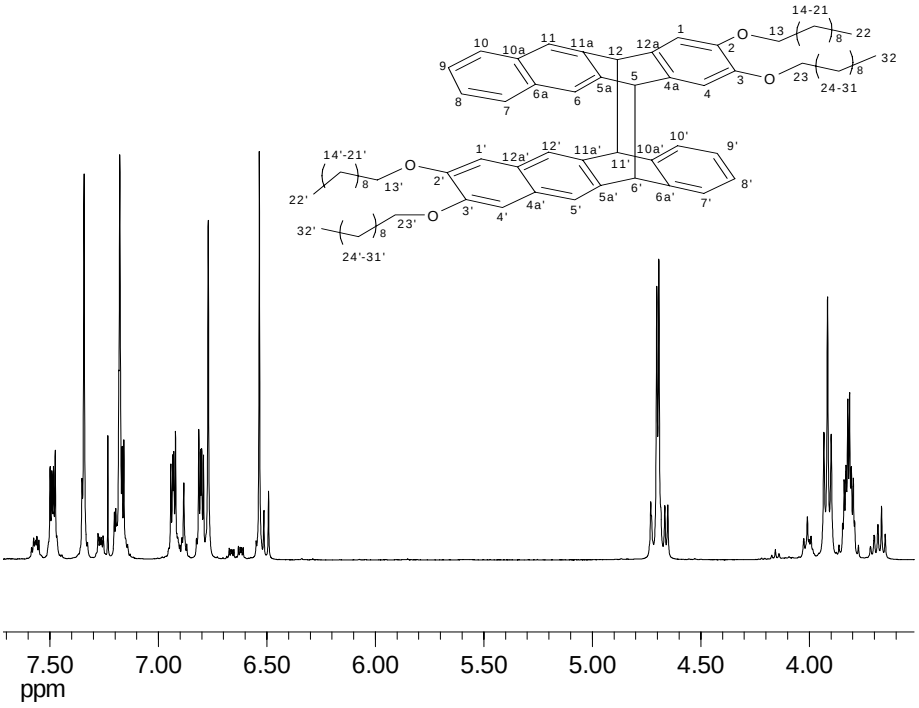

Figure 52 **^{1}H NMR spectrum of 91 (including O-CH_2)**

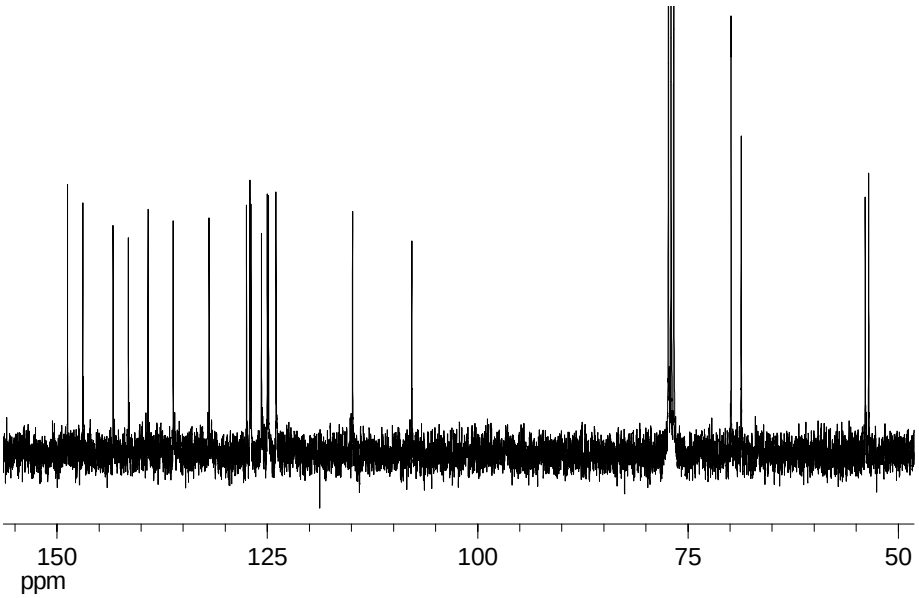

Figure 53 **^{13}C NMR spectrum of 91 (alkyl chains excluded)**

4.4.2.1 Structure elucidation of the photoproducts

The structural elucidation of the 2,3-DDOT photodimers can be divided into two parts. The first task is to determine the structure of the individual decks of the dimers. This information is gained by one- and two dimensional NMR spectra. Thus, the ring undergoing photodimerisation (or the different rings in **91** and **92**) can be determined as well as the question whether a symmetric dimerisation (same rings on both decks) or an unsymmetrical dimerisation took place.

As mentioned in Chapter 4.3.1, the best way to further distinguish the hth- from the htt dimers would be the X-ray analysis of single crystals of the compounds **87**, **88**, **91**, and **92**. This was prevented by the high solubility of the dimers, in addition to the thermal instability leading to monomerization when dissolved. After column chromatography and removal of the solvent, oils were generally obtained that showed slow evolution of the monomer color. The absolute structure of **91** could be derived from ROESY experiments, showing couplings between 4/1-H and 10'/7'-H. Still, it should be noted that ROESY experiments on **87**, **88** and **92** did not lead to comparable through space couplings, providing the full characterization of mixed dimers between 5,12-DDOT (**85**) and tetracene (**82**) (see Chapter 4.6.1.3.1). In the case of the 5,12-DDOT dimers (see Chapter 4.5.3.1) comparison of the shape of the fluorescence spectra led to the absolute structure. The spectra of the 2,3-DDOT dimers are presented in Figure 54.

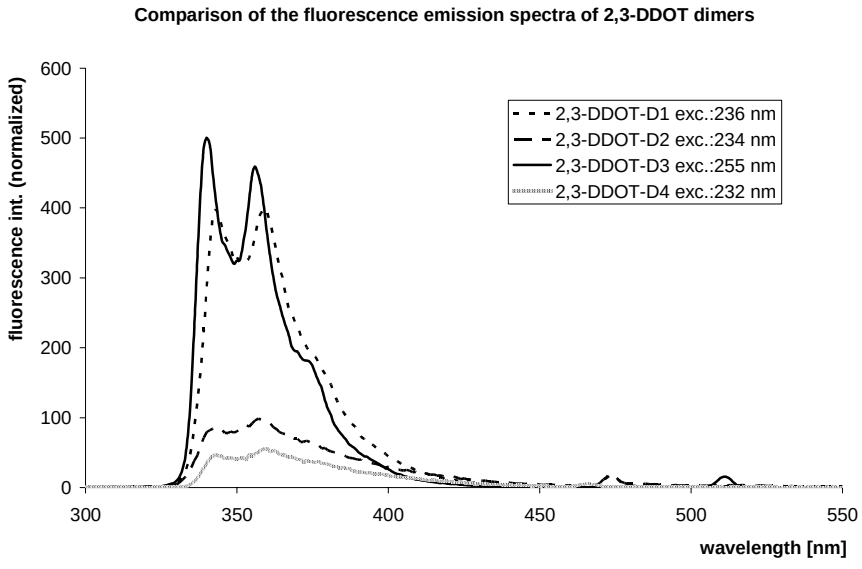

Figure 54 **Comparison of the fluorescence emission spectra 2,3-DDOT dimers 87, 88, 91 and 92**

Figure 54 shows the similarity between the dimers 2,3-DDOT-D1 (**87**) and 2,3-DDOT-D3 (**88**) as well as the similarity between 2,3-DDOT-D2 (**92**) and 2,3-DDOT-D4 (**91**) but no distinct difference between the hth- and the htt dimers is visible, unlike in the 5,12-DDOT case (see Chapter 4.5.3.1).

Another way to distinguish the dimers is the comparison of the UV/Vis spectra of different dimers. Those results will be presented in Chapter 4.7 as they are of general interest to all dimers.

As ROESY experiments did not provide sufficient information for all 2,3-DDOT dimers, the chemical shifts of 9/8/9'/8'-H (**87** and **88**) or 9'/8'-H (**92** and **91**) were used as differentiation. When Figure 46, Figure 48, Figure 50 and Figure 52 are compared, it is obvious, that the H-atoms 9/8/9'/8' respectively 9'/8' are above the naphthalene core of the second deck in the case of the htt dimers. This leads to a shielding of the protons, resulting in a distinct upfield shift as shown in the next table.

hth-photodimers of 2,3-DDOT		htt-photodimers of 2,3-DDOT	
D1 (**87**)	D4 (**91**)	D3 (**88**)	D2 (**92**)
δ (9/8/9'/8'-H)	δ (9'/8'-H)	δ (9/8/9'/8'-H)	δ (9'/8'-H)
6.81 ppm (center)	6.80 ppm (center)	6.59 ppm (center)	6.62 ppm (center)

Table 33 **^{1}H NMR shifts to distinguish the 2,3-DDOT photodimers**

As the respective NMR signals give the same information in all cases of tetracene photodimerization, they were used generally as secondary reference (see following chapters).

4.5 5,12-Disubstituted tetracenes

As mentioned before, 5,12-disubstituted tetracenes are analogues of 9,10-disubstituted anthracenes. The main difference, when photochemistry is considered, is the absorption in the visible range and the presence of two reactive rings, when photodimerization is considered.

4.5.1 Retrosynthesis of 5,12-didecyloxytetracene (85)

As, until now, no 5,12-disubstituted alkoxy-tetracenes are known, a synthetic approach had to be developed.

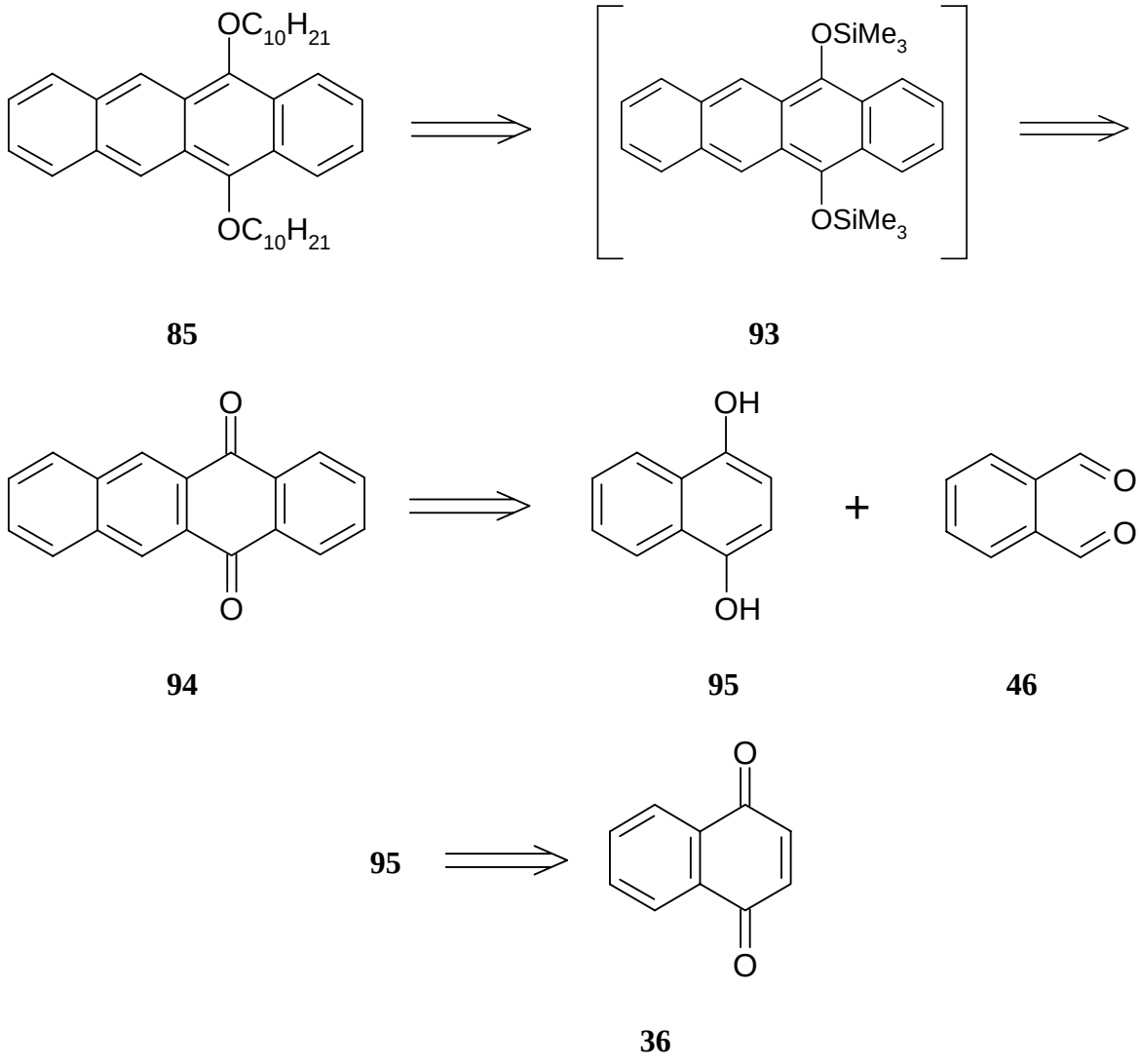

85 **93** **94** **95** **46** **95** **36**

Scheme 21 Retrosynthetic evaluation of 5,12-DDOT (85)

Using the synthesis of 2,3-dialkoxy-tetracenes (**2**) (see Chapter 2), the alkylation of 5,12-dihydroxytetracene would be the synthesis of choice. This intermediate has been published in 1931 by Fieser et al.[64] along with numerous other 5,12-disubstituted tetracenes. The main problem is already presented in this early literature: the low stability towards oxidation. As in the comparison between dihydroacenes and the corresponding acenes,[65] the disruption of the π-conjugation stabilizes the molecule. Therefore acene-quinones are generally more stable than the corresponding *p*-dihydroxy acenes.[58] In order to prevent the reoxidation of 5,12-dihydroxy-tetracene to 5,12-tetracene-quinone (**94**), protection of the free OH function was mandatory. This was accomplished by silylation following the 5,12-bis(trimethylsilyloxy)-tetracene (**93**) synthesis presented by Bouas-Laurent et al. in 1970.[66] The further synthesis contains the preparation of the 5,12-tetracene-quinone (**94**) and the alkylation of the 5,12-bis(trimethylsilyloxy)-tetracene (**93**), as presented in the following chapters.

4.5.1.1 Synthesis of 5,12-didecyloxy-tetracene (85)

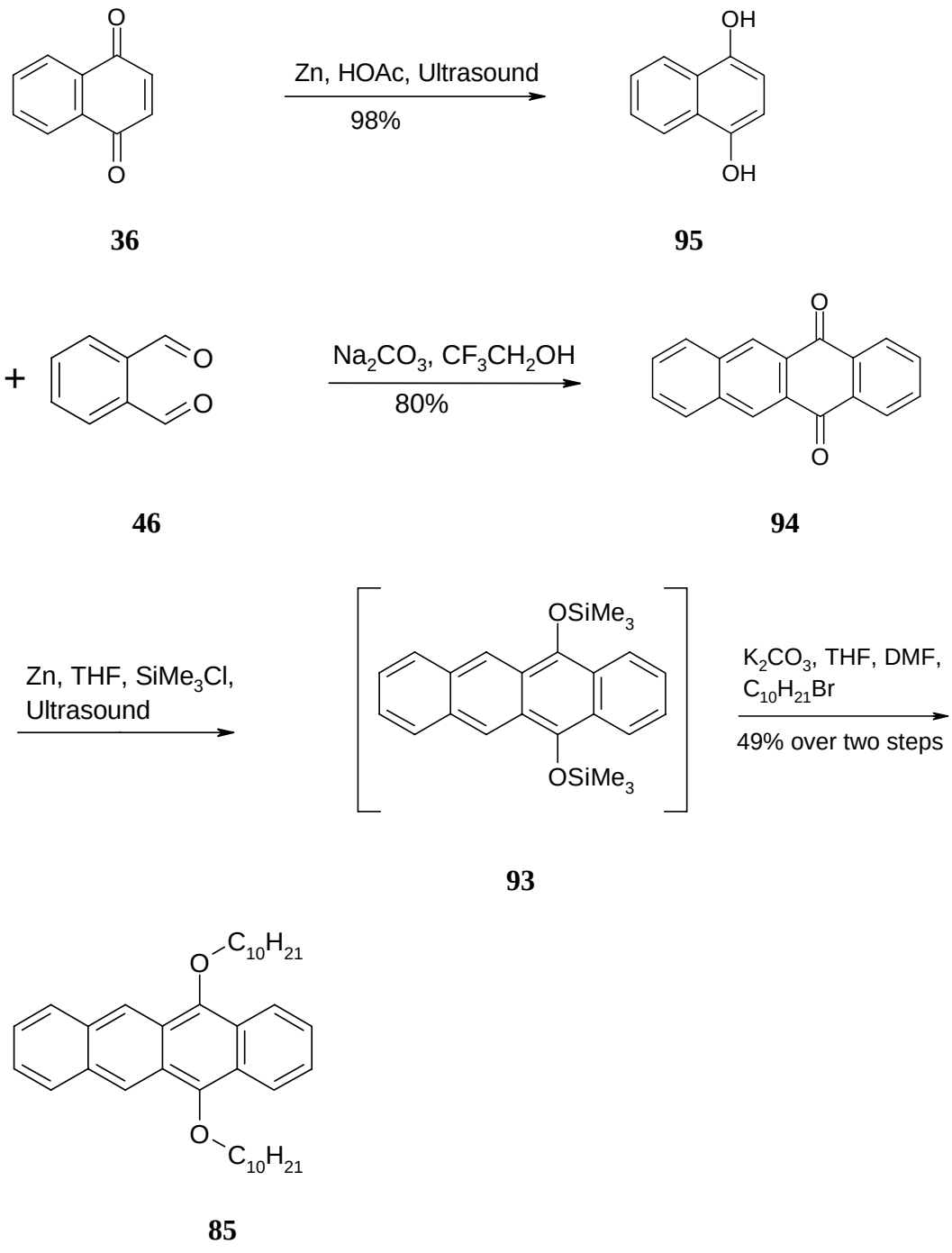

36 **95** **46** **94** **93** **85**

Scheme 22 **Synthesis of 5,12-DDOT (85)**

4.5.1.2 Explanation of the individual synthetic steps

4.5.1.2.1 Synthesis of 1,4-dihydroxy-naphthalene (**95**)

As mentioned in Chapter 2.5.1.3, many procedures exist to reduce naphthoquinones to the corresponding hydroquinones. In the course of this work, Zn/glacial acetic acid under ultrasound conditions was used as described by Marchand et al. in 1991.[24]

The only problem concerning the given procedure is the fast reoxidation of the hydroquinone in solution. This makes purification by column chromatography or recrystallization nearly impossible. The relatively poor solubility of the starting material drives the reoxidation further as the starting material tends to precipitate. Since the reduction proceeds in nearly quantitative yield (see Chapter 7.3.4.1) and traces of the quinone are easily removed on the next reaction step, those problems are not considered further.

The structure of the product was assigned by one- and two dimensional NMR spectroscopy (data not provided in the literature).

Entry	δ (H)	multiplicity	coupling (*J* or *N* [Hz])	correlation
a	8.36	s		OH
b	8.21	m_c (AA'XX')	*N* = 9.8 Hz	8/5-H
c	7.48	m_c (AA'XX')	*N* = 9.7 Hz	7/6-H
d	6.76	s		3/2-H

Table 34 **^{1}H NMR correlation of 95**

Entry	δ (C)	multiplicity	correlation	HSQC	HMBC
A	146.8	s	C-4/1	-	(a),b,d
B	126.7	s	C-8a/4a	-	(a),b,c,d
C	125.7	d	C-7/6	c	b
D	122.8	d	C-8/5	b	c
E	108.6	d	C-3/2	d	(a)

Table 35 **^{13}C NMR correlation of 95**

70 eV mass spectrometry shows [M^+] at *m/z* = 160 as well as a fragment with *m/z* = 131. This can be related to [M^+]-CO-H. In the IR spectrum the OH-absorption is registered at 3267 cm^{-1} and the characteristic quinone absorptions (around 1670 and 1570 cm^{-1}) are absent. This gives further proof to the assigned structure.

4.5.1.2.2 Synthesis of 5,12-tetracene-quinone (**94**)

5,12-Tetracene-quinone (**94**) was first reported as an oxidation product of tetracene (oxidation with fuming HNO_3 in acetic acid) by Gabriel and Leupold in 1898.[67] A rational synthesis had already been proposed in 1931 by Waldmann et al.,[68] using 3-benzoyl-[2]naphthoic acid as a precursor and Friedel-Crafts conditions for the reaction ($AlCl_3$ in NaCl). More recent methods rely on the fusion of two building blocks like 1,4-naphthoquinone with α,α,α',α'-tetrabromo-o-xylene (Cava et al. in 1959[69]) and sodium iodide or 1,4-naphthoquinone with 2-(dimethoxymethyl)benzylic alcohol (Smith et al. in 1983[70]). In the present study, a modification of the synthesis by Serpaud et al was used.[17]

The condensation of 1,4-dihydroxynaphthalene (**95**) with phthalic dialdehyde (**46**) can be accomplished under basic conditions. The synthesis starting from these precursors is favorable as both are either commercially available or easy to prepare in one step from commercially available products (see Chapter 7.3.4.2). Originally, sodium hydroxide was used at high temperature (140 °C) and low pressure (1 torr).[17] This led to the desired product in 70-90% yield, depending on the applied procedure. Working in solution is preferable when working on a large scale, thus sodium carbonate as a base and *2,2,2*-trifluorethanol as solvent, also presented in the article by Serpaud et al.[17] were chosen. The poor solubility of the product is a major driving force of the reaction and facilitates work-up.

As the full characterization of the product is not reported in the original literature, the complete NMR and 70 eV mass spectral data are given here. The coupling constants were, again, calculated iteratively using the WinDAISY software, the relative error of the calculation (R-factor) equals 0.84%.

The ^{1}H NMR spectrum contains four signals of the AA'XX' respectively BB'YY' type.

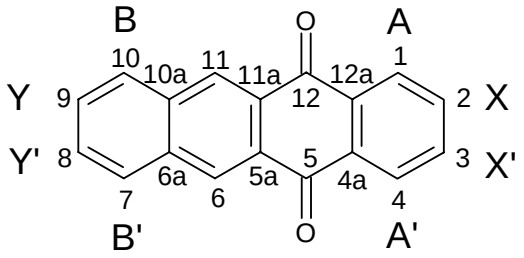

94

4/1-H, (δ = 8.40 (center)), 3/2-H (δ = 7.83 (center)) are showing the following coupling constants: $^{3}J_{AX/A'X'}$ = 7.8 Hz; $^{4}J_{AX'/A'X}$ = 1.3 Hz; $^{5}J_{AA'}$ = 0.6 Hz; $^{3}J_{XX'}$ = 7.4 Hz.

10/7-H (δ = 8.11 (center)), and 9/8-H (δ = 7.71 (center)) are showing the following coupling constants: $^{3}J_{BX/B'X'}$ = 8.3 Hz; $^{4}J_{BY'/B'Y}$ = 1.2 Hz; $^{5}J_{BB'}$ = 0.7 Hz; $^{3}J_{YY'}$ = 6.9 Hz.

As in the case of other acenes (see Chapters 2.5.1.7 and 2.8.1.5) the "inner" protons are deshielded and hence shifted downfield. The ^{1}H NMR spectrum is completed by a singlet for 11/6-H at δ = 8.87, deshielded by the proximity to the carbonyl function in the quinone.

The ^{13}C NMR spectrum shows the most downfield signal, as expected, at δ = 183.0, characteristic for the C=O. Following upfield are the signals for C-10a/a and C-12a/4a at δ = 135.2 and 135.5. The last signal (C-11a/5a, δ=129.8) is less deshielded and separated from the former signals by two H-bearing C-atoms (C-3/2 and C-10/7, δ = 134.2 and 130.1). The spectrum is completed by the other H-bearing C-atom signals at δ = 129.6, 129.5 and 127.5 (C-11/6, C-9/8 and C-4/1).

The mass spectrum shows [M^{+}] at *m/z* = 258 and characteristic fragments at *m/z* = 230 (loss of CO) and 202 (loss of two molecules CO). The IR spectrum displays the expected absorption bands of the quinone system at 1671 and 1578 cm^{-1}, the UV spectrum is dominated by strong absorption bands in the far UV (λ = 238 and 282 nm), the yellow color can be explained by the most bathochromic absorption at λ = 390 nm.

4.5.1.2.3 Synthesis of 5,12-didecyloxy-tetracene (**85**)

As explained in Chapter 4.5.1, the synthesis of 5,12-DDOT **85** starting from 5,12-tetracene-quinone (**94**) is a two step reaction, following a route successfully employed for anthracene derivatives.[71] First the quinone has to undergo a two electron reduction to the stage of the hydroquinone, which is protected by silylation with $SiMe_3Cl$. The reaction is carried out, using Zn in THF under ultrasound conditions to shorten the reaction time (see Chapter 7.3.4.3). To prevent reoxidation, all solvents are saturated with Ar. The progress of the reaction can easily be seen by the deep red color of the product and the increase in solubility (the starting quinone **94** in nearly insoluble in THF). As even the protected hydroquinone is fairly instable (especially in solution), the intermediate is separated from the Zn residue, the solvent as well as the excess of $SiMe_3Cl$ is removed under vacuum and the intermediate is used without further purification or characterization. The next step of the synthesis has again to be carried out with thoroughly Ar purged solvents to prevent reoxidation.

The relatively poor yield (49% over the two steps) can be explained partly by reoxidation (the starting quinone can be detected by TLC as a side product) and by the need to purify the product by several runs of column chromatography. Still, slow decomposition can be detected in the NMR spectra. The product is characterized by one- and two dimensional NMR spectroscopy as well as low- and high resolution 70 eV mass spectrometry.

Entry	δ (H)	multiplicity	coupling (J or N [Hz])	correlation
a	8.90	s		11/6-H
b	8.27	m_c (AA'XX')	N = 10.1 Hz	4/1-H
c	8.03	m_c (BB'YY')	N = 9.8 Hz	10/7-H
d	7.41	m_c (AA'XX')	N = 6.8 Hz	9/8-H
e	7.39	m_c (BB'YY')	N = 7.0 Hz	3/2-H
f	4.26	t	^3J = 6.7 Hz	23/13-H
g	2.15-2.08	m		chain
h	1.75-1.68	m		chain
i	1.55-1.30	m		chain
j	0.91-0.88	m		32/22-H

Table 36 **^{1}H NMR correlation of 85**

Entry	δ (C)	multiplicity	correlation	HSQC	HMBC
A	147.5	s	C-12/5	-	a,b
B	131.2	s	C-10a/6a	-	a,c,d
C	128.7	d	C-10/7	c	a,d
D	125.4	d	C-9/8	d	c
E	124.7	d	C-3/2	e	b
F	124.6	s	C-11a/5a	-	a
G	124.0	s	C-12a/4a	-	b,e
H	122.8	d	C-4/1	b	e
I	121.4	d	C-11/6	a	c
J	76.3	t	C-23/13	f	g
K	31.9	t	chain	i	i,j
L	30.8	t	chain	g	f
M	29.7	t	chain	i	g,i
N	29.6	t	chain	i	i
O	29.4	t	chain	i	i
P	26.3	t	chain	h	f,g
Q	22.7	t	chain	i	j
R	14.1	qu	C-32/22	j	i

Table 37 **^{13}C NMR correlation of 85**

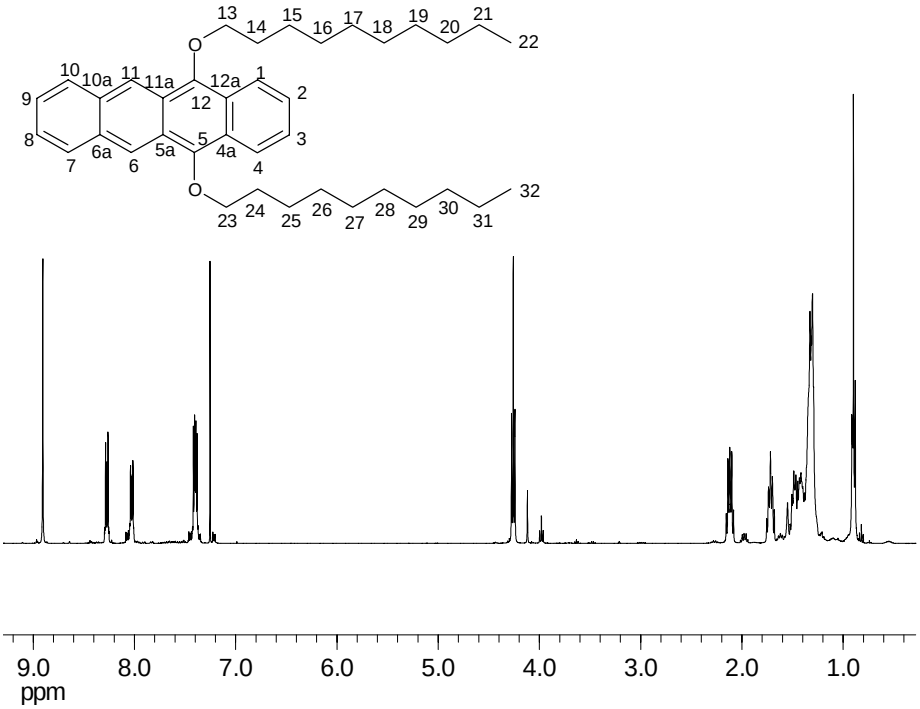

Figure 55 **^{1}H NMR spectrum of 85**

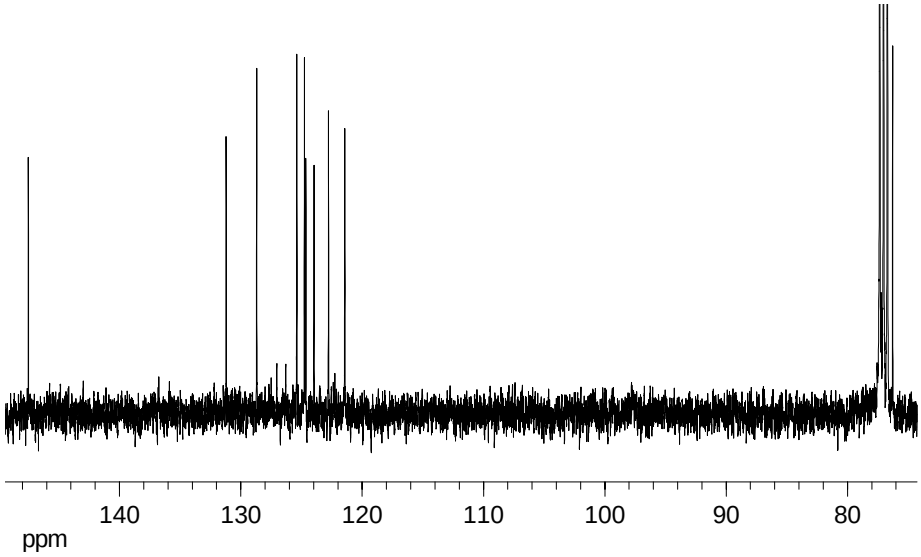

Figure 56 **^{13}C NMR spectrum of 85 (aromatic region, including C-23/13)**

When the ^{1}H NMR spectrum of 5,12-DDOT (**85**) is compared with the spectrum of the precursor (tetracene-5,12-quinone (**94**)), relative and absolute differences can be detected concerning the aromatic part of the molecule. In contrast to the quinone, 9/8-H appears downfield from 3/2-H (*vide supra*). In absolute values, all signals of the hydrocarbon (with the exception of 11/6-H) are shifted upfield, compared to the corresponding signals in the quinone **94**.

Although the ^{1}H NMR spectra of the quinone **94** and the substituted tetracene **85** are similar, this is not the case for their ^{13}C NMR spectra. Not only the carbon atom of the former C=O group is shifted upfield by 35.5 ppm, but the order of appearance of the other signals changes, too (see Chapter 7.3.4.2 and 7.3.4.3).

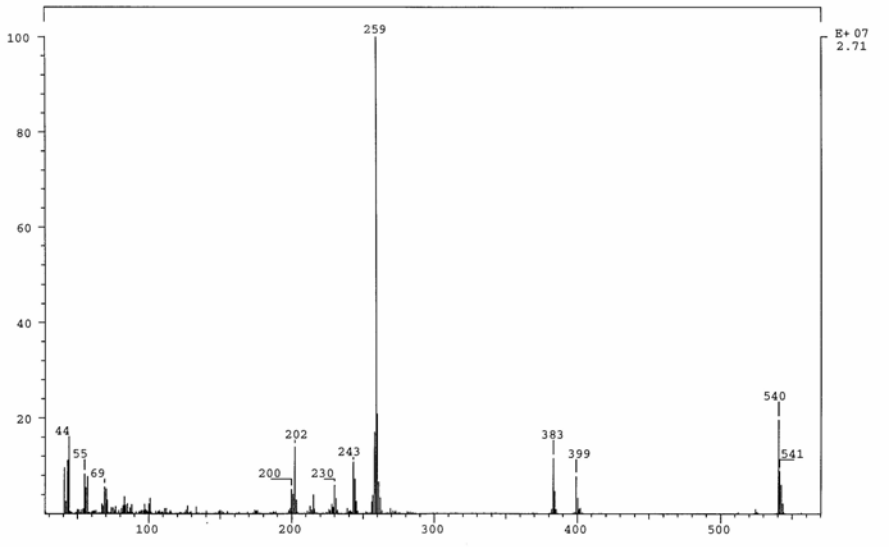

Figure 57 70 eV mass spectrum of 85

The structural assignment is further assisted by 70 eV mass spectrometry, showing [M^+] at *m/z* = 540 and fragments at *m/z* = 399, 383, 259 and 243. These can be explained by successive cleavage of $C_{10}H_{21}$ followed by loss of oxygen. This fragmentation occurs twice, leading to the fragments mentioned above. The IR spectrum shows characteristic bands at 2916 and 2850 cm^{-1} deriving from the CH_2-vibrations. The UV/Vis spectrum exhibits a sharp absorption in the far UV (λ = 285 nm) and a well structured bathochromic absorption in the visible range (λ = 403 to 505 nm), causing the deep red color of **85**.

4.5.2 Possible photoproducts

When the [4+4]photodimerization of 5,12-disubstituted tetracenes is considered, one interesting difference to the unsubstituted tetracene and the 2,3-disubstituted tetracenes is obvious. In this case, two different rings can undergo photocycloaddition, the substituted (in this case electron rich) and the unsubstituted (relatively electron poor). In principle, "mixed dimers" between both modes of dimerization are possible. These "crossed dimers" in the case of anthracenes (i. e. dimerization of anthracene with 9,10-didecyloxy-anthracene) were published by Fages et al.,[72] showing that *para*-dialkoxy substituted rings in anthracenes can undergo photocycloaddition, when the steric demand allows this.

This leads to the following six possible photodimers, again only considering reaction at the center rings.

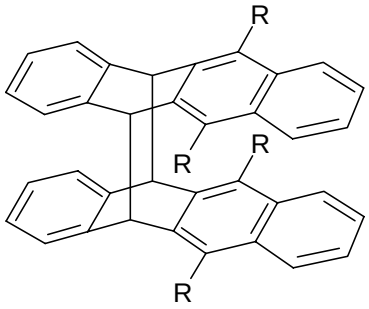

96

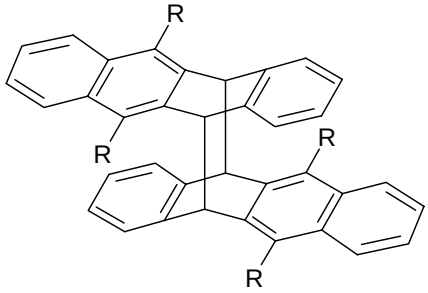

97

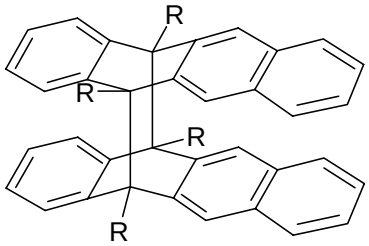

98

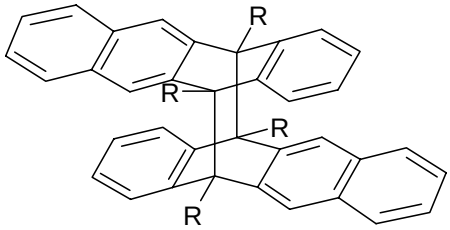

99

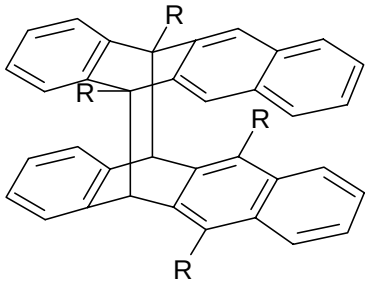

100

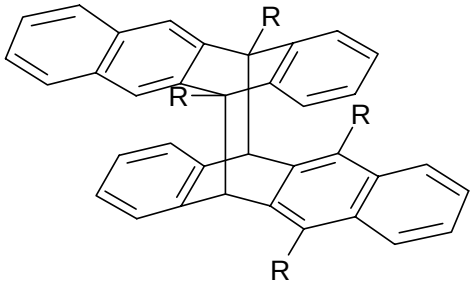

101

Scheme 23 **Possible photodimers of 5,12-disubstituted tetracenes (in this study: R = $OC_{10}H_{21}$)**

4.5.3 Irradiation of 5,12-DDOT (**85**)

5,12-DDOT (**85**) was dimerized by irradiation in Ar-purged cyclohexane. Two photoproducts were obtained and separated by column chromatography. The structures of these dimers were determined by NMR spectroscopy and fluorescence spectra (see Chapter 4.6.1). Further structural data derived from UV- and IR spectra. 70 eV mass spectrometry led to monomerization and only the fragments of the monomer are detectable (see Chapter 7.3.5.2).

5,12-DDOT-D1 (**96**)

Entry	δ (H)	multiplicity	coupling (*J* or *N* [Hz])	correlation
a	7.78	m_c (AA'XX')	*N* = 9.7 Hz	1/1'/4/4'-H
b	7.24	m_c (AA'XX')	*N* = 9.6 Hz	2/2'/3/3'-H
c	6.98	m_c (BB'YY')	*N* = 8.7 Hz	10/10'/7/7'-H
d	6.83	m_c (BB'YY')	*N* = 8.6 Hz	9/9'/8/8'-H
e	5.35	s		11/11'/6/6'-H
f	4.19-4.13	m		23/23'/13/13'-Hα or Hβ
g	3.73-3.65	m		23/23'/13/13'-Hα or Hβ
h	2.04-1.91	m		chain
i	1.71-1.62	m		chain
j	1.54-1.22	m		chain
k	0.97-0.86	m		32/32'/ 22/22'-H

Table 38 **^{1}H NMR correlation of 96**

Entry	δ (C)	multiplicity	correlation	HSQC	HMBC
A	146.9	s	C-12/12'/5/5'	-	a,e
B	143.6	s	C-10a/10a'/6a/6a'	-	c,d,e
C	132.6	s	C-11a/11a'/5a/5a'	-	e
D	127.9	s	C-12a/12a'/4a/4a'	-	a,b
E	127.1	d	C-10/10'/7/7'	c	d
F	125.8	d	C-9/9'/8/8'	d	c
G	125.1	d	C-3/3'/2/2'	b	a
H	122.4	d	C-4/4'/1/1'	a	b
I	75.2	t	C-23/23'/13/13'	f,g	h,i
J	46.7	d	C-11/11'/6/6'	e	c,(e)
K-P	32.0-22.7	t	chain	-	-
Q	14.2	q	C-32/32'/22/22'	k	j

Table 39 **^{13}C NMR correlation of 96**

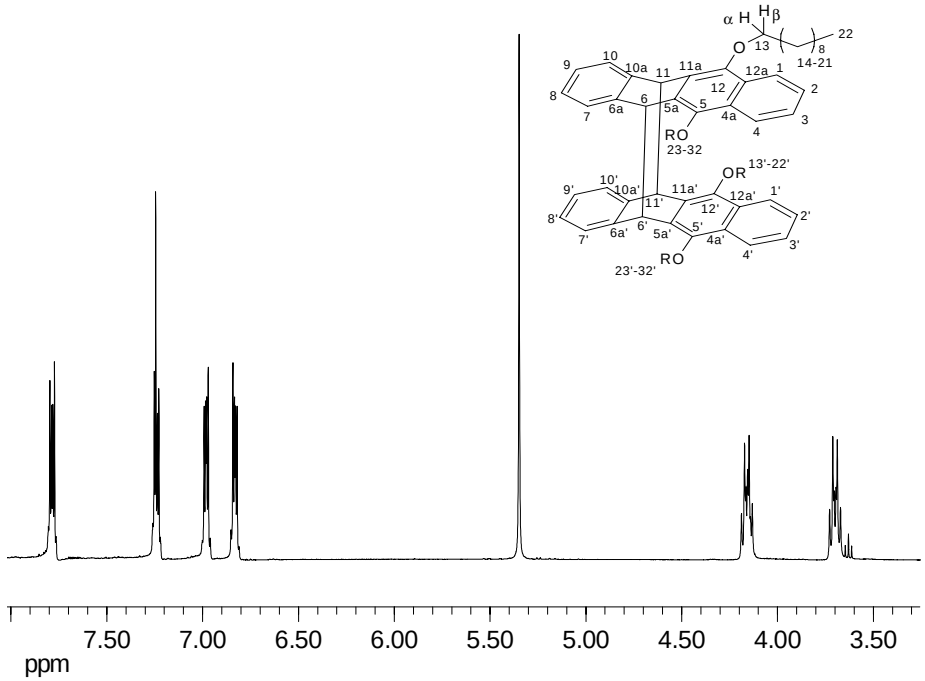

Figure 58 **^{1}H NMR spectrum of 96 (aromatic region, including O-CH_2)**

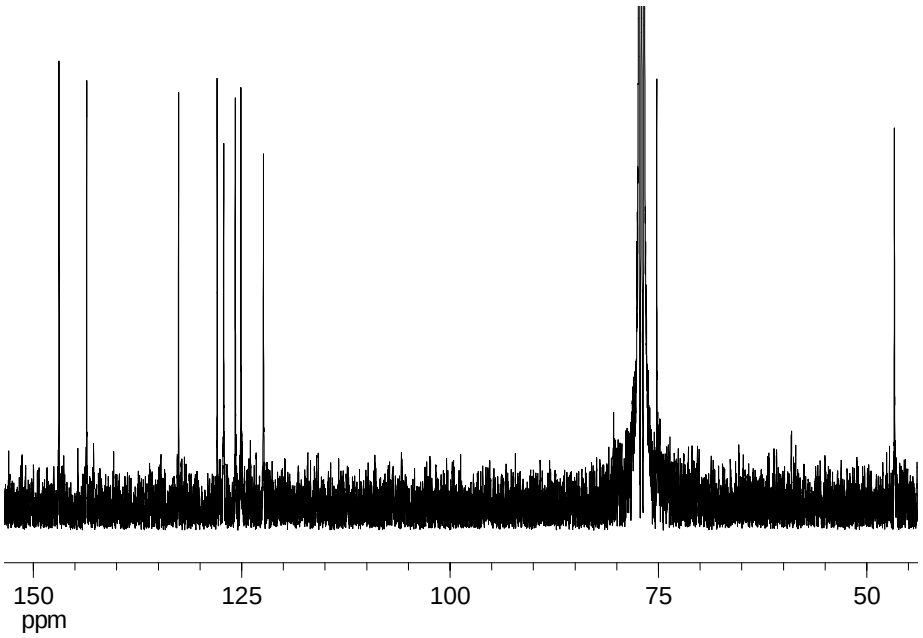

Figure 59 **^{13}C NMR spectrum of 96**

5,12-DDOT-D2 (**97**)

Entry	δ (H)	multiplicity	coupling (*J* or *N* [Hz])	correlation
a	7.86	m_c (AA'XX')	*N* = 9.6 Hz	1/1'/4/4'-H
b	7.32	m_c (AA'XX')	*N* = 9.6 Hz	2/2'/3/3'-H
c	7.02	m_c (BB'YY')	*N* = 8.7 Hz	10/10'/7/7'-H
d	6.70	m_c (BB'YY')	*N* = 8.6 Hz	9/9'/8/8'-H
e	5.32	s		11/11'/6/6'-H
f	4.16-4.10	m		23/23'/13/13'-Hα or Hβ
g	3.88-3.83	m		23/23'/13/13'-Hα or Hβ
h	2.07-2.00	m		chain
i	1.77-1.64	m		chain
j	1.58-1.27	m		chain
k	0.96-0.86	m		32/32'/ 22/22'-H

Table 40 **^{1}H NMR correlation of 97**

Entry	δ (C)	multiplicity	correlation	HSQC	HMBC
A	146.6	s	C-12/12'/5/5'	-	a,e
B	142.8	s	C-10a/10a'/6a/6a'	-	c,d,e
C	132.4	s	C-11a/11a'/5a/5a'	-	e
D	127.7	s	C-12a/12a'/4a/4a'	-	a,b
E	127.0	d	C-10/10'/7/7'	c	d
F	125.9	d	C-9/9'/8/8'	d	c
G	125.0	d	C-3/3'/2/2'	b	a
H	122.3	d	C-4/4'/1/1'	a	b
I	75.0	t	C-23/23'/13/13'	f,g	h
J	46.6	d	C-11/11'/6/6'	e	c,(e)
K-P	32.0-22.7	t	chain	-	-
Q	14.1	q	C-32/32'/22/22'	k	j

Table 41 **^{13}C NMR correlation of 97**

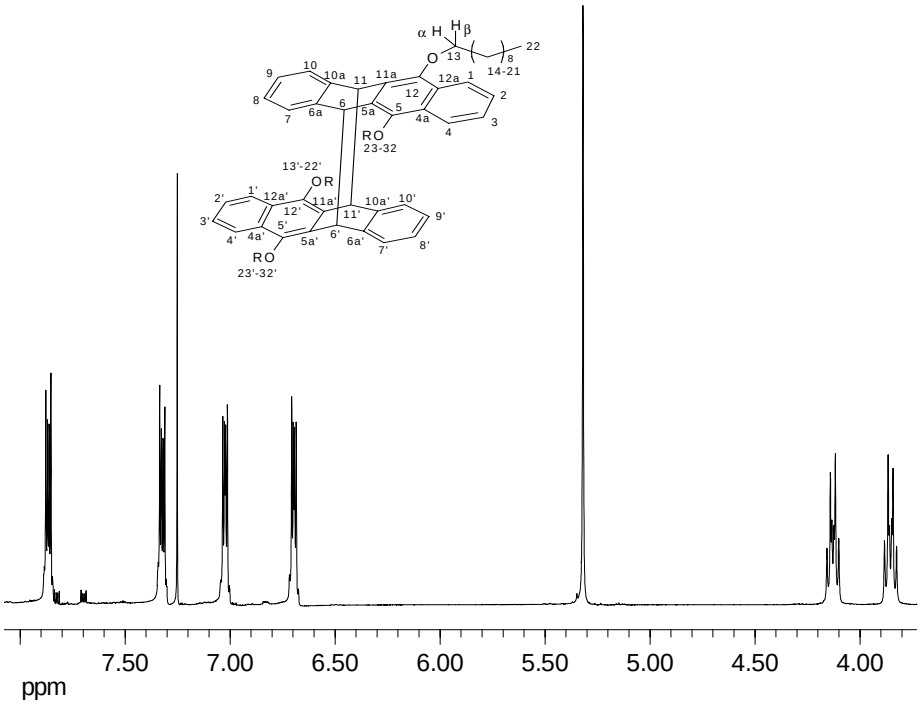

Figure 60 **^{1}H NMR spectrum of 97 (aromatic region, including O-CH_2)**

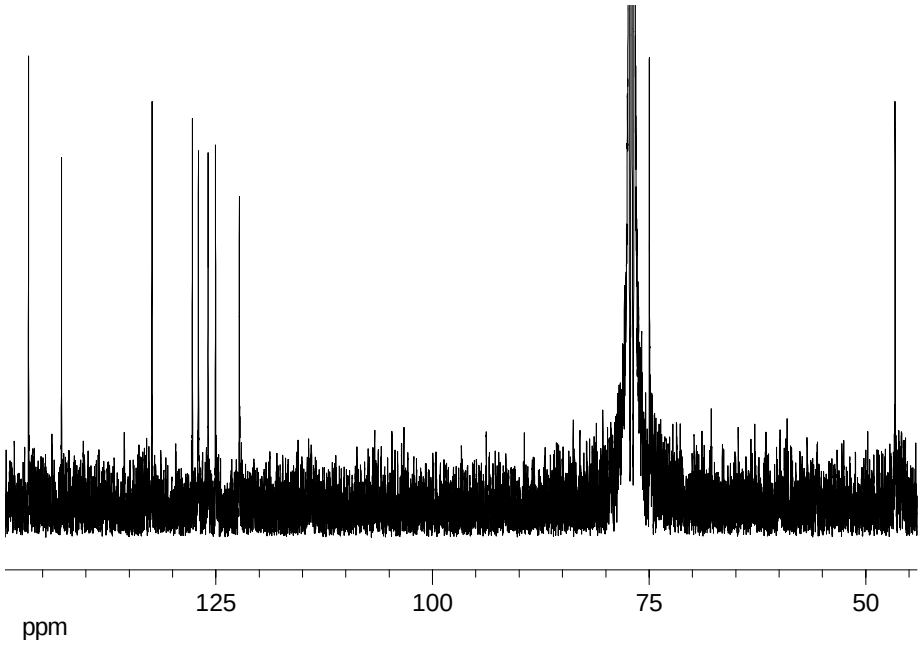

Figure 61 **^{13}C NMR spectrum of 97**

4.5.3.1 Differentiation of the photodimers 96 and 97

As NMR spectroscopy again allows only to determine the structure of the "single decks" but not the differentiation between hth and htt dimers, different methods had to be found. Depending on the structure, the differentiation can be derived from NOESY or ROSY spectra but this is difficult in the case of symmetric dimers as **96** and **97**.

The fluorescence spectra of 5,12-DDOT-D1 (**96**) and 5,12-DDOT-D2 (**97**), upon irradiation at 240 nm, show characteristic differences as seen in Figure 62.

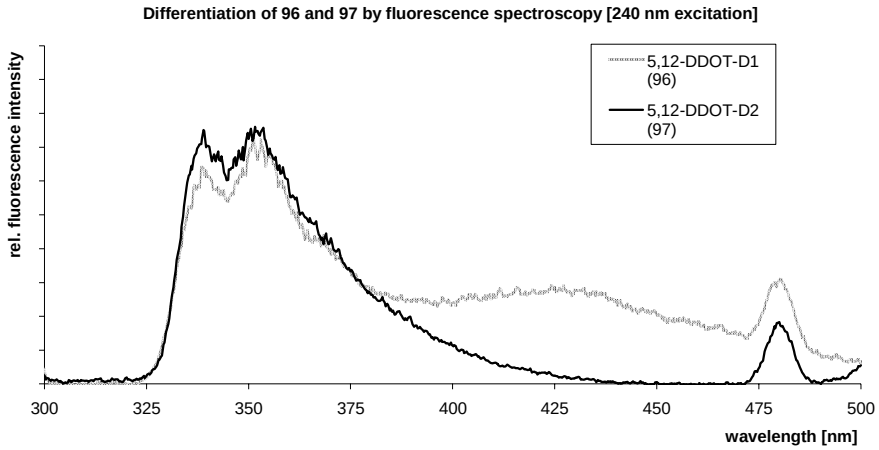

Figure 62 Comparison of the emission-spectra of 96 and 97

Figure 62 shows that 5,12-DDOT-D1 (**96**), exhibits a bathochromically shifted fluorescence emission when excitated at 240 nm. This can be attributed to a naphthalene excimer fluorescence that is only possible in the case of the hth dimer. While the absence of such an excimer fluorescence qualifies 5,12-DDOT-D2 (**97**) as the htt dimer.

The chemical shifts of 9/9'/8/8'-H of both dimers can be taken as further proof:

hth-photodimer	htt-photodimer
5,12-DDOT-D1 (**96**)	5,12-DDOT-D2 (**97**)
δ (9/8/9'/8'-H)	δ (9/8/9'/8'-H)
6.83 ppm (center)	6.70 ppm (center)

Table 42 ^{1}H NMR shifts to distinguish the 5,12-DDOT photodimers

4.5.4 Further investigation of 96 and 97

4.5.4.1 Reaction-quantum-yields of the 5,12-DDOT-dimerization

Since 5,12-DDOT (**85**) undergoes dimerization to a larger extent, the efficiency of the process was measured by determining its quantum yield.

The reaction quantum yield $\phi_{(dim)}$ of the photodimerization is defined as the relative amount of photons leading to dimerization in comparison to the total amount of photons absorbed by the sample.

The measurement of $\phi_{(dim)}$ contains thus two measurements: the decay of the monomer absorption (that is transferred into the number of reacting molecules by the Lambert-Beer law) and the total light output of the lamp at the irradiation wavelength (439 nm).

The quantum-yield of the 5,12-DDOT (**85**) dimerization was measured relatively to the photochemical reduction of $K_3Fe(C_2O_4)_3 \bullet 3H_2O$ (Parker actinometer).[73]

Two samples of 5,12-DDOT (**85**) were prepared in 1 mm optical cuvettes, degassed by freeze-thaw-cycles and then irradiated with a 2 kW xenon-lamp at 439 nm. The volumes of the solution were determined by calibration of the height of solution in the cell and are calculated after the freeze thaw procedure. The initial concentration is determined, using the optical density of the solutions at 440 and 469 nm.

The intensity of the absorbed light in the Parker solution is calculated by:

$$I_0 = \frac{abs\,(510nm) \cdot V(Par\,\mathrm{ker}) \cdot N_A}{\varepsilon(510nm) \cdot l \cdot t(irr) \cdot \phi(436, 0.15M)} \qquad \textbf{Equation 3}$$

After calculation of the constants Equation 3 leads to:

$$I_0 = \frac{abs\,(510nm)}{t(irr)} \cdot 1{,}3429 \cdot 10^{18}\left[h\nu / sek\right] \qquad \textbf{Equation 4}$$

Where abs (510) is the absorption of the iron (II)-complex, relatively to a solution of unirradiated Parker actinometer. Two volumes of Parker solution were irradiated before and after the irradiation of the samples, proving the time stable photon output of the lamp.

Intensity before the sample-irradiation	Intensity after the sample-irradiation	average
$3.79 \bullet 10^{15}$ hν/sek	$3.67 \bullet 10^{15}$ hν/sek	
$3.87 \bullet 10^{15}$ hν/sek	$3.86 \bullet 10^{15}$ hν/sek	
		$(3.80 \pm 0.09) \bullet 10^{15}$ hν/sek

Table 43 Determination of the photon output

The number of molecules of 5,12-DDOT (**85**) reacting were calculated by:

$$\Delta(abs) = abs(before) - abs(after)$$ **Equation 5**

$$\Delta n(5{,}12 - DDOT) = \frac{\Delta(abs) \cdot V \cdot N_A}{\varepsilon \cdot l}$$ **Equation 6**

With the volumes of cell one and two before and after irradiation (285 µl), the irradiation times (2400 s (cell 1) and 900 s (cell 2)), the path length (1 mm) and the following values for the absorption at 440 and 469 nm, $\phi_{(dim)}$ can be determined

cell	λ [nm]	ε [$mol^{-1}lcm^{-1}$]	OD before	OD after	Δ OD	Δ c [mol/l] $*10^{-4}$	Δ n [molecules] $*10^{16}$
1	440	2341	1.126	0.998	0.128	5.50	9.43
	469	4452	2.166	1.913	0.253	5.70	9.78
2	440	2341	1.124	1.063	0.061	2.59	4.44
	469	4452	2.165	2.037	0.128	2.88	4.94

Table 44 Calculation of the number of reacted 5,12-DDOT (85) molecules

Δn (cell 1) = $9.61*10^{16}$ molecules;

Δn (cell 2) = $4.69*10^{16}$ molecules

It has to be kept in mind that one excited molecule of 5,12-DDOT (**85**) reacts with one molecule in the groundstate and that the OD of the cells decreases due to the dimerization. This is taken into consideration by correction of the I_0 values

cell	T (before)	T (after)	∅ (T)	correction
1	8.29%	11.0%	9.65%	0.904
2	8.49%	9.66%	9.08%	0.909

Table 45 Correction of the absorbed light by transmission before and after irradiation

with T being the transmission at the irradiation wavelength.

$\phi_{(dim)}$ is calculated on the basis of Equation 7:

$$\phi(\text{dim}) = \frac{n(transformed)}{2 \cdot I_{ein}}$$
$$I_{ein} = I_0 \cdot t \cdot correction$$

Equation 7

leading to the following values:

cell 1: $5.8 \cdot 10^{-3}$; cell 2: $7.4 \cdot 10^{-3}$; $\phi_{(dim)} = 6.6 \cdot 10^{-3}$

This value should be seen in comparison with the photodimerization quantum yields of alkoxy substituted anthracenes, especially with the one for 1,4-DDOT, as the electronic situation (dimerization adjacent to the substitution) is similar. Desvergne et al. have published these measurements in 1988.[74] The values vary between $3.7 \bullet 10^{-2}$ in the case of 1,5-DDOT, $3.2 \bullet 10^{-2}$ in the case of 1,8-DDOT, $6.5 \bullet 10^{-3}$ for 1,4-DDOT and $1.0 \bullet 10^{-3}$ for the centrosymmetric dimer of 2,6-DDOT. Especially for the 1,4-didecyloxy-anthracene, the value is in good agreement to the one found for 5,12-DDOT (**85**).

4.5.4.2 Thermal and photochemical decomposition of 96 and 97

To monitor the thermal dissociation of the 5,12-DDOT dimers is of interest for various reasons. First it provides a further way to distinguish the two dimers, since the decomposition rate should be different for the centrosymmetric and the planosymmetric dimer. Secondly, the possibility of a photochemically/thermally switchable molecule is of interest for different practical applications.[50] To test these properties, the thermal decomposition of the two photodimers was examined in solution by recording the UV absorption of the formed monomer.

The two dimers were dissolved in hexane or MCH and the UV-spectra were monitored over a period of 90 minutes at a given, constant temperature (308 K and 342 K). This experiment gives an answer to the relative decomposition of 5,12-DDOT-D1 **96** and 5,12-DDOT-D2 **97**.

The simple dissociation of the dimers would lead to a first order kinetic, *i. e.* a logarithmic increase of the monomer concentration that can be monitored by UV spectroscopy of the lower energy absorption of the monomer.

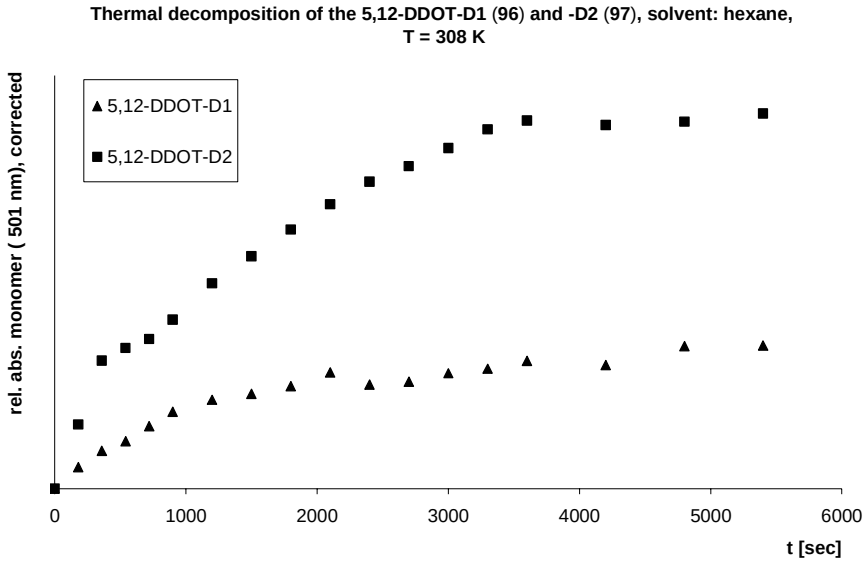

Figure 63 **Thermal decomposition of 96 and 97 in hexane, T = 308 K**

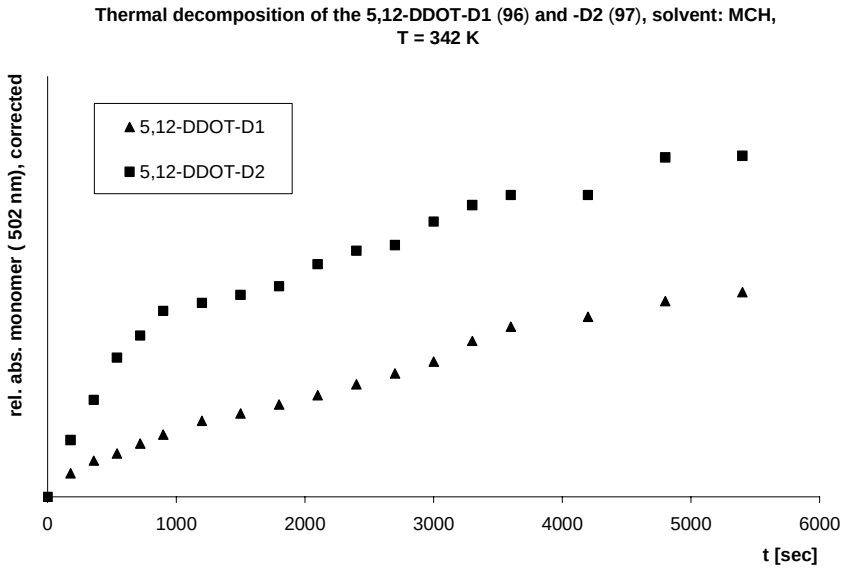

Figure 64 **Thermal decomposition of 96 and 97 in MCH, T = 342 K**

The data of the monomerization of the two dimers are presented in Figure 63 and Figure 64.

For the cleavage, it can be seen that the decomposition of 5,12-DDOT-D2 (**97**) is nearly twice as fast as the decomposition of its isomer **96**.

Kinetic analysis of the thermal decomposition of the dimers at two different temperatures can give an idea of the activation energy of the dissociation. The data of the thermal dissociation is transferred into a ln(c(monomer)) versus t diagram (see Appendix I D)

A pure monomerization of **96** and **97** should result in linear plots of ln (c(monomer)) over time. This is not the case, and it can be concluded that either the monomer or the dimers are thermally instable and undergo general degradation under the measurement conditions. Another possibility is that the monomer undergoes thermal dimerization, leading to an equilibrium. These difficulties prevent the calculation of activation energies of the different dimer dissociations. Still, a discernible difference of the thermal stability in solution of 5,12-DDOT-D1 and 5,12-DDOT-D2 can be recognized.

Further information on the different dissociation rates can be derived from molecular modeling calculations. It is thus interesting to note, that with different methods (force field and density functional theory calculations) no significant difference in the ground state energies between **96** and **97** could be found. Still it has to be kept in mind that calculations in the gas phase might not display the same behavior as the molecules show in solution.

Next to the possibility of thermal reversibility of the dimerization, it is often possible to influence the reaction by applying light of different wavelengths, *i. e.* to use photochromic properties of a molecule. Photochromism is the light induced reversible change of color.[75] As **96** and **97** do not absorb light in the visible range it is likely to assume photochromism.

The degassed solutions which had been used to determine the dimerization quantum yield of 5,12-DDOT (**85**) were irradiated with light of shorter wavelength to induce the dissociation of the dimers. As in the case of thermal dissociation, the dissociation can be observed by the increase of the monomer absorption. To prevent thermal reactions, a monochromator was used.

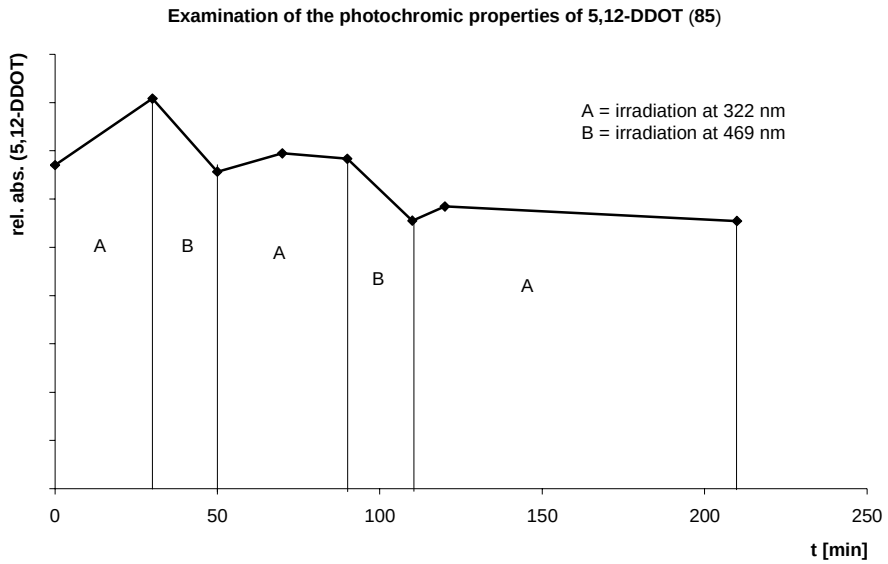

Figure 65 Examination of the photochromic properties of 5,12-DDOT (85) and its dimers 96 and 97

Figure 65 shows that the mixture of the dimers 5,12-DDOT-D1 **96** and 5,12-DDOT-D2 **97** photodissociats on irradiation at 322 nm (increase of the monomer absorption in the parts A). When the mixture is again irradiated at 469 nm, the amount of monomer decreases (parts B).

Still, 5,12-DDOT (**85**) is not a photochromic substance in the pure sense of the definition.[75] As the monomer concentration does not regain the value it had at the beginning of the experiment, no pure dimerization/monomerization takes place, but a decomposition of the monomer parallel to the photoreaction. This can be seen in detail in the part of Figure 65, time 110 to 210 minutes, where the monomer absorption decreases after a long irradiation at 322 nm.

4.6 Crossed photodimers of 5,12-DDOT (85) and tetracene (82)

4.6.1 Possible photoproducts

That 9,10-DDOA (**1**) does not give any photoproducts upon irradiation,[3] can be attributed to steric overload of the most reactive (9,10/9',10') positions. One convincing proof of this rationalization is provided by the formation of mixed photodimers between 9,10-DDOA (**1**) and anthracene.[72]

When a 1:1 mixture of tetracene (**82**) and 5,12-DDOT (**85**) is irradiated together, three groups of dimers can be formed: The two groups of "pure dimers" and the mixed dimers. The pure dimers of tetracene (**82**) and 5,12-DDOT (**85**) are discussed in the Chapters 4.3.2 and 4.5.3, the mixed dimers are described in the following Scheme 24.

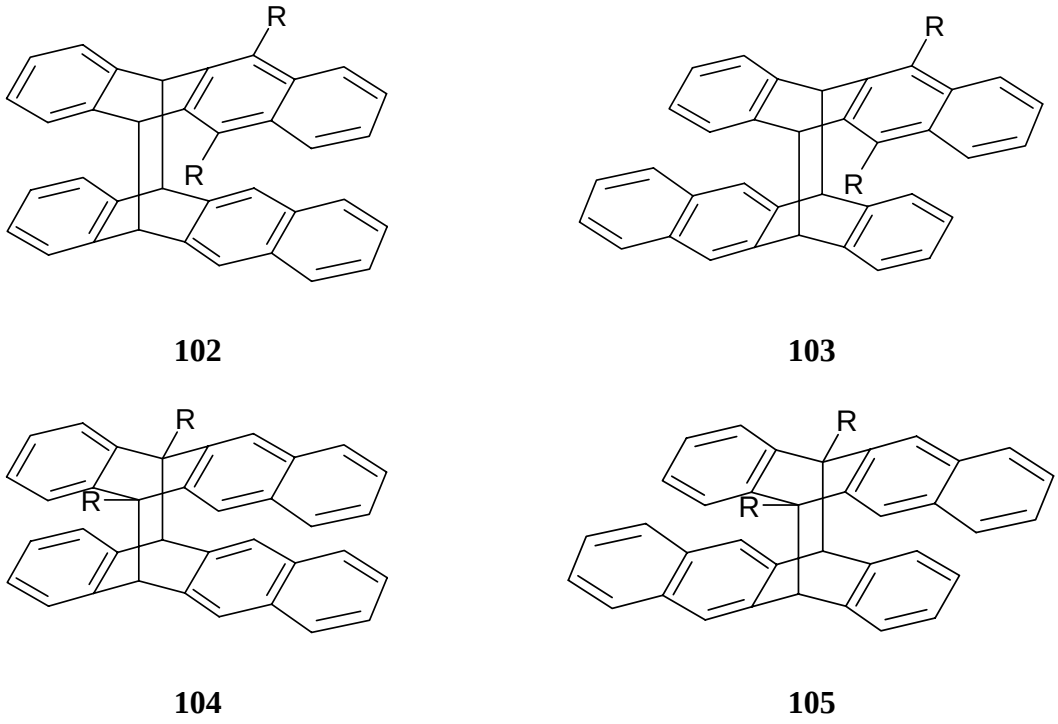

102 **103**

104 **105**

Scheme 24 **Possible mixed dimers of tetracene (82) and 5,12-DDOT (85) (R = $OC_{10}H_{21}$)**

Unlike in the 9,10-DDOA/anthracene case, two reactive rings (one substituted, one unsubstituted) are present, it will hence be interesting to investigate the product distribution.

4.6.2 Irradiation of a mixture of 5,12-DDOT (85) and tetracene (82)

When a 1:1 mixture of tetracene (**82**) and 5,12-DDOT (**85**) is irradiated in Ar saturated cyclohexane, dimers of all three classes could be detected by TLC and crude NMR spectra. The main problem of this experiment is the separation of the different products. To facilitate the task, only the groups of new dimers (in comparison to the already known pure dimers) as detected by thin layer chromatography, were separated. The pure tetracene dimers **83** and **84** were separated from the mixture by rinsing the residue of the reaction, after removal of the cyclohexane, with pentane. This residue showed only the two pure tetracene dimers which were not separated from each other.

The pentane soluble fraction, a red oil, contained the pure 5,12-DDOT dimers **96** and **97** (detectable by TLC), traces of 5,12-DDOT (**85**) and mixed dimers of 5,12-DDOT/ tetracene. The fraction containing those new dimers (23%) was further separated using several runs of flash chromatography. From the possible four dimers containing 5,12-DDOT (**85**) and tetracene (**82**), only two were observed and could be separated to determine the structures by one and two dimensional NMR spectroscopy, as well as UV/Vis- and IR spectroscopy.

4.6.2.1 Mixed dimers

5,12-DDOT-T-D1 (**102**) (hth dimer)

Entry	δ (H)	multiplicity	coupling (J or N [Hz])	correlation
a	7.76	m_c (AA'XX')	N = 9.7 Hz	4/1-H
b	7.49	m_c (BB'YY')	N = 9.4 Hz	22/19-H
c	7.45	s		23/18-H
d	7.21	m_c (AA'XX')	N = 9.6 Hz	3/2-H
e	7.18	m_c (BB'YY')	N = 9.4 Hz	21/20-H
f	7.00-6.97	m		16/13 or 10/7-H
g	6.86-6.83	m		15/14 or 9/8-H
h	5.33	d	^3J = 11.2 Hz	11/6-H
i	4.86	d	^3J = 11.2 Hz	24/17-H
j	4.17-4.11	m		35/25-H_α or H_β
k	3.86-3.82	m		35/25-H_α or H_β
l,m,n	2.08-2.00 1.72-1.57 1.55-1.34	m		chain
o	0.92	t	^3J = 6.9 Hz	44/34-H

Table 46 **^{1}H NMR correlation of 102**

Entry	δ (C)	multiplicity	correlation	HSQC	HMBC
A	146.8	s	C-12/5	-	a,h
B	143.1	s	C-24a/16a or 10a/6a	-	f,g,h,i
C	143.07	s	C-24a/16a or 10a/6a	-	f,g,h,i
D	141.0	s	C-23a/17a	-	c,h,i
E	132.2	s	C-11a/5a	-	h,i
F	131.9	s	C-22a/18a	-	b,c,e
G	127.7	s	C-12a/4a	-	a,d
H	127.2	d	C-16/13 or C-10/7	f	g
I	127.13	d	C-16/13 or C-10/7	f (b)	(c),(e),g
J	127.10	d	C-22/19	b	c,e,(g)
K	125.89	d	C-15/14 or 9/8	g	f
L	125.85	d	C-15/14 or 9/8	g	f
M	125.4	d	C-23/18	c	b,i
N	125.15	d	C-21/20	e	(a),b
O	125.06	d	C-3/2	d	a
P	122.3	d	C-4/1	a	d
Q	74.7	t	C-35/25	j,k	l,m
R	53.6	d	C-24/17	i	b,f,h
S	47.0	d	C-11/6	h	f,i
T-AA	32.0-22.7	t	chain	-	-
AB	14.2	q	C-44/34	o	n

Table 47 **^{13}C NMR correlation of 102**

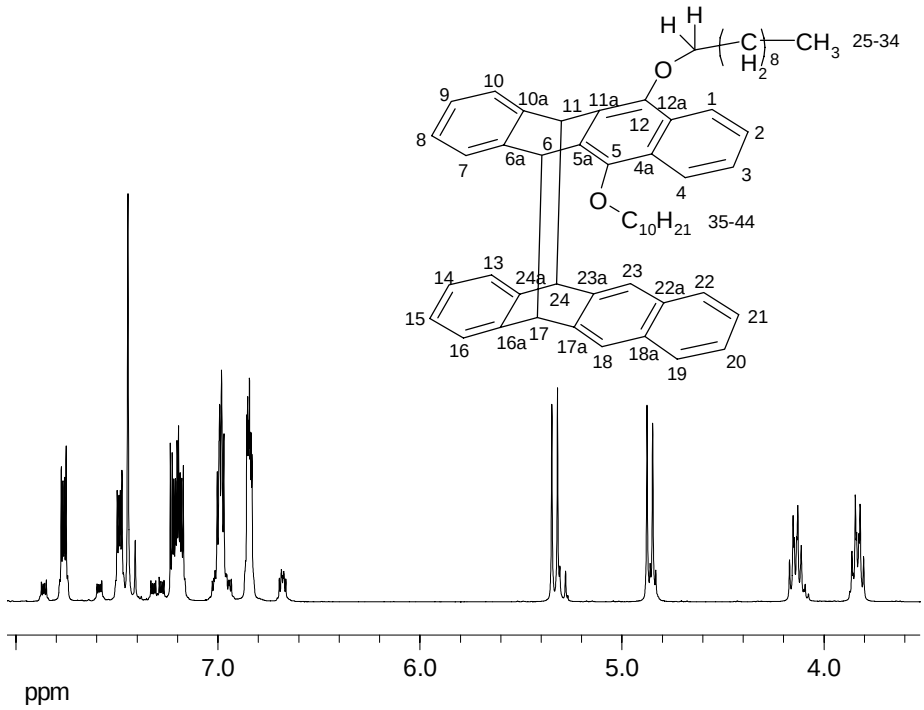

Figure 66 **^{1}H NMR spectrum of 102 (aromatic region including O-CH_2)**

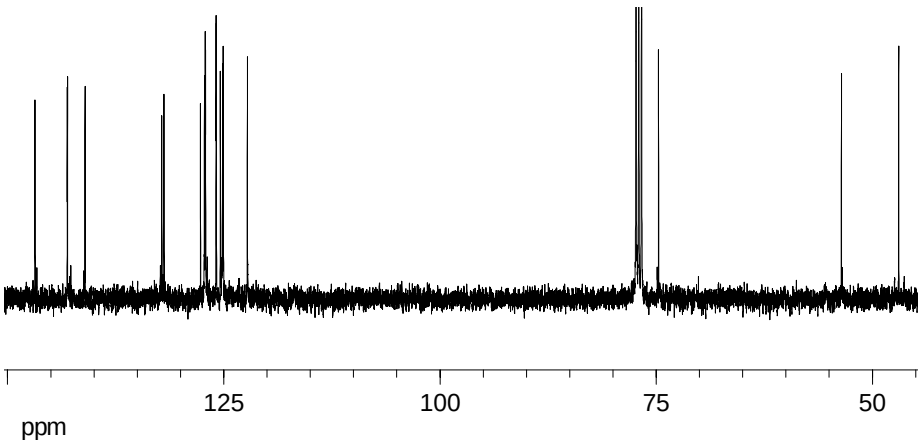

Figure 67 **^{13}C NMR spectrum of 102 (aromatic region including C-35/25)**

5,12-DDOT-T-D2 (**103**) (htt-dimer)

Entry	δ (H)	multiplicity	coupling (*J* or *N* [Hz])	correlation
a	7.86	m_c (AA'WW')	*N* = 9.6 Hz	4/1-H
b	7.59	m_c (BB'XX')	*N* = 9.4 Hz	22/19-H
c	7.41	s		23/18-H
d	7.32	m_c (AA'WW')	*N* = 9.6 Hz	3/2-H
e	7.28	m_c (BB'XX')	*N* = 9.4 Hz	21/20-H
f	7.02	m_c (CC'YY')	*N* = 8.7 Hz	16/13-H
g	6.94	m_c (DD'XX')	*N* = 8.7 Hz	10/7-H
h	6.69-6.66	m		15/14-H and 9/8-H
i	5.29	d	^3J = 11.2 Hz	11/6-H
j	4.85	d	^3J = 11.2 Hz	24/17-H
k	4.13-4.09	m		35/25-H_α or H_β
l	3.87-3.82	m		35/25-H_α or H_β
m	2.08-2.00	m		chain
n	1.72-1.65	m		chain
o	1.53-1.26	m		chain
p	0.92	t	^3J = 6.9 Hz	44/34-H

Table 48 **^{1}H NMR correlation of 103**

Entry	δ (C)	multiplicity	correlation	HSQC	HMBC
A	146.6	s	C-12/5	-	a,i
B	142.8	s	C-10a/6a	-	g,h,j
C	142.7	s	C-24a/16a	-	f,h,i
D	141.2	s	C-23a/17a	-	c,(i),j
E	132.3	s	C-11a/5a	-	i,(j)
F	132.0	s	C-22a/18a	-	b,c,d/e
G	127.7	s	C-12a/4a	-	a,(d/e)
H	127.3	d	C-10/7	g	h,i
I	127.1	d	C-22/19	b	c,d/e
J	126.9	d	C-16/13	f	h,j
K	125.88	d	C-9/8 or C-16/13	h	f,g
L	125.86	d	C-9/8 or C-16/13	h	f,g
M	125.2	d	C-23/18	c	b,j
N	125.1	d	C-3/2 or C-21/20	d,e	a,b
O	122.3	d	C-4/1	a	d
P	74.9	t	C-35/25	k,l	m
Q	53.5	d	C-24/17	j	c,f,i
R	47.0	d	C-11/6	i	g,j
S-Z	32.0-22.7	t	chain	-	-
AA	14.2	q	C-44/34	p	o

Table 49 **^{13}C NMR correlation of 103**

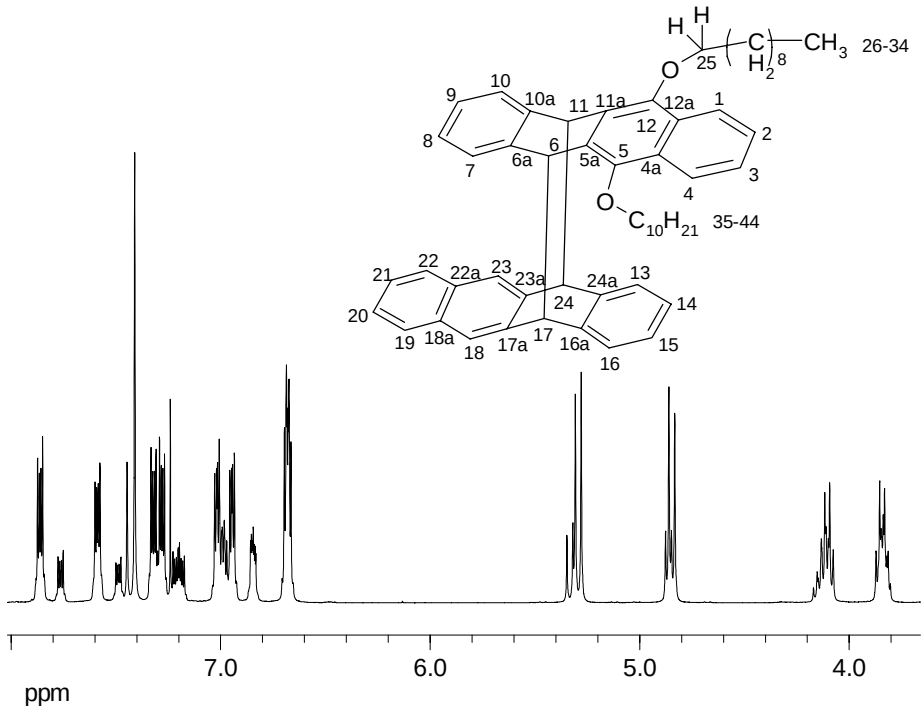

Figure 68 **^{1}H NMR spectrum of 103 (aromatic region including O-CH_2)**

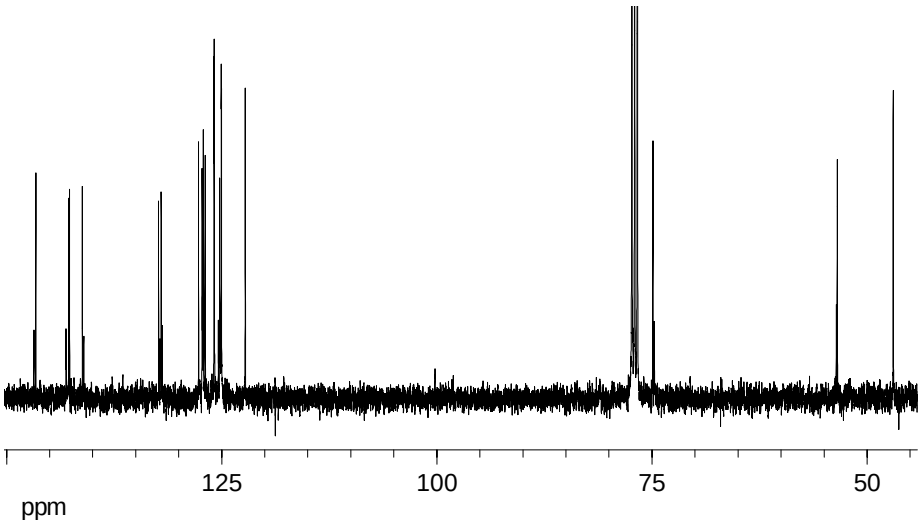

Figure 69 **^{13}C NMR spectrum of 103 (aromatic region including C-25/35)**

4.6.2.2 Structural elucidation

The relative orientation of the two decks of **102** and **103** was determined by ROESY experiments, well suited in the case of unsymmetrical dimers. In the case of **102** coupling between the OCH_2-H and 23/18-H indicates the hth orientation, while in the case of **103**, coupling between 10/7-H and 23/18-H leads to the htt orientation.

Like in the cases of the 2,3-DDOT- and the pure 5,12-DDOT dimers, the chemical shifts of the 9/8-H and 15/14-H signals are a further proof of the assigned structure.

hth-photodimer	htt-photodimer
5,12-DDOT-T-D1 (**102**)	5,12-DDOT-T-D2 (**103**)
δ (15/14- and 9/8-H)	δ (15/14- and 9/8-H)
6.85 ppm (center)	6.68 ppm (center)

Table 50 **^{1}H NMR shifts to distinguish the 5,12-DDOT-T photodimers**

The preparative photodimerization of 5,12-DDOT (**85**) with tetracene (**82**) shows two main results. The general product distribution shows no preference between the monomers. Dimers of all the three groups (pure and mixed) are formed. When the mixed dimers are considered, it can be stated that the electron rich (alkoxy substituted) ring does not take part in the dimerization, leading only to two of the possible mixed dimers.

Compared to the results from the anthracene/9,10-DDOA dimerization[72] the reactivity of the substituted ring appears to be lower than that of the unsubstituted center ring. Still, the anthracene/9,10-DDOA results show that the substituted ring is more reactive than the outer rings.

4.7 Summary of the structural elucidation of tetracene dimers

In the curse of this study on the structures of different alkoxy-tetracene photodimers, the structural elucidation was mainly performed on the basis of one- and two dimensional NMR experiments. In the cases of unsymmetrical dimers (**91**, **102** and **103**) ROESY experiments were employed. Coupling between the two decks is weak. Thus mostly protons adjacent to the newly formed connection showed an effect, while differences in the outer rings did not lead to ROESY coupling signals.

In the case of the 5,12-DDOT dimers **96** and **97** there is a distinct difference in the fluorescence spectra. The hth dimer shows a bathochromically shifted naphthalene excimer fluorescence. This technique has proven inefficient in the case of the 2,3-DDOT dimers though.

One general possibility to differentiate between the dimers are the chemical shifts of the H atoms at the benzenic subunit of the dimers. In the case of the htt dimers the center of the signal corresponding to the *o*-H atoms is shifted upfield by 0.13 to 0.23 ppm probably due to the shielding by the aromatic naphthalene unit.

This can even be used as further proof of the structural assignment in the case of the pure tetracene dimers, even if only from **84** the spectrum is available, so far. With $\delta_{(center)}$ = 6.85 ppm the chemical shift in question (2/3/2'/3'-H) indicates a hth structure.

Further structural information can be derived by comparison of the UV spectra of the different dimers as shown below.

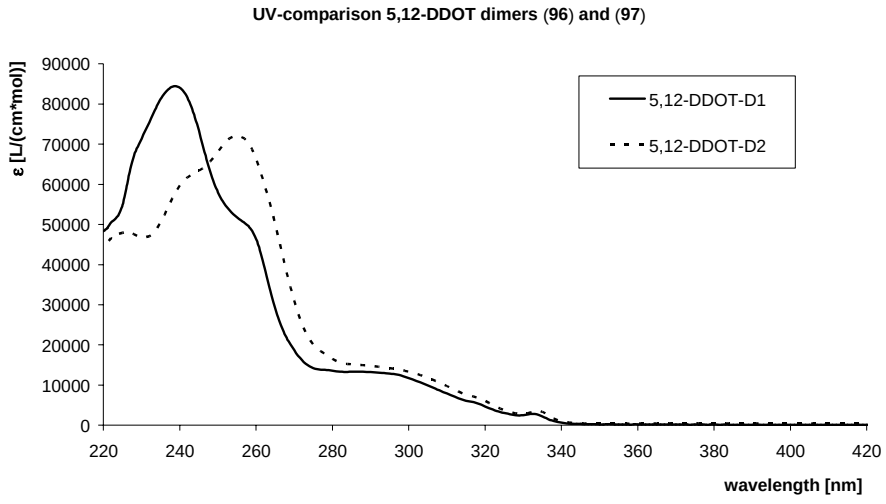

Figure 70 UV/Vis spectra of 96 and 97

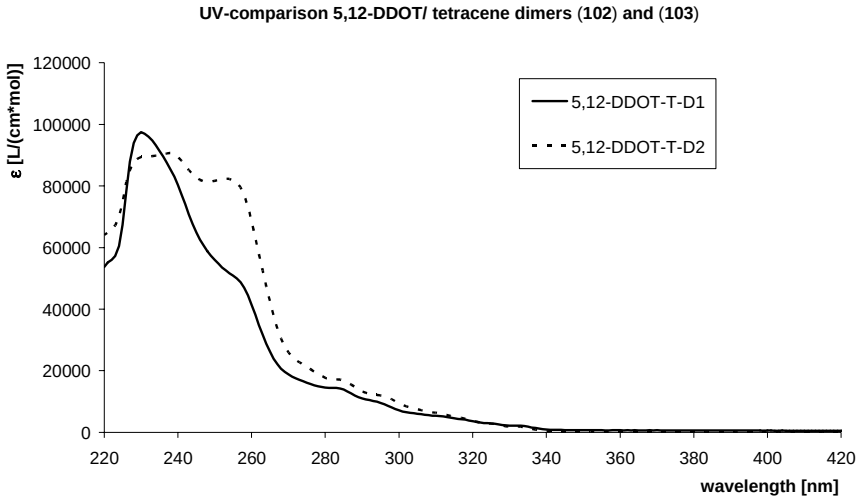

Figure 71 **UV/Vis spectra of 102 and 103**

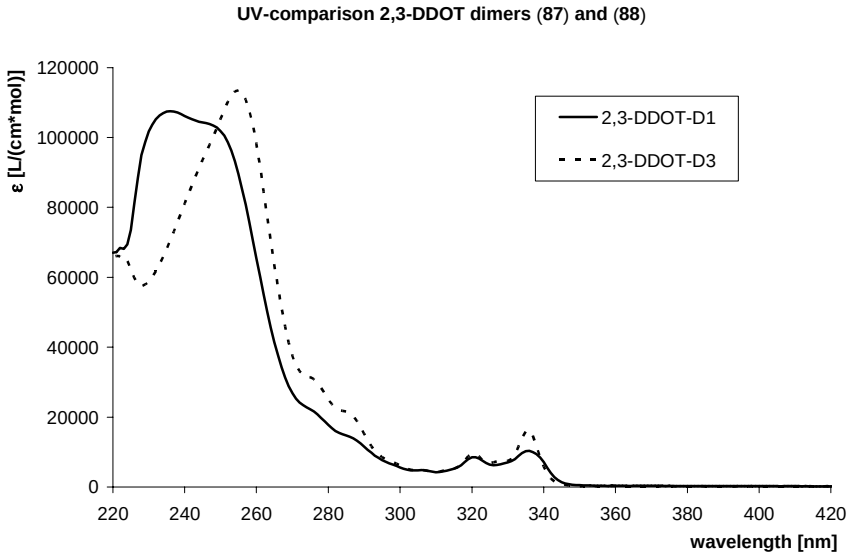

Figure 72 **UV/Vis spectra of 87 and 88**

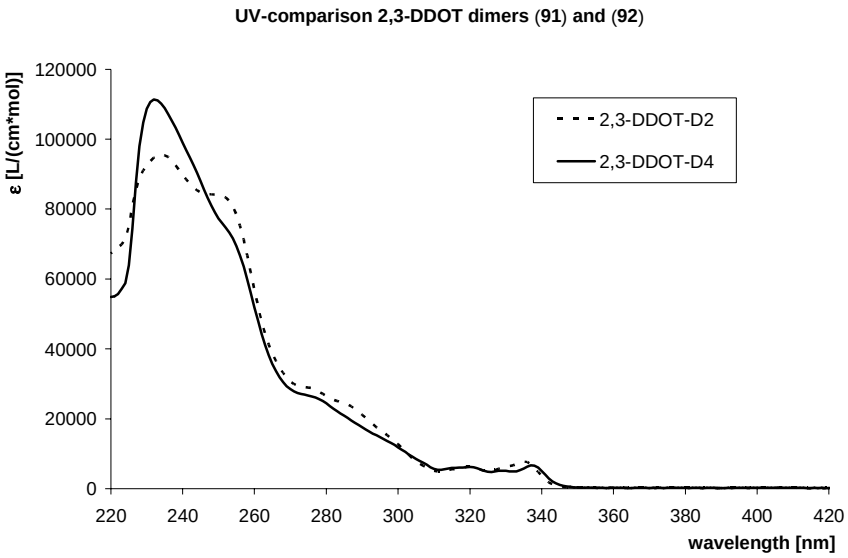

Figure 73 UV/Vis spectra of 92 and 91

It can be seen from Figure 70, Figure 71, Figure 72 and Figure 73 that the htt dimers (indicated by dotted lines) generally show a more bathochromic absorption when compared to the hth dimers. The same trend can be observed in the case of the pure tetracene dimers, when the published UV/Vis spectra are considered.[7] This trend is most prominent in the case of the "pure" dimers and can probably be explained by the difference in the dipole moment which should be only quite small in the case of the 5,12-DDOT/tetracene dimers (as only one part contains alkoxy functions) and in the case of the unsymmetrical 2,3-DDOT dimers, as the different arrangement of the naphthalene units is counteracted by the arrangement of the alkoxy chains.

5 Photophysical examination of various tetracenes

In a homogeneous system, the decay mechanism of excited molecules is routinely studied by measuring fluorescence lifetimes $\tau_{(fl)}$ and fluorescence quantum yields $\phi_{(fl)}$.[76] This leads to the calculation of the radiative and nonradiative decay rate constants, using the following equation:

$$\phi_{(fl)} = \frac{k_{FM}}{k} \qquad \textbf{Equation 8}$$

Here $\phi_{(fl)}$ is the fluorescence quantum yield, k is the total decay rate constant (the reciprocal of the fluorescence lifetime $\tau_{(fl)}$), and k_{FM} is the radiative decay rate constant.

Simple transformation leads to Equation 9:

$$k_{FM} = \frac{\phi_{(fl)}}{\tau_{(fl)}} \qquad \textbf{Equation 9}$$

The spectroscopic properties of the different substituted tetracenes can be compared with the properties of pure tetracene on the one hand and with substituted anthracenes on the other. The fluorescence quantum yields of 5,12-DDOT (**85**), 2,3-DDOT (**86**) and 2,3-DHdOT (**111**) were measured relative to perylene as a common fluorescence standard. Furthermore, the fluorescence life times of 5,12-DDOT (**85**), 2,3-DDOT (**86**) and 2,3-DHdOT (**111**) were determined by single photon counting.

The principles of the two measurements will be explained in the following chapters.

5.1 Measurement principles

5.1.1 Fluorescence quantum yield

The fluorescence quantum yield ($\phi_{(fl)}$) is defined as the ratio of photons causing fluorescence to the total amount of photons absorbed by the sample.

$$\phi(fl) = \frac{h\nu(fluorescence)}{h\nu(total)} \qquad \textbf{Equation 10}$$

The number of photons causing fluorescence can easily be determined by calculation of the area under the curve of the fluorescence emission of a given sample. Like in the case of the dimerization quantum yield (see Chapter 4.5.3.2) the main difficulty rests in the measurement of the number of photons emitted by the lamp of a given fluorescence spectrometer.

This is generally performed by comparison to the known fluorescence quantum yield of a standard sample at the same wavelength as the measured sample, since the measurement of the absolute emission is rather difficult.[77]

One commonly used reference compound is perylene, due to its high photostability and the nearly quantitative fluorescence quantum yield at ambient temperature (ϕ(fl)≈1).[78] To prevent reabsorption of the fluorescence photons emitted, all measurements were carried out at high dilution. The differences in refractive indices of the sample- and reference solvents were taken into consideration, as well as the different absorbance (OD) of the reference and the sample, leading to Equation 11:

$$\phi_{(fl)} = \frac{(n_d^{20})^2(S)}{(n_d^{20})^2(R)} \cdot \frac{A(S)}{A(R)} \cdot \frac{abs(R)}{abs(S)} \cdot \phi_{(fl)}(R) \qquad \textbf{Equation 11}$$

n^d_{20} = refractive index of the solvent, S = sample, R = reference, A = area, abs = absorbance, $\phi_{(fl)}$ = Fluorescence-quantum yield

$\phi_{(F)}$ (R) in cyclohexane = 0.94, n^d_{20} (cyclohexane) = 1.426, n^d_{20} (MCH) = 1.422.

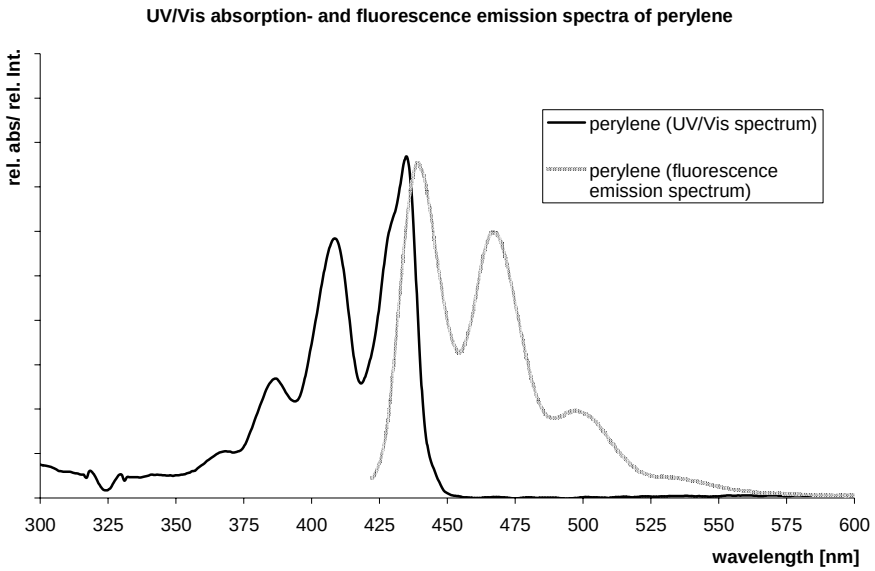

Figure 74 Absorption and emission spectra of perylene

5.1.2 Fluorescence life time[79]

The measurement of the fluorescence decay by single photon counting rests on the following principles: the probability of deactivation of a single activated molecule by fluorescence at a given time after activation is proportional to the fluorescence intensity at this time. If only a single fluorescence photon of all the photons after activation is detected at a given time, the experiment leads to the fluorescence decay curve as a probability curve, provided the measurements are accumulated several times. To ensure that only a single photon of each measurement is detected until the next activation, the rate of detection should only amount 2% of the pulse rate. This may lead to relatively long measurement times, one of the drawbacks of the single photon technique.

Generally flash lamps are used, which exhibit an activation pulse having a half width of 1-4 ns. As this time approximately corresponds to the fluorescence decay times, the real fluorescence time function F(t) has to be calculated from the experimental fluorescence decay function D(t) and the lamp pulse function L(t).

One principal problem of the fluorescence decay measurement is the need of identical conditions under which the fluorescence and the lamp pulse are recorded. The systematical error of the measurement depends of the apparatus (photomultiplier, detection electronics and the monochromator) having an own half width, as well as of the registered wavelength.

Another important influence is the color effect of the photomultiplier. This can be explained by the velocity dependence of the photoelectrons, detected by the photomultiplier, from the wavelength of the photons that led to emission of the photoelectrons. The dependency leads to a time shift between lamp pulse and fluorescence, described by the shift parameter δ. The experimental signal (from which the fluorescence signal is calculated) can be described by:

$$D(t) = \int_0^t L(t - s + \delta)F(s)ds \qquad \textbf{Equation 12}$$

Without providing a full theoretical analysis of the underlying mathematical procedures, it can be stated that the fluorescence decay F(t) is determined from Equation 12 by iterative reconvolution. A theoretical function D'(t) is fitted by variation of the parameters to the experimental curve D(t) by non-linear regression.

Two parameters are generally used to show the quality of this regression. The square error χ^2 and the Durbin-Watson factor DW. They are defined by the following equations and provided directly by the measurement software:

$$\chi^2 = \frac{\sum_{i=n(a)}^{n(e)} R_i^2}{\nu} \qquad \textbf{Equation 13}$$

$$\text{with } R_i = \frac{D(t_i) - D'(t_i)}{\sqrt{D(t_i)}} \qquad \textbf{Equation 14}$$

where ν is the number of degrees of freedom ($\nu = n_e - n_a + 1 - p$), p is the number of fit parameters and $n_e - n_a + 1$ equals the number of channels used to fit the curve.

$$DW = \frac{\sum_{i=n(a)+1}^{n(e)} (R_i - R_{i-1})^2}{\nu\chi^2} \qquad \textbf{Equation 15}$$

In Chapter 5.3 the fluorescence decay times as well as the χ^2 and DW values are presented for the different tetracenes.

5.2 Results of the fluorescence quantum yield measurements

The fluorescence and UV/Vis-spectroscopic measurements were carried out at the "Laboratoire de Physico-Chimie Moléculaire,(CNRS, UMR 5803) Université Bordeaux 1".

5.2.1 Fluorescence-quantum-yield of 5,12-DDOT (**85**)

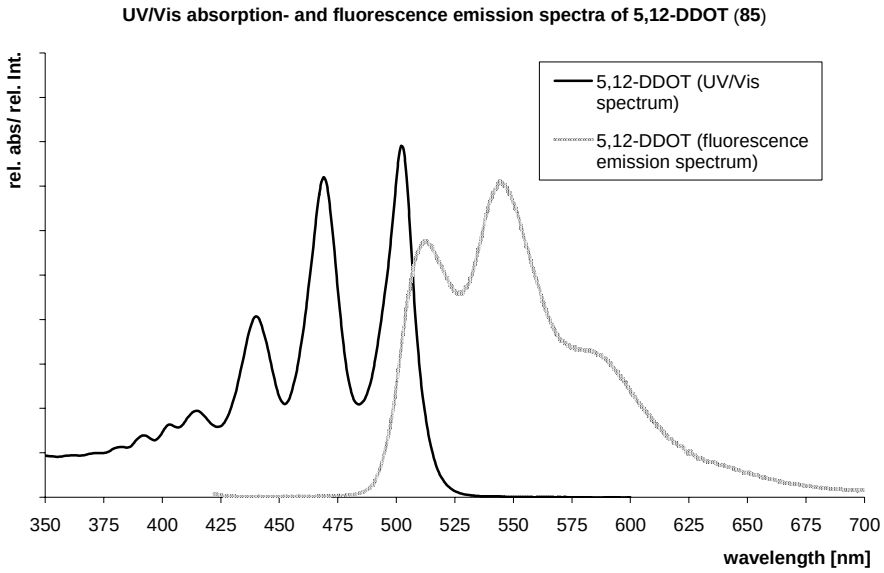

Figure 75 **Absorption- and emission spectra of 5,12-DDOT (85)**

λ(S)	λ(R)	OD(S)	OD(R)	A(S)	A(R)	$\phi_{(F)}$(S)
408	408	0.080	0.072	226001	376125	0.51
418	418	0.092	0.032	275077	174232	0.51
						∅ = 0.51

Table 51 **Calculation of ϕ(fl) of 5,12-DDOT (85)**

5.2.2 **Fluorescence-quantum-yield of 2,3-DDOT (86)**

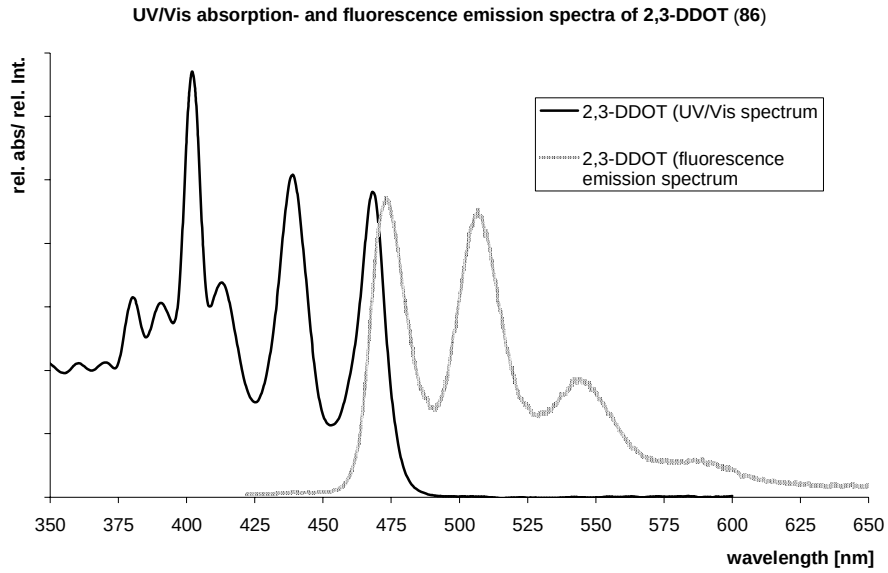

Figure 76 **Absorption- and emission spectra of 2,3-DDOT (86)**

λ(S)	λ(R)	OD(S)	OD(R)	A(S)	A(R)	$\phi_{(F)}$(S)
408 nm	408 nm	0.060	0.094	26743	151896	0.26
392 nm	392 nm	0.060	0.035	23756	62945	0.21
418 nm	418 nm	0.051	0.041	22146	70434	0.24
426 nm	426 nm	0.030	0.078	14146	118780	0.29
						∅ = 0.25

Table 52 **Calculation of ϕ (fl) of 2,3-DDOT (86)**

5.2.3 **Fluorescence-quantum-yield of 2,3-DHdOT (111)**

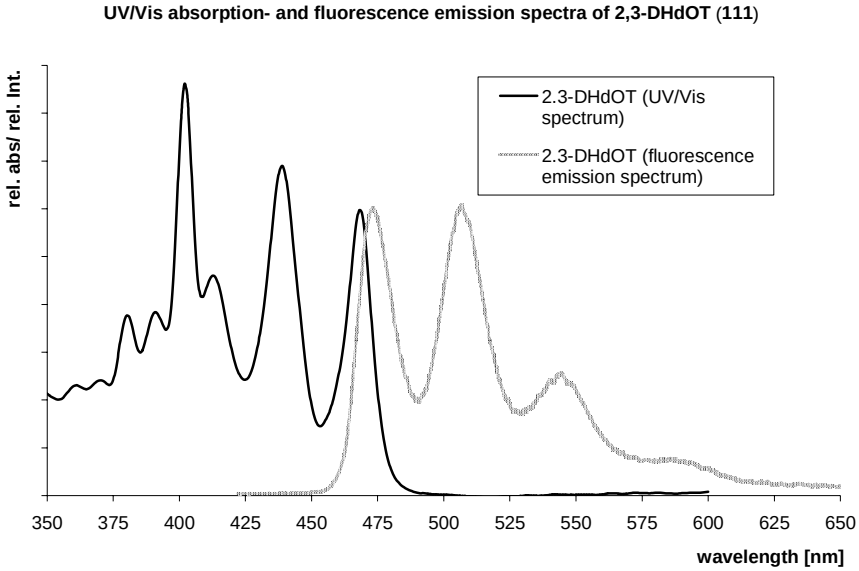

Figure 77 **Absorption- and emission spectra of 2,3-DHdOT (111)**

λ(S)	λ(R)	OD(S)	OD(R)	A(S)	A(R)	$\phi_{(F)}$(S)
408 nm	408 nm	0.104	0.120	35711	182639	0.21
392 nm	392 nm	0.094	0.045	31070	77170	0.18
418 nm	418 nm	0.088	0.053	28599	86297	0.19
426 nm	426 nm	0.061	0.100	18356	144999	0.20
						∅ = 0.20

Table 53 **Calculation of ϕ (fl) of 2,3-DHdOT (111)**

5.2.4 Discussion of the results

Comparison of the fluorescence quantum yields of 2,3-DDOT (**86**) and 2,3-DHdOT (**111**) shows a good agreement (0.25 and 0.2 respectively). Still, the two values demonstrate the limits of the measurement. It is reasonable to assume the same value for $\phi_{(fl)}$ for both substances, as the spectroscopic characteristics should be the same. This should be kept in mind, when these values are compared with results for other acenes.

On the other hand, with 0.51 in the case of 5,12-DDOT (**85**) $\phi_{(fl)}$ is twice as high as the value for the 2,3-disubstituted alkoxy tetracenes.

When looking for acenes to compare those values with, it is reasonable to make a relative comparison with 9,10-DDOA and 2,3-DDOA (**1**). As shown by Brotin et al.[3] the value is 0.19 in the case of 2,3-DDOA (**1**) and 0.86 for 9,10-DDOA, respectively (both measured in MCH).

It can be seen that even if the differences are larger in the anthracene case, the fluorescence quantum yield of the *p*-disubstituted alkoxy acenes is generally larger than that of *o*-disubstituted alkoxy acenes.

5.3 Results of the fluorescence lifetime measurements

The single photon counting measurements to determine the fluorescence decay rates were carried out at the "Laboratoire de Physico-Chimie Moléculaire, (CNRS, UMR 5803) Université Bordeaux 1".

Substance ($\lambda_{(emiss)}$)	Solvent	τ [ns]	χ^2	DW
5,12-DDOT	MCH (degassed)	25.0	1,13	1.85
2,3-DDOT (508 nm)	MCH (degassed)	8.3	1.20	1.67
2,3-DHdOT	MCH (degassed)	8.3	1.16	1.73

Table 54 Fluorescence lifetimes of different alkoxy-tetracenes

5.3.1 Discussion of the results

As seen in Table 54, with 25 ns the fluorescence lifetime of 5,12-DDOT (**85**) is far longer than the life times of the 2,3-disubstituted alkoxy tetracenes **86** and **111**. With 8.3 ns 2,3-DDOT (**86**) and 2,3-DHdOT (**111**) show the same fluorescence decay time, a result that was to be expected.

Comparing those results to those of similarly substituted anthracenes, the same trend can be seen. 2,3-DDOA (**1**) exhibits a $\tau_{(fl)}$ 0f 4.2 ns, while 9,10-DDOA exhibits $\tau_{(fl)}$ of 13.8 ns.[3]

5.4 Radiative decay rate constant

Following Equation 9 (see Chapter 5), the radiative decay rate constant of the three examined alkoxytetracenes can be calculated and compared:

Substance	k_{FM}
5,12-DDOT (**85**)	0.020 ns^{-1}
2,3-DDOT (**86**)	0.030 ns^{-1}
2,3-DHdOT (**111**)	0.024 ns^{-1}

Table 55 Radiative decay rate constants of alkoxytetracenes

It can be seen that the values for k_{FM} are in the same order of magnitude for all three samples. While this is not astonishing in the case of 2,3-DDOT and 2,3-DHdOT (bearing the same chromophore), it is noteworthy in the case of 5,12-DDOT.

Again, these results are compared to the radiative rate constants of dialkoxyanthracenes, calculated from the results published by Brotin et al.[3]

Substance	k_{FM}
2,3-DDOA (**1**)	0.045 ns^{-1}
9,10-DDOA	0.062 ns^{-1}
1,4-DDOA	0.046 ns^{-1}

Table 56 Radiative rate constants of alkoxy-anthracenes, calculated from[3]

When the values for 9,10-DDOA and 2,3-DDOA (**1**) are compared, it can be seen that, unlike in the tetracene case, the k_{FM} values for the *p*-disubstituted anthracene are higher than the values for the *o*-disubstituted anthracene. The value for 1,4-DDOA (as another *p*-disubstituted alkoxy-anthracene) is fairly similar to the one for 2,3-DDOA, indicating that the ring being substituted has a larger influence on the radiative rate constant than the *o*- or *p*-substitution pattern. Before a full comparisons can be made in the case of the tetracenes, more synthetic work needs to be carried out but it can be stated that the k_{FM} values for the tetracenes **85** and **86**, **111** are smaller than the values obtained for similarly substituted anthracenes.[3]

6 Summary

2,3-Dialkoxy-tetracenes (**2**) (chain length 1, 4, 6, 10 and 16 C-atoms) have been synthesized according to Scheme 25.

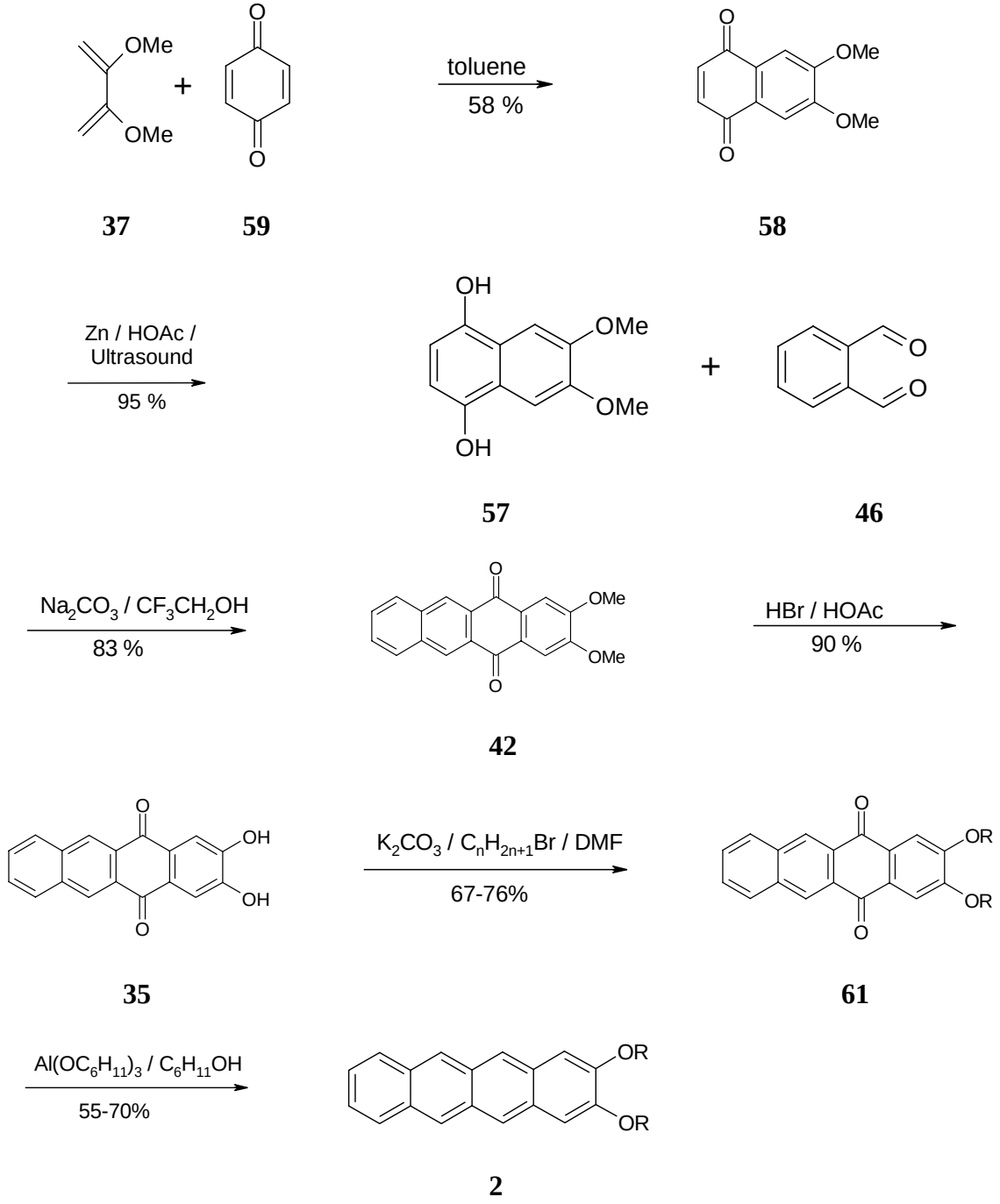

Scheme 25 **Synthesis of 2,3-dialkoxy-tetracenes** (**2**)

Overall this sequence furnished the 2,3-dialkoxy-tetracenes (**2**) in acceptable yields (21% 6 steps).

Gel formation of the 2,3-dialkoxy-tetracenes **2** with various organic solvents was examined under aspects of chain length and temperature dependency. Three kinds of experiments were performed: inverted tube tests to study macroscopic gel formation, temperature dependent UV/Vis spectroscopy to gain insight into the thermodynamics of the gel formation and AFM (atomic force microscopy) measurements to study the microscopic structures of the formed gels.

The inverted tube tests have shown that the minimum chain length for 2,3-dialkoxy-tetracenes (**2**) to form gels is around C-6. The best results (stable gels with the minimum of gelator) were obtained with 2,3-dihexadecyloxy-tetracene (**111**). This shows that the larger aromatic core, in comparison to 2,3-didecyloxy-anthracene (**1**), has to be compensated by longer chains to increase the solubility. Another difference to the parent molecule is a shift in polarity, when the solvents that form gels are considered. 2,3-DHdOT (**111**) forms gels mainly in apolar solvents, the best results (0.55 mg/mL at ambient temperature) were obtained with cyclohexane, while the best solvent in the case of 2,3-DDOA (**1**) is methanol.

UV/Vis spectroscopic experiments provided a first insight into the thermodynamics of gel formation and the melting of gels. It was shown that the phase transitions are subject to a hysteresis. Furthermore, the thermodynamic values (ΔG) for the formation (ΔG_F) and the melting (ΔG_M) of the gels of 2,3-DDOT (**86**) and 2,3-DHdOT (**111**) in two solvents (cyclohexane and n-hexanol) are fairly similar. In the case of the gel melting the values spread over a wider range. This similarity, along with the comparison of the UV/Vis-spectra of gel forming 2,3-dialkoxy-tetracenes in the gel state with spectra measured in solid state (KBr pellets) gives a first idea of the mode of gel formation. It involves dry gels, i. e. no solvent molecules are incorporated in the gelator structures.

Those structures were more closely examined using AFM measurements leading to an estimation of the size of the fibers formed. The smallest structures measured so far exhibit a size of 200 nm (diameter) and several µm (length) and the measurements show a bridged, net like structure of the gelator (e. g. 2,3-DHdOT (**111**) in nonane, 0.5 mg/mL) that immobilizes the solvent, thus forming the gel.

Having shown the gel forming capacities of 2,3-dialkoxy-tetracenes, 2,3-dialkoxy-pentacenes were synthesized, using the well established route to investigate the gel formation of 2,3-disubstituted pentacenes. The main synthetic difference was the use of naphthalene-2,3-dicarboxaldehyde (**52**) instead of phthalic dialdehyde (see Scheme 25). This led to the formation of 2,3-dimethoxypentacene-5,14-quinone (**77**) as the key intermediate of the 2,3-dialkoxy-pentacene synthesis.

Analysis of the gel forming properties of the resulting 2,3-dihexadecyloxy-pentacene (**115**) by AFM- and inverted tube methods showed that even pentacenes are able to form gels, even if the poor solubility limits the solvents to high boiling halogenated ones (the best results were obtained with 1,1,2,2-tetrachloroethane). Furthermore, instability towards oxidation limited the measurements for 2,3-disubstituted pentacenes.

The photochemistry of substituted tetracenes was examined, using 2,3-dialkoxy-tetracenes (**2**) and 5,12-DDOT (**85**) as analogues of 2,3-DDOA (**1**) and 9,10-DDOA.

The tetracene 5,12-DDOT (**85**) was synthesized in a two step reaction starting from 5,12-tetracene-quinone (**94**) by Zn reduction followed directly by alkylation, as shown in Scheme 26.

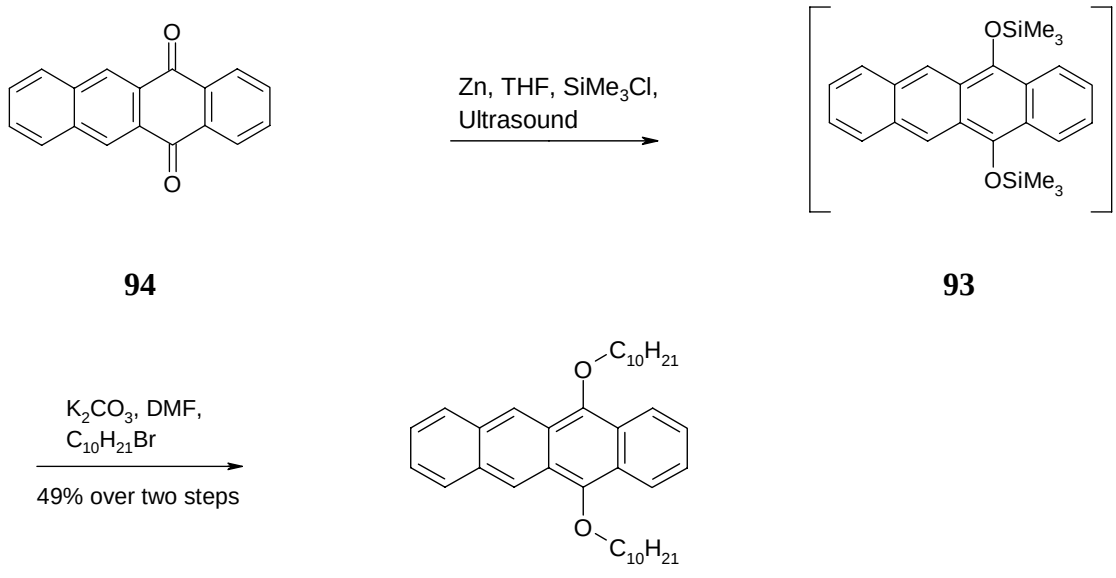

Scheme 26 Synthesis of 5,12-DDOT (**85**)

The irradiation of 2,3-DDOT (**86**) led to several photodimers, in contrast to the 2,3-DDOA irradiation, that does not provide photodimers. Still, the dimers that can be seen as analogues of 2,3-DDOA (**1**) were not formed.

In the case of the 5,12-DDOT (**85**) neither the pure 5,12-DDOT-dimerization, nor the crossed dimerization of 5,12-DDOT (**85**) with tetracene led to dimers under participation of the alkoxy substituted ring. This is in contrast to the results of the dimerization of 9,10-DDOA with anthracene that leads to the 9,10-photodimers.

The structures of the different photodimers were investigated by NMR spectroscopy as well as fluorescence- and UV/Vis-spectroscopy to distinguish the head-to-head from the head-to tail dimers.

To supplement the photochemical results, measurements of the fluorescence quantum yields of 5,12-DDOT (**85**), 2,3-DDOT (**86**) and 2,3-DHdOT (**111**) were measured along with measurements of the fluorescence life times of the compounds to determine the radiative decay rate constants.

5,12-DDOT dimerisation was shown to be thermally and photochemically reversible, even if the degradation of the substrate under thermal or UV photochemical conditions was observed.

7 Experimental part

7.1 Techniques and equipment

Thin layer chromatography (TLC): TLC- plates „Polygram Sil G/UV_{254}“, Macherey & Nagel Co. (Düren).

Column chromatography: Flash chromatography was carried out with “Kieselgel 60” (70-230 mesh), Merck KgaA (Darmstadt) under N_2 pressure.

Melting points: “Meltemp” electrical melting point apparatus, uncorrected.

Irradiations: The preparative irradiations were carried out in Ar purged solvents with a 1000 W halogen lamp in a glass vessel (Duran: transmittance 5% at 285 nm, 10% at 290 nm).

NMR-spectroscopy: Unless otherwise mentioned, ^{1}H and ^{13}C NMR spectra were measured in deuterated chloroform using tetramethylsilane (TMS) as internal standard. The multiplicities are abbreviated as follows: s = singlet, d = doublet, t = triplet, q = quartet, m = multiplet, m_c = multiplet center (used for higher order spin systems).

The coupling constants for the AA'XX'-spin system of compounds **42**, **94** and **109** were analyzed by iterative calculation, using the WinDAISY® 4.1 software (Bruker Rheinstetten). The calculations were performed by Professor Dr. L. Ernst, TU Braunschweig. R-Factors are generally better than 0.85%.

In the cases where the spin system was not calculated, the distance between the outer signals is given in Hz (*N*-values).

The solid state TOS NMR spectra of **83** and **84** were measured at 4 kHz, using the CH_2 signal of adamanthane (δ = 28.8) as indirect standard.

The following spectrometers were used: Bruker AC 200: ^{1}H NMR (200.2 MHz), ^{13}C (50.3 MHz)

Bruker DRX 400: ^{1}H NMR (400.1 MHz), ^{13}C (100.6 MHz)

Mass spectrometry: Finnigan MAT 8430 Spectrometer. Unless otherwise noted 70 eV electron impact (EI) ionization was used. High resolution spectra were taken by “peak matching” with a precision of ± 2 ppm.

IR spectroscopy: As KBr pellets on a Nicolet 320 FT-IR-spectrometer or on a diamond ATR spectrometer Bruker Tensor 27. The intensity of the bands is abbreviated with w (weak, up to 33% of the most intense band), m (medium, 34 - 67% of the most intense band), s (strong, more than 68% of the most intense band).

UV/Vis absorption spectroscopy: Beckman UV 5230 spectrometer. As solvent DCM of spectroscopic pure quality was used, unless otherwise stated. The temperature dependent spectra of the gelators, as well as the absorption spectra to calculate the fluorescence quantum yields were measured at the Laboratoire de Chimie Organique et Organometallique at the Université Bordeaux I on a Hitachi U-3300 spectrometer.

Fluorescence spectroscopy: 1680 Spex double-spectrometer at the Laboratoire de Chimie Organique et Organometallique, Université Bordeaux I. The fluorescence spectra to distinguish the 2,3-DDOT-photodimers were measured at the TU Braunschweig.

Elementary analysis (EA): The elementary analysis of the compounds were measured at the Institut für Pharmazeutische Chemie and the Institut für Anorganische und Analytische Chemie, Technischen Universität Braunschweig.

Fluorescence life times: Single photon timing technique (Applied Photophysics), decay parameters determined by nonlinear least squares deconvolution method, using the DECAN (1.0) program, provided by F. De Schryver. Excitation has been performed by a pulsed H_2 arc-lamp combined to a band-pass filter, detection has been performed after a monochromator by photomultiplier. Measured at the Laboratoire de Chimie Organique et Organometallique, Université Bordeaux I.

7.2 General working procedures (GWP)

7.2.1 GWP 1 (alkylation of dihydroxy-acene-quinones)

The hydroxyacenequinone is dissolved in dry DMF (17 mL/mmol). It is deprotonated over 1 h with K_2CO_3 (1.25 equivalents per OH group) under N_2. After this time the alkylbromide is added (1.1 equivalents per OH group) over a period of 1 h. The mixture is refluxed for further 3 h. After completion of the reaction the mixture is allowed to cool to room temp. The solvent is evaporated under vacuum. Column chromatography (silica; DCM/ pentane) gave the product.

7.2.2 GWP 2 (reduction of alkoxy-acene-quinones)

Al powder (6-12 equivalents calculated on the basis of the alkoxy-acene-quinone), $HgCl_2$ (0.2 mg/mmol Al), CCl_4 (2 µL/mmol Al) and dry cyclohexanol (0.5-1.0 mL/mmol Al) were refluxed under N_2 or Ar for 3 h (formation of the alkoxide can be observed by formation of a dark grey solution). The reaction vessel is protected against direct light and the alkoxy-acene-quinone is added to the cooled down solution. The mixture is refluxed for 1.5 to 3 h. Work up is carried out as described for the individual experiments.

7.2.3 GWP 3 (photodimerization)

The different tetracenes are dissolved/suspended in cyclohexane in a Teflon® capped glass reactor equipped with a magnetic stirrer. The concentration is chosen to be formally 0.05 M. The solution is saturated with Ar (1 min per mL of solution), the reactor is closed and irradiated for 24-48 h with a 1000 W halogen lamp. After the reaction time has passed, the reaction is allowed to cool to room temp., the solvent is evaporated under vacuum and the resulting mixture is separated, using column chromatography under the conditions mentioned in the individual experimental chapters.

7.3 Synthetic procedures

7.3.1 2,3-Dialkoxy-tetracene synthesis

7.3.1.1 2,3-Dimethoxy-buta-1,3-diene (37)[11]

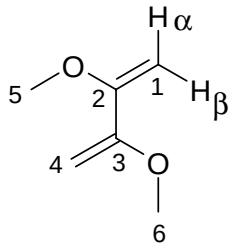

37

Butan-2,3-dione (**60)** (39 mL, 0.44 mol), trimethylorthoformiate (148 mL, 1.35 mol) and 115 mL of dry methanol are saturated with N_2 for 1.5 h. 6 drops of conc. sulfuric acid are added and the mixture is refluxed for 18 h under N_2. Excess reagents are distilled off (110 °C), $NH_4H_2PO_4$ (56 mg) and hydroquinone (70 mg) are added, and the crude product is distilled several times until reasonable purity (controlled by GC) is reached. The product is obtained as a colorless liquid, b. p. 132-135 °C, 90% pure, 14.4 g (29%).

^{1}H NMR (400 MHz, $CDCl_3$): δ = 4.68 (d, ^1J = 1.50 Hz, 2 H, 1/4-H_α), 4.15 (d, ^1J = 1.52 Hz, 2 H, 1/4-H_β), 3.63 (s, 6 H, 5/6-H).

^{13}C NMR (100 MHz, $CDCl_3$): δ = 156.5 (s, C-2/3), 82.4 (t, C-1/4), 55.0 (q, C-5/6).

The spectral data agree with the data given in the literature. [11]

7.3.1.2 6,7-Dimethoxy-1,4-naphthoquinone (58)[20]

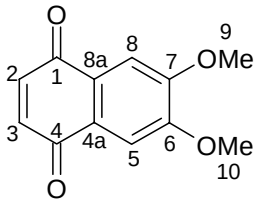

58

Benzoquinone (**59**) (33.1 g, 0.31 mol) is dissolved in anhydrous toluene (42 mL, 140 °C temperature of the oil bath). 2,3-Dimethoxybuta-1,3-diene (**37**) (9.9 g, 90% GC-purity, 75.4 mmol) is added and the mixture is stirred for 40 h under N_2. The mixture is allowed to cool to room temp., the residue is washed with pentane and afterwards with hot water to remove the excess of **59** as well as the formed hydroquinone. After the crude product has been washed several times with acetone the residue (9.62 g, 58%) is obtained as a brownish-yellow solid of appreciable purity for synthetic use. Further purification can be achieved by sublimation at 220 °C/ 0.1 hPa.

m. p.: 242 °C (acetone).

IR (KBr): $\tilde{\nu}_{max}$ = 3442 cm^{-1} (m), 1655 (m), 1611 (w), 1585 (s), 1513 (m), 1314 (s).

^{1}H NMR (400 MHz, $CDCl_3$): δ = 7.49 (s, 2 H, 8/5-H), 6.88 (s, 2 H, 3/2-H), 4.03 (s, 6 H, 10/9-H).

^{13}C NMR (100 MHz, $CDCl_3$): δ = 184.5 (s, C-4/1), 153.5 (s, C-7/6), 138.3 (d, C-3/2), 126.7 (s, C-8a/4a), 107.8 (d, C-8/5), 56.5 (q, C-10/9).

UV (DCM): λ_{max} (lg ε) = 208 nm (4.47), 228 (4.00), 268 (4.38), 278 (4.29, shoulder), 352 (3.42), 410 (3.34).

MS (70 eV): *m/z* (%) = 218 (100) [M^+], 203 (14) [M^+–CH_3], 188 (7) [M^+–2*CH_3], 175 (13) [M^+–CO–CH_3].

The spectral data agree with those given in the literature. [20]

7.3.1.3 1,4-Dihydroxy-6,7-dimethoxy-naphthalene (57)[24]

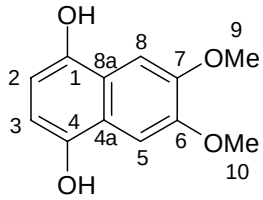

57

6,7-Dimethoxy-naphtho-1,4-quinone (**58**) (3.6 g, 16.5 mmol) is suspended in 108 mL of glacial acetic acid. 2.15 g (33 mmol) Zn dust is added in four portions and after each addition the suspension is sonicated for 20 min in a 130 W ultrasound bath. The reaction is complete, when the product is dissolved totally and the solution above the Zn residue is only slightly brownish. The mixture is diluted with 100 mL of ethyl acetate and the $Zn/Zn(OAc)_2$ precipitate is filtered off and washed with ethyl acetate. The solvent is removed under vacuum, the solid product washed with pentane and dried in high vacuum. The crude product (3.47 g, 95%) is directly used for further reaction.

m. p.: 178-182 °C (decomposition).

IR (KBr): $\tilde{\nu}_{max}$ = 3236 cm^{-1} (m), 1612 (s), 1497 (s), 1268 (s), 1259 (s), 1202 (s).

^{1}H NMR (400 MHz, acetone-d_6): δ = 8.19 - 8.07 (br.-s, 2 H, OH), 7.48 (s, 2 H, 8/5-H), 6.58 (s, 2 H, 2/3-H), 3.92 (s, 6 H, 10/9-H).

^{13}C NMR (100 MHz, acetone-d_6): δ = 150.2 (s, C-7/6), 146.0 (s, C-4/1), 122.0 (s, C-8a/4a), 107.3 (d, C-3/2), 102.3 (d, C-8/5), 55.8 (q, C-10/9).

MS (70 eV): *m/z* (%) = 220 (100) [M^+], 218 (36) [M^+-2H], 205 (8) [M^+-CH_3], 177 (12) [M^+-CH_3-CO].

HRMS: *m/z* calcd. for $C_{12}H_{12}O_4$ [M^+]: 220.0736; found 220.0726 ± 1 ppm.

7.3.1.4 2,3-Dimethoxy-tetracene-5,12-quinone (42)[17]

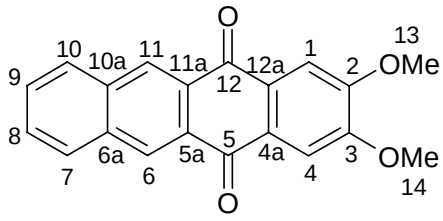

42

1,4-Dihydroxy-6,7-dimethoxy-naphthalene (**57**) (3.47 g, 15.8 mmol), phthalic dialdehyde (**46**) (2.32 g, 17.3 mmol), Na_2CO_3 (3.35 g, 31.6 mmol) and 2,2,2-trifluorethanol (79 mL) are mixed in a dry vessel under N_2. The mixture is refluxed for 4 h, allowed to cool to room temp. and stirred with 80 mL of water. The residue is filtered off, washed with water, acetone and diethyl ether. The product (4.18 g, 83%) is obtained as a dark yellow solid. Further purification can be achieved by recrystallization from ethyl acetate.

m. p.: 295 °C (ethyl acetate).

R_f (DCM): 0.08.

IR (KBr): $\tilde{\nu}_{max}$ = 3443 cm^{-1} (w), 3054 (w), 2999 (w), 2941 (w), 2837 (w), 1666 (s), 1620 (w), 1579 (s), 1510 (m), 1467 (m), 1455 (m), 1443 (m), 1400 (m), 1375 (m), 1308 (s).

^{1}H NMR (400 MHz, $CDCl_3$): δ = 8.78 (s, 2 H, 11/6-H), 8.08 (m_c, $^3J_{AX/A'X'}$ = 8.3 Hz, $^4J_{AX'/A'X}$ = 1.2 Hz, $^5J_{AA'}$ = 0.7 Hz, $^3J_{XX'}$ = 6.9 Hz, 2 H, 10/7-H), 7.77 (s, 2 H, 4/1-H), 7.68 (m_c, $^3J_{XA/X'A'}$ = 8.3 Hz, $^4J_{X'A/XA'}$ = 1.2 Hz, $^5J_{AA'}$ = 0.7 Hz, $^3J_{XX'}$ = 6.9 Hz, 2 H, 9/8-H), 4.08 (s, 6 H, 14/13-H).

^{13}C NMR (100 MHz, $CDCl_3$): δ = 182.2 (s, C-12/5), 153.9 (s, C-3/2), 135.0 (s, C-10a/6a), 130.1 (d, C-10/7), 129.9 (s, C-11a/5a), 129.5 (s, C-12a/4a), 129.3 (d, C-9/8), 129.2 (d, C-11/6), 108.5 (d, C-4/1), 56.6 (q, C-14/13).

UV (DCM): λ_{max} (lg ε) =204 nm (4.38), 236 (4.58), 298 (4.74), 386 (3.81).

MS (70 eV): *m/z* (%) = 318 (100) [M^+], 303 (12) [M^+-CH_3], 289 (9) [M^+-CH_3-CH_2], 275 (11) [M^+-CH_3-CO), 247 (20) [M^+-2CO-CH_3].

Elemental analysis: $C_{20}H_{14}O_4$ (318.33): calcd. C 75.46, H 4.43; found C 74.91, H 4.39.

7.3.1.5 2,3-Dihydroxy-tetracene-5,12-quinone (35)

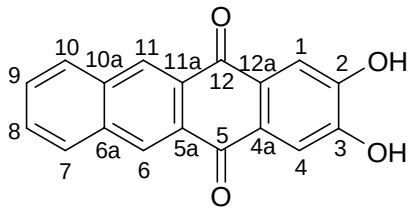

35

a) Demethylation with HBr/HOAc[30]

2,3-Dimethoxy-tetracene-5,12-quinone (**42**) (4.18 g, 13.1 mmol) is refluxed for 24 h in 92 mL of concentrated HBr solution (w = 48%). After addition of glacial acetic acid (92 mL) reflux is maintained for further 24 h. The suspension is allowed to cool to room temp. and diluted with 200 mL of water. After filtration the residue is washed with water, acetone and diethyl ether and dried in high vacuum. The product (3.42 g, 90%) is obtained as a slight green solid and used for further synthesis without purification.

b) Demethylation with pyridine•HCl[31]

2,3-Dimethoxy-tetracene-5,12-quinone (**42**) (1.0 g, 3.14 mmol), is mixed with pyridine*HCl (10.9 g, 94.3 mmol) under N_2. The mixture is heated in a sand bath to 200 - 240 °C, where the pyridinium salt is molten. The mixture is stirred for 3 h and allowed to cool to room temp. Water is added and the insoluble residue is filtered, washed with 2 N hydrochloric acid, methanol and diethyl ether to yield 820 mg (90%) of 2,3-dihydroxy-tetracene-5,12-quinone (**35**).

c) Demethylation with BBr_3[26]

2,3-Dimethoxy-tetracene-5,12-quinone (**42**) (0.4 g, 1.26 mmol) is suspended in 80 mL of anhydrous DCM under N_2. Under strong stirring a solution of BBr_3 (3.0 mL, 1 molar in DCM) is added and the mixture is stirred for 14 h at room temp. 8 mL of methanol is added and the solvent is evaporated under reduced pressure. Thin layer chromatography shows only partly cleavage of the ether. The crude mixture was directly alkylated under standard conditions (GWP 1), leading to 70 mg (10%) **56**, 66 mg (12%) of the singly demethylated/ alkylated product and 180 mg (45%) of unreacted starting material. Longer reaction times or higher temperatures did not improve the results.

m. p.: 314 °C (decomp.).

IR (ATR): $\tilde{\nu}_{max}$ = 3469 cm^{-1} (w), 3270 (m), 1670 (s), 1648 (m), 1575 (s), 1514 (m), 1499 (m), 1454 (m), 1401 (m), 1303 (s).

UV (DMSO): λ_{max} (lg ε) = 253 nm (4.20), 303 (4.65), 374 (4.01), 538 (3.09).

^{1}H NMR (400 MHz, DMSO-d_6): δ = 10.68 (s, 2 H, OH), 8.68 (s, 2 H, 11/6-H), 8.21 (m_c, *N* = 9.4 Hz, 2 H, 10/7-H), 7.73 (m_c, *N* = 9.5 Hz, 2 H, 9/8-H), 7.57 (s, 2 H, 4/1-H).

^{13}C NMR (100 MHz, DMSO-d_6): δ = 181.3 (s, C-12/5), 151.8 (s, C-3/2), 134,4 (s, C-10a/6a), 130,0 (d, C-10/7), 129.8 (s, C-11a/5a), 129.4 (d, C-9/8), 128.4 (d, C-11/6), 128.0 (s, C-12a/4a), 113.0 (d, C-4/1).

MS (70 eV): *m/z* (%) = 290 (100) [M^+], 262 (22) [M^+-CO], 234 (14) [M^+-2 CO].

Elemental analysis: Due to imperfect demethylation, no elemental analysis was performed.

7.3.1.6 2,3-Dibutoxy-tetracene-5,12-quinone (106)[11]

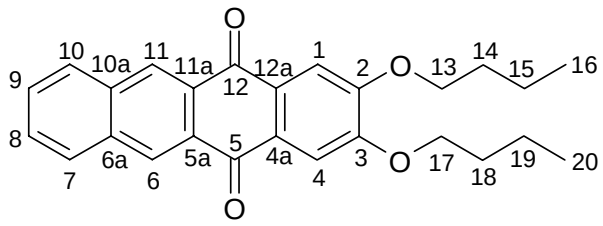

106

GWP 1: 2,3-Dihydroxy-tetracene-5,12-quinone (**35**) (1.00 g, 3.45 mmol), K_2CO_3 (1.19 g, 8.63 mmol), DMF (60 mL), C_4H_9Br (1.04 g, 7.59 mmol). The product is obtained as a yellow solid (0.93 g, 67%).

m. p.: 201 °C (ethyl acetate).

R_f (DCM): 0.53.

IR (ATR): $\tilde{\nu}_{max}$ = 3084 cm^{-1} (w), 3056 (w), 3029 (w), 2955 (m), 2938 (w), 2905 (w), 2867 (w), 1661 (s), 1618 (w), 1575 (s), 1508 (m), 1455 (m), 1399 (m), 1374 (m), 1300 (s).

^{1}H NMR (400 MHz, $CDCl_3$): δ = 8.76 (s, 2 H, 11/6-H), 8.06 (m_c, *N* = 9.4 Hz, 2 H, 10/7-H), 7.73 (s, 2 H, 4/1-H), 7.65 (m_c, *N* = 9.5 Hz, 2 H, 9/8-H), 4.21 (t, ^{3}J = 6.6 Hz, 4 H, 17/13-H), 1.93-1.86 (m, 4 H, chain), 1.61-1.51 (m, 4 H, chain), 1.03 (t, ^{3}J = 7.4 Hz, 6 H, 20/16-H).

^{13}C NMR (100 MHz, $CDCl_3$): δ = 182.3 (s, C-12/5), 153.9 (s, C-3/2), 135.0 (s, C-10a/6a), 130.04 (s, C-11a/5a), 130.02 (d, C-10/7), 129.20 (s, C-12a/4a), 129.15 (d, C-9/8), 129.1 (d, C-11/6), 109.4 (d, C-4/1), 69.1 (t, C-17/13), 31.0 (t, chain), 19.2 (t, chain), 13.8 (q, C-20/16).

The aromatic ^{13}C-signals were assigned by comparison with **107** and **108**.

UV (DCM): λ_{max} (lg ε) = 238 nm (4.76), 302 (4.90), 390 (4.05).

MS (70 eV): *m/z* (%) = 402 (25) [M^+], 346 (9) [M^+-C_4H_8], 290 (100) [M^+-C_8H_{16}].

Elemental analysis: $C_{26}H_{26}O_4$ (402.49): calcd. C 77.59, H 6.51; found C 77.74, H 6.50.

7.3.1.7 2,3-Dihexyloxy-tetracene-5,12-quinone (107)[11]

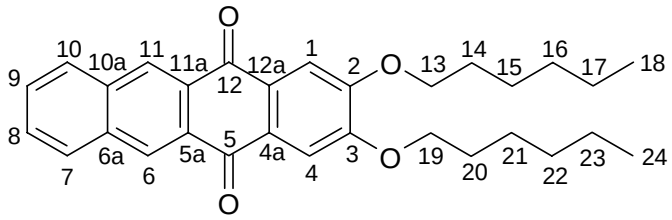

107

GWP 1: 2,3-Dihydroxy-tetracene-5,12-quinone (**35**) (1.0 g, 3.45 mmol), K_2CO_3 (1.19 g, 8.63 mmol), DMF (60 mL), $C_6H_{13}Br$ (1.25 g, 7.59 mmol). The product is obtained as a yellow solid (1.17 g, 74%).

m. p.: 154 °C (ethyl acetate).

R_f (DCM): 0.62.

IR (KBr): $\tilde{\nu}_{max}$ = 3450 cm^{-1} (w), 3084 (w), 3058 (w), 2949 (w), 2926 (w), 2883 (w), 2857 (w), 1662 (s), 1620 (w), 1574 (s), 1510 (w), 1457 (w), 1399 (m), 1375 (w), 1309 (s).

^{1}H NMR (400 MHz, $CDCl_3$): δ = 8.77 (s, 2 H, 11/6-H), 8.07 (m_c, *N* = 9.5 Hz, 2 H, 10/7-H), 7.74 (s, 2 H, 4/1-H), 7.66 (m_c, *N* = 9.5 Hz, 2 H, 9/8-H), 4.21 (t, ^3J = 6.7 Hz, 4 H, 19/13-H), 1.94-1.87 (m, 4 H, chain), 1.59-1.49 (m, 4 H, chain), 1.43-1.32 (m, 8 H, chain), 0.94-0.91 (m, 6 H, 24/18-H).

^{13}C NMR (100 MHz, $CDCl_3$): δ = 182.4 (s, C-12/5), 153.9 (s, C-3/2), 135.0 (s, C-10a/6a), 130.04 (s, C-11a/5a), 130.02 (d, C-10/7), 129.22 (s, C-12a/4a), 129.17 (d, C-9/8), 129.1 (d, C-11/6), 109.4 (d, C-4/1), 69.4 (t, C-19/13), 31.5 (t, chain), 28.9 (t, chain), 25.6 (t, chain), 22.6 (t, chain), 14.0 (q, C-24/18).

UV (DCM): λ_{max} (lg ε) = 238 nm (4.67), 303 (4.81), 338 (4.00 sh), 390 (3.95).

MS (70 eV): *m/z* (%) = 458 (25) [M^+], 374 (10) [M^+-C_6H_{12}], 290 (100) [M^+- 2*C_6H_{12}].

Elemental analysis: $C_{30}H_{34}O_4$ (458.60): calcd. C 78.57, H 7.47; found C 78.26, H 7.38.

7.3.1.8 2,3-Didecyloxy-tetracene-5,12-quinone (56)[11]

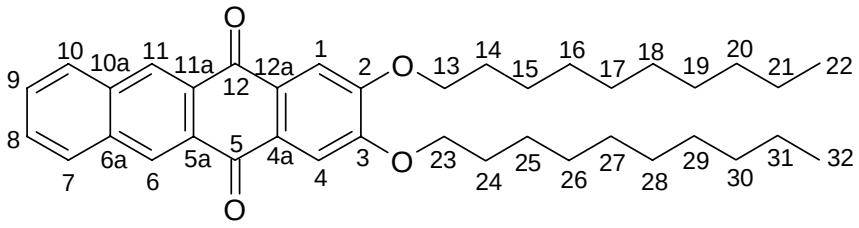

56

GWP 1: 2,3-Dihydroxy-tetracene-5,12-quinone (**35**) (3.90 g, 13.4 mmol), K_2CO_3 (4.64 g, 33.6 mmol), DMF (230 mL), $C_{10}H_{21}Br$ (6.52 g, 29.5 mmol). The product is obtained as a waxy yellow solid (5.8 g, 76%).

m. p.: 132 °C (ethyl acetate).

R_f (DCM): 0.70.

IR (ATR): $\tilde{\nu}_{max}$ = 3081 cm^{-1} (w), 3057 (w), 2916 (s), 2870 (m), 2847 (m), 1670 (s), 1620 (w), 1580 (s), 1506 (m), 1456 (m), 1399 (m), 1373 (m), 1306 (s).

^{1}H NMR (400 MHz, $CDCl_3$): δ = 8.75 (s, 2 H, 11/6-H), 8.05 (m_c, *N* = 9.5 Hz, 2 H, 10/7-H), 7.72 (s, 2 H, 4/1-H), 7.65 (m_c, *N* = 9.4 Hz, 2 H, 9/8-H), 4.20 (t, ^3J = 6.7 Hz, 4 H, 23/13-H), 1.94-1.87 (m, 4 H, chain), 1.55-1.28 (m, 28 H, chain), 0.89 (t, ^3J = 7.0 Hz, 6 H, 32/22-H).

^{13}C NMR (100 MHz, $CDCl_3$): δ = 182.3 (s, C-12/5), 153.9 (s, C-3/2), 135.0 (s, C-10a/6a), 130.0 (s, C-11a/5a), 130.0 (d, C-10/7), 129.2 (s, C-12a/4a), 129.1 (d, C-9/8), 129.0 (d, C-11/6), 109.4 (d, C-4/1), 69.4 (t, C-23/13), 31.9, 29.60, 29.56, 29.4, 29.3, 28.9, 25.9, 22.7 (t, chain), 14.1 (q, C-32/22).

The aromatic ^{13}C-signals were assigned by comparison with **107** and **108**.

UV (DCM): λ_{max} (lg ε) = 238 nm (4.70), 302 (4.83), 390 (3.97).

MS (70 eV): *m/z* (%) = 570 (59) [M^+], 430 (35) [M^+-$C_{10}H_{20}$], 290 (100) [M^+- 2* $C_{10}H_{20}$].

Elemental analysis: $C_{38}H_{50}O_4$ (570.81): calcd. C 79.94, H 8.83; found C 79.82, H 8.88.

7.3.1.9 2,3-Dihexadecyloxy-tetracene-5,12-quinone (**108**)[11]

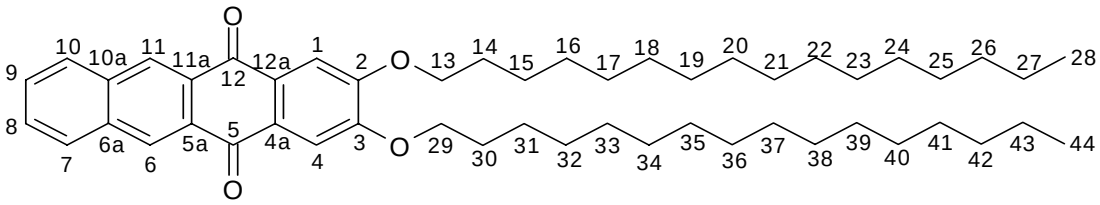

108

GWP 1: 2,3-Dihydroxy-tetracene-5,12-quinone (**35**) (2.0 g, 6.89 mmol), K_2CO_3 (2.38 g, 17.2 mmol), dimethylformamide (120 mL), $C_{16}H_{33}Br$ (4.63 g, 15.2 mmol). The product is obtained as a waxy yellow solid (3.62 g, 71%).

m. p.: 126 °C (ethyl acetate).

R_f (DCM): 0.75.

IR (ATR): $\tilde{\nu}_{max}$ = 3086 cm^{-1} (w), 3058 (w), 3033 (w) 2962 (w), 2916 (s), 2848 (s), 1660 (m), 1620 (w), 1574 (s), 1506 (m), 1463 (m), 1399 (m), 1374 (w), 1304 (s).

^{1}H NMR (400 MHz, $CDCl_3$): δ = 8.77 (s, 2 H, 11/6-H), 8.07 (m_c, *N* = 9.4 Hz, 2 H, 10/7-H), 7.74 (s, 2 H, 4/1-H), 7.66 (m_c, *N* = 9.5 Hz, 2 H, 9/8-H), 4.21 (t, ^3J = 6.6 Hz, 4 H, 29/13-H), 1.94-1.87 (m, 4 H, chain), 1.55-1.26 (m, 52 H, chain), 0.86 (t, ^3J 7.0 Hz, 6 H, 44/28-H).

^{13}C NMR (100 MHz, $CDCl_3$): δ = 182.3 (s, C-12/5), 153.9 (s, C-3/2), 135.0 (s, C-10a/6a), 130.08 (s, C-11a/5a), 130.02 (d, C-10/7), 129.24 (s, C-12a/4a), 129.16 (d, C-9/8), 129.06 (d, C-11/6), 109.5 (d, C-4/1), 69.4 (t, C-29/13), 35.2, 34.0, 31.9, 29.7, 29.7, 29.5, 29.3, 29.0, 26.0, 24.7 (t, chain), 14.1 (q, C-44/28).

UV (DCM): λ_{max} (lg ε) = 238 nm (4.68), 302 (4.82), 386 (4.00).

MS (70 eV): *m/z* (%) = 738 (28) [M^+], 514 (11) [M^+-$C_{16}H_{32}$], 290 (16) [M^+-$C_{32}H_{66}$].

Elemental analysis: $C_{50}H_{74}O_4$ (739.14): calcd. C 81.25, H 10.09; found C 80.91, H 10.03.

7.3.1.10 2,3-Dimethoxy-tetracene (73)[39]

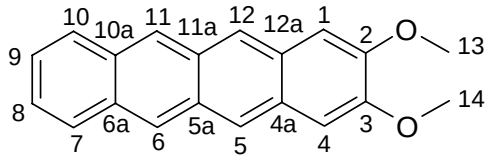

73

GWP 2: 2,3-Dimethoxy-tetracene-5,12-quinone (**42**) (0.64 g, 2.01 mmol), Al (330 mg, 12.1 mmol), $HgCl_2$ (2 mg), CCl_4 (20 µL), cyclohexanol (12 mL), reaction time 2.5 h.

Work-up: The mixture is decomposed with a solution of 7.5 mL HCl (w = 32%) and 7.5 mL of ethanol. The crude product is filtered, washed with ethanol and recrystallized from ethyl acetate (protected from direct light): yellow solid (0.32 g, 55%).

m. p.: 298 - 302 °C(decomp.).

IR (ATR): $\tilde{\nu}_{max}$ = 3007 cm^{-1} (w), 2975 (w), 2947 (w), 2906 (w), 2841 (w), 1633 (w), 1553 (m), 1515 (w), 1483 (s), 1450 (m), 1432 (s), 1295 (m), 1267 (m), 1224 (s).

^{1}H NMR (400 MHz, $CDCl_3$): δ = 8.56 (s, 2 H, 11/6-H), 8.43 (s, 2 H, 12/5-H), 7.98 (m_c, *N* = 9.8 Hz, 2 H, 10/7-H), 7.37 (m_c, *N* = 9.8 Hz, 2 H, 9/8-H), 7.17 (s, 2 H, 4/1-H), 4.06 (s, 6 H, 13/14-H).

^{13}C NMR (100 MHz, $CDCl_3$): δ = 150.3 (s, C-3/2), 131.1 (s, C-10a/6a), 129.8 (s, C-11a/5a), 128.9 (s, C-12a/4a), 128.2 (d, C-10/7), 125.5 (d, C-11/6), 124.7 (d, C-9/8), 123.6 (d, C-12/5), 104.3 (d, C-4/1), 55.9 (q, C-14/13).

The aromatic ^{13}C-signals were assigned by comparison with **109**.

UV (DCM): λ_{max} (lg ε) = 260 nm (4.45), 282 (4.83), 288 (4.84), 380 (3.44), 402 (3.77), 414 (3.51), 440 (3.72), 470 (3.68).

MS (70 eV): *m/z* (%) = 288 (100) [M^+], 273 (4) [M^+-CH_3], 245 (33) [M^+-CH_3-CO], 202 (16) [M^+-2CH_3-2CO].

HRMS: *m/z* calcd. for $C_{20}H_{16}O_2$ [M^+]: 288.1150; found 288.1145 ± 1 ppm.

7.3.1.11 2,3-Dibutoxy-tetracene (109) [39]

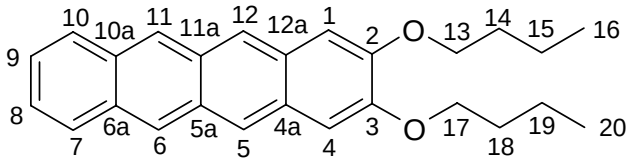

109

GWP 2: 2,3-Dibutoxy-tetracene-5,12-quinone (**106**) (0.70 g, 1.74 mmol), Al (282 mg, 10.4 mmol), $HgCl_2$ (2 mg), CCl_4 (20 µL), cyclohexanol (10.4 mL), reaction time 3 h.

Work-up: The mixture is decomposed with a solution of 5 mL HCl (w = 32%) and 5 mL of ethanol. The crude product is filtered, washed with ethanol and recrystallized from ethyl acetate (protected from direct light): orange fluorescent solid (0.42 g, 65%).

m. p.: 251 °C (ethyl acetate).

R_f (DCM): 0.81.

IR (ATR): $\tilde{\nu}_{max}$ = 3069 cm^{-1} (w), 3044 (w), 2957 (m), 2931 (m), 2870 (m), 1632 (w), 1553 (m), 1516 (w), 1485 (m), 1460 (m), 1396 (m), 1379 (m), 1296 (m), 1233 (m), 1211 (m).

^{1}H NMR (400 MHz, $CDCl_3$): δ = 8.52 (s, 2 H, 11/6-H), 8.37 (s, 2 H, 12/5-H), 7.95 (m_c, $^3J_{AX/A'X'}$ = 8.7 Hz, $^4J_{AX'/A'X}$ = 1.2 Hz, $^5J_{AA'}$ = 0.9 Hz, $^3J_{XX'}$ = 6.5 Hz, 2 H, 10/7-H), 7.35 (m_c, $^3J_{XA/X'A'}$ = 8.7 Hz, $^4J_{X'A/XA'}$ = 1.2 Hz, $^5J_{AA'}$ = 0.9 Hz, $^3J_{XX'}$ = 6.5 Hz, 2 H, 9/8-H), 7.13 (s, 2 H, 4/1-H), 4.16 (t, ^3J = 6.6 Hz, 4 H, 13/17-H), 1.96-1.89 (m, 4 H, chain), 1.63-1.54 (m, 4 H, chain), 1.03 (t, ^3J = 7.4 Hz, 6H, 16/20-H).

^{13}C NMR (100 MHz, $CDCl_3$): δ = 150.3 (s, C-3/2), 131.0 (s, C-10a/6a), 129.7 (s, C-11a/5a), 129.1 (s, C-12a/4a), 128.2 (d, C-10/7), 125.4 (d, C-11/6), 124.6 (d, C-9/8), 123.3 (d, C-12/5), 105.3 (d, C-4/1), 68.5 (t, C-13/17), 31.1 (t, chain), 19.4 (t, chain), 13.9 (q, C-16/20).

UV (DCM): λ_{max} (lg ε) = 292 nm (4.91), 382 (3.40), 404 (3.70), 444 (3.67), 472 (3.51).

MS (70 eV): *m/z* (%) = 372 (95) [M^+], 316 (24) [M^+-C_4H_8], 260 (100) [M^+-C_8H_{16}], 231 (29) [M^+-C_8H_{16}-CHO].

HRMS: *m/z* calcd. for $C_{26}H_{20}O_2$ [M^+]: 372.2089; found 372.2085 ± 1 ppm.

7.3.1.12 2,3-Dihexyloxy-tetracene (110)[39]

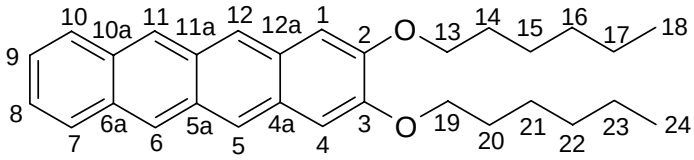

110

GWP 2: 2,3-Dihexyloxy-tetracene-5,12-quinone (**107**) (0.5 g, 1.09 mmol), Al (180 mg, 6.54 mmol), $HgCl_2$ (3 mg), CCl_4 (30 µL), cyclohexanol (6.5 mL), reaction time 3 h.

Work-up: The mixture is decomposed with a solution of 12 mL HCl (w = 32%) and 12 mL of ethanol. The crude product is filtered, washed with ethanol and recrystallized from ethyl acetate (protected from direct light): orange fluorescent solid (0.33 g, 70%).

m. p.: 181°C (ethyl acetate).

R_f (DCM): 0.84.

IR (ATR): $\tilde{\nu}_{max}$ = 2917 cm^{-1} (w), 2848 (w), 1669 (w), 1621 (w), 1578 (m), 1508 (w), 1457 (w), 1400 (w), 1374 (w), 1305 (s).

^{1}H NMR (400 MHz, $CDCl_3$): δ = 8.53 (s, 2 H, 11/6-H), 8.38 (s, 2 H, 12/5-H), 7.96 (m_c, *N* = 9.8 Hz, 2 H, 10/7-H), 7.35 (m_c, *N* = 9.8 Hz, 2 H, 9/8-H), 7.14 (s, 2 H, 4/1-H), 4.16 (t, ^3J = 6.6 Hz, 4 H, 13/19-H), 1.97-1.90 (m, 4 H, chain), 1.59-1.27 (m, 12 H, chain), 0.95-0.92 (m, 6 H, 18/24-H).

^{13}C NMR (100 MHz, $CDCl_3$): δ = 150.2 (s, C-3/2), 131.0 (s, C-10a/6a), 129.7 (s, C-11a/5a), 129.1 (s, C-12a/4a), 128.2 (d, C-10/7), 125.4 (d, C-11/6), 124.6 (d, C-9/8), 123.3 (d, C-12/5), 105.2 (d, C-4/1), 68.7 (t, C-13/19), 31.6 (t, chain), 29.0 (t, chain), 25.8 (t, chain), 22.6 (t, chain), 14.0 (q, C-18/24).

The aromatic ^{13}C-signals were assigned by comparison with **109**.

UV (DCM): λ_{max} (lg ε) = 292 nm (4.93), 382 (3.61), 404 (3.77), 416 (3.53), 444 (3.58), 472 (3.51).

MS (70 eV): *m/z* (%) = 428 (100) [M^+], 344 (26) [M^+-C_6H_{12}], 260 (98) [M^+-$C_{12}H_{24}$].

HRMS: *m/z* calcd. for $C_{30}H_{36}O_2$ [M^+]: 428.2715; found 428.2707 ± 1 ppm.

7.3.1.13 2,3-Didecyloxy-tetracene (86) [39]

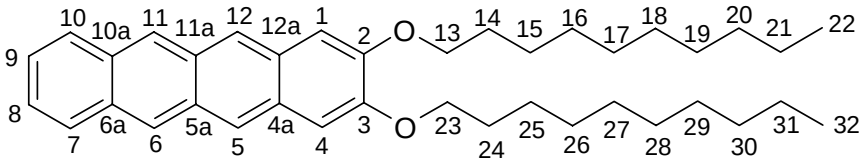

86

GWP 2: 2,3-Didecyloxy-tetracene-5,12-quinone (**56**) (1.50 g, 2.63 mmol), Al (425 mg, 15.8 mmol), $HgCl_2$ (3 mg), CCl_4 (30 µL), cyclohexanol (15.8 mL), reaction time 3 h.

Work-up: The mixture is decomposed with a solution of 30 mL HCl (w = 32%) and 30 mL of ethanol. The crude product is filtered, washed with ethanol and recrystallized from ethyl acetate (protected from direct light): yellow fluorescent solid (0.94 g, 66%).

m. p.: 172 - 173°C (ethyl acetate).

R_f (DCM/pentane (1:4)): 0.53.

IR (KBr): $\tilde{\nu}_{max}$ = 3448 cm^{-1} (w), 3048 (w), 2956 (m), 2920 (s), 2873 (m), 2852 (s), 1636 (w), 1557 (w), 1488 (m), 1479 (m), 1467 (m), 1301 (m), 1241 (s).

^{1}H NMR (400 MHz, $CDCl_3$): δ = 8.54 (s, 2 H, 11/6-H), 8.39 (s, 2 H, 12/5-H), 7.96 (m_c, *N* = 9.8 Hz, 2 H, 10/7-H), 7.36 (m_c, *N* = 9.8 Hz, 2 H, 9/8-H), 7.14 (s, 2 H, 4/1-H), 4.16 (t, ^3J = 6.6 Hz, 4 H, 13/23-H) 1.98- 0.86 (m, 38 H, chain).

^{13}C NMR (100 MHz, $CDCl_3$): δ = 150.2 (s, C-3/2) 130.9 (s, C-10a/6a), 129.7 (s, C-11a/5a), 129.1 (s, C-12a/4a), 128.2 (d, C-10/7), 125.4 (d, C-11/6), 124.6 (d, C-9/8), 123.3 (d, C-12/5), 105.2 (d, C-4/1), 68.7 (t, C-13/23), 31.9, 29.7, 29.6, 29.5, 29.4, 29.0, 26.1, 22.7 (t, chain), 14.1 (q, C-22/32).

The aromatic ^{13}C-signals were assigned by comparison with **109**.

UV (DCM): λ_{max} (lg ε) = 262 nm (4.47), 284 (4.91, sh), 292 (5.10), 382 (3.55), 404 (3.86), 416 (3.55), 444 (3.74), 472 (3.67).

MS (70 eV): *m/z* (%) = 540 (100) [M^+], 400 (20) [M^+-$C_{10}H_{20}$], 260 (65) [M^+-$C_{20}H_{40}$].

HRMS: *m/z* calcd. for $C_{38}H_{52}O_2$ [M^+]: 540.3967; found 540.3949 ± 1 ppm.

7.3.1.14 2,3-Dihexadecyloxy-tetracene (**111**)[39]

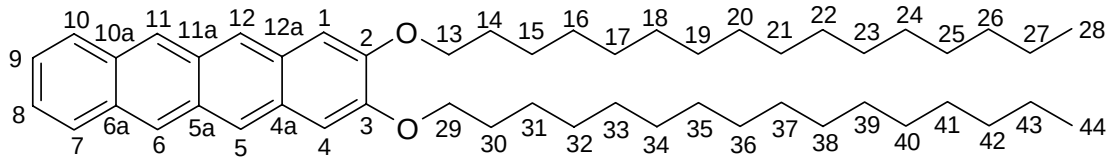

111

GWP 2: 2,3-Hexadecyloxy-tetracene-5,12-quinone (**108**) (1.63 g, 2.21 mmol), Al (715 mg, 26.5 mmol), $HgCl_2$ (30 mg), CCl_4 (100 µL), cyclohexanol (53 mL), reaction time 2 h.

Work-up: The mixture is decomposed with a solution of 25 mL HCl (w = 32%) and 25 mL of ethanol. The crude product is filtered, washed with ethanol and recrystallized from ethyl acetate/methanol (protected from direct light): yellow fluorescent solid (1.10 g, 70%).

m. p.: 144 °C (ethyl acetate/methanol).

R_f (DCM/ pentane (1:4)): 0.58.

IR (ATR): $\tilde{\nu}_{max}$ = 3045 cm^{-1} (w), 2957 (m), 2915 (s), 2847 (s), 1635 (w), 1556 (w), 1482 (m), 1464 (s), 1397 (w), 1378 (w), 1299 (m), 1265 (w), 1238 (s).

^{1}H NMR (400 MHz, $CDCl_3$): δ = 8.53 (s, 2 H, 11/6-H), 8.38 (s, 2 H, 12/5-H), 7.96 (m_c, *N* = 9.8 Hz, 2 H, 10/7-H), 7.35 (m_c, *N* = 9.8 Hz, 2 H, 9/8-H), 7.14 (s, 2 H, 4/1-H), 4.16 (t, ^3J = 6.6 Hz, 4 H, 13/29-H), 1.98-1.91 (m, 4 H, chain), 1.59-1.26 (m, 52 H, chain), 0.88 (t, ^3J = 6.8 Hz, 6 H, 28/44-H).

^{13}C NMR (100 MHz, $CDCl_3$): δ = 150.2 (s, C-3/2) 131.0 (s, C-10a/6a), 129.7 (s, C-11a/5a), 129.1 (s, C-12a/4a), 128.2 (d, C-10/7), 125.4 (d, C-11/6), 124.6 (d, C-9/8), 123.3 (d, C-12/5), 105.2 (d, C-4/1), 68.7 (t, C-13/29), 31.9, 29.74, 29.68, 29.5, 29.4, 29.0, 26.1, 22.7 (t, chain), 14.1 (q, C-28/44) not all of the 16 C atoms of the chain are resolved.

The aromatic ^{13}C-signals were assigned by comparison with **109**.

UV (DCM): λ_{max} (lg ε) = 228 nm (4.13), 262 (4.41), 292 (5.02), 382 (3.55), 404 (3.82), 444 (3.68), 472 (3.62).

MS (70 eV): *m/z* (%) = 708 (100) [M^+], 484 (14) [M^+-$C_{16}H_{32}$], 260 (73) [M^+-2*$C_{16}H_{32}$].

HRMS: *m/z* calcd. for $C_{30}H_{36}O_2$ [M^+]: 708.5845; found 708.5813 ± 1 ppm.

7.3.1.14.1 Demethylation of 2,3-dimethoxy-tetracene (**73**) *with BBr_3*

a) In DCM: 2,3-Dimethoxy-tetracene (**73**, 100 mg, 0.35 mmol) is suspended in 80 mL of dry DCM. At room temp., BBr_3 (1 M solution in hexane, 1.38 mL, 1.38 mmol) is added by syringe and the mixture is stirred for 18 h at room temp. under N_2. Methanol (5 mL) is added, the solvent is removed and the solid precipitate is directly used for alkylation under standard conditions (GWP 1) using K_2CO_3 (140 mg, 1.04 mmol), $C_{10}H_{21}Br$ (170 mg, 0.76 mmol) and DMF (10 mL). After column chromatography 18 mg (10%) of 2,3-didecyloxy tetracene (**86**) was obtained along with 14 mg (14%) unreacted starting material and 14 mg (10%) of 2-decyloxy-3-methoxy-tetracene, resulting from partial demethylation.

b) In toluene: 2,3-Dimethoxy-tetracene (**73**, 200 mg, 0.69 mmol) is suspended in 100 mL of anhydrous toluene (saturated with Ar for 30 min). At room temp., BBr_3 (1 M solution in hexane, 4.2 mL, 4.16 mmol) is added by syringe and the mixture is stirred for 12 h at reflux temperature under Ar. Methanol (14 mL) is added, the solvent is removed and the solid precipitate is directly used for alkylation under standard conditions (GWP 1) using K_2CO_3 (290 mg, 2.08 mmol), $C_6H_{13}Br$ (340 mg, 2.08 mmol) and DMF (12 mL, saturated with Ar for 15 min). After chromatography 48 mg (16%) of 2,3-dihexyloxy-tetracene (**110**) was obtained along with 20 mg (10%) of unreacted starting material and 46 mg (19%) of 2-hexyloxy-3-methoxy-tetracene, formed by partial demethylation.

7.3.1.14.2 Attempted demethylation of 2,3-dimethoxy-tetracene (**73**) *with pyridine hydrochloride*

2,3-Dimethoxy-tetracene (**73**, 400 mg, 1.39 mmol) is mixed with pyridine•HCl (4.82 g, 41.7 mmol) under Ar. The mixture is heated until an outer temperature (sand bath) of 230 °C is reached, and the molten salt mixture is stirred for 2.5 h at this temperature. After letting the mixture cool down to room temp. it is stirred with water to dissolve the pyridine salt. After filtration, no product residue could be obtained.

The reaction is repeated, using 200 mg (0.70 mmol) of **73** and 2.40 g (21 mmol) of pyridine•HCl. The reaction temp. is kept below 205 °C. After 30 min the mixture is allowed to cool down and washed with water, methanol and ether. The resulting residue (130 mg, 65%) is identified as starting material.

7.3.2 2,3-Didecyloxy-anthracene (1) synthesis

7.3.2.1 2,3-Dimethoxy-9,10-anthraquinone (38)[11]

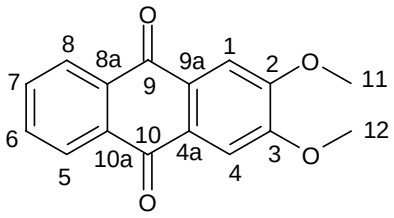

38

1,4-Naphthoquinone (**36**) (3.0 g, 19.0 mmol) is dissolved in 4.5 mL of anhydrous toluene under N_2. At an oil-bath temperature of 120 °C, 2,3-dimethoxy-buta-1,3-diene (**37**) (6.0 g, 47.4 mmol) is added dropwise. The mixture is stirred for 18 h at 120 °C. The solvent is evaporated and the crude mixture is suspended in a solution of methanol/DCM (1:1). KOH (2.0 g) is added and air is bubbled through the suspension for 2 h. 200 mL of water is added and the aqueous solution is extracted three times with DCM. The organic solution is washed with water, dried (Na_2SO_4), and the solvent is evaporated. The crude product is recrystallized from ethyl acetate to yield 2.34 g (46%) of a yellow solid.

m. p.: 244°C (ethyl acetate).

R_f (DCM/pentane (1:1)): 0.05.

IR (ATR): $\tilde{\nu}_{max}$ = 3301 cm^{-1} (w), 3083 (w), 3062 (w), 3019 (w), 2996 (w), 2943 (w), 2864 (w), 2836 (w), 1655 (s), 1572 (s), 1512 (s), 1451 (m), 1373 (m), 1333 (s), 1307 (s).

^{1}H NMR (400 MHz, $CDCl_3$): δ = 8.28 (m_c, *N* = 9.1 Hz, 2 H, 8/5-H), 7.78 (m_c, *N* = 9.1 Hz, 2 H, 7/6-H), 7.72 (s, 2 H, 4/1-H), 4.09 (s, 6 H, 12/11-H).

^{13}C NMR (100 MHz, $CDCl_3$): δ = 182.4 (s, C-10/9), 153.8 (s, C-3/2), 133.7 (d, C-7/6), 133.5 (s, C-10a/8a), 128.4 (s, C-9a/4a), 126.9 (d, C-8/5), 108.3 (d, C-4/1), 56.5 (q, C-12/11).

UV (DCM): λ_{max} (lg ε) = 224 nm (3.96), 234 nm (4.16), 242 (4.26), 248 (4.29), 270 (4.59), 282 (4.44, sh), 330 (3.61), 364 (3.52), 392 (3.28).

MS (70 eV): *m/z* (%) = 268 (100) [M^+], 253 (13) [M^+-CH_3], 238 (18) [M^+-$2CH_3$], 225 (16) [M^+-CH_3-CO], 197 (28) [M^+-$2CH_3$-2CO].

The spectral data agree with those given in the literature.[11]

7.3.2.2 2,3-Dihydroxy-9,10-anthraquinone (28)

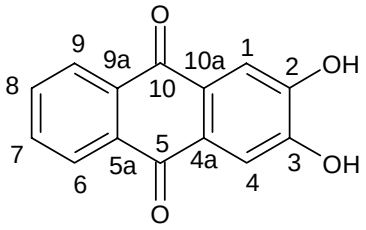

28

2,3-Dimethoxy-9,10-anthraquinone (**38**) (1.00 g, 3.73 mmol) is suspended in 26 mL of HBr (w = 48%) and the suspension heated to reflux for 12 h. After addition of 26 mL of glacial acetic acid, reflux is maintained for further 12 h. The suspension is diluted with 70 mL of water, filtered and the residue is washed with water, methanol and diethyl ether. The product is obtained as a yellow solid (0.8 g, 90%).

m. p.: 320 °C (decomp.).

IR (ATR): $\tilde{\nu}_{max}$ = 3077 cm^{-1} (w), 2956 (w), 2927 (m), 2857 (w), 1666 (s), 1574 (s), 1512 (m), 1464 (m), 1372 (m), 1304 (s), 1217 (s).

^{1}H NMR (400 MHz, DMSO-d_6): δ= 10.65 (s, 2 H, OH) 8.10 (m_c, *N* = 9.1 Hz, 2 H, 9/6-H), 7.84 (m_c, *N* = 9.1 Hz, 2 H, 8/7-H), 7.51 (s, 2 H, 4/1-H).

^{13}C NMR (100 MHz, DMSO-d_6): δ= 181.7 (s, C-10/5), 151.6 (s, C-3/2), 134.0 (d, C-8/7), 133.2 (s, C-9a/5a), 126.9 (d, C-9/6), 126.4 (s, C-10a/4a), 113.0 (d, C-4/1).

UV (DMSO): λ_{max} (lg ε) = 288 nm (4.50), 398 (3.21).

MS (70 eV)**:** *m/z* (%) = 240 (100) [M^+], 212 (7) [M^+-CO], 184 (7) [M^+-2•CO].

The spectral data agree with those given in the literature.[11]

7.3.2.3 2,3-Didecyloxy-9,10-anthraquinone (**8**)[11]

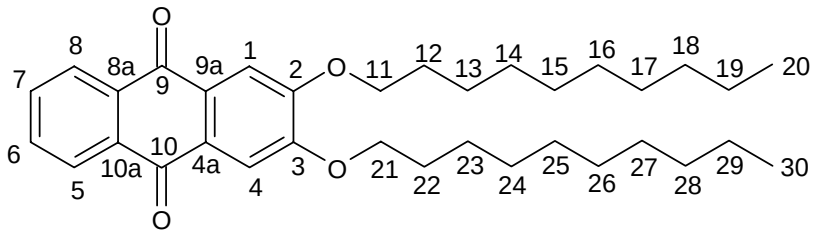

8

GWP 1: 2,3-Dihydroxy-9,10-anthraquinone (**28**) (1.96 g, 7.83 mmol), K_2CO_3 (5.40 g, 39.2 mmol), DMF (50 mL), $C_{10}H_{21}Br$ (4.33 g, 19.6 mmol). The product is obtained as a yellow solid (4.04 g, 95%).

m. p.: 101°C (ethyl acetate).

R_f (DCM/pentane (1:2)): 0.11.

IR (ATR): $\tilde{\nu}_{max}$ = 2958 cm^{-1} (w), 2918 (m), 2850 (m), 1669 (m), 1574 (s), 1513 (m), 1465 (m), 1375 (m), 1330 (s), 1308 (s), 1218 (s).

^{1}H NMR (400 MHz, $CDCl_3$): δ = 8.29 (m_c, *N* = 9.1 Hz, 2 H, 8/5-H), 7.78 (m_c, *N* = 9.1 Hz, 2 H, 7/6-H), 7.71 (s, 2 H, 4/1-H), 4.23 (t, ^3J = 6.6 Hz, 4 H, 11/21-H), 1.97-1.90 (m, 4 H, chain), 1.58-1.32 (m, 14 H, chain), 0.94-0.91 (m, 6 H, 20/30-H).

^{13}C NMR (100 MHz, $CDCl_3$): δ = 182.6 (s, C-10/9), 153.8 (s, C-3/2), 133.7 (d, C-7/6), 133.6 (s, C-10a/8a), 128.1 (s, C-9a/4a), 126.9 (d, C-8/5), 109.3 (s, C-4/1), 69.4 (t, C-21/11), 31.9, 29.59, 29.56, 29.3, 28.9, 25.9, 22.7 (t, chain, not all C-atoms resolved), 14.1 (q, C-30/20).

UV (DCM): λ_{max} (lg ε) = 281 nm (4.68, sh), 289 (4.72), 394 (3.45).

MS (70 eV): *m/z* (%) = 520 (34) [M^+], 380 (21) [M^+-$C_{10}H_{20}$], 364 (61) [M^+-$C_{10}H_{20}O$], 240 (100) [M^+-$C_{20}H_{40}$], 225 (90) [M^+-$C_{20}H_{40}O$ + H], 224 (89) [M^+-$C_{20}H_{40}O$].

The spectral data agree with those given in the literature.[11]

7.3.2.4 2,3-Didecyloxy-anthracene (**1**)

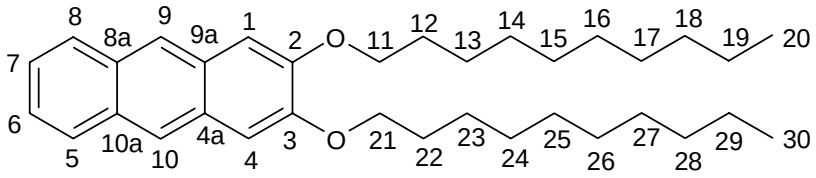

1

GWP 2: 2,3-Didecyloxy-9,10-anthraquinone (**8**) (4.54 g, 8.71 mmol), Al 1.27 g, 46.9 mmol), $HgCl_2$ (8 mg), CCl_4 (80 µL), cyclohexanol (50 mL), reaction time 12 h.

Work-up: The mixture is decomposed with 50 mL of hydrochloric acid (16%), diluted with water and extracted several times with DCM. The organic solution is dried (Na_2SO_4) and the solvent evaporated under vacuum. The crude product is purified by column chromatography, on silica with DCM/pentane (1:1). The product is finally recrystallized from pentane to yield 1.66 g (39%) 2,3-didecyloxy-anthracene (**1**).

m. p.: 92°C (pentane).

R_f (DCM/pentane (1:4)): 0.60.

IR (KBr): $\tilde{\nu}_{max}$ = 3441 cm^{-1} (w), 3049 (w), 2919 (s), 2851 (s), 1630 (w), 1569 (w), 1491 (m), 1467 (s), 1385 (w), 1288 (m), 1262 (w), 1223 (s).

^{1}H NMR (400 MHz, $CDCl_3$): δ = 8.17 (s, 2 H, 10/9-H), 7.90 (m_c, *N* = 9.7 Hz, 2 H, 8/5-H), 7.37 (m_c, *N* = 9.7 Hz, 2 H, 7/6-H), 7.17 (s, 2 H, 4/1-H), 4.14 (t, ^3J = 6.6, 4 H, 21/11-H), 1.94-1.89 (m, 4 H, chain), 1.57-1.27 (m, 28 H, chain), 0.89 (t, ^3J = 6.9 Hz, 6 H, 30/20-H).

^{13}C NMR (100 MHz, $CDCl_3$): δ = 150.1 (d, C-3/2), 130.7 (s, C-10a/8a), 128.7 (s, C-9a/4a), 127.6 (d, C-8/5), 124.4 (d, C-7/6), 123.7 (d, C-10/9), 105.9 (d, C-4/1), 68.7 (t, C-21/11), 31.9, 29.66, 29.60, 29.46, 29.37, 29.1, 26.1, 22.7 (t, chain, not all C-atoms resolved), 14.1 (q, C-30/20).

UV (DCM): λ_{max} (lg ε) = 264 nm (4.92), 326 (3.53), 342 (3.74), 360 (3.85), 368 (3.79), 378 (3.66).

MS (70 eV): *m/z* (%) = 490 (74) [M^+], 350 (26) [M^+-$C_{10}H_{20}$], 334 (17) [M^+-$OC_{10}H_{20}$], 210 (100) [M^+-2*$C_{10}H_{20}$], 194 (48) [M^+-2*$OC_{10}H_{20}$].

The spectral data agree with those given in the literature.[11]

7.3.3 2,3-Dialkoxy-pentacene synthesis

7.3.3.1 Naphthalene-2,3-dicarboxaldehyde[14]

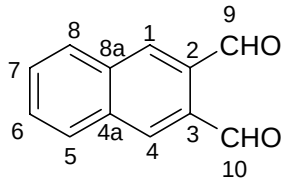

52

Phthalic dialdehyde (**46**, 6.00 g, 44.7 mmol), glacial acetic acid (3 mL), water (4.5 mL), 2,5-dimethoxy-tetrahydrofuran (**47**, 6.7 mL, 49.2 mmol) and three drops of piperidine are heated to reflux for 15 h. The reaction mixture is stirred with 20 mL of water and the precipitate is filtered off. After washing with water, methanol and diethyl ether the crude product is obtained by chromatographic separation from polymeric side products (DCM, silica). After evaporation of the solvent, the crude product is sublimed (130 °C) to yield 1.06 g (19%) of a yellow solid.

m. p.: 132 °C.

R_f (DCM): 0.31.

IR (KBr): $\tilde{\nu}_{max}$ = 3452 (w), 1702 (m), 1683 (s), 1656 (m), 1650 (m), 1621 (m), 1586 (w), 1573 (w), 1561 (w), 1463 (m), 1446 (m), 1321 (w), 1252 (m).

^{1}H NMR (400 MHz, $CDCl_3$): δ = 10.64 (s, 2 H, 10/9-H), 8.45 (s, 2 H, 4/1-H), 8.06 (m_c, *N* = 9.4 Hz, 2 H, 8/5-H), 7.75 (m_c, *N* = 9.5 Hz, 2 H, 7/6-H).

^{13}C NMR (100 MHz, $CDCl_3$): δ = 192.5 (s, C-10/9), 134.4 (d, C-4/1 or C-8a/4a), 134.4 (s, C-4/1 or C-8a/4a), 132.8 (s, C-3/2), 130.0 (d, C-7/6), 129.6 (d, C-8/5).

UV (CH_3CN): λ_{max} (lg ε) = 216 nm (4.24), 258 (4.74), 284 (3.82), 294 (3.72), 346 (3.52), 360 (3.57).

MS (70 eV): *m/z* (%) = 184(92) [M^+], 156 (48) [M^+-CO], 155 (100) [M^+-CHO], 127 (80) [M^+-CO-CHO].

The spectral data agree with those given in the literature.[14]

7.3.3.2 2,3-Dimethoxy-pentacene-5,14-quinone

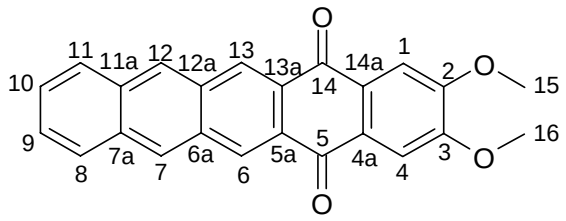

77

1,4-Dihydroxy-6,7-dimethoxy-naphthalene (**57**, 0.35 g, 1.59 mmol), naphthalene-2,3-dicarboxaldehyde (**52**, 0.29 g, 1.59 mmol), Na_2CO_3 (0.34 g, 3.18 mmol) and CF_3CH_2OH (8 mL) are mixed under N_2. The mixture is heated to reflux for 4 h, then diluted with 10 mL of water and the precipitate is filtered off. After washing with water, methanol and diethyl ether, the product is obtained as an orange solid (0.52 g, 89%).

m.p.: 340 °C (decomp.).

R_f (DCM): 0.13.

IR (ATR): $\tilde{\nu}_{max}$ = 3083 cm^{-1} (w), 3044 (w), 3019 (w), 2967 (w), 2947 (w), 1664 (s), 1582 (s), 1535 (w), 1501 (m), 1469 (m), 1446 (m), 1418 (m), 1367 (m), 1307 (m).

^{1}H NMR (400 MHz, $CDCl_3$): δ = 9.00 (s, 2 H, 13/6-H), 8.67 (s, 2 H, 12/7-H), 8.07 (m_c, *N* = 9.7 Hz, 2 H, 11/8-H), 7.81 (s, 2 H, 4/1-H), 7.59 (m_c, *N* = 9.7 Hz, 2 H, 10/9-H), 4.10 (s, 6H, 16/15-H).

Due to the poor solubility in the common deuterated solvents, no ^{13}C NMR spectrum could be measured. The ^{1}H signals were determined by comparison with 2,3-didecyloxy-tetracene-5,14-quinone (**112**).

UV (DCM): λ_{max} (lg ε) = 262 nm (4.91), 309 (4.49), 325 (4.63), 340 (4.75), 409 (3.88), 456 (3.95).

MS (70 eV): *m/z* (%) = 368 (100) [M^+], 353 (4) [M^+-CH_3], 325 (8) [M^+-CH_3-CO].

HRMS: *m/z* calcd. for $C_{24}H_{16}O_4$ [M^+]: 368.1049; found 368.1039 ± 1 ppm.

7.3.3.3 2,3-Dihydroxy-pentacene-5,14-quinone[30]

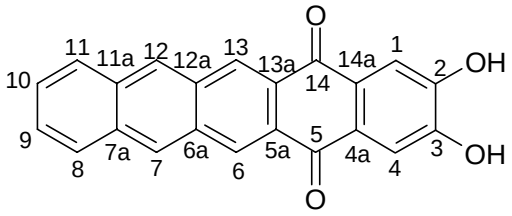

76

2,3-Dimethoxy-pentacene-5,14-quinone (**77**, 1.39 g, 3.77 mmol) is suspended in 75 mL of aqueous HBr (w = 48%). The suspension is heated to reflux for 4 d, diluted with 75 mL of glacial acetic acid and again heated for 2 d. The mixture is diluted with water, filtered and the residue is washed with water, methanol and diethyl ether. The crude mixture of **76**, **77** and traces of the partially demethylated starting material is directly alkylated without further purification.

7.3.3.4 2,3-Didecyloxy-pentacene-5,14-quinone (112)

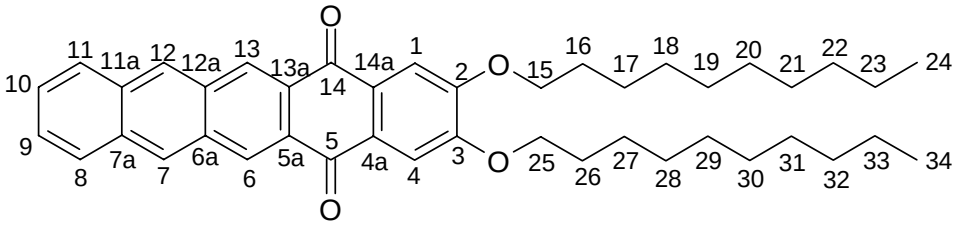

112

GWP 1: 2,3-Dihydroxy-5,14-pentacenequinone (**76**) (1.50 g, 4.32 mmol), K_2CO_3 (1.50 g, 10.8 mmol), DMF (75 mL), $C_{10}H_{21}Br$ (2.1 g, 9.5 mmol). The product is obtained as an orange solid (1.66 g, 62%).

m. p.: 206 °C (ethyl acetate).

R_f (DCM/pentane (1:1)): 0.21.

IR (ATR): $\tilde{\nu}_{max}$ = 3081 cm^{-1} (w), 3057 (w), 2916 (s), 2870 (m), 2847 (m), 1670 (s), 1620 (w), 1580 (s), 1506 (m), 1456 (m), 1399 (m), 1373 (m), 1306 (s).

^{1}H NMR (400 MHz, $CDCl_3$): δ = 8.96 (s, 2 H, 13/6-H), 8.64 (s, 2 H, 12/7-H), 8.05 (m_c, *N* = 9.7 Hz, 2 H, 11/8-H), 7.75 (s, 2 H, 4/1-H), 7.57 (m_c, *N* = 9.7 Hz, 2 H, 10/9-H), 4.21 (t, ^3J = 6.6 Hz, 4 H, 25/15-H), 1.95-1.88 (m, 4 H, chain), 1.56-1.19 (m, 28 H, chain), 0.91-0.86 (m, 6 H, 34/24-H).

^{13}C NMR (100 MHz, $CDCl_3$): δ = 182.1 (s, C-14/5), 154.0 (s, C-3/2), 133.5 (s, C-11a/7a), 131.7 (s, C-12a/6a), 130.6 (d, C-13/6), 129.8 (d, C-12/7), 129.7 (s, C-14a/4a), 129.2 (s, C-13a/5a), 128.6 (d, C-11/8), 127.3 (d, C10/9), 109.4 (d, C-4/1), 69.4 (t, C-25/15), 31.9, 29.62, 29.58, 29.38, 29.36, 29.0, 26.0, 22.7 (t, chain), 14.1 (q, C-34/24).

UV (DCM): λ_{max} (lg ε) = 262 nm (4.91), 312 (4.49, sh), 325 (4.65), 339 (4.77), 456 (3.95).

MS (70 eV): *m/z* (%) = 620 (100) [M^+], 480 (32) [M^+-$C_{10}H_{20}$], 340 (49) [M^+-$C_{20}H_{40}$], 311 (8) [M^+-$C_{20}H_{40}$-CHO].

Elemental analysis: $C_{42}H_{52}O_4$ (620.87): calcd. C 81.24, H 8.46; found C 80.79, H 8.48.

7.3.3.5 2,3-Dihexadecyloxy-pentacene-5,14-quinone (**113**)

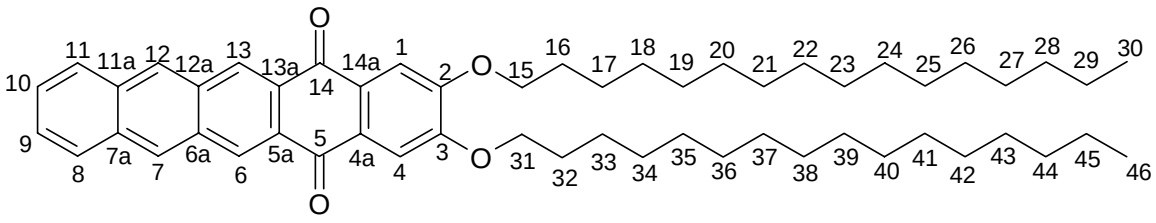

113

GWP 1: 2,3-Dihydroxy-pentacene-5,14-quinone (**76**) (0.80 g, 2.35 mmol), K_2CO_3 (0.97 g, 7.05 mmol), DMF (15 mL), $C_{16}H_{33}Br$ (2.15 g, 7.05 mmol). The product is obtained as an orange solid (1.05 g, 57%).

m. p.: 170 - 172 °C (ethyl acetate).

R_f (DCM/pentane (1:1)): 0.28.

IR (ATR): $\tilde{\nu}_{max}$ = 3044 cm^{-1} (w), 2917 (s), 2849 (s), 1668 (m), 1573 (s), 1508 (m), 1466 (m), 1449 (m), 1421 (w), 1376 (m), 1318 (s), 1274 (m).

^{1}H NMR (400 MHz, $CDCl_3$): δ = 8.96 (s, 2 H, 13/6-H), 8.64 (s, 2 H, 12/7-H), 8.05 (m_c, *N* = 9.7 Hz, 2 H, 11/8-H), 7.75 (s, 2 H, 4/1-H), 7.57 (m_c, *N* = 9.7 Hz, 2 H, 10/9-H), 4.21 (t, ^3J = 6.6 Hz, 4 H, 31/15-H), 1.95-1.88 (m, 4 H, chain), 1.56-1.22 (m, 52 H, chain), 0.88 (t, ^3J = 6.8 Hz, 6 H, 46/30-H).

^{13}C NMR (100 MHz, $CDCl_3$): δ = 182.1 (s, C-14/5), 154.0 (s, C-3/2), 133.5 (s, C-11a/7a), 131.7 (s, C-12a/6a), 130.7 (d, C-13/6), 129.8 (d, C-12/7), 129.7 (s, C-14a/4a), 129.2 (s, C-13a/5a), 128.6 (d, C-11/8), 127.3 (d, C-10/9), 109.4 (d, C-4/1), 69.4 (t, C-31/15), 31.9, 29.73, 29.68, 29.63, 29.4, 29.0, 26.0, 22.7 (t, chain, not all C-atoms resolved), 14.1 (qu, C-46/30).

UV (DCM): λ_{max} (lg ε) = 262 nm (4.88), 325 (4.62), 339 (4.74), 455 (3.93).

MS (70 eV): *m/z* (%) = 788 (100) [M^+], 564 (20) [M^+-$C_{16}H_{32}$], 340 (29) [M^+-$C_{32}H_{64}$], 311 (7) [M^+-$C_{32}H_{64}$-CHO].

HRMS: *m/z* calcd. for $C_{54}H_{76}O_4$ [M^+]: 788.5744; found 788.5749 ± 1 ppm.

7.3.3.6 2,3-Didecyloxy-pentacene (114)

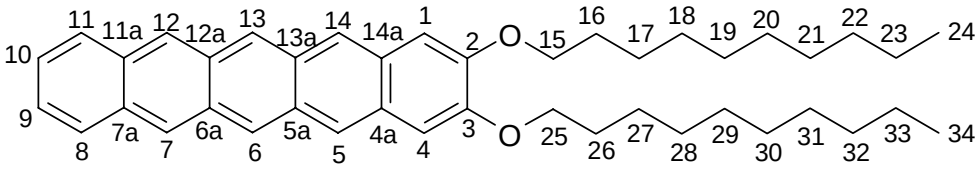

114

GWP 2: All reaction- and work-up steps were carried out under Ar and the solvents for the work up were saturated with argon.

2,3-Didecyloxy-pentacene-5,14-quinone (**112**) (0.25 g, 0.40 mmol), Al (109 mg, 4.0 mmol), $HgCl_2$ (2 mg), CCl_4 (20 µL), cyclohexanol (4 mL), reaction time 2 h.

Work-up: The mixture is decomposed with a solution of 2.5 mL HCl (w = 32%) and 2.5 mL of ethanol. The crude product is filtered, washed with ethanol and diethyl ether: dark blue solid (51 mg, 22%).

m. p.: 235 - 240 °C (decomp.).

IR (ATR): $\tilde{\nu}_{max}$ = 2921 cm^{-1} (s), 2852 (s), 1707 (w), 1667 (w), 1614 (w), 1501 (m), 1463 (s), 1415 (w), 1385 (w), 1306 (w), 1253 (s), 1211 (m).

MS (70 eV): m/z (%) = 590 (100) [M^+], 450 (11) [M^+-$C_{10}H_{20}$], 310 (36) [M^+-$C_{20}H_{40}$], 281 (17) [M^+-$C_{20}H_{40}$-CHO], 265 (8) [M^+-$C_{20}H_{40}$-CHO-O].

HRMS: *m/z* calcd. for $C_{42}H_{54}O_2$ [M^+]: 590.4124; found 590.4110 ± 1 ppm.

7.3.3.7 2,3-Dihexadecyloxy-pentacene (115)

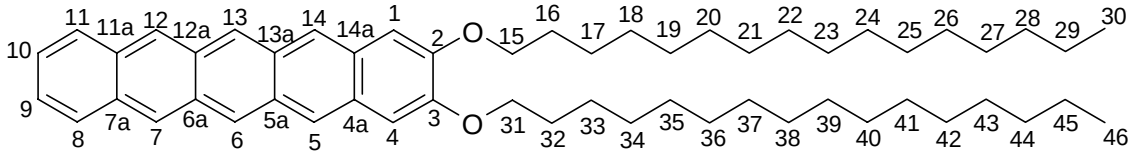

115

GWP 2: All reaction- and work-up steps were carried out under Ar and the solvents for the work up were saturated with Ar.

2,3-Dihexadecyloxy-pentacene-5,14-quinone (**113**) (400 mg, 0.51 mmol), Al (137 mg, 5.06 mmol), $HgCl_2$ (10 mg), CCl_4 (20 µL), cyclohexanol (5 mL), reaction time 1/2 h

Work-up: The mixture is decomposed with a solution of 3 mL HCl (W = 32%) and 3 mL of ethanol. The crude product is filtered off, washed with ethanol and diethyl ether. To separate the crude product from remaining Al, it is hot-extracted using Ar-saturated $CHCl_3$. The product is obtained as a dark blue solid (94 mg, 24%).

m. p.: 199 - 205 °C (decomp., $CHCl_3$).

IR (ATR): $\tilde{\nu}_{max}$ = 3048 cm^{-1} (w), 2917 (s), 2849 (s), 1672 (w), 1633 (w), 1555 (w), 1463 (s), 1380 (w), 1306 (m), 1253 (s), 1211 (m).

^{1}H NMR (400 MHz, 1,2,2,2-tetrachloroethane-d_2, 81 °C): δ = 8.83 (s, 2 H, 13/6-H), 8.63 (s, 2 H, 12/7-H), 8.40 (s, 2 H, 14/5-H), 7.94 (m_c, *N* = 9.8 Hz, 2 H, 11/8-H), 7.33 (m_c, *N* = 9.9 Hz, 2 H, 10/9-H), 7.11 (s, 2 H, 4/1-H), 4.18 (t, ^3J = 6.5 Hz, 4 H, 31/15-H), 1.98-1.91 (m, 4 H, chain), 1.63-1.56 (m, 4 H, chain), 1.48-1.31 (m, 48 H, chain), 0.92 (t, ^3J = 6.8 Hz, 6 H, 46/30-H).

^{13}C NMR (100 MHz, 1,2,2,2-tetrachloroethane-d_2 81 °C): δ = 150.8 (s, C-3/2), 131.2 (s, C-11a/7a), 129.7 (s, C-13a/5a or 12a/6a), 129.5 (s, C-14a/4a), 128.2 (d, C-11/8), 125.9 (d, C-12/7), 125.1 (d, C-13/6), 124.7 (d, C-10/9), 122.9 (d, C-14/5), 105.8 (d, C-4/1), 68.9 (t, C-31/15), 31.7, 29.5, 29.4, 29.2, 29.1, 29.0, 26.0, 22.4 (t, chain, not all C-atoms resolved), 13.8 (q, C-46/30).

UV (2,2,3,3-tetrachloroethane): λ_{max} = 309 nm, 321, 348, 433, 498, 536, 580.

The UV/Vis spectrum could only be measured qualitatively as the concentration could not be determined (saturated solution).

MS (70 eV): *m/z* (%) = 758 (100) [M^+], 534 (10) [M^+-$C_{16}H_{32}$], 310 (45) [M^+-$C_{32}H_{64}$], 281 (16) [M^+-$C_{32}H_{64}$-CHO].

HRMS: *m/z* calcd. for $C_{54}H_{78}O_2$ [M^+]: 758.6002; found 758.6022 ± 1 ppm.

7.3.4 5,12-Dialkoxy-tetracene synthesis

7.3.4.1 1,4-Dihydroxy-naphthalene (95)[24]

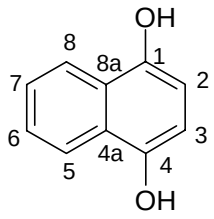

95

1,4-Naphthoquinone (**36**) (10.0 g, 63.2 mmol) is suspended is glacial acetic acid (150 mL) Zn powder (16.5 g, 253 mmol) is added in portions of 4.13 g and the suspension is sonicated in a 130 W ultrasound bath for 15 min after each addition. After the reaction is finished (the solution over the Zn/ $Zn(OAc)_2$ is clear and only slightly colored). The mixture is diluted with ethyl acetate, filtered from the Zn/ ZnOAc residue and the solvent is evaporated. The product is dried *in vacuo* to yield 9.94 g (98%) and used without further purification.

m. p.:184 °C (decomp.).

IR (ATR): $\tilde{\nu}_{max}$ = 3267 cm^{-1} (m), 3062 (w), 1817 (w), 1641 (m), 1595 (m), 1478 (m), 1399 (m), 1325 (s), 1263 (s).

^{1}H NMR (400 MHz, acetone d_6): δ = 8.36 (s, 2 H, OH), 8.21 (m_c, *N* = 9.8 Hz, 2 H, 8/5-H), 7.48 (m_c, *N* = 9.7 Hz, 2 H, 7/6-H), 6.76 (s, 2 H, 3/2-H).

^{13}C NMR (100 MHz, acetone d_6): δ = 146.8 (s, C-4/1), 126.7 (s, C-8a/4a), 125.7 (d, C-7/6), 122.8 (d, C-8/5), 108.6 (d, C-3/2).

MS (70 eV): *m/z* (%) = 160 (100) [M^+], 131 (21) [M^+-CO+H].

The spectral data agree with those given in the literature.[24]

7.3.4.2 Tetracene-5,12-quinone (94)[17]

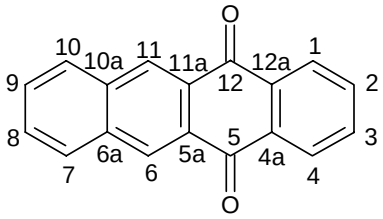

94

1,4-Dihydroxy-naphthalene (**95**) (9.94 g, 62.0 mmol), phthalic dialdehyde (**46**) (8.31 g, 62 mmol), Na_2CO_3 (13.1 g, 124 mmol) and 2,2,2-trifluorethanol (200 mL) are mixed under N_2. The mixture is heated to reflux for 6 h. The mixture is allowed to cool down to room temp. and diluted with 400 mL of water. The residue is removed by filtration, washed with water, acetone and diethyl ether. The product is obtained as a yellow solid (12.9 g, 80%).

m. p.: 294 °C (ethyl acetate).

IR (ATR): $\tilde{\nu}_{max}$ = 3316 cm^{-1} (w), 3066 (w), 3040 (w), 1671 (s), 1613 (m), 1578 (m), 1507 (w), 1455 (m), 1395 (m), 1358 (w), 1324 (m), 1279 (s).

^{1}H NMR (400 MHz, $CDCl_3$): δ = 8.87 (s, 2 H, 11/6-H), 8.40 (m_c, $^3J_{AX/A'X'}$ = 7.8 Hz; $^4J_{AX'/A'X}$ = 1.3 Hz; $^5J_{AA'}$ = 0.6 Hz; $^3J_{XX'}$ = 7.4 Hz, 2 H, 4/1-H), 8.11 (m_c, $^3J_{BY/B'Y'}$ = 8.3 Hz; $^4J_{BY'/B'Y}$ = 1.2 Hz; $^5J_{BB'}$ = 0.7 Hz; $^3J_{YY'}$ = 6.9 Hz, 2 H, 10/7-H), 7.83 (m_c, $^3J_{AX/A'X'}$ = 7.8 Hz; $^4J_{AX'/A'X}$ = 1.3 Hz; $^5J_{AA'}$ = 0.6 Hz; $^3J_{XX'}$ = 7.4 Hz, 2 H, 3/2-H), 7.71 (m_c, $^3J_{BY/B'Y'}$ = 8.3 Hz; $^4J_{BY'/B'Y}$ = 1.2 Hz; $^5J_{BB'}$ = 0.7 Hz; $^3J_{YY'}$ = 6.9 Hz 2 H, 9/8-H).

^{13}C NMR (100 MHz, $CDCl_3$): δ = 183.0 (s, C-12/5), 135.2 (s, C-10a/6a), 134.5 (s, C-12a/4a), 134.2 (d, C-3/2), 130.1 (d, C-10/7), 129.8 (s, C-11a/5a), 129.6 (d, C-11/6), 129.5 (d, C-9/8), 127.5 (d, C-4/1).

UV (DCM): λ_{max} (lg ε) = 238 nm (4.65), 242 (4.61 sh), 282 (4.51), 292 (4.53), 312 (3.93 sh), 390 (3.74).

MS (70 eV): *m/z* (%) = 258 (100) [M^+], 230 (37) [M^+-CO], 202 (55) [M^+-2CO].

The spectral data agree with those given in the literature.[17]

7.3.4.3 5,12-Didecyloxy-tetracene (85)

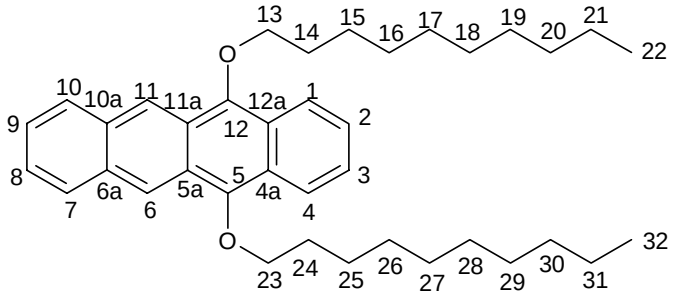

85

A dried and Ar filled Schlenk-flask is charged with 12 mL of THF (dried over potassium) and trimethylchlorosilane (1.32 g, 11.8 mmol). The solution is saturated with Ar for 20 min. Zn (770 mg, 11.8 mmol, activated with HCl) is added and the suspension is again saturated with Ar for 10 min. Tetracene-5,12-quinone (**94**, 0.76 g, 2.95 mmol) is added and the mixture is ultrasonicated until a bright red solution results. This solution is separated from the Zn residue by syringe and the solvent is evaporated in vacuo.

A dried, Ar filled apparatus is charged with K_2CO_3 (11.8 mmol, 1.63 g) and the above intermediate (*vide supra*). 20 mL of anhydrous DMF is added and the suspension is saturated with Ar for 20 min. The suspension is heated to reflux temperature and $C_{10}H_{21}Br$ is added (6.49 mmol, 1.44 g) over a period of 30 min. The mixture is refluxed until TLC shows no further reaction and the color has changed to brown-orange (14 h).

The reaction mixture is diluted with water and extracted with diethyl ether. The organic solution is washed several times with water, dried (Na_2SO_4), and the solvent is evaporated under vacuum.

The crude product is purified several times by column chromatography, with silica and pentane/ diethyl ether (2%). The product (780 mg, 49%) crystallizes after several days in the refrigerator as a waxy red solid.

m. p.: 48 °C.

R_f (diethyl ether (5%)/pentane): 0.48.

IR (ATR): $\tilde{\nu}_{max}$ = 3070 cm^{-1} (w), 3041 (w), 2955 (m), 2916 (s), 2872 (m), 2850 (s), 1629 (w), 1469 (m), 1449 (w), 1404 (m), 1347 (s), 1315 (m).

^{1}H NMR (400 MHz, $CDCl_3$): 8.90 (s, 2 H, 11/6-H), 8.27 (m_c, *N* = 10.1 Hz, 2 H, 4/1-H), 8.03 (m_c, *N* = 9.8 Hz 2 H, 10/7-H), 7.41 (m_c, *N* = 6.8 Hz, 2 H, 9/8-H), 7.39 (m_c, *N* = 7.0 Hz, 2 H, 3/2-H), 4.26 (t, ^{3}J = 6.7 Hz, 4 H, 13/23-H), 2.15-2.08 (m, 4 H, chain), 1.75-1.68 (m, 4 H, chain), 1.55-1.30 (m, 24 H, chain), 0.91-0.88 (m, 6 H, chain).

^{13}C NMR (100 MHz, $CDCl_3$): 147.5 (s, C-12/5), 131.2 (s, C-10a/6a), 128.7 (d, C-10/7), 125.4 (d, C-9/8), 124.7 (d, C-3/2), 124.6 (s, C-11a/5a), 124.0 (s, C-12a/4a), 122.8 (d, C-4/1), 121.4 (d, C-11/6), 76.3 (t, C-13/23), 31.9, 30.8, 29.7, 29.6, 29.4, 26.3, 22.7 (t, chain, not all C-atoms resolved), 14.1 (qu, C-22/32).

UV (DCM): λ_{max} (lg ε) = 285 nm (5.20), 304 (4.11), 403 (3.13), 3.15), 443 (3.54), 472 (3.81), 505 (3.83).

MS (70 eV): *m/z* (%) = 540 (20) [M^+], 399 (8) [M^+-$C_{10}H_{21}$], 383 (11) [M^+-$C_{10}H_{21}O$], 259 (100) [M^+-$C_{20}H_{41}$].

HRMS: *m/z* calcd. for $C_{38}H_{52}O_2$ [M^+]: 540.3967; found 540.3954 ± 1 ppm.

7.3.5 Photoreactions

7.3.5.1 Photodimerization of 2,3-DDOT (**86**)

GWP 3: 2,3-Didecyloxy-tetracene (**86**) (600 mg, 1.11 mmol), cyclohexane (22 mL), solvent for chromatographic separation: DCM/ pentane (1:3) to pure DCM, further separation of the dimers by several runs of column chromatography, solvent: 15% DCM/ pentane to 25% DCM/ pentane.

Besides 123 mg (21%) of **86** the following dimers were obtained as waxy, nearly colorless solids:

2,3-DDOT-D1 (**87**): 61 mg (10%)

2,3-DDOT-D2 (**92**): 67 mg (11%)

2,3-DDOT-D3 (**88**): 85 mg (15%)

2,3-DDOT-D4 (**91**): 94 mg (including D5) (16%)

7.3.5.1.1 2,3-DDOT-D1 (**87**)

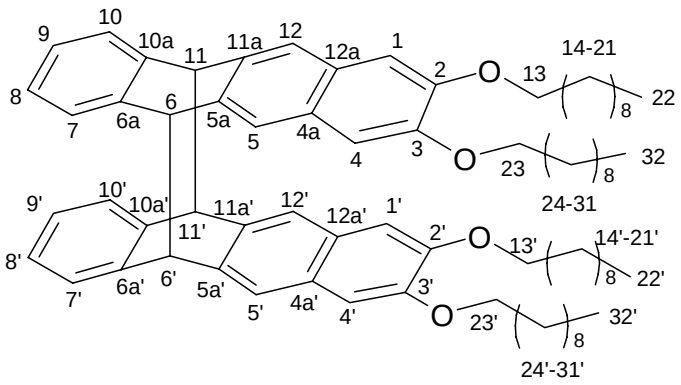

87

IR (ATR): $\tilde{\nu}_{max}$ = 2922 cm^{-1} (s), 2853 (s), 1613 (w), 1505 (m), 1488 (w), 1462 (s), 1414 (w), 1386 (w), 1259 (s), 1195 (w), 1161 (s).

^{1}H NMR (400 MHz, $CDCl_3$): δ = 7.20 (s, 4 H, 12/5/12'5'-H), 6.94 (m_c, *N* = 8.6 Hz, 4 H, 10/7/10'/7'-H), 6.81 (m_c, *N* = 8.7 Hz, 4 H, 9/8/9'/8'-H), 6.80 (s, 4 H, 4/1/4'/1'-H), 4.74 (s, 4 H, 11/6/11'/6'-H), 3.94-3.91 (m, 8 H, 23/13/23'/13'-H), 1.80-1.77 (m, 8 H, chain), 1.44-1.42 (m, 8 H, chain), 1.31-1.26 (m, 32 H, chain), 0.89-0.86 (m, 12 H, 22/32/22'/32'-H).

^{13}C NMR (100 MHz, $CDCl_3$): δ = 148.8 (s, C-3/2/3'/2'), 143.6 (s, C-10a/6a/10a'/6a'), 139.2 (s, C-11a/5a/11a'/5a'), 127.5 (s, C-12a/4a/12a'/4a'), 127.0 (d, C-10/7/10'/7'), 125.6 (d, C-9/8/9'/8'), 124.0 (d, C-12/5/12'/5'), 107.9 (d, C-4/1/4'/1'), 68.7 (t, C-23/13/23'/13'), 53.9 (d, C-11/6/11'/6'), 31.9, 29.63, 29.58, 29.45, 29.35, 29.2, 26.1, 22.7 (t, chain), 14.1 (q, C-32/22/32'/22').

UV (DCM): λ_{max} (lg ε) = 236 nm (5.03), 245 (5.02, sh), 305 (3.68), 321 (3.93), 336 (4.01).

7.3.5.1.2 2,3-DDOT-D2(**92**)

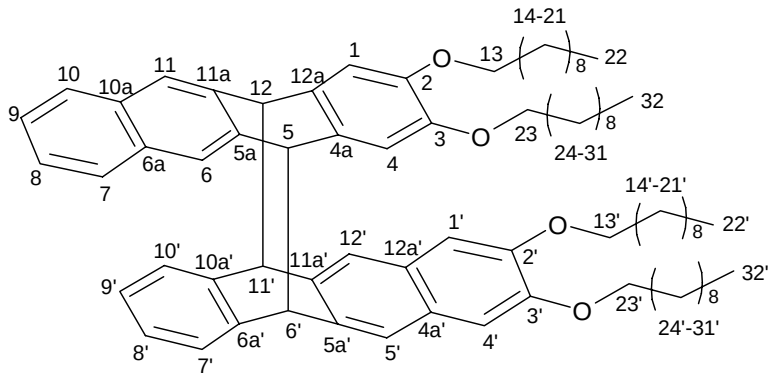

92

IR (ATR): $\tilde{\nu}_{max}$ = 2921 cm^{-1} (s), 2852 (s), 1611 (w); 1502 (m), 1462 (m), 1415 (w), 1382 (w), 1307 (m), 1256 (s), 1187 (w), 1162 (m).

^{1}H NMR (400 MHz, $CDCl_3$): δ = 7.57 (m_c, *N* = 9.4 Hz, 2 H, 10/7-H), 7.35 (s, 2 H, 11/6-H), 7.27 (m_c, *N* = 9.4 Hz, 2 H, 9/8-H), 7.20 (s, 2 H, 12'/5'-H), 6.89-6.87 (m, 4 H, 4'/1'-H and 10'/7'-H), 6.62 (m_c, *N* = 8.6 Hz, 2 H, 9'/8'-H), 6.51 (s, 2 H, 4/1-H), 4.69 (s, 2 H, 11'/6'-H), 4.68 (s, 2 H, 12/5-H), 4.03-3.99 (m, 4 H, 23'/13'-H), 3.72-3.68 (m, 4 H, 23/13-H), 1.91-1.82 (m, 4 H, chain), 1.59-1.44 (m, 8 H, chain), 1.37-1.25 (m, 52 H, chain), 0.90-0.86 (m, 12 H, 32/32'/22/22'-H).

^{13}C NMR (100 MHz, $CDCl_3$): 149.0 (s, C-3'/2'), 146.9 (s, C-3/2), 143.2 (s, C-10a'/6a'), 141.7 (s, C-11a/5a), 139.2 (s, C-11a'/5a'), 136.1 (s, C-12a/4a), 132.0 (s, C-10a/6a), 127.7 (s, C-12a'/4a'), 127.10 (d, C-10/7), 127.05 (d, C-10'/7'), 125.6 (d, C-9'/8'), 124.93 (d, C-9/8), 124.88 (d, C-11/6), 123.9 (d, C-12'/5'), 115.1 (d, C-4/1), 108.0 (d, C-4'/1'), 69.9 (t, C-23/13), 68.9 (t, C-23'/13'), 53.9 (d, C-11'/6'), 53.5 (d, C-12/5), 31.9, 29.68, 29.65, 29.61, 29.5, 29.4, 29.38, 29.2, 29.16, 26.13, 29.09, 26.0, 22.7 (t, chain), 14.1 (q, C-32/32'/22/22').

UV (DCM): λ_{max} (lg ε) = 234 nm (4.38), 248 (4.32, sh), 274 (3.87, sh), 320 (3.19), 335 (3.29).

7.3.5.1.3 2,3-DDOT-D3(**88**)

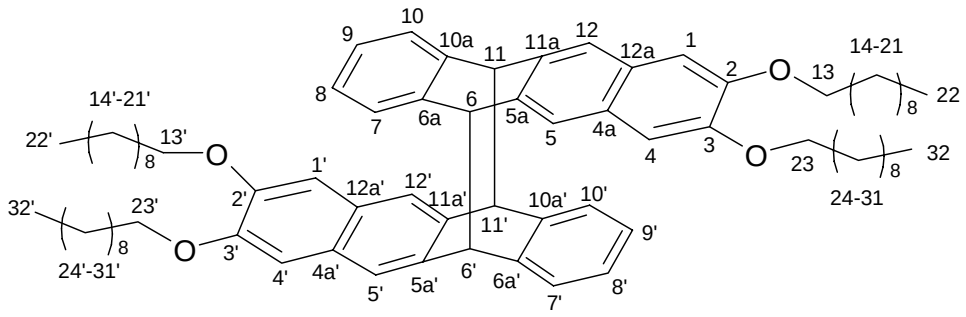

88

IR (ATR): $\tilde{\nu}_{max}$ = 2956 cm^{-1} (m), 2920 (s), 2852 (s), 1613 (w), 1501 (m), 1464 (m), 1406 (w), 1390 (w), 1251 (s), 1199 (m), 1158 (m), 1110 (m), 1014 (w).

^{1}H NMR (400 MHz, $CDCl_3$): δ = 7.12 (s, 4 H, 12,5,12',5'-H), 6.83 (m_c, *N* = 8.7 Hz, 4 H, 10,7,10',7'-H), 6.81 (s, 4 H, 4,1,4',1'-H), 6.59 (m_c, *N* = 8.7 Hz, 4 H, 9,8,9',8'-H), 4.66 (s, 4 H, 11,6,11',6'-H), 3.98-3.89 (m, 8 H, 23,13,23',13'-H), 1.79-1.73 (m, 8 H, chain), 1.44-1.35 (m, 8 H, chain), 1.30-1.20 (m, 56 H, chain), 0.83-0.80 (m, 12 H, 32,22,32',22'-H).

^{13}C NMR (100 MHz, $CDCl_3$): δ = 148.8 (s, C-3,2,3',2'), 143.2 (s, C-10a,6a,10a',6a'), 139.4 (s, C-11a,5a,11a',5a'), 127.5 (s, C-12a,4a,12a',4a'), 127.0 (d, C-10,7,10',7'), 125.5 (d, C-9,8,9',8'), 123.8 (d, C-12,5,12',5'), 107.8 (d, C-4,1,4',1'), 68.7 (t, C-23,13,23',13'), 53.8 (d, C-11,6,11',6'), 31.9, 29.6, 29.59, 29.5, 29.4, 29.2, 26.1, 22.7 (t, chain), 14.1 (q, C-32,22,32',22').

UV (DCM): λ_{max} (lg ε) = 255 nm (5.06), 320 (3.98), 336 (4.21).

7.3.5.1.4 2,3-DDOT-D4 (**91**)

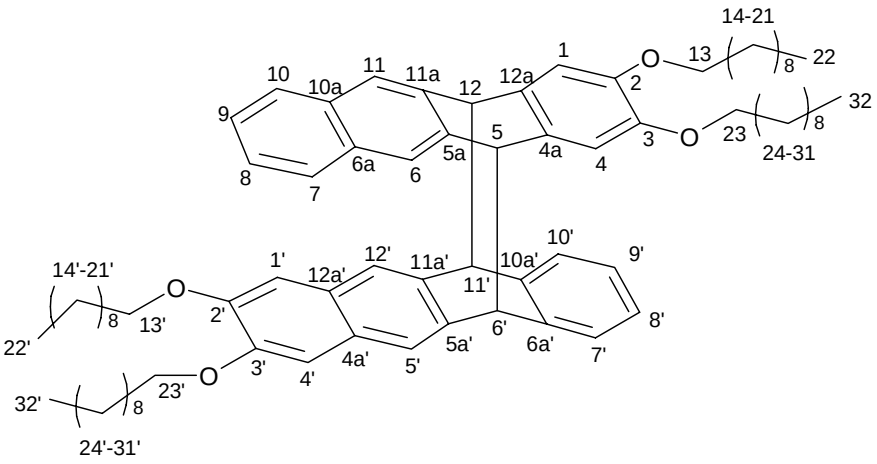

91

IR (ATR): $\tilde{\nu}_{max}$ = 2922 cm^{-1} (s), 2853 (s), 1612 (w); 1501 (s), 1462 (m), 1415 (w), 1382 (w), 1304 (m), 1257 (s), 1229 (s), 1161 (m), 1110 (w), 1080 (w).

^{1}H NMR (400 MHz, $CDCl_3$): δ = 7.49 (m_c, *N* = 9.4 Hz, 2 H, 10/7-H), 7.34 (s, 2 H, 11/6-H), 7.18-7.16 (m, 4 H 9/8-H and 12'/5'-H), 6.93 (m_c, *N* = 8.7 Hz, 2 H, 10'/7'-H), 6.80 (m_c, *N* = 8.6 Hz, 2 H, 9'/8'-H), 6.77 (s, 2 H, 4'/1'-H), 6.53 (s, 2 H, 4/1-H), 4.70 (s, 2 H, 11'/6'-H), 4.69 (s, 2 H, 12/5-H), 3.92 (t, ^{3}J = 6.7 Hz, 4 H, 23'/13'-H), 3.84-3.78 (m, 4 H, 23/13-H), 1.79-1.75 (m, 4 H, chain), 1.69-1.65 (m, 4 H, chain), 1.42-1.25 (m, 56 H, chain), 0.90-0.86 (m, 12 H, 32/22/32'/22'-H).

^{13}C NMR (100 MHz, $CDCl_3$): δ = 148.7 (s, C-3'/2'), 146.9 (s, C-3/2), 143.3 (s, C-10a'/6a'), 141.5 (s, C-11a/5a), 139.2 (s, C-11a'/5a'), 136.2 (s, C-12a/4a), 131.9 (s, C-10a/6a), 127.5 (s, C-12a'/4a'), 127.1 (d, C-10/7), 126.9 (d, C-10'/7'), 125.7 (d, C-9'/8'), 125.0 (d, C-11/6), 124.9 (d, C-9/8), 124.0 (d, C-12'/5'), 114.9 (d, C-4/1), 107.8 (d, C-4'/1'), 69.9 (t, C-23/13), 68.7 (t, C-23'/13'), 53.9 (d, C-11'/6'), 53.5 (d, C-12/5), 31.9, 29.65, 29.61, 29.56, 29.43, 29.41, 29.36, 29.34, 29.26, 29.1, 26.04, 25.96, 25.87, 22.7 (t, chain), 14.1 (q, C-32/22/32'/22').

UV (DCM): λ_{max} (lg ε) = 232 nm (5.05), 320 (3.79), 329 (3.71), 337 (3.82).

7.3.5.2 Photodimerization of 5,12-didecyloxy-tetracene (85)

GWP 3: 5,12-didecyloxy-tetracene (**85**, 500 mg, 0.92 mmol), cyclohexane (18.4 mL), solvent for chromatographic separation: diethyl ether (5%)/pentane.

Two photoproducts 5,12-DDOT-D1 (**96**) and 5,12-DDOT-D2 (**97**) were obtained as white powders, 104 mg each (0.092 mmol, 20%).

Due to the larger amount of starting material, the irradiation was carried out for 5 d. A similar experiment, using 320 mg **85** and 12 mL of cyclohexane, irradiation for 48 h led to comparable results.

7.3.5.2.1 5,12-DDOT-D1 (96)

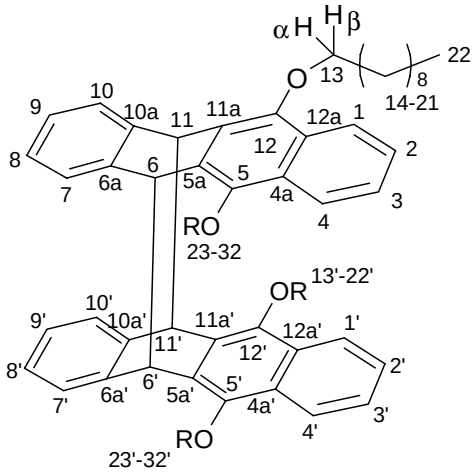

96

m. p.: 70 °C.

R_f (diethyl ether (10%)/pentane): 0.66.

IR (ATR): $\tilde{\nu}_{max}$ = 3068 cm^{-1} (w), 3022 (w), 2957 (m), 2922 (s), 2852 (s), 1712 (m), 1598 (w), 1454 (m), 1347 (s), 1319 (w), 1272 (m).

^{1}H NMR (400 MHz, $CDCl_3$): δ = 7.78 (m_c, *N* = 9.7 Hz, 4 H, 1/1'/4/4'-H), 7.24 (m_c, *N* = 9.6 Hz, 4 H, 2/2'/3/3'-H), 6.98 (m_c, *N* = 8.7 Hz, 4 H, 10/10'/7/7'-H), 6.83 (m_c, *N* = 8.6 Hz, 4 H, 9/9'/8/8'-H), 5.35 (s, 4 H, 11/11'/6/6'-H), 4.19-4.13 (m, 4 H, 23/23'/13/13'-Hα or Hβ), 3.73-3.65 (m, 4 H, 23/23'/13/13'-Hα or Hβ), 2.04-1.91 (m, 8 H, chain), 1.71-1.62 (m, 8 H, chain), 1.54-1.22 (m, 48 H, chain), 0.97-0.86 (m, 12 H, 32/32'/ 22/22'-H).

^{13}C NMR (100 MHz, $CDCl_3$): 146.9 (s, C-12/12'/5/5'), 143.6 (s, C-10a/10a'/6a/6a'), 132.6 (s, C-11a/11a'/5a/5a'), 127.9 (s, C-12a/12a'/4a/4a'), 127.1 (d, C-10/10'/7/7'), 125.8 (d, C-9/9'/8/8'), 125.1 (d, C-3/3'/2/2'), 122.4 (d, C-4/4'/1/1'), 75.2 (t, C-23/23'/13/13'), 46.7 (d, C-11/11'/6/6'), 32.0, 30.8, 29.90, 29.86, 29.81, 29.5, 25.5, 22.7 (t, chain), 14.2 (q, C-32/32'/22/22').

UV (DCM): λ_{max} (lg ε) = 239 nm (4.93), 287 (4.13), 332 (3.45).

MS (70 eV): *m/z* (%) = 540 (11) [monomer], 259 (100) [monomer - $C_{20}H_{41}$].

7.3.5.2.2 5,12-DDOT-D2 (**97**)

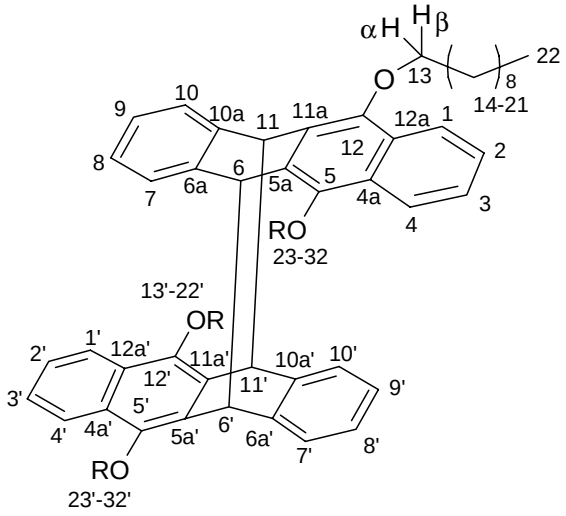

97

m. p.: 125 °C.

R_f (diethyl ether (10%)/pentane): 0.62.

IR (ATR): $\tilde{\nu}_{max}$ = 3072 cm^{-1} (w), 3020 (w), 2960 (m), 2916 (s), 2849 (s), 1674 (w), 1627 (w), 1601 (w), 1503 (w), 1455 (m), 1346 (s), 1321 (m), 1271 (m).

^{1}H NMR (400 MHz, $CDCl_3$): δ = 7.86 (m_c, *N* = 9.6 Hz, 4 H, 1/1'/4/4'-H), 7.32 (m_c, *N* = 9.6 Hz, 4 H, 2/2'/3/3'-H), 7.02 (m_c, *N* = 8.7 Hz, 4 H, 10/10'/7/7'-H), 6.70 (m_c, *N* = 8.6 Hz, 4 H, 9/9'/8/8'-H), 5.32 (s, 4 H, 11/11'/6/6'-H), 4.16-4.10 (m, 4 H, 23/23'/13/13'-Hα or Hβ), 3.88-3.83 (m, 4 H, 23/23'/13/13'-Hα or Hβ), 2.07-2.00 (m, 8 H, chain), 1.77-1.64 (m, 8 H, chain), 1.58-1.27 (m, 48 H, chain), 0.96-0.86 (m, 12 H, 32/32'/ 22/22'-H).

^{13}C NMR (100 MHz, $CDCl_3$): 146.6 (s, C-12/12'/5/5'), 142.8 (s, C-10a/10a'/6a/6a), 132.4 (s, C-11a/11a'/5a/5a'), 127.7 (s, C-12a/12a'/4a/4a'), 127.0 (d, C-10/10'/7/7'), 125.9 (d, C-9/9'/8/8'), 125.0 (d, C-3/3'/2/2'), 122.3 (d, C-4/4'/1/1'), 75.0 (t, C-23/23'/13/13'), 46.6 (d, C-11/11'/6/6'), 32.0, 30.7, 29.80, 29.77, 29.4, 26.5, 22.7 (t, chain, not all C-atoms resolved), 14.1 (q, C-32/32'/22/22').

UV (DCM): λ_{max} (lg ε) = 255 nm (4.86), 288 (4.17), 334 (3.56).

MS (70 eV): *m/z* (%) = 540 (11) [monomer], 259 (100) [monomer - $C_{20}H_{41}$].

7.3.5.3 Crossed photodimerization of 5,12-didecyloxy-tetracene (85) with tetracene (82)

GWP 3: Tetracene (**82**) (171 mg, 0.75 mmol), 5,12-didecyloxy-tetracene (**85**, 406 mg, 0.75 mmol), cyclohexane (30 mL).

Prior to chromatographic separation of the soluble products the mixture was triturated with pentane to separate the pure tetracene dimers (insoluble) from the pure 5,12-DDOT dimers and the mixed dimers.

The two tetracene dimers were identified by comparison of the IR-spectra using the pure dimers (see below). The solid residue did not show any other products and was not separated. Amount of pure tetracene dimers: 102 mg (60%)

Solvent for chromatographic separation of the pentane soluble products: diethyl ether (2%)/pentane.

Besides the pure 5,12-DDOT dimers **96** and **97** (identified by thin layer chromatography and ^{1}H NMR spectra), a fraction of new dimers was isolated, containing two mixed dimers **102** and **103**, 131 mg (23%).

5,12-DDOT-T-D1 (**102**)

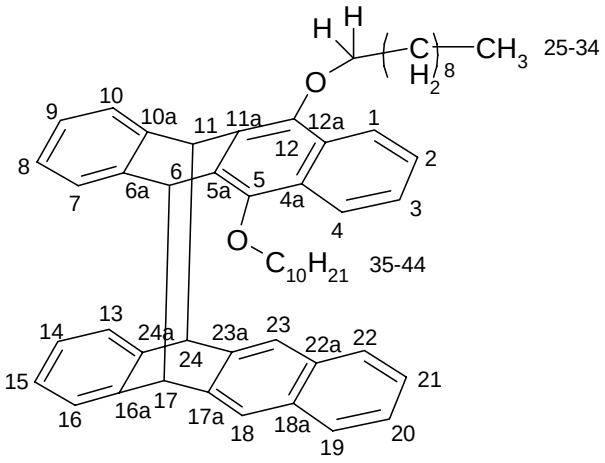

102

IR (ATR): $\tilde{\nu}_{max}$ = 3067 cm^{-1} (w), 3019 (w), 2922 (s), 2853 (s), 1600 (w), 1502 (w), 1484 (w), 1456 (m), 1347 (s), 1320 (m), 1293 (w), 1266 (w), 1229 (w), 1171 (w), 1093 (m).

^{1}H NMR (400 MHz, $CDCl_3$): δ = 7.76 (m_c, *N* = 9.7 Hz, 2 H, 4/1-H), 7.49 (m_c, *N* = 9.4 Hz, 2 H, 22/19-H), 7.45 (s, 2 H, 23/18-H), 7.21 (m_c, *N* = 9.6 Hz, 2 H, 3/2-H), 7.18 (m_c, *N* = 9.4 Hz, 2 H, 21/20-H), 7.00-6.97 (m, 4 H, 16/13-H or 10/7-H), 6.86-6.83 (m, 4 H, 15/14-H or 9/8-H), 5.33 (d, ^{3}J = 11.2 Hz, 2 H, 11/6-H), 4.86 (d, ^{3}J = 11.2 Hz, 2 H, 24/17-H), 4.17-4.11 (m, 2 H, 35/25-H_α or 35/25-H_β), 3.86-3.82 (m, 2 H, 35/25-H_α or 35/25-H_β), 2.08-2.00 (m, 4 H, chain), 1.72-1.57 (m, 4 H, chain), 1.55-1.34 (m, 24 H, chain), 0.92 (t, ^{3}J = 6.9 Hz, 6 H, 44/34-H).

^{13}C NMR (100 MHz, $CDCl_3$): δ = 146.8 (s, C-12/5), 143.1 (s, C-24a/16a or C-10a/6a), 143.07 (s, C-24a/16a or C-10a/6a), 141.0 (s, C-23a/17a), 132.2 (s, C-11a/5a), 131.9 (s, C-22a/18a), 127.7 (s, C-12a/4a), 127.2 (d, C-16/13 or C-10/7), 127.13 (d, C-16/13 or C-10/7), 127.10 (d, C-22/19), 125.89 (d, C-15/14 or C-9/8), 125.85 (d, C-15/14 or C-9/8), 125.4 (d, C-23/18), 125.15 (d, C-21/20), 125.06 (d, C-3/2), 122.3 (d, C-4/1), 74.7 (t, C-35/25), 53.6 (d, C-24/17), 47.0 (d, C-11/6), 32.0, 30.6, 29.8, 29.73, 29.71, 29.43, 26.3, 22.7 (t, chain), 14.2 (q, C-44/34).

UV (DCM): λ_{max} (lg ε) = 230 nm (5.02), 281 (4.19, sh).

5,12-DDOT-T-D2 (**103**)

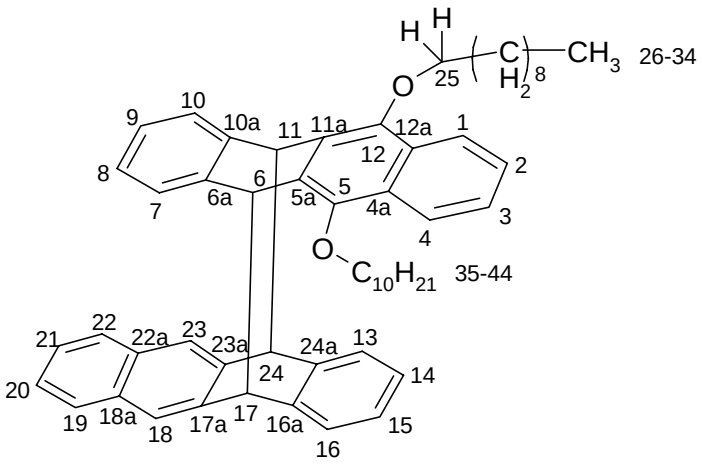

103

IR (ATR): $\tilde{\nu}_{max}$ = 3066 cm^{-1} (w), 3021 (w), 2922 (s), 2852 (s), 1599 (w), 1501 (w), 1483 (w), 1456 (m), 1347 (s), 1320 (m), 1294 (w), 1265 (w), 1233 (w), 1171 (w), 1101 (m).

^{1}H NMR (400 MHz, $CDCl_3$): δ = 7.86 (m_c, *N* = 9.6 Hz, 2 H, 4/1-H), 7.59 (m_c, *N* = 9.4 Hz, 2 H, 22/19-H), 7.41 (s, 2 H, 23/18-H), 7.32 (m_c, *N* = 9.6 Hz, 2 H, 3/2-H), 7.28 (m_c, *N* = 9.4 Hz, 2 H, 21/20-H), 7.02 (m_c, *N* = 8.7 Hz, 2 H, 16/13-H), 6.94 (m_c, *N* = 8.7 Hz, 2 H, 10/7-H), 6.69-6.66 (m, 4 H, 15/14-H and 9/8-H), 5.29 (d, ^{3}J = 11.2 Hz, 2 H, 11/6-H), 4.85 (d, ^{3}J = 11.2 Hz, 2 H, 24/17-H), 4.13-4.09 (m, 2 H, 35/25-H_α or H_β), 3.87-3.82 (m, 2 H, 35/25-H_α or H_β), 2.08-2.00 (m, 4 H, chain), 1.72-1.65 (m, 4 H, chain), 1.53-1.26 (m, 28 H, chain), 0.92 (t, ^{3}J = 6.9 Hz, 6 H, 44/34-H).

^{13}C NMR (100 MHz, $CDCl_3$): δ = 146.6 (s, C-12/5), 142.8 (s, C-10a/6a), 142.7 (s, C-24a/16a), 141.2 (s, C-23a/17a), 132.3 (s, C-11a/5a), 132.0 (s, C-22a/18a), 127.7 (s, C-12a/4a), 127.3 (d, C-10/7), 127.1 (d, C-22/19), 126.9 (d, C-16/13), 125.88 (d, C-9/8 or C-15/14), 125.86 (d, C-9/8 or C-15/14), 125.2 (d, C-23/18), 125.1 (d, C-3/2 or C-21/20), 122.3 (d, C-4/1), 74.9 (t, C-35/25), 53.5 (d, C-24/17), 47.0 (d, C-11/6), 32.0, 30.6, 29.8, 29.7, 29.7, 29.4, 26.3, 22.7 (t, chain), 14.2 (q, C-44/34).

UV (DCM): λ_{max} (lg ε) = 238 nm (4.96), 253 (4.92).

7.3.5.3.1 Photodimerization of tetracene (**82**)

GWP 3: Tetracene (**82**, 362 mg, 1.59 mmol), cyclohexane (32 mL), solvent for recrystallization: toluene.

Tetracene-D1 (**83**) (211 mg, 58%) was obtained as white powder (poorly soluble in boiling toluene)

Tetracene-D2 (**84**) (114 mg, 31%) was obtained from the toluene solution after evaporation of the solvent.

Tetracene-D1 (**83**)

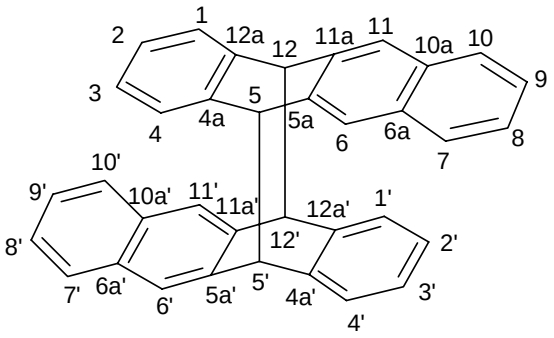

83

Only solid state NMR could be used due to the poor solubility, discussion of the results see Chapter 4.3.2.

IR (ATR): $\tilde{\nu}_{max}$ = 3062 cm^{-1} (w), 3039 (w), 3015 (w), 2919 (w), 1499 (w), 1479 (m), 1456 (m), 1456 (m), 1354 (w), 1312 (w), 1221 (w), 1102 (w), 1030 (w), 978 (w), 951 (m), 885 (s), 746 (s).

Tetracene-D2 (**84**)

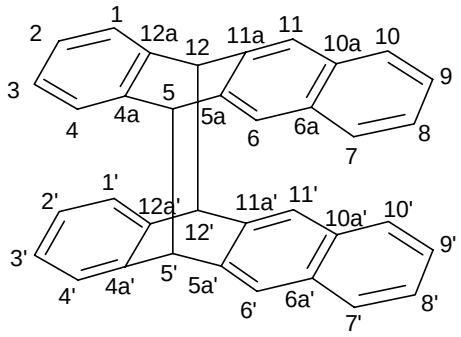

84

IR (ATR): $\tilde{\nu}_{max}$ = 3043 cm^{-1} (w), 3018 (w), 2921 (w), 1499 (w), 1501 (w), 1483 (m), 1458 (m), 1388 (w), 1353 (w), 1312 (w), 1261 (w), 1096 (w), 1021 (w), 978 (w), 956 (m), 900 (s), 741 (s).

^{1}H NMR (400 MHz, $CDCl_3$): δ = 7.49 (m_c, *N* = 9.4 Hz, 4 H, 10/7/10´/7´-H), 7.39 (s, 4 H, 11/6/11´/6´-H), 7.17 (m_c, *N* = 9.5 Hz, 4 H, 9/8/9´/8´-H), 6.98 (m_c, *N* = 8.7 Hz, 4 H, 4/1/4´/1´-H), 6.85 (m_c, *N* = 8.7 Hz, 4 H, 3/2/3´/2´-H), 4.84 (s, 4 H, 12/5/12´/5´-H).

^{13}C NMR (100 MHz, $CDCl_3$): δ = 143.0 (s, C-12a/4a/12a´/4a´), 141.0 (s, C-11a/5a/11a´/5a´), 132.0 (s, C-10a/6a/10a´/6a´), 127.14 (d, C-4/1/4´/1´), 127.12 (d, C-10/7/10´/7´), 125.9 (d, C-3/2/3´/2´), 125.4 (d, C-11/6/11´/6´), 125.0 (d, C-9/8/9´/8´), 53.8 (d, C-12/5/12´/5´).

The results of the solid state NMR experiments are discussed in Chapter 4.3.2

Appendix I: Gel formation measurements

A) Inverted tube tests, solvent screening

Abbreviations: G = gel formation, P = precipitation of the gelator upon cooling, IS = gelator is insoluble in the boiling solvent, L = gelator stays dissolved after cooling, VS = the gelator stays dissolved but the viscosity of the solvent increases visibly.

I) 2,3-DDOT (**86**)

Solvent	β [mg/mL]	c [10^{-3} mol/L]	RT	-24°C
methanol	10.6	19.6	IS	-
	1.07	1.98	IS	-
ethanol	13.5	25	P	-
2-propanol	10.1	18.7	P	-
	4.83	8.9	P	-
n-butanol	0.993	1.84	P	-
n-hexanol	2.64	4.89	G	-
	0.968	1.79	L	L
n-octanol	2.69	4.98	G	-
	1.02	1.89	L	L (+4°)
n-decanol	2.49	4.61	G	-
	0.994	1.84	L	-
n-hexane	11.4	21.1	G	-
	5.43	10.1	G	-
n-heptane	2.62	4.85	P	-
	0.988	1.83	P	-
n-nonane	2.45	4.54	P	-
	0.991	1.83	P	-
n-$C_{14}H_{30}$	2.45	4.54	P	-
	1.02	1.89	P	-
cyclohexane	6.01	11.1	G	-
	3.6	6.7	G	-
	2.1	3.9	G	-
	1.1	2.0	VS	-
MCH	5.5	$1.0*10^{-2}$	G	-

1,2-propylene-carbonate	8.8	16	IS	-
	4.34	8.0	P	-
chloroform	9.6	18	L	G
	21.3	39.4	L	G
DCM	4.89	9.05	L	G
	2.59	4.80	L	VS
DMF	2.50	4.63	G	-
	1.03	1.91	L	VS
acetone	2.55	4.72	P	-
	1.02	1.89	L	P

Table 57 Solvent screening of 2,3-DDOT (86)

II) 2,3-DHdOT (**111**)

Solvent	β [mg/mL]	c [10^{-3} mol/L]	RT	-24°C
methanol	2.37	3.34	IS	-
	1.08	1.52	P	-
ethanol	2.64	3.72	IS	-
	0.974	1.37	P	-
2-propanol	2.57	3.62	IS	-
	0.978	1.38	P	-
n-butanol	1.63	2.30	P	-
	1.30	1.83	P	-
n-hexanol	1.67	2.36	VS	-
	1.24	1.75	VS	-
	0.16	0.226	L	-
n-octanol	0.70	0.987	G	-
n-decanol	1.55	1.37	G	-
	0.97	1.19	G	-
	0.20	0.282	L	-
n-hexane	2.22	3.13	G	-
	0.85	1.20	G	-
n-heptane	0.61	0.860	G	-
n-nonane	2.36	3.33	G	-

	1.12	1.58	G	-
	0.13	0.183	L	-
n-$C_{14}H_{30}$	2.44	3.44	G	-
	0.993	1.40	G	-
cyclohexane	1.26	1.78	G	-
	0.55	0.776	G	-
	0.23	0.324	L	-
MCH	0.68	0.995	VS	-
chloroform	5.11	7.21	L	L
	2.41	3.40	L	L
DCM	5.31	7.49	G	-
	2.63	3.71	L	VS
DMF	2.42	3.41	P	-
	1.02	1.44	P	-
1,2-propylene-carbonate	2.39	3.37	IS	-
	0.985	1.39	IS	-
acetone	2.45	3.46	G	-
	1.00	1.41	P	-

Table 58 Solvent screening of 2,3-DHdOT (111)

III) 2,3-DHdOP (**115**)

Solvent	β [mg/mL]	c [10^{-3} mol/L]	RT	-24°C
toluene	5 mg/ ml	6.6	IS	-
chloroform	5 mg/ ml	6.6	G + P	-
1,1,2,2-tetrachloro-ethane	10 mg/ ml	13	G	-

Table 59 Solvent screening of 2,3-DHdOP (115)

B) Thermodynamic data of the gel formation using UV/Vis-spectroscopy

B-1) 2,3-DDOT (**86**)/cyclohexane

Concentrations measured: $c_1 = 4.1 \bullet 10^{-4}$ M (0.22 mg/mL), $c_2 = 8.7 \bullet 10^{-4}$ M (0.47 mg/mL), $c_3 = 2.3 \bullet 10^{-3}$ M (1.24 mg/mL), $c_4 = 3.5 \bullet 10^{-3}$ M (1.89 mg/mL), $c_5 = 4.6 \bullet 10^{-3}$ M (2.48 mg/mL), $c_6 = 5.5 \bullet 10^{-3}$ M (2.97 mg/mL).

Half melting- and formation points

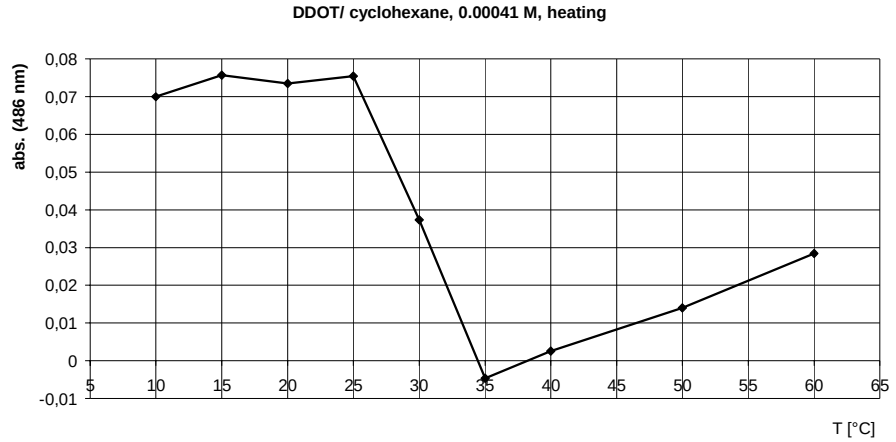

T (melting) = 30 °C

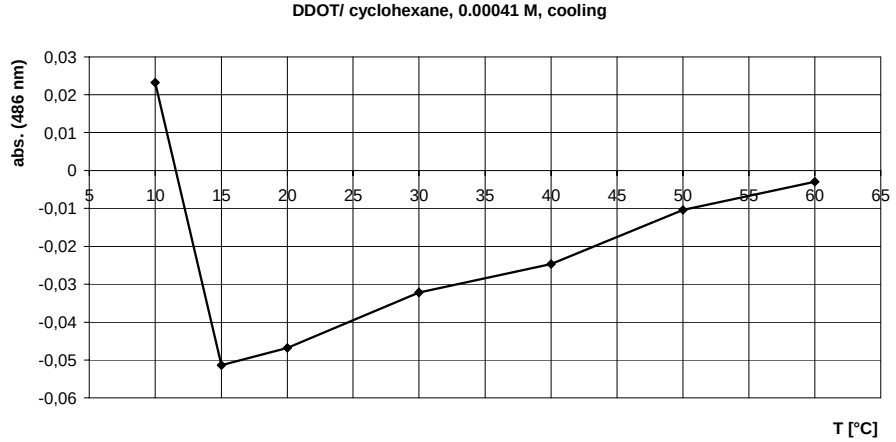

T (formation) = 12 °C

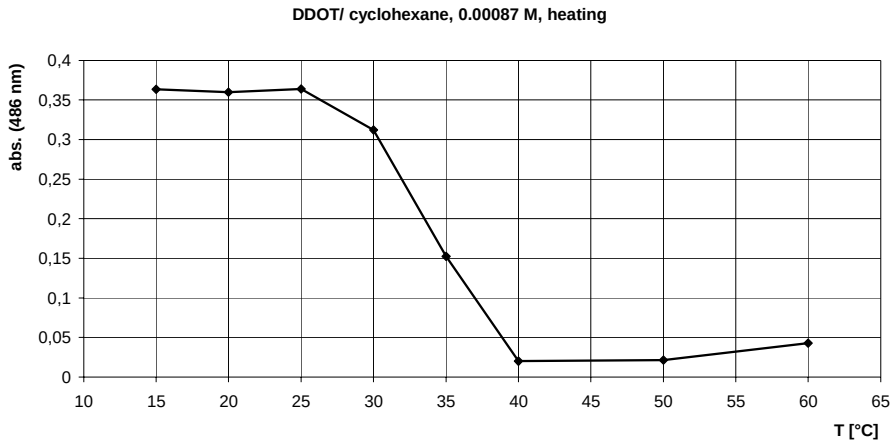

T (melting) = 34°C

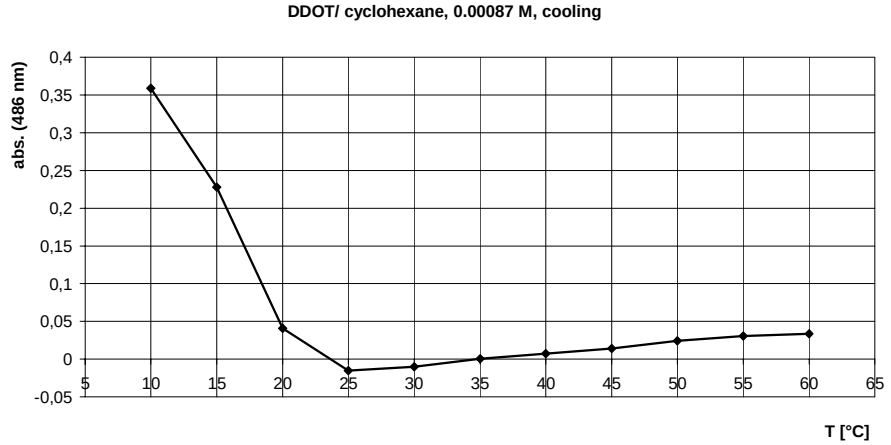

T (formation) = 17°C

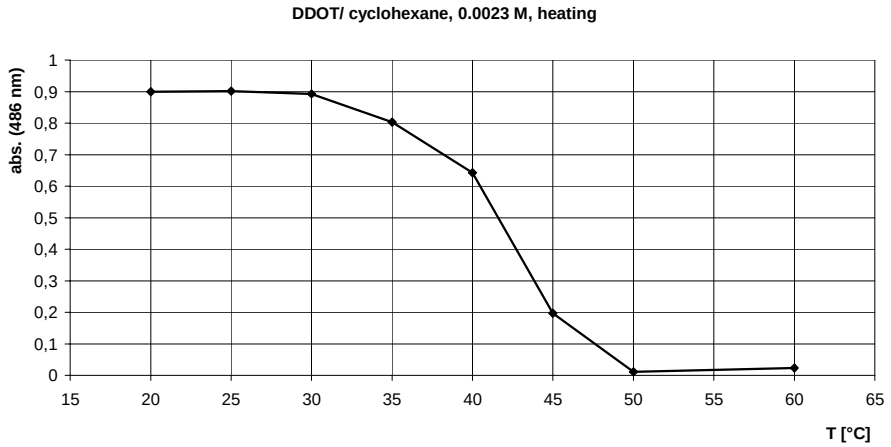

T (melting) = 42 °C

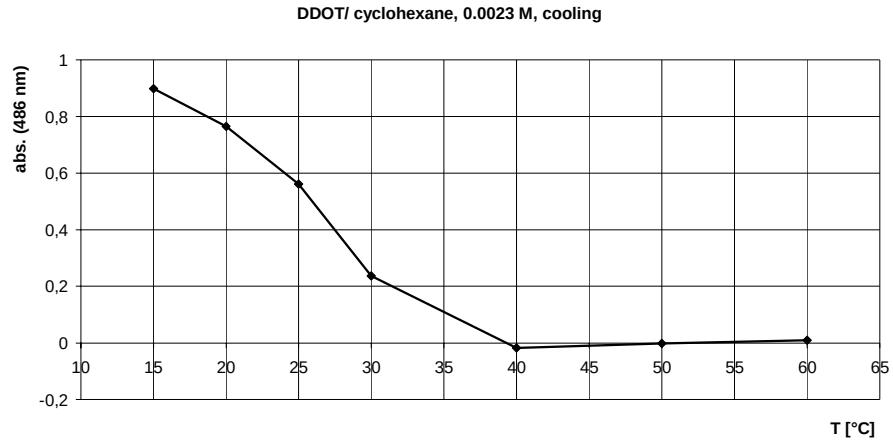

T (formation) = 26 °C

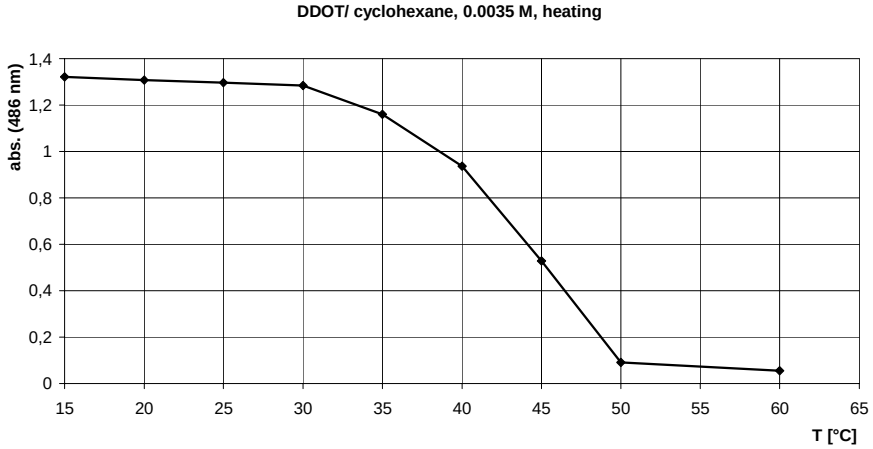

T (melting) = 43 °C

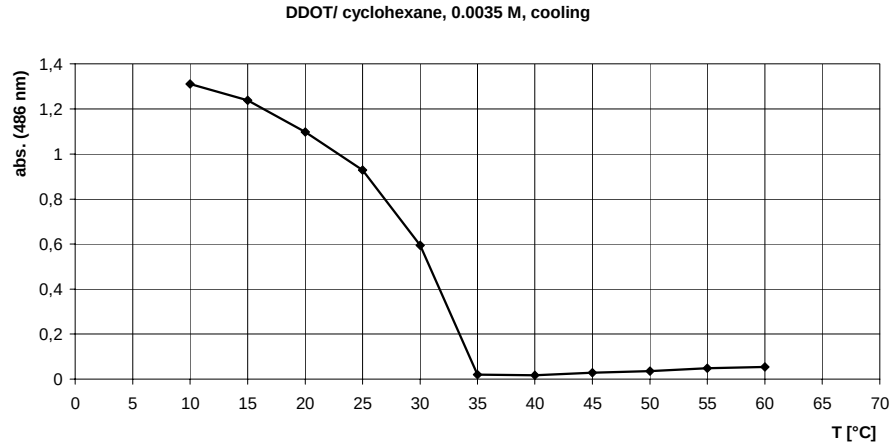

T (formation) = 29 °C

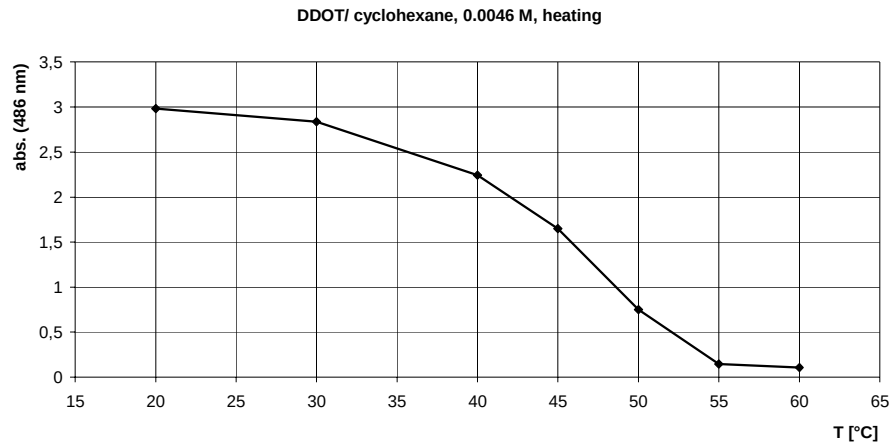

T (melting) = 45 °C

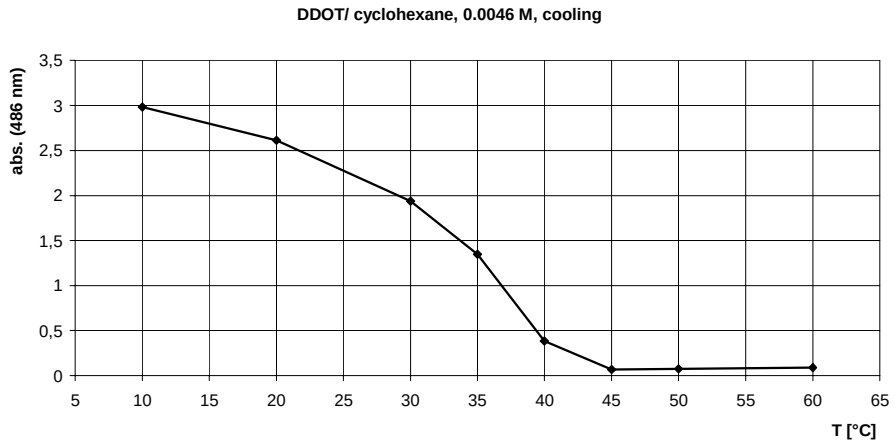

T (formation) = 33 °C

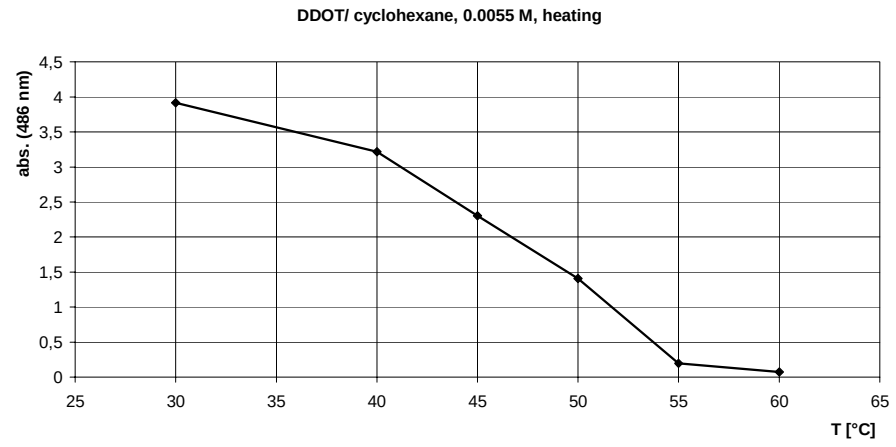

T (melting) = 47 °C

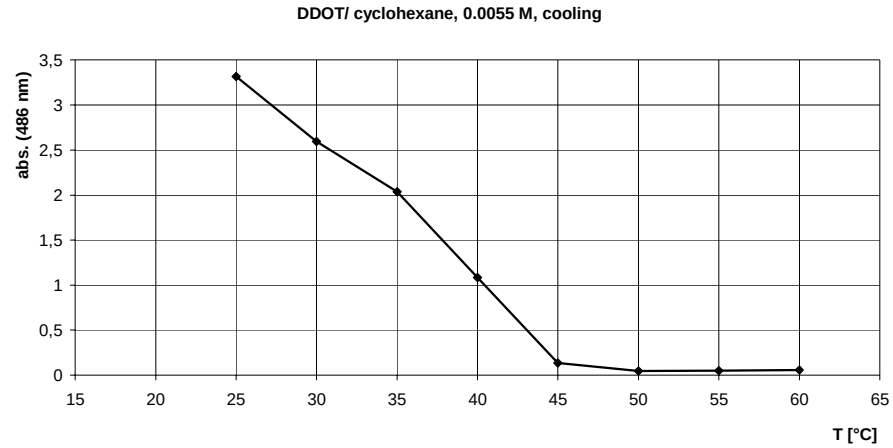

T (formation) = 37 °C

Phase transition diagram (2,3-DDOT (**86**)/cyclohexane)

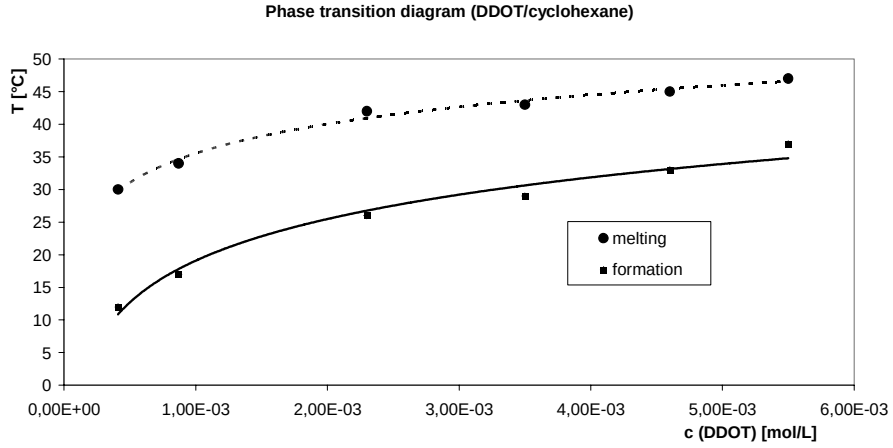

Determination of the thermodynamic properties (ΔH, ΔS, 2,3-DDOT (**86**)/cyclohexane)

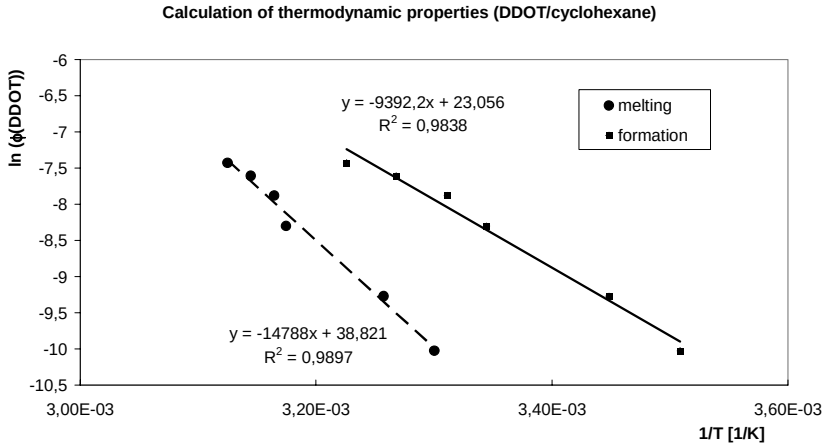

B-2) 2,3-DDOT (**86**)/hexanol

Concentrations measured: $c_1 = 4.1 \bullet 10^{-4}$ M (0.22 mg/mL), $c_2 = 9.8 \bullet 10^{-4}$ M (0.53 mg/mL), $c_3 = 1.5 \bullet 10^{-3}$ M (0.81 mg/mL), $c_4 = 2.1 \bullet 10^{-3}$ M (1.13 mg/mL).

Half melting points

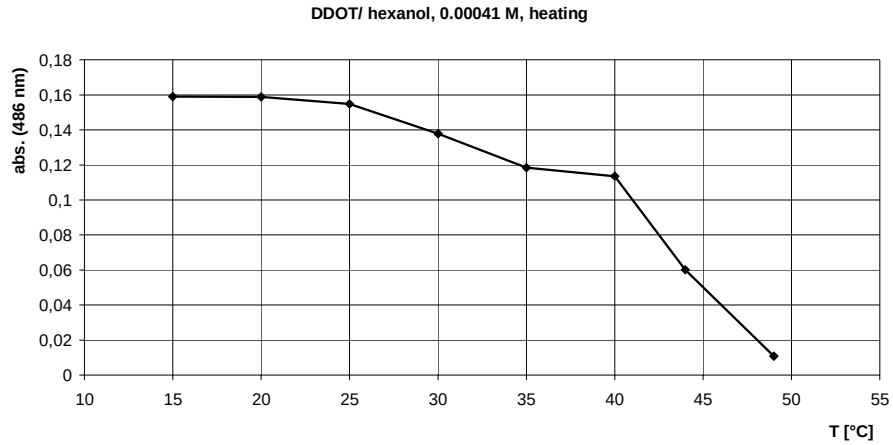

T (melting) = 40 °C

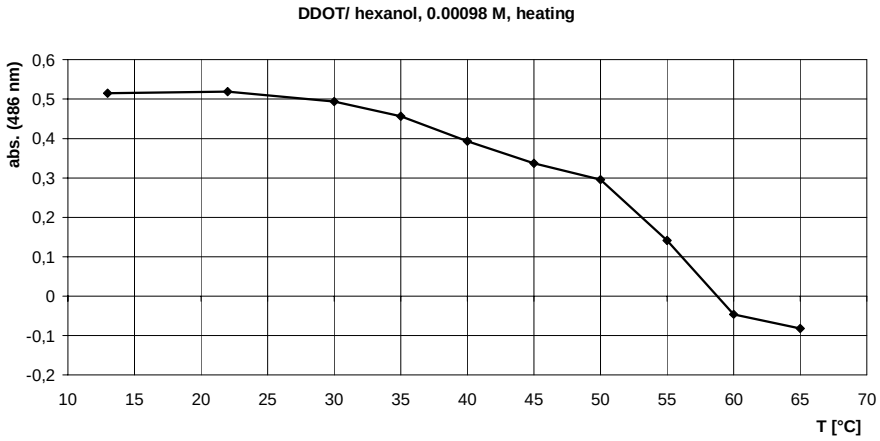

T (melting) = 52 °C

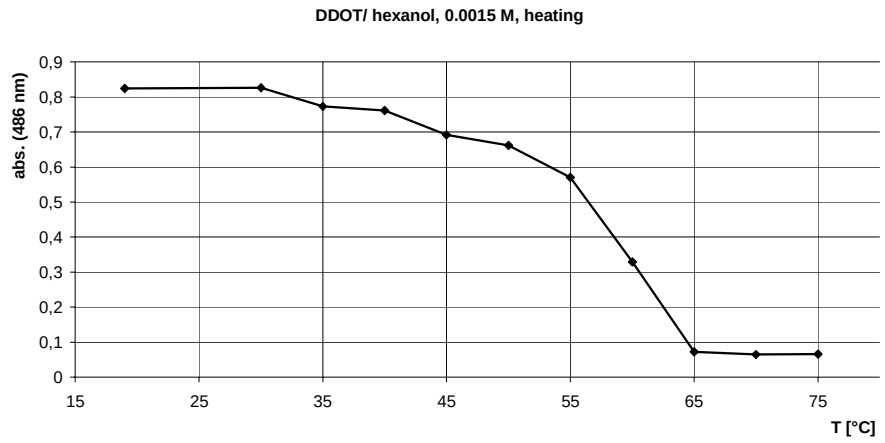

T (melting) = 53 °C

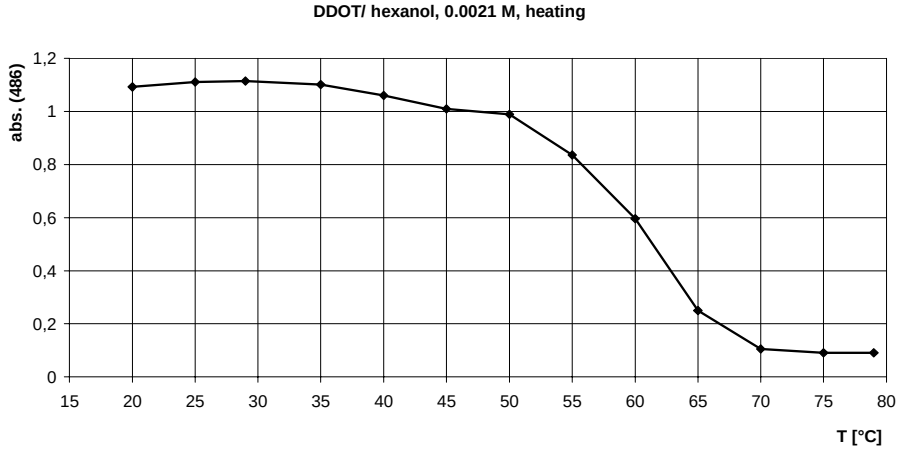

T (melting) = 60 °C

Phase transition diagram (2,3-DDOT (**86**)/ hexanol, melting)

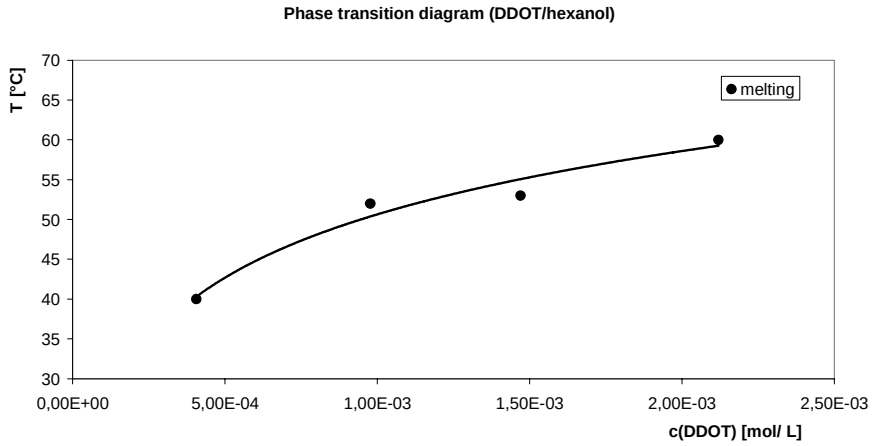

Determination of thermodynamic properties (ΔH, ΔS, 2,3-DDOT (**86**)/ hexanol)

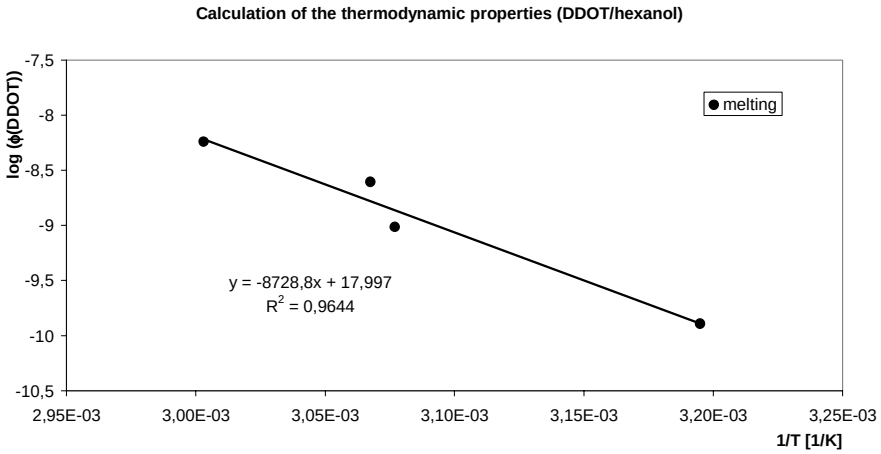

B-3) 2,3-DHdOT (**111**)/ cyclohexane

Concentrations measured: $c_1 = 4.1 \bullet 10^{-4}$ M (0.287 mg/ml), $c_2 = 7.0 \bullet 10^{-4}$ M (0.497 mg/mL), $c_3 = 1.0 \bullet 10^{-3}$ M (0.718 mg/mL), $c_4 = 2.0 \bullet 10^{-3}$ M (1.39 mg/mL), $c_5 = 2.7 \bullet 10^{-3}$ M (1.88 mg/mL).

Half melting- and formation points

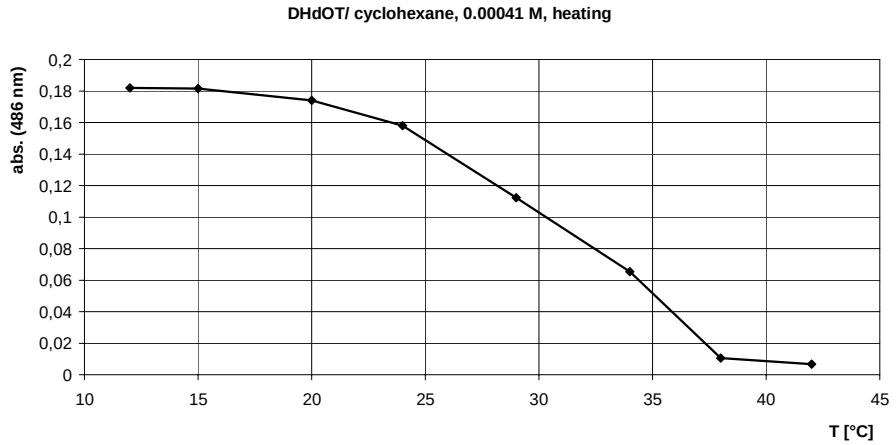

T (melting) = 31 °C

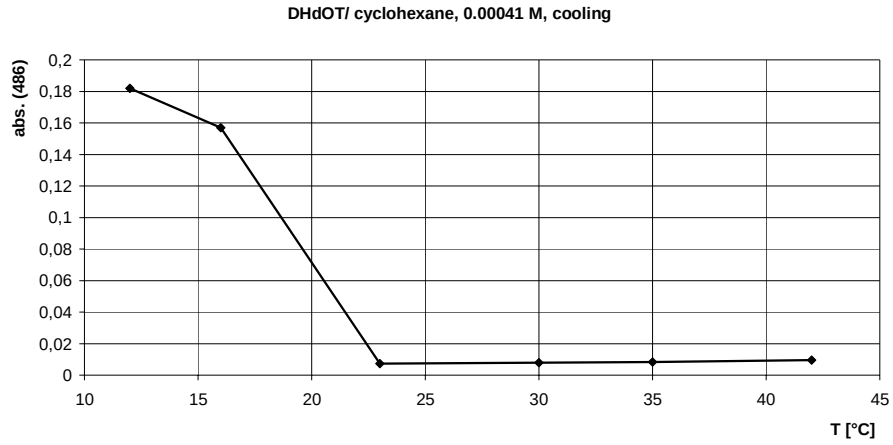

T (formation) = 19 °C

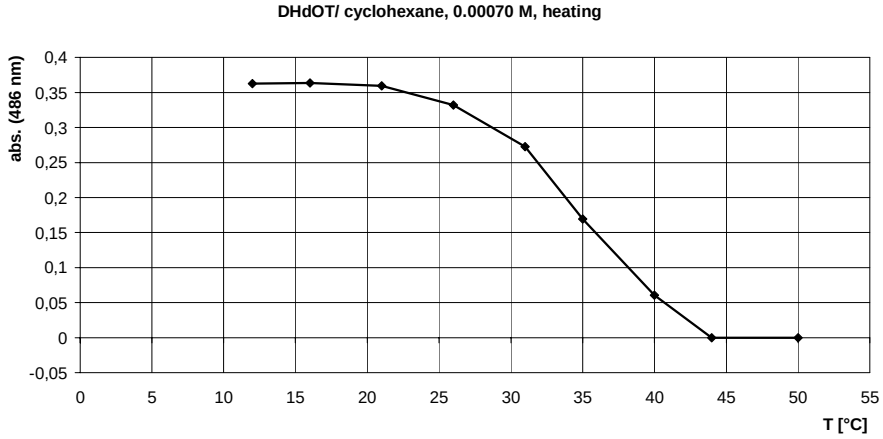

T (melting) = 35 °C

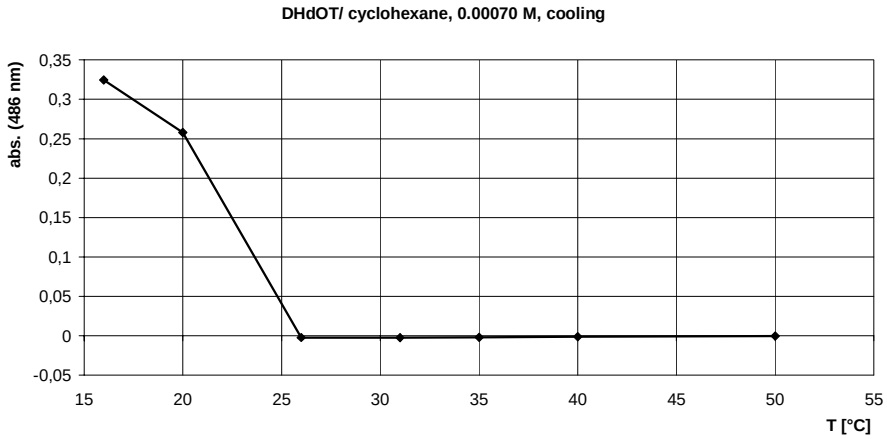

T (formation) = 22 °C

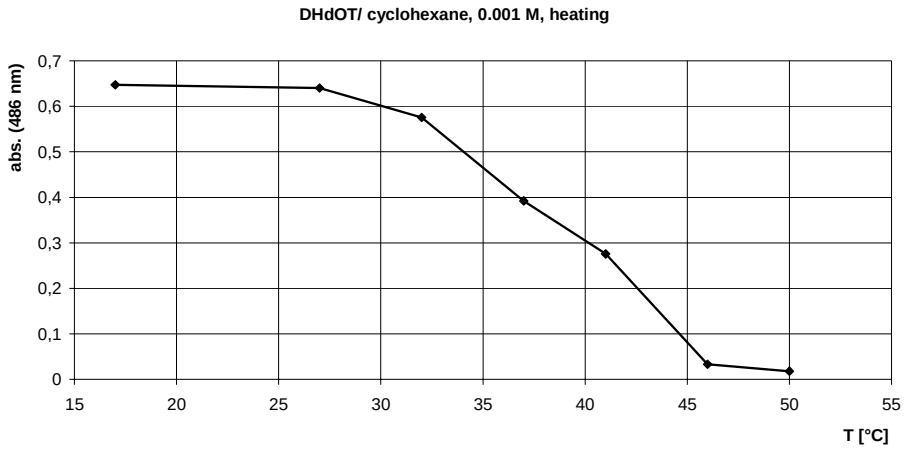

T (melting) = 39 °C

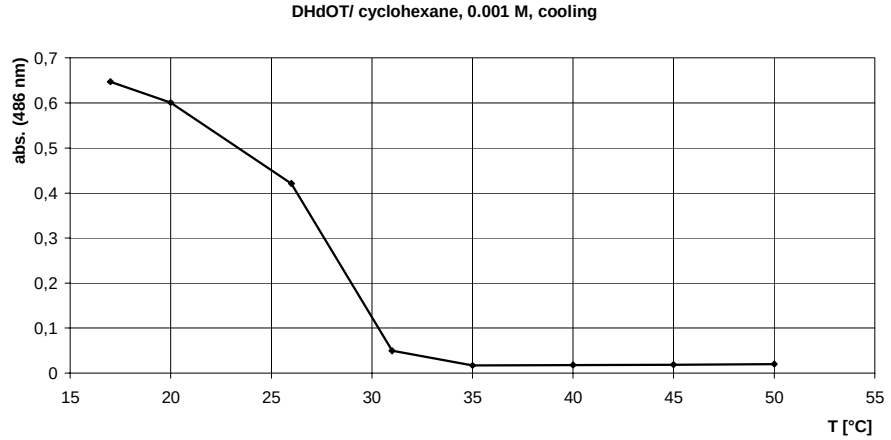

T (formation) = 27 °C

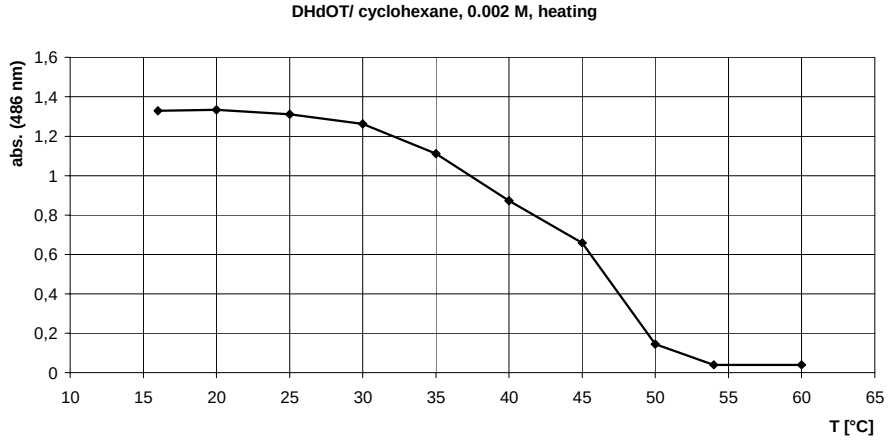

T (melting) = 45 °C

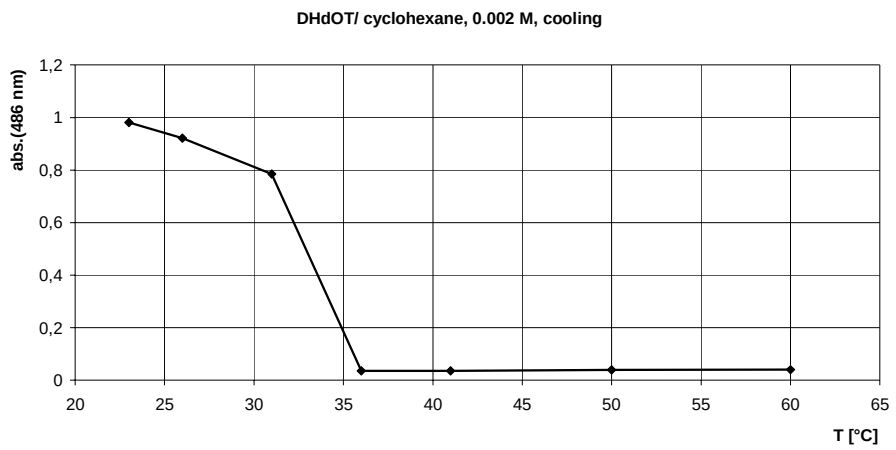

T (formation) = 33 °C

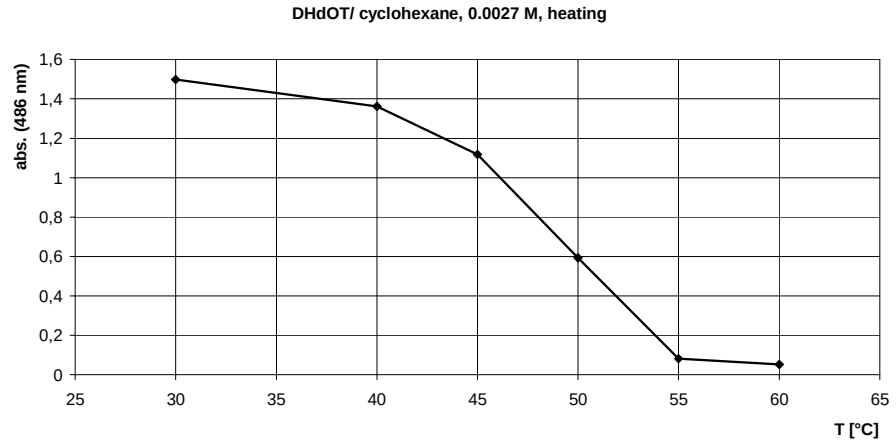

T (melting) = 48 °C

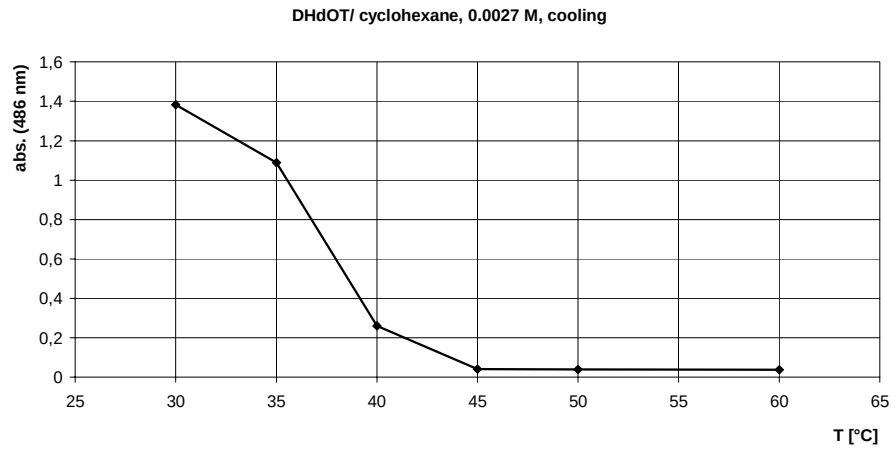

T (formation) = 37 °C

Phase transition diagram (2,3-DHdOT (**111**)/cyclohexane)

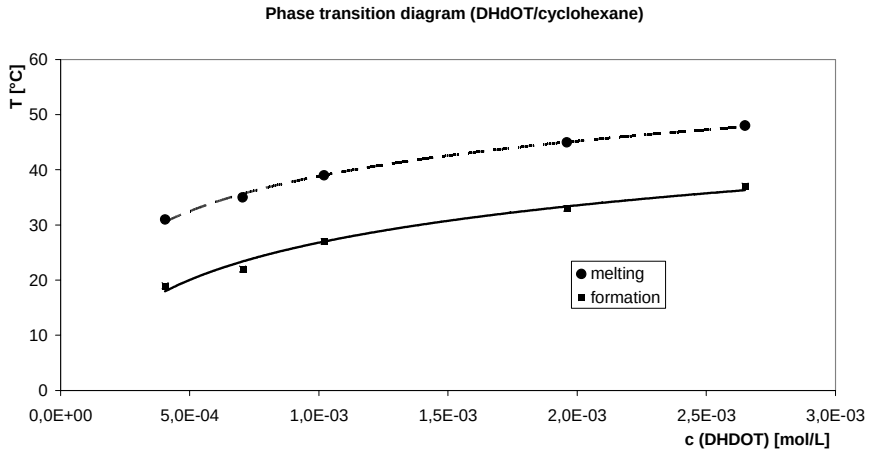

Determination of the thermodynamic properties (ΔH, ΔS, 2,3-DHdOT (**111**)/cyclohexane)

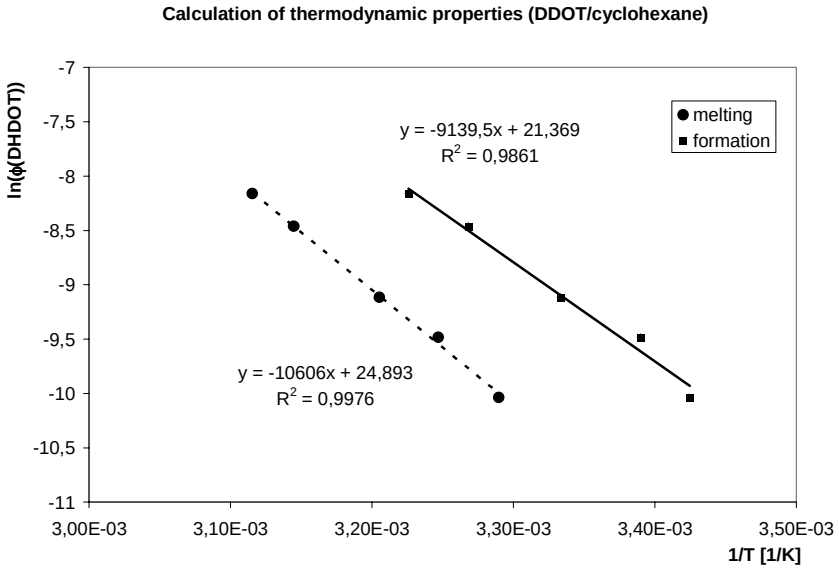

B-4) 2,3-DHdOT (**111**)/hexanol

Concentrations measured: $c_1 = 43.1 \bullet 10^{-4}$ M (0.222 mg/mL), $c_2 = 7.2 \bullet 10^{-4}$ M (0.512 mg/mL), $c_3 = 1.2 \bullet 10^{-3}$ M (0.815 mg/mL), $c_4 = 1.4 \bullet 10^{-3}$ M (1.00 mg/mL).

Half-melting points

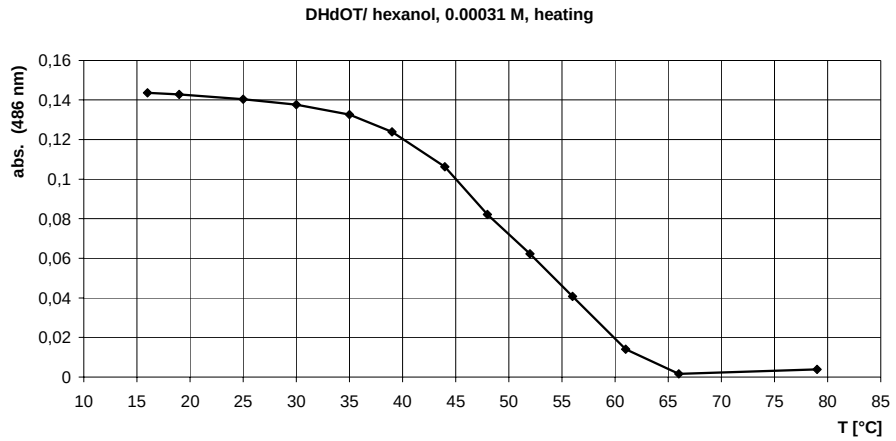

T (melting) = 50 °C

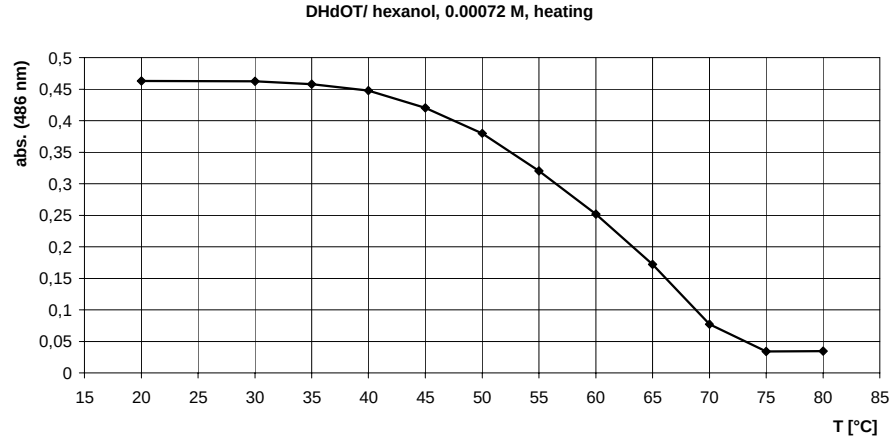

T (melting) = 60 °C

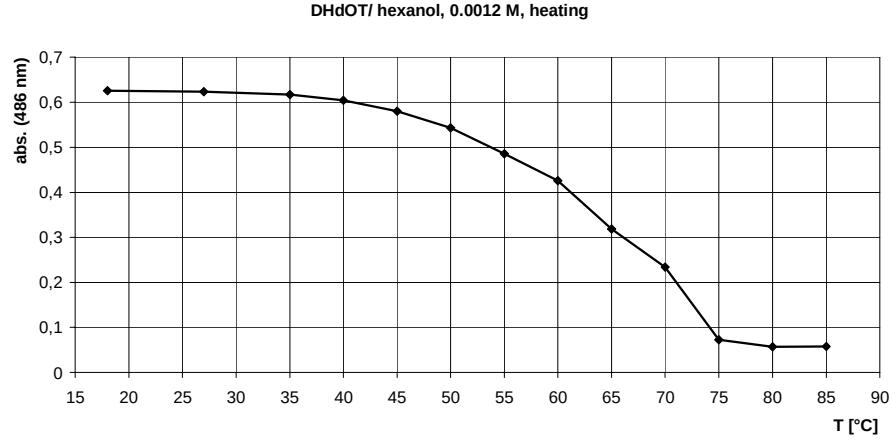

T (melting) = 64 °C

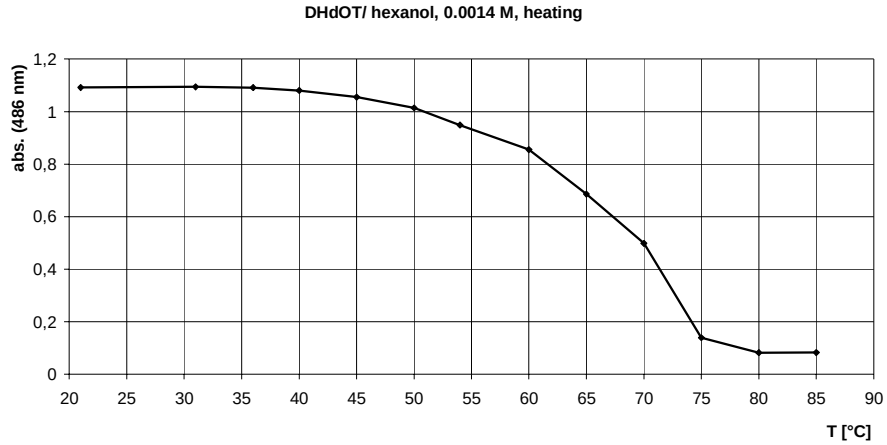

T (melting) = 65 °C

Phase transition diagram (2,3-DHdOT (**111**)/hexanol, melting)

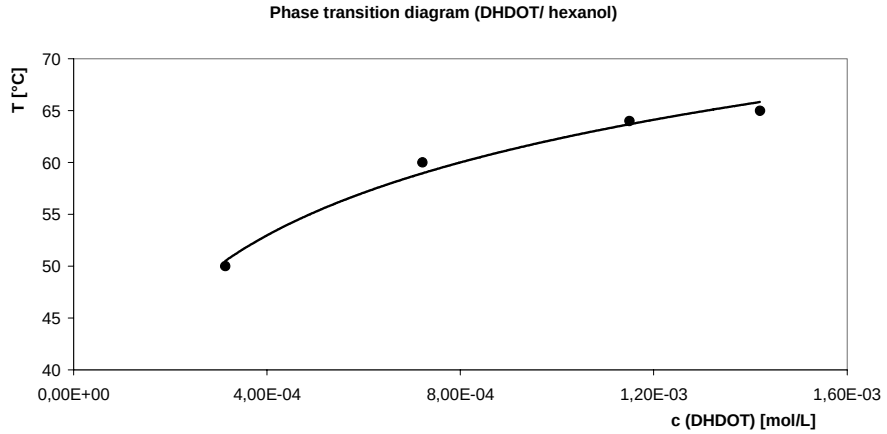

Determination of thermodynamic properties (ΔH, ΔS, 2,3-DHdOT (**111**)/hexanol)

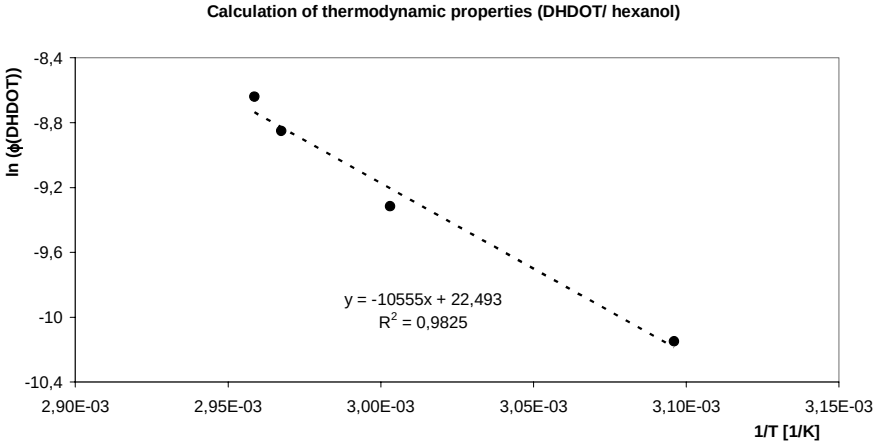

C) Cooperative behavior of 2,3-DDOA (**1**) *and 2,3-DDOT* (**86**)

C.1) Solvent: hexanol

$c_{(2,3\text{-DDOA})} = 4.05 \bullet 10^{-3}$ M, $c_{(2,3\text{-DDOT})} = 4.06 \bullet 10^{-4}$ M

$\lambda_{(\text{obs, 2,3-DDOA-gel})} = 382$ nm; $\lambda_{(\text{obs, 2,3-DDOT-gel})} = 482$ nm

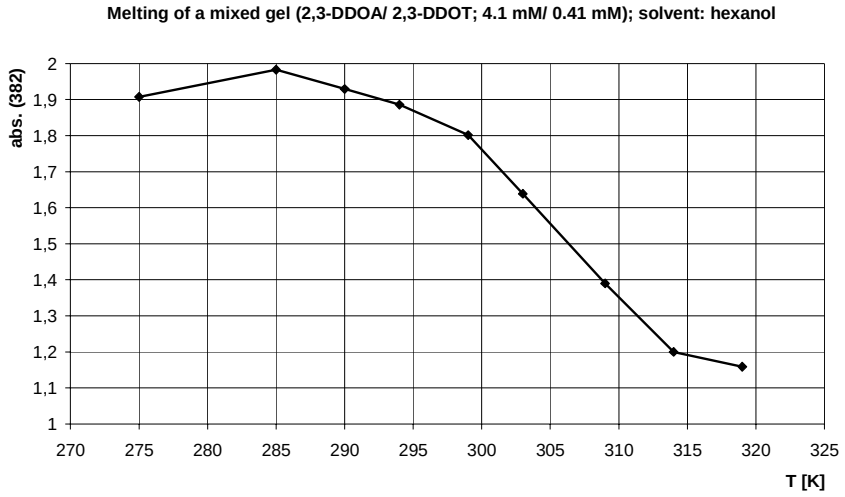

Half-melting-point (DDOA) = 305 K

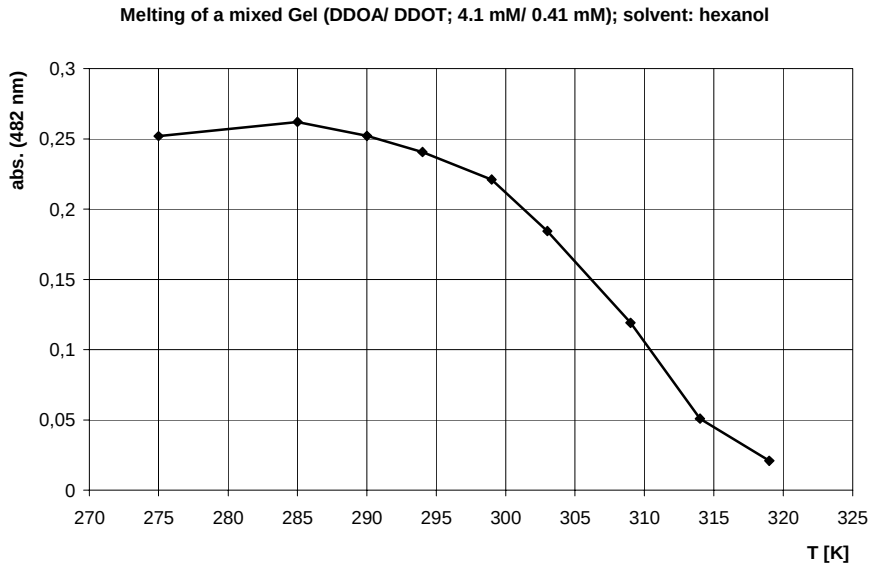

Half-melting-point (DDOT) = 307 K

C.2) Solvent: MCH

$c_{(2,3\text{-DDOA})} = 1.07 \bullet 10^{-3}$ M, $c_{(2,3\text{-DDOT})} = 0.98 \bullet 10^{-4}$ M

$\lambda_{(\text{obs, 2,3-DDOA-gel})} = 384$ nm; $\lambda_{(\text{obs, 2,3-DDOT-gel})} = 483$ nm

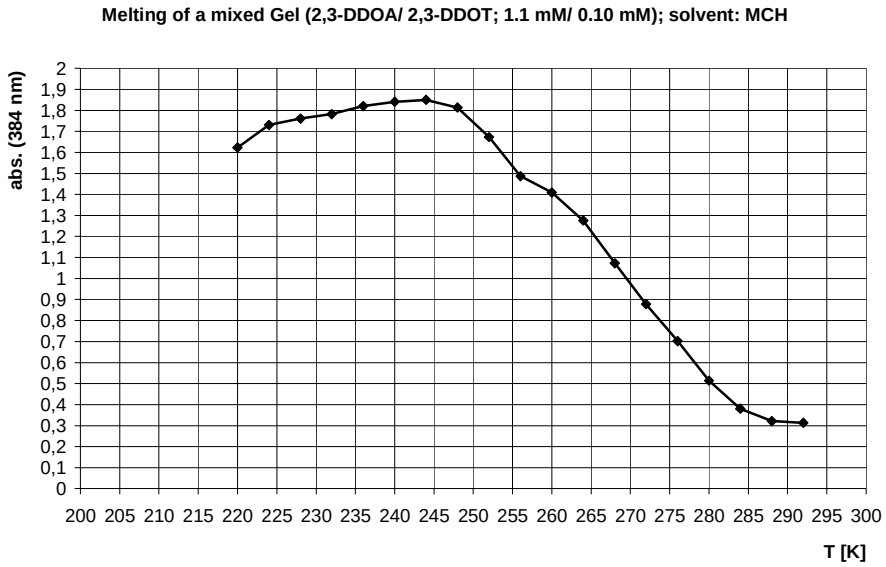

Half-melting-point (2,3-DDOA) = 269 K

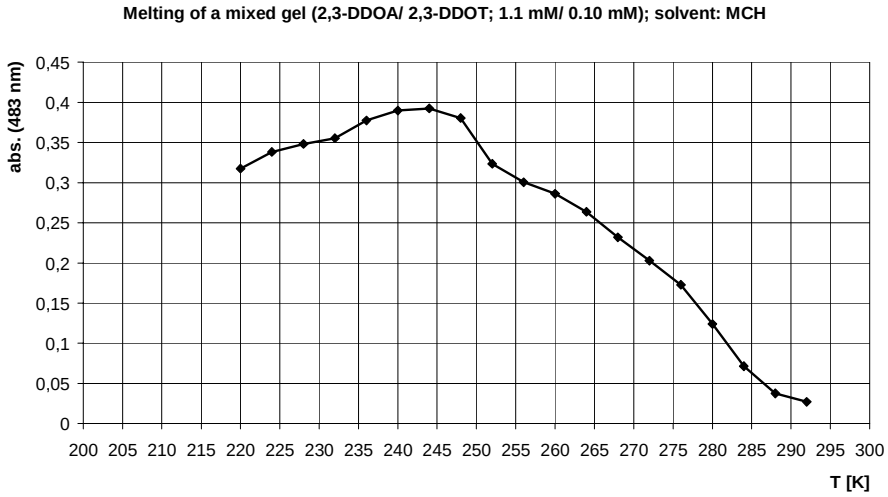

Half-melting-point (2,3-DDOT) = 273 K

D) Thermal dissociation of 96 *and* 97.

D.1) Dissociation of 96, hexane, 308 K

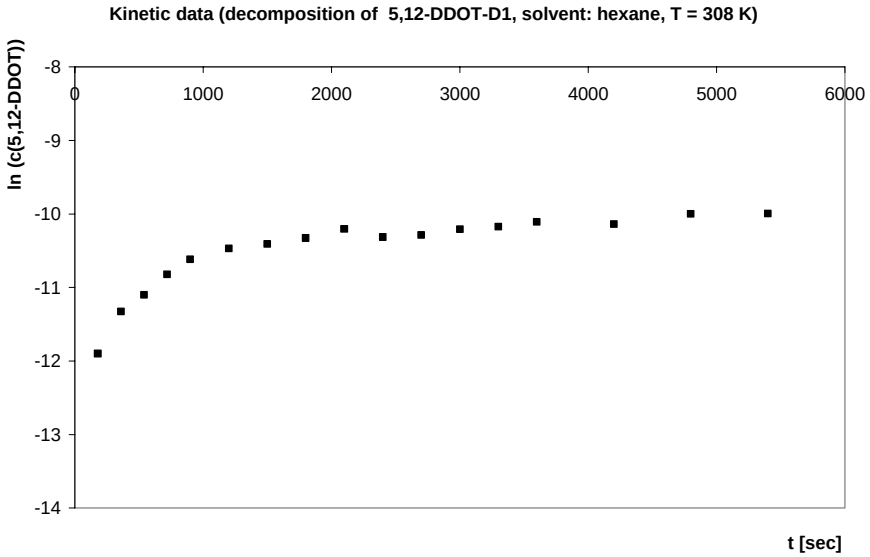

D.2) Dissociation of 96, MCH, 342 K

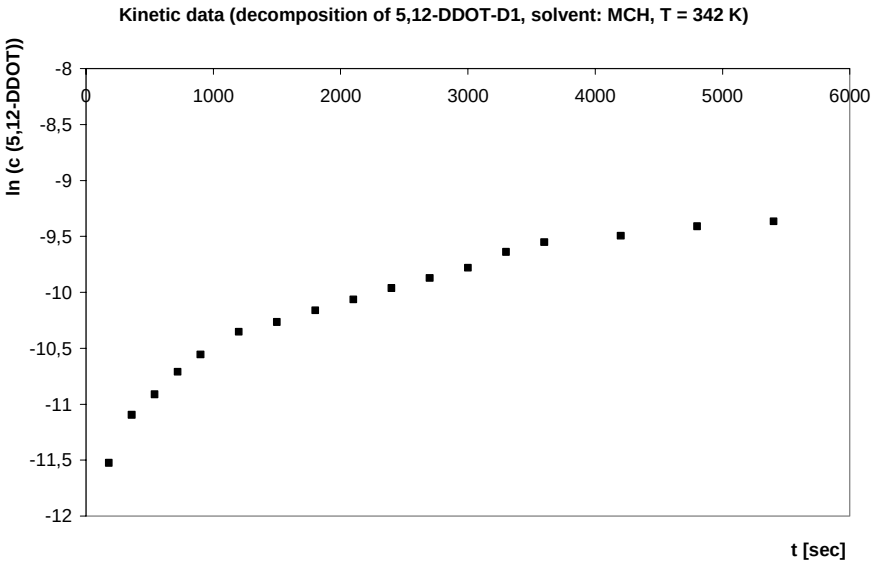

D.3) Dissociation of 97, hexane, 308 K

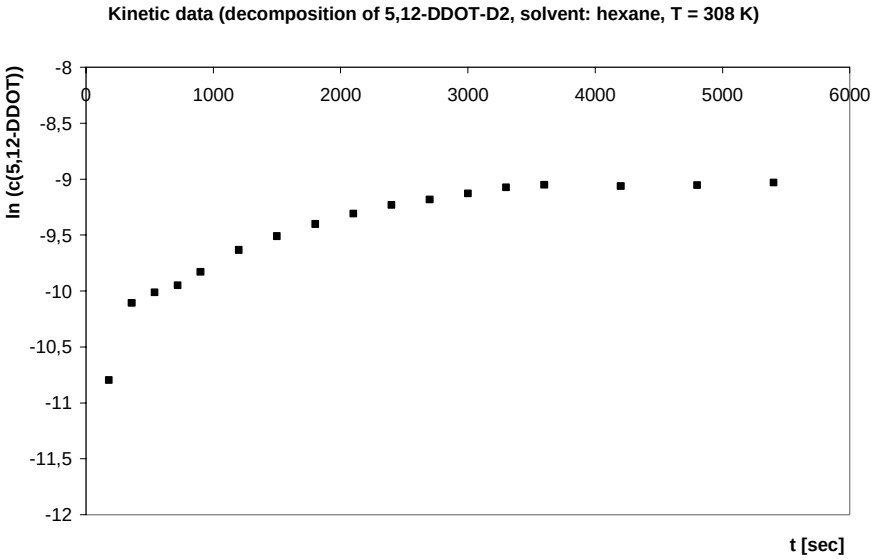

D.4) Dissociation of 97, MCH, 342 K

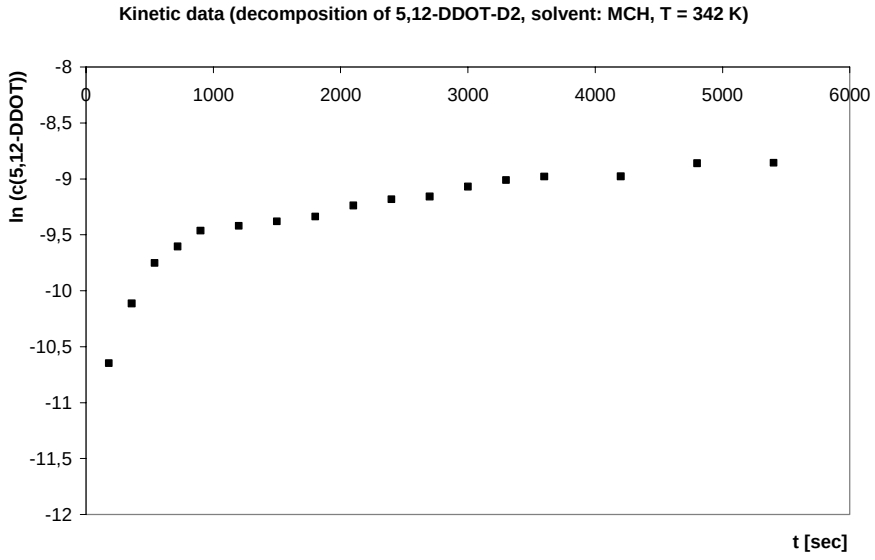

Appendix II: Commonly used abbreviations

A) Substance abbreviations

2,3-DMOT: 2,3-Dimethoxy-tetracene (**73**)

2,3-DBOT: 2,3-Dibutoxy-tetracene (**109**)

2,3-DHOT: 2,3-Dihexyloxy-tetracene (**110**)

2,3-DDOT: 2,3-Didecyloxy-tetracene (**86**)

5,12-DDOT: 5,12-Didecyloxy-tetracene (**85**)

2,3-DHdOT: 2,3-Dihexadecyloxy-tetracene (**111**)

2,3-DDOA: 2,3-Didecyloxy-anthracene (**1**)

2,3-DDOP: 2,3-Didecyloxy-pentacene (**114**)

2,3-DHdOP: 2,3-Dihexadecyloxy-pentacene (**115**)

2,3-DDOT dimers:

- 2,3-DDOT-D1 (**87**)
- 2,3-DDOT-D2 (**92**)
- 2,3-DDOT-D3 (**88**)
- 2,3-DDOT-D4 (**91**)

5,12-DDOT dimers:

- 5,12-DDOT-D1 (**96**)
- 5,12-DDOT-D2 (**97**)

Mixed dimers between 5,12-DDOT and tetracene (**82**):

- 5,12-DDOT-T-D1 (**102**)
- 5,12-DDOT-T-D2 (**103**)

Tetracene dimers:

- Tetracene-D1 (**83**)
- Tetracene-D2 (**84**)

hth = head to head dimer; htt = head to tail dimer

B) Abbreviations of commonly used solvents and chemical substances

DCM: Dichloromethane

MCH: Methylcyclohexane

DMF: *N*,*N*-Dimethylformamide

TEMPO: Tetramethylpiperidin-nitroxyl

Appendix III: Literature

[1] a) P. Terech, R. G. Weiss, *Chem Rev.*, **1997**, 97, 3133-3159; b) A. T. Polishuk, J. Am. Soc. Lubn. Eng., **1977**, *33*, 133-138; c) N. Pilpel, *Chem. Rev.*, **1963**, *63*, 221-234; d) O. Martin-Borret, R. Ramasseul, R. Rassat, *Bull. Soc. Chim. Fr.*, **1979**, 401-408; e) T. Itoh, D. E. Katsoulis, I. Mita, *J. Mater. Chem.*, **1993**, *3*, 1303-1305; f) K. Murata, M. Aoki, T. Susuki, T. Harada, H. Kawabata, T. Komori, F. Ohseto, K. Ueda, S. Shinkai, *J. Am. Chem. Soc.*, **1994**, *116*, 6664-66676; g) J. Campbell, M. Kuzma, M. Labes, *Mol. Cryst. Liq. Cryst.*, **1983**, *95*, 45-50; h) P. Terech, C. Chachaty, J. Gaillard, A. M. Godquin-Giroud, *J. Phys. Fr.*, **1987**, *48*, 663-671; R. Ramasseul, P. Maldivi, J. C. Marchon, *Liquid Crystals*, **1993**, *13*, 729-733; j) R. J. Twieg, T. P. Russel, R. Siemens, J. F. Rabolt, *Macromolecules*, **1985**, *18*, 1361-1362; k) J.-M. Lehn, M. Mascal, A. DeCian, J. Fisher, *J. Chem. Soc., Chem. Commun.*, **1990**, 479-481.

[2] T. Brotin, R. Utermöhlen, F. Fages, H. Bouas-Laurent, J.-P. Desvergne, *J. Chem. Soc., Chem. Commun.*, **1991,** 416-418.

[3] T. Brotin, J. Waluk, J.-P. Desvergne, H. Bouas-Laurent, J. Michl, *Photochem. Photobiol.*, **1992**, 335-347.

[4] H. Bouas-Laurent, A. Castellan, J.-P. Desvergne, R. Lapouyade, *Chem. Soc. Rev.*, **2000**, *29*, 43-55.

[5] Photochromism: Molecules and Systems, H. Dürr, H. Bouas-Laurent (eds.), Elsevier, Amsterdam, **2003**, chapter 14, 583.

[6] H. Bouas-Laurent, A. Castellan, *J. Chem. Soc., Chem. Comm.*, **1970**, 1648-1649.

[7] R. Lapouyade, A. Nourmamode, H. Bouas-Laurent, *Tetrahedron*, **1980**, 2311-2316.

[8] H. G. Bungenberg de Jong, *Colloid Science II*, **1949** ed. H. R. Kruyt, (Elsevier Publ. Co., Inc., Amsterdam).

[9] P. J. Flory, *Faraday Discuss. Chem. Soc.*, **1974**, 57, 7-18.

[10] P. Terech, I. Furman, H. Bouas-Laurent, J. P. Desvergne, R. Ramasseul, R. G. Weiss; *J. Chem Soc., Faraday Discuss.*, **1995**, 101, 345-358.

[11] J.-L. Pozzo, G. M. Clavier, M. Colomes, H. Bouas-Laurent, *Tetrahedron*, **1997**, 53 6377-6390.

[12] D. N. Gupta, P. Hodge, N. Khan; *J. Chem. Soc., Perkin Trans. 1*, **1981**, 689-696.

[13] D. M. Bowles, J. E. Anthony, *Org. Lett.*, **2000**, 2, 85-87.

[14] A. Mallouli, Y. Lepage, *Synthesis*, **1980**, *9*, 689.

[15] R. W. Franck, P. B. Gupta; *J. Org. Chem.*, **1985**, *50*, 4632-4635.

[16] J. Reichwagen, *Diploma Thesis*, Braunschweig **2001**.

[17] B. Serpaud, Y. Lepage, *Bull. Soc. Chim. Fr.*, **1977**, 5, 539-542.

[18] R. Adams, T. A. Geissmann, R. B. Baker, H. M. Teeter, *J. Am. Chem. Soc.*, 63, **1941**, 528-534.

[19] J. W. Grissom, G. U. Gunawardena, *Tetrahedron Lett.*, 36, **1995**, 4951-4954.

[20] X. Zhang, B. W. Fox, J. A. Hadfield, *Synth. Comm.*, **1996**, 26, 49-62.

[21] R. T. Plimpton, *J. Chem. Soc.*, **1880**, 37, 633-645.

[22] H. Laatsch, *Justus Liebigs Ann. Chem.*, **1985**, 251-274.

[23] V. P. Papageorgiou, E. A. Couladouras, Z. F. Plyta, S. A. Haroutouniau, *J. Org. Chem.*, **1997**, 62, 6-10.

[24] A. P. Marchand, G. M. Reddy, *Synthesis*, **1991**, 3, 198-200.

[25] E. Barranco, N. Martín, J. L. Seguro, C. Seoane, *Tetrahedron*, **1993**, 49 , 4881-4892.

[26] M. Albrecht, M. Schneider, *Synthesis*, **2000**, *11*, 1557-1560.

[27] M. V. Bhatt, S. S. El-Morey, *Synthesis*, **1982**, *12*, 1048-1050.

[28] S. Andersson, *Synthesis*, **1985**, *4*, 437-439.

[29] A. Robertson, R. B. Waters, *J. Chem. Soc.*, **1933**, 83-86.

[30] G. Grethe, V. Toome, H. L. Lee, M. Uskakovic, A. Brossi, *J. Org. Chem.*, **1968**, 504-508.

[31] N. P. Buu-Hoi, D. Lavit, *J. Org. Chem.*, **1956**, 21-23.

[32] A. Williamson, *Justus Liebigs Ann. Chem.*, **1851**, *77*, 37-49.

[33] K. Lagodzinski, *Ber. Dtsch. Chem. Ges.*, **1895**, *28*, 1533-1535.

[34] R. Broene, F. Diederich, *Tetrahedron Lett.*, **1991**, *32*, 5227-5230.

[35] T. R. Criswell, B. H. Klanderman, *J. Org. Chem.*, **1974**, *39*, 770-774.

[36] S. Coffey, V. Boyd, *J. Chem. Soc.*, **1954**, 2468-2470.

[37] H. Meerwein, R. Schmidt, *Justus Liebigs Ann. Chem.*, **1926**, *444*, 221-238.

[38] W. Ponndorf, *Angew. Chem.*, **1926**, *39*, 138-143.

[39] U. Müller, M. Adam, K. Müllen, *Chem. Ber.*, **1994**, *127*, 437-444.

[40] D. Perepichka, M. Bendikov, H. Meng, F. Wudl, *J. Am. Chem. Soc.*, **2003**, *125*, 10190-10191.

[41] G. S. Tulevski, Q. Miao, M. Fukuto, R. Abram, B. Ocko, R. Pindak, M. L. Steigerwald, C. R. Kagan, C. Nuckolls, *J. Am. Chem. Soc.*, **2004**, *126*, 15048-15050.

[42] N. Vets, M. Smet, W. Dehaen, *Tetrahedron Lett.*, **2004**, 7287-7289.

[43] A. Afzali, C. D. Dimitrakopoulos, T. L. Breen, *J. Am. Chem. Soc.*, **2002**, 8812-8813.

[44] M. M. Payne, J. H. Delcamp, S. R. Parkin, J. E. Anthony, *Org. Lett.*, **2004**, 1609-1612.

[45] Y. Sakamoto, T. Suzuki, M. Kobayashi, Y. Gao, Y. Fukai, Y. Inoue, F. Sato, S. Tokito, *J. Am. Chem. Soc.*, **2004**, 8138-8140.

[46] J. W. Cook, L. Hunter, R. Schoental, *J. Chem. Soc.*, **1949**, Suppl. Issue, 228.

[47] F. Weygand, K. G. Kinkel, D. Tietjen, *Chem. Ber.*, **1950**, *83*, 394-399.

[48] W. Ried, H. Bodem, *Chem. Ber.*, **1956**, *89*, 708-712.

[49] R. G. Carlson, K. Srinivasachar, R. S. Givens, B. K. Matuszewski, *J. Org. Chem.*, **1986**, *51*, 3978-3983.

[50] Photochromism: Molecules and Systems, H. Dürr and H. Bouas-Laurent (eds.), revised edition, Elsevier, Amsterdam **2003**, chapter 14, p. 584.

[51] K. Lagodzinski, *Ber. Dtsch. Chem. Ges.*, **1895**, *28*, 116-119.

[52] J. R. Johnson, W. H. Lobling, G. W. Bodamer, *J. Am. Chem. Soc.*, **1941**, 63, 131-135.

[53] J.-P. Desvergne, T. Brotin, D. Meerschaut, G. Clavier, F. Placin, J.-L. Pozzo and H. Bouas-Laurent, unpublished data.

[54] P. Terech, D. Meerschaut, J.-P. Desvergne, M. Colomes and H. Bouas-Laurent, *J. Colloid Interface Sci.*, **2003**, 441-445.

[55] A. Del Guerzo, J. Reichwagen, H. Hopf, C. Belin, H. Bouas-Laurent, J.-P. Desvergne: Self-Assembled Fibers with Tunable Optical Properties: Organogels of Anthracene and Tetracene Derivatives (Poster), HRSMC & EPA Summer School "New Perspectives in Photochemistry" Egmond aan Zee, **2003**.

[56] Analytical chemistry: the authentic text to the FECS curriculum analytical chemistry/ ed. by R. Kellner, J.-M. Mermet, M. Otto, H.M. Widmer; Weinheim **1998**.

[57] R. B. Woodward, R. Hoffmann, *Angew. Chem., Int. Ed.*, **1969**, 781-853, *Angew. Chem.*, **1969**, 797-870.

[58] B. A. Hess, jr., L. S. Schaad, *J. Am. Chem. Soc.*, **1971**, 305-310.

[59] J.-P. Desvergne, F. Fages, I. Frisch, H. Bouas-Laurent, *J. Chem. Soc., Chem. Commun.*, **1988**, 1413-1415.

[60] R. Calas, R. Lalande, *Bull. Soc. Chim. Fr.*, **1959**, 770-772.

[61] N. C. Yang, H. Shou, T. Wang, J. Masnovi, *J. Am. Chem. Soc.*, **1980**, 102, 6652-6654.

[62] T. Brotin, J.-P. Desvergne, F. Fages, R. Utermöhlen, R. Bonneau, H. Bouas-Laurent, *Photochem. Photobiol.*, **1992**, 349-358.

[63] L. B. Birks, *Photochem. Photobiol.*, **1963**, 493 [quoted in 7].

[64] L. F. Fieser, *J. Am. Chem. Soc.*, **1931**, 53, 2329-2338.

[65] M. Zander, Polycyclische Aromaten: Kohlenwasserstoffe und Fullerene, Stuttgart: Teubner, **1995**.

[66] P. Labandibar, R. Lapouyade, H. Bouas-Laurent, *C. R. Hebd. Seances Acad. Sci. Ser. C*, **1971**, 272, 1257-1260.

[67] S. Gabriel, E. Leupold, *Ber. Dtsch. Chem. Ges.*, **1898**, , 31 1272-1286.

[68] H. Waldmann, H. Mathiowetz, *Ber. Dtsch. Chem. Ges.*, **1931**, 64, 1713-1721.

[69] M. P. Cava, A. A. Deana, K. Muth, *J. Am Chem. Soc.*, **1959**, 81, 6458-6460.

[70] J. G. Smith, P. W. Dibble, *J. Org. Chem.*, **1983**, 48, 5361-5362.

[71] D. Marquis, J.-P. Desvergne, H. Bouas-Laurent, *J. Org. Chem.*, **1995**, *60*, 7984-7996.

[72] F. Fages, J.-P. Desvergne, H. Bouas-Laurent, *Bull. Soc. Chim. Fr.*, **1985**, 959-964.

[73] C. G. Hatchard, C. A. Parker, *Proc. R. Soc. Lond. A*, **1956**, 518-535.

[74] F. Fages, J.-P. Desvergne, I. Frisch, H. Bouas-Laurent, *J. Chem. Soc., Chem. Commun.*, **1988**, 1413-1415.

[75] H. Bouas-Laurent, H. Dürr, *Pure Appl. Chem.*, **2001,** 73, 639-665.

[76] Y. S. Liu, P. de Mayo, W. R. Ware, *J. Phys. Chem.*, **1993**, 5995-6001.

[77] J. Olmstedt, *J. Phys. Chem.*, **1979**, *83***,** 2581-2584.

[78] H. Langhals, *Nachr. Chem. Techn. Lab.*, **1980**, 28, 716-718.

[79] T. Salthammer, *Fluoreszensspektroskopische Untersuchungen von Energie-übertragungsprozessen an Perylen und 3,9-Dibromperylen*, Dissertation, Braunschweig, **1990**, 24-40.

Lebenslauf

Jens Reichwagen

geboren am 17. Januar 1974

in Hamburg

ledig

Promotion

	04/ 2005	Disputation
	02/ 2005	Einreichen der Disserttation
seit	10/ 2001	Promotion am Institut für Organische Chemie, TU Braunschweig; Mentor: Professor Dr. Henning Hopf *Thema der Dissertation:* Synthesis of acene based organic gelators. Examination of the spectroscopical, photochemical and rheological properties
seit	05/ 2004	Wissenschaftliche Hilfskraft am Institut für Anorganische und Analytische Chemie, TU Braunschweig
04/ 2002 - 03/ 2004		Promotionsstipendium des Fonds der Chemischen Industrie
10/ 2001 - 03/ 2002		Wissenschaftliche Hilfskraft am Institut für Organische Chemie, TU Braunschweig
07/ 2003 - 08/ 2003		Forschungen an der Université Bordeaux I bei
und		Professor Dr.Henri Bouas-Laurent
06/ 2002 - 07/ 2002		

Hochschulbildung

09/ 2001	Abschluss des Diplomstudiums Chemie an der TU Braunschweig *Thema der Diplomarbeit:* 2,3-Didecyloxytetracen als neuer Gel-Bildner.
08/ 1998 - 05/ 2001	Hauptstudium mit Vertiefungsrichtung Ökologische Chemie und Abfallanalytik

05/ 1999 - 04/ 2001	Studienbegleitendes Stipendium der Hoechst Stiftung
10/ 1996 - 08/ 1998	Grundstudium.

Berufsausbildung

08/ 1993 - 06/ 1996	Ausbildung zum Chemielaboranten im Staatlichen Veterinäruntersuchungsamt für Fische und Fischwaren, Cuxhaven.

Schulbildung

08/ 1986 - 05/ 1993	Gymnasium Cuxhaven.
08/ 1980 - 06/ 1986	Grundschule und Orientierungsstufe Franzenburg

Katastrophenschutzdienst

10/ 1996 - 11/ 1999	Deutsches Rotes Kreuz, Braunschweig
11/ 1992 - 10/ 1996	Fernmeldezug der Stadt Cuxhaven